Winter 2016

Small Solar Wind Transients 1995 - 2014: Properties, Modeling, and Effects on the Magnetosphere

Wenyuan Yu
University of New Hampshire, Durham

Small Solar Wind Transients 1995 - 2014: Properties, Modeling, and Effects on the Magnetosphere

BY

WENYUAN YU

B.A. in Applied Physics, Wuhan University, 2008

M.S. in Physics, Wuhan University, 2010

DISSERTATION

Submitted to the University of New Hampshire

in partial fulfillment of

the requirements for the degree of

Doctor of Philosophy

in

Physics

December, 2016

This dissertation has been examined and approved in partial fulfillment of the requirements for the degree of Doctor of Philosophy in Physics by:

Dissertation Director, Charles J. Farrugia
Research Professor of Physics, University of New Hampshire

Noé Lugaz
Research Associate Professor of Physics

Antoinette B. Galvin
Research Professor of Physics

Roy B. Torbert
Professor of Physics

Dawn C. Meredith
Professor of Physics

On November 10, 2016

Original approval signatures are on file with the University of New Hampshire Graduate School.

Dedication

This dissertation is dedicated to my family for supporting me during my Ph.D. study. I also dedicate this thesis to Dr. Charles Farrugia and Dr. Noé Lugaz, whose great help and teach on the space physics made this dissertation.

Acknowledgments

I would like to express my sincerest appreciation to my advisors Dr. Charles Farrugia and Dr. Noé Lugaz. Thanks to their generous support, I can finally make this dissertation. I would like to thank Fathima Muzamil and Nada Al-haddad for their encourages during my dissertation writing process. This dissertation was supported by NASA and NSF grants. Thanks to my thesis defense committee members Charles Farrugia, Noé Lugaz, Antoinette Galvin, Roy Torbert and Dawn Meredith for their comments and patience on the thesis. Finally, thanks to Guanlai Li and Lily Li for all their support during my Ph.D. studies.

Table of Contents

List of Tables

List of Figures

ABSTRACT

Small Solar Wind Transients 1995 - 2014: Properties, Modeling, and Effects on the Magnetosphere

by

Wenyuan Yu

University of New Hampshire, December, 2016

Using case studies and statistical analysis on a large data sample we investigate properties of small solar wind transients (STs) and discuss their modeling. The observations are from the Wind and STEREO spacecraft. By "small" we mean a duration of 0.5-12 hours. We do not restrict ourselves to magnetic flux ropes. Having arrived at a definition based on an extension of previous work, we apply an automated algorithm to search for STs. In one chapter we focus on the solar activity minimum years 2007-2009. We find an average ST duration of ∼4.3 hours, with 75% lasting less than 6 hours. A major difference from large-scale transients (i.e. ICMEs) in the same solar minimum is that the low proton temperature (T_p) is not a robust signature of STs, which is opposite to the trend in ICMEs. Further, the plasma β (electrons + protons) ~ 1 and thus force free modeling of flux rope STs may not be appropriate. We then examine a much wider sample covering almost 2 solar cycles (1995-2014). After Alfvénic fluctuations are removed, we obtain about 2000 STs. We find that their occurrence frequency has a two-fold dependence: it is (i) correlated strongly with slow solar wind speeds, and (ii) anti-correlated with solar activity, as monitored by the sunspot number. As regards (i) we find that over 80% of STs occur in the slow wind (< 450 km/s). The anti-correlation with solar cycle activity is contrary to what is observed with ICMEs. Most of the STs convect with the ambient solar wind. Studying the normalized expansion parameter, we conclude that many STs do not expand at all, i.e. they are static structures. Only $\sim$ 5 % of STs show enhanced values of iron charge states. We also find that the plasma beta of STs depends on solar activity level, being $<<$ 1 for maximum and of order 1 or more for solar minimum. Thus non-force free models should be used in solar minimum years while the force free models could be used in solar maximum. Motivated by these results, we then explore ST modeling with static, non-force free methods, using two analytical (with circular and elliptical cross-sections, respectively) and one numerical model (Grad-Shafranov reconstruction). We illustrate and compare results for 8 examples of flux rope STs. The two analytical models give fairly similar results. We show that our non-force free models can also fit the data as well, or even better, than the force free model. Grad-Shafranov reconstruction shows that the small flux ropes tend to have elliptical cross-section. Finally, we address some aspects of the disturbances in the Earth's magnetosphere, focusing on substorms and storms. We find substorm occurrence to be relatively common during passages of STs at Earth: $\sim$47% of STs of duration 1-5 hours were associated with substorms, a conclusion reached in other studies but here valid over a much larger data set. Further, about 3% of these STs were associated with geomagnetic storms.

Chapter 1

Introduction

As a magnetized planet orbiting the Sun at 1 AU, the Earth's plasma and magnetic field environment is strongly affected by solar activity. The Sun continuously releases a stream of charged particles, referred to as the solar wind (Parker [1958]). Measurements of the solar wind properties have been made routinely near 1 AU by spacecraft since the late 1960s (e.g. IMP8, ISEE, Wind, ACE, STEREO). The solar wind has both corotating and transient components. The transient solar wind is released from the Sun and propagates away from it, while the corotating component rotates with the Sun.

Researchers commonly distinguish between the slow and fast solar winds because they typically emanate from different regions of the Sun and exhibit different properties in interplanetary space (see for example, Schwenn [1983], for the inner heliosphere using Helios data, and review by Isenberg [1991]). The speeds of the solar wind at 1 AU are usually observed to be in the range 300-800 km/s. A dividing line at 450 km/s is usually used to separate the slow ($< 450km/s$) from the fast solar winds ($\geq 450km/s$). The former is associated with open field regions above or adjacent to the heliomagnetic streamer belt, while the latter is associated with the heliospheric current sheets from closed regions of the Sun (Phillips et al. [1995]; Feldman et al. [2005]). Their occurrence frequency changes with the solar activity cycle, whose average duration is 11 years as determined from changes in the number of sunspots (SSN) (http://www.sidc.be/silso/datafiles). The percentage of the fast solar wind is high during the solar maximum phase while it is low during solar minimum activity.

The large transient structures in the solar wind cause some of the strongest disturbances in the Earth's magnetosphere. They can give rise to strong aurorae, reaches lower latitudes, and cause damage to satellites and electrical facilities, which may result in the long-lasting power outages (Board et al. [2008]). Study of these transient structures is therefore essential to understand the near-Earth space environment, resulting in the development of the field of space weather in the past 50 years. The transient structures can be divided into two categories: large transients and small transients, based on the observed durations. That is, they have large and small spatial dimensions. As a rough estimate, at 1 AU these are of order 0.2 and 0.02 AU, respectively.

The large transients are also known as interplanetary coronal mass ejections (ICMEs). They, and their subset called magnetic clouds (MCs; Burlaga et al. [1981]), have been widely studied both for their intrinsic interest as well as because they can give rise to strong disturbances in planetary magnetospheres such as the terrestrial one.

Small transients (STs) in the solar wind have been studied for over 2 decades. STs which have a magnetic flux rope (FR) geometry were discovered and modeled by Moldwin et al. [1995, 2000] in a linear force free approach. Then, as more and more small flux ropes were observed, scientists also paid more attention to these smaller ones. STs can also cause disturbances in the Earth's magnetosphere. This is one reason for studying them. By understanding these transient structures, we can learn how they affect the interplanetary space and contribute to space weather efforts. For example, do STs contribute significant geoeffects in the magnetosphere at solar minimum when the contribution of large transients is low?

1.1 Large Transients

Large-scale transients (ICMEs) have attracted considerable interest since their discovery in satellite observations in the 1970s. Their frequency of occurrence is known to increase significantly with solar activity (Robbrecht et al. [2009]; Wang and Colaninno [2014]).

The passage of most ICMEs near Earth lasts for 1-2 days. If they are MCs, their geometry is often modeled as a large magnetic flux rope. Figure 1-1 (Figure 1, Richardson and Cane [2010]) shows a sketch of a MC whose field lines are still connected to the Sun. Inside the MC, this topology leads to the observation of heat flux electrons moving both parallel and opposite to the magnetic field lines, i.e. counterstreaming electrons. The ICME is also driving a shock ahead of it. The magnetic field between the ICME and the shock, i.e. the ICME sheath, is turbulent, unlike there is an orderly field inside the ICME. Shock, sheath and ICME material all contribute to the disturbances seen in a planetary magnetosphere.

ICMEs have many signatures (see table 1.1), such as high magnetic field strengths, low proton temperatures, high α particle/proton number density ratios, enhanced iron charge states, etc. (see e.g. Richardson and Cane [2010]). A subset of ICMEs are called MCs (Burlaga et al. [1981]). MCs are characterized by an above-average magnetic field strength, and a large and smooth rotation of the field vector in a plasma of low proton temperature and/or proton beta (T_p and β_p) (Burlaga et al. [1981], Klein and Burlaga [1982]). They have been modeled as magnetic flux ropes (Burlaga et al. [1981], Goldstein [1983]) in a linear force-free approximation (Burlaga [1988], Lepping et al. [1990]).

ICMEs/MCs occupy a central place in discussions of space weather at Earth. This is because these configurations typically possess physical parameters which may reach up to extreme values that last for several hours (see e.g. Farrugia et al. [1997] and Figure 1-2). To illustrate, Figure 1-2 shows proton and magnetic field observation of a MC which was observed by the ACE spacecraft on November 20, 2003. ACE was orbiting the L1 Lagrangian point, which is about 250 Earth radii away from Earth in the sunward direction. This MC caused one of the strongest geomagnetic storms in solar cycle 23 where the depression of the Earth field, measured by the so-called storm-time Dst index was about -500 nT. From top to bottom, the panels show the proton density, the bulk speed, proton temperature (in purple, the expected temperature for normal solar wind expansion), the α/proton number density ratio, the dynamic pressure, the components of the magnetic field in GSE coordinates and the total field and the proton beta. The GSE coordinate system has its axis centered at Earth and pointing to the Sun, the Y axis points toward dusk such that the (XY) plane is the ecliptic plane and the Z axis is directed perpendicular to the ecliptic plane so that the XYZ system is right-handed. Some of the signatures characterizing ICMEs and MCs are observed here: (i) low proton temperature, (ii) high values of α/proton density ratios reaching up to 20 %, (iii) strong magnetic field, and (iv) smooth and large rotations of its components. Another important parameter is the dynamic pressure (panel 5), which reached very high values when compared to typical values of about 2-3 nPa.

Magnetic flux ropes are clear structures and many years have been devoted in trying to model them. Scientists created many models, both analytical and numerical (for example, Lundquist [1950], Mulligan and Russell [2001], Hidalgo et al. [2002a], Hidalgo et al. [2002b], Hidalgo [2003], Hidalgo [2005], Marubashi and Lepping [2007], Hu and Sonnerup [2001], Hu and Sonnerup [2002]) to study them, in order to obtain information about this kind of structures (e.g., the orientation, sizes, and variations with time, and so on). A very popular

Table 1.1: Typical signatures of different types of solar wind transients. For further details, see text.

Transients	Signatures
ICME	B enhancement; B rotation ($\geq 30\%$); low B variance; proton temperature decrease (robust); discontinuity at boundaries; MCs ($\sim 30\%$); high α/proton number density ratio; enhanced iron charge states; bidirectional electrons; cosmic ray depletions; velocity expansion; density decrease; enhancements of Fe/O; elevated oxygen charge states.
MC	B enhancement; large-scale rotation of the magnetic field vector; low proton temperature and low proton β;
ST	Duration between [0.5, 12] hours observed at 1AU; B enhancement; low proton β or low proton temperature; low Alfvén Mach number; high T_e/T_p ratio; small velocity expansion; bidirectional electrons (some of them); high iron charge state (some of them).
FR - ST	Smooth rotations of the magnetic components; B enhancement; duration between [0.5, 12] hours observed at 1 AU; low Alfvén Mach number; low proton β or low proton temperature; small velocity expansion; high T_e/T_p ratio; high iron charge state; et al.

model is that of Lundquist [1950], which considered the flux ropes which were linearly force - free (i.e. $J \times B = 0$, which implies $J = \alpha B$, and α here is constant).

The limitation of this approach is that the data input to these models is usually from one spacecraft crossing a very large structure. The STEREO mission has brought improvements on this. The capabilities of Heliospheric Imagers (Eyles et al. [2009]) on STEREO/SECCHI (Howard et al. [2008]) to remotely sense these large structures as they erupt from the Sun and propagate through the inner heliosphere allow comparisons with in situ observations. Much effort is being invested in the prediction of the arrival time and in situ properties from remote sensing observations (see e.g. Rollett et al. [2012], Möstl et al. [2011] and references therein) under various assumptions for the shape of the transients (e.g. The Fixed - Phi Kahler and Webb [2007] and the Harmonic Mean Lugaz et al. [2009]).

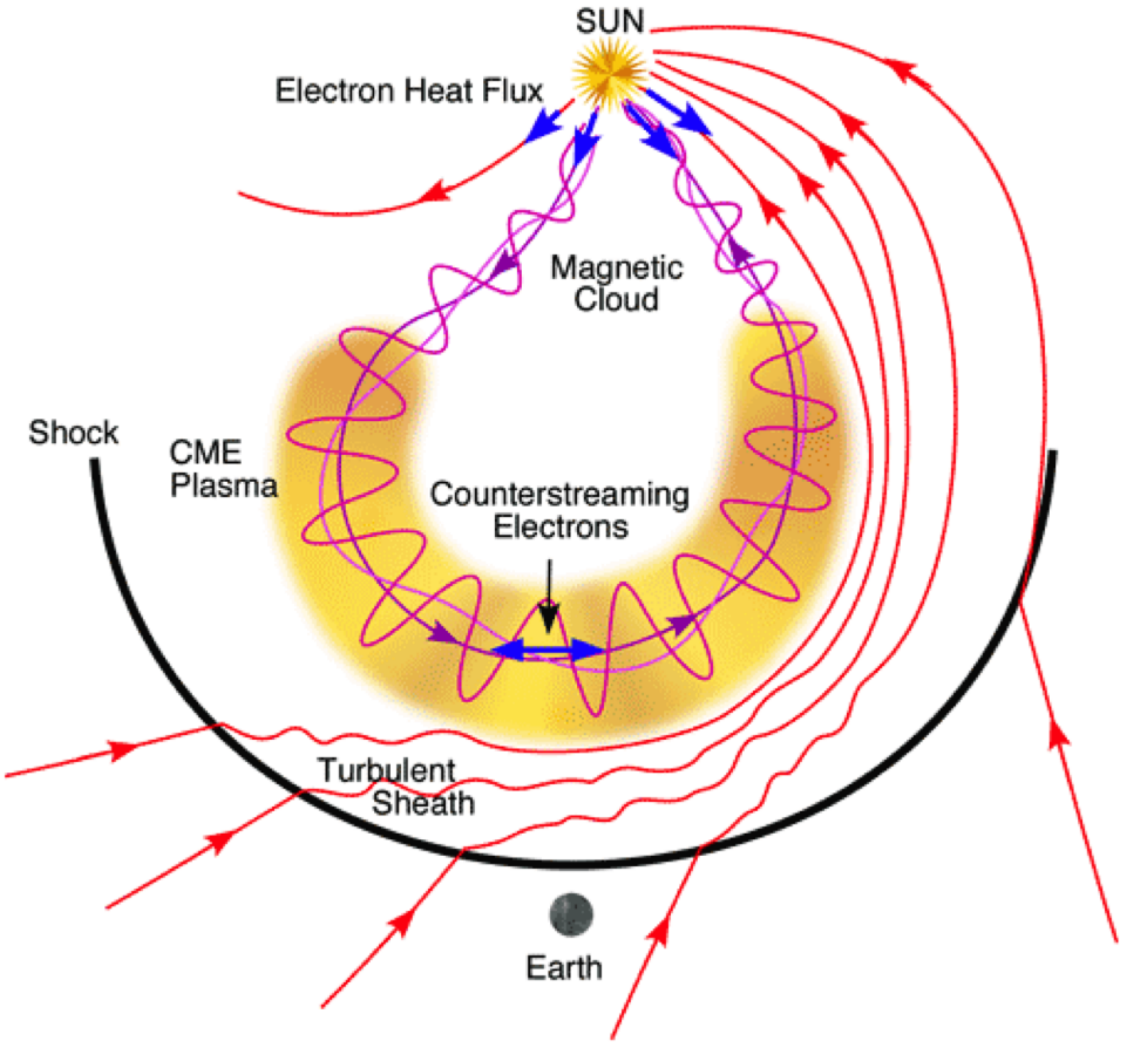

Figure 1-1: An ICME with MC (https://ase.tufts.edu/cosmos/pictures/Sept09/Fig8_7.MagCloud.gif).

1.2 Small Transients

Small transients (STs) in the solar wind have also attracted considerable interest, although for different reasons. By "small" we mean configurations whose passage at Earth may last from a few tens of minutes to a few hours. Some of these STs also have the geometry of small magnetic flux ropes. Indeed, attention has also been repeatedly drawn to the presence of small flux ropes in the solar wind (e.g. Moldwin et al. [2000], Feng et al. [2007, 2008],

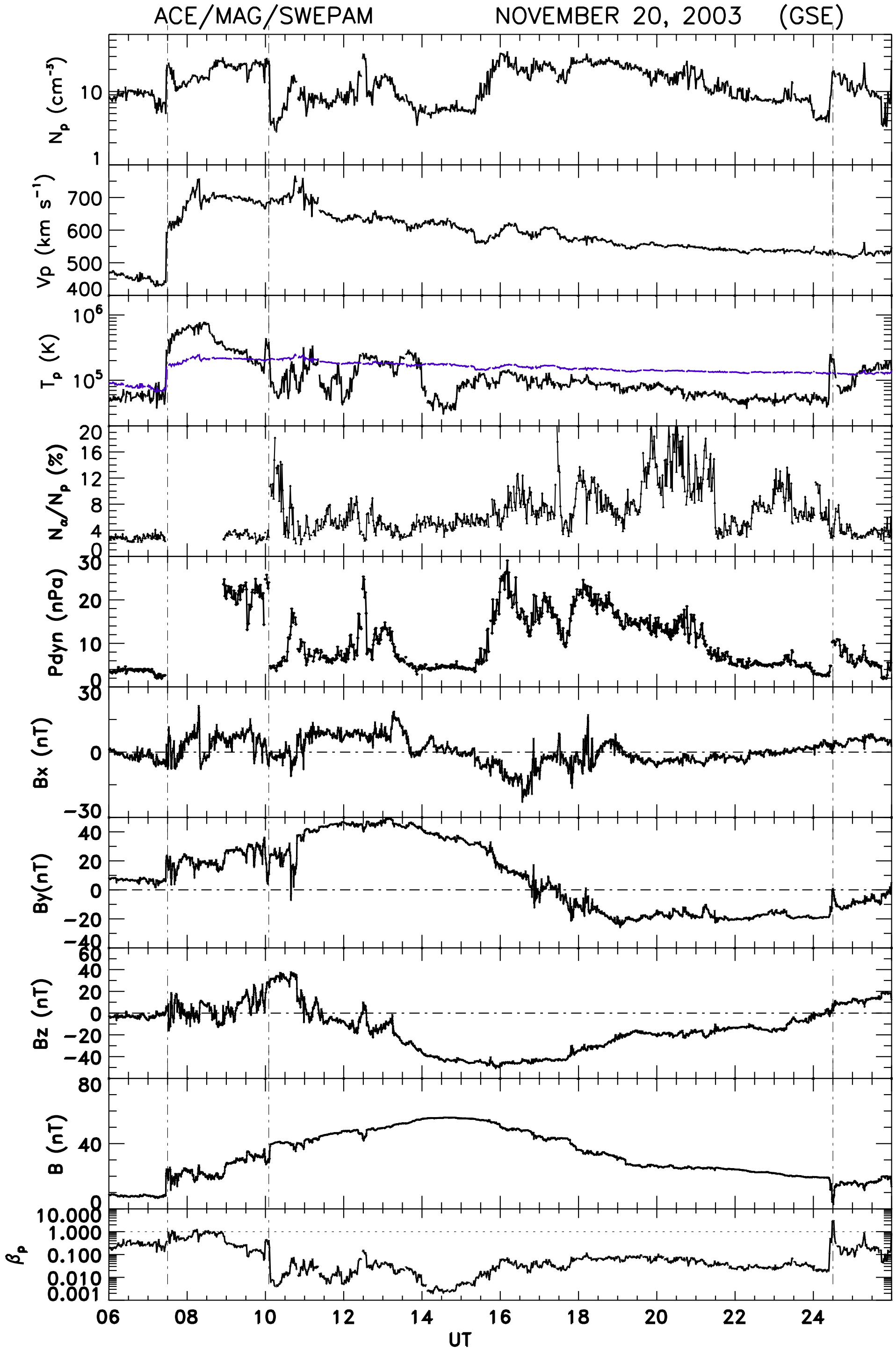

Figure 1-2: A MC observed by ACE spacecraft on November 20, 2003.

Cartwright and Moldwin [2008, 2010], Ruan et al. [2009]). These studies of small solar wind flux ropes (FRs) came after the discovery of small flux ropes in the geomagnetic tail (Slavin et al. [2003], Moldwin and Hughes [1991]).

The flux rope structure studied by Moldwin et al. [1995] was observed by Ulysses at 5 AU. Aside from its size, it had properties different from those of large MCs, such as high proton temperature and plasma β, and no enhancement of the α/proton relative abundance. Eleven small flux ropes, this time from IMP8 and Wind observations at 1 AU in 1995 -1997 (solar minimum and early rising phase of cycle 23) were reported by Moldwin et al. [2000]. Some properties were similar to those of magnetic clouds (Burlaga et al. [1981]) while others were not. Importantly, the small flux ropes at 1 AU showed a lack of radial expansion. This static property was also confirmed by Kilpua et al. [2009].

An example of a ST is shown in figure 1-3. It was observed by STB on June 11, 2010. Its duration is 1.67 hrs, shown between two vertical guidelines. From top to bottom the figure shows the total field strength (B), the field components in RTN coordinates (B_R, B_T, B_N), the proton bulk speed (V_p), density (N_p) and temperature (in red is the expected temperature, T_{exp}; in black is the proton temperature, T_p), the Alfvén Mach number (M_A), β (in black is the proton beta, β_p; in red is the plasma beta, β_{plasma} with alphas not included in its calculation), and the pressures (proton pressure in blue, magnetic pressure in red, and the total pressure in black). B is about three times the yearly average, its components all have flat profiles in this ST. The V_p is steady. N_p is lower than surrounding values. T_p is much less than T_{exp}. Parameter M_A is much less than the yearly average. β_p is very small, less than 0.1, while the β_{plasma} is ~ 0.5. While this event does not have a flux rope structure, the above properties identify it as a ST.

A main question that has been raised in these studies concerns the possible relation

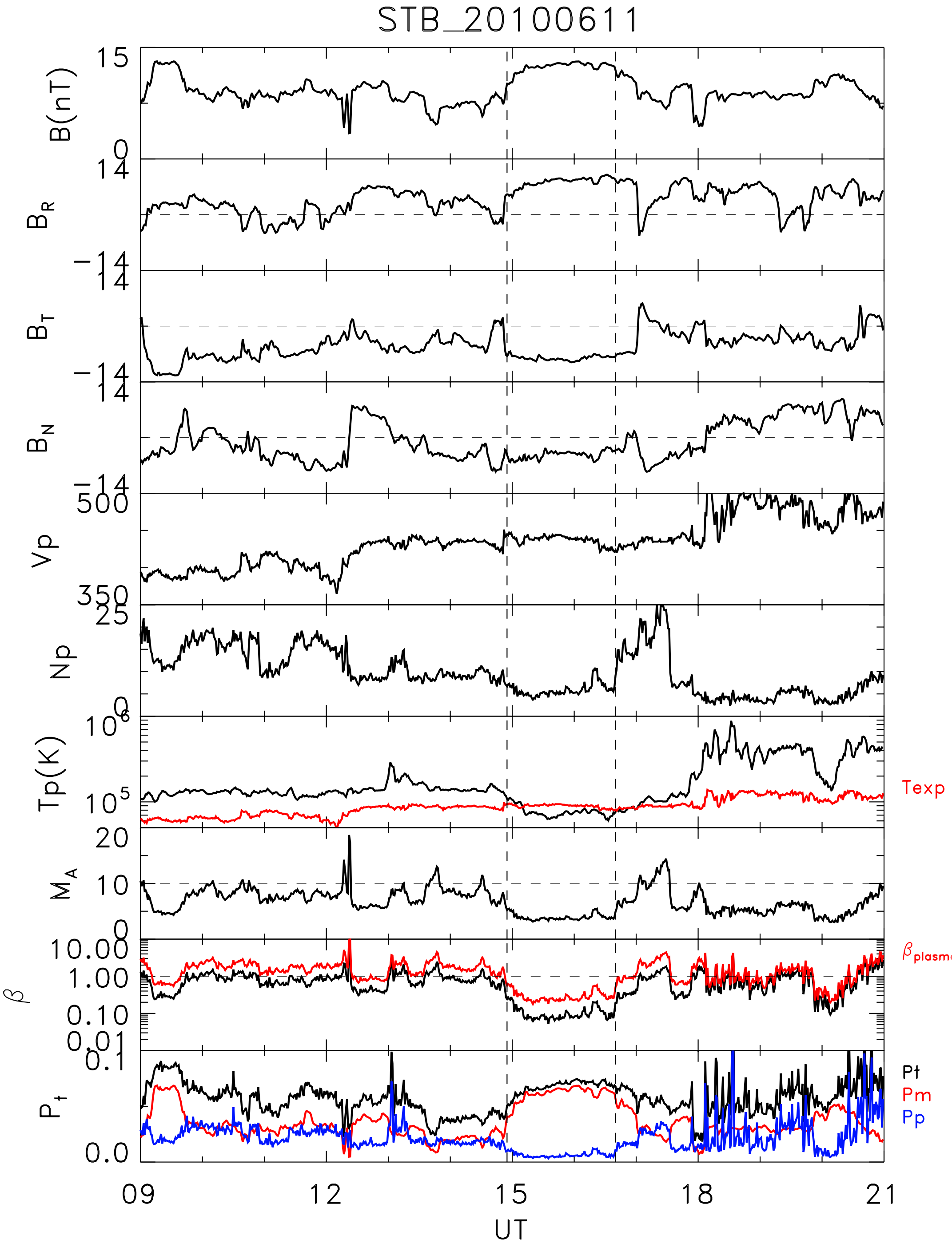

Figure 1-3: A ST observed by Wind spacecraft on June 11, 2010.

between these STs and the large-scale ICMEs/MCs. A further, related question concerns their origin: Do STs originate at the Sun or, rather, in heliospheric processes, such as through reconnection at the heliospheric current sheet (HCS)?

A debate was started, which is still ongoing, as to where STs originate. Using a larger data base (68 samples in 1995-2005) Cartwright and Moldwin [2008, 2010] proposed the view that the small flux ropes are produced by reconnection across the heliospheric current sheet (HCS). However, Feng et al. [2007, 2008] proposed a different mechanism. They analyzed over 100 small and intermediate magnetic flux ropes during solar cycle 23 (1995 - 2005) observed by the Wind spacecraft. (The cases studied had little overlap with the list of Cartwright and Moldwin.) The distributions of their sizes and energies exhibited a continuous variation, and the distribution of the axial orientations was similar to that of MCs. The authors suggested that small- and intermediate magnetic flux ropes originated from solar eruptions just like magnetic clouds. In recent work, Tian et al. [2010] concluded that small flux ropes could be created both in the solar wind and near the Sun (see also Rouillard et al. [2011]). Janvier et al. [2014b] also studied small FRs from existing tables, and showed that the small FRs may originate in blowout X-ray jets or multi-reconnection processes, or they may be created at the heliospheric current sheet.

The analytical models proposed to study the MCs can also be used to study the small flux ropes. And in some sense, these models are more reliable on these small flux ropes because of their static property (Moldwin et al. [2000]; Kilpua et al. [2009], Yu et al. [2014, 2016]), since the models refer to magnetohydrostatic equilibrium.

1.3 Geoeffectiveness of solar wind transients

ICMEs/MCs may give rise to strong disturbances in the magnetosphere. This is mainly due to reconnection of their magnetic field lines with the magnetospheric field lines. This process converts magnetic energy into particle energy, where the particles are heated and accelerated. Magnetic storms and substorms are two main appearances of geomagnetic activity. In addition, as also shown by Farrugia et al. [1995]; Lavraud and Borovsky [2008], these magnetically-dominated structures can also alter the structure of the Earth's magnetosheath.

The magnetic storm is a temporary disturbance of the Earth's magnetosphere. The essential feature of it is a ring current which has been energized. It can be monitored by the Dst index (the disturbance storm time) or SYM-H, which is a higher resolution version of Dst index. An example of the Dst measurements during a geomagnetic storm is shown in Figure 1-4. It has three phases, as marked. There is an initial phase where there is a sudden increase in Dst value. This is due to the arrival of the shock, which compresses the magnetosphere. It is followed by a main phase with a sharp decrease in Dst. This phase usually lasts a few hours, and the strength of the storm is given by the lowest value of the Dst index. Then a recovery phase follows, which may last for a few days.

The magnetic substorm is a result of dayside merging of the magnetic fields which is created by the southward B_z component in the ICME. This process loads magnetic flux into the tail (the loading phase). When, later, reconnection happens in the near-magnetotail, this energy is released to the particles in the high latitude ionosphere and plasma sheet. The substorm also has three phases, namely, the growth phase (i.e. the energy loading process); the expansion phase (the energy unloading process), and the recovery phase, when the magnetosphere returns to a quiet state.

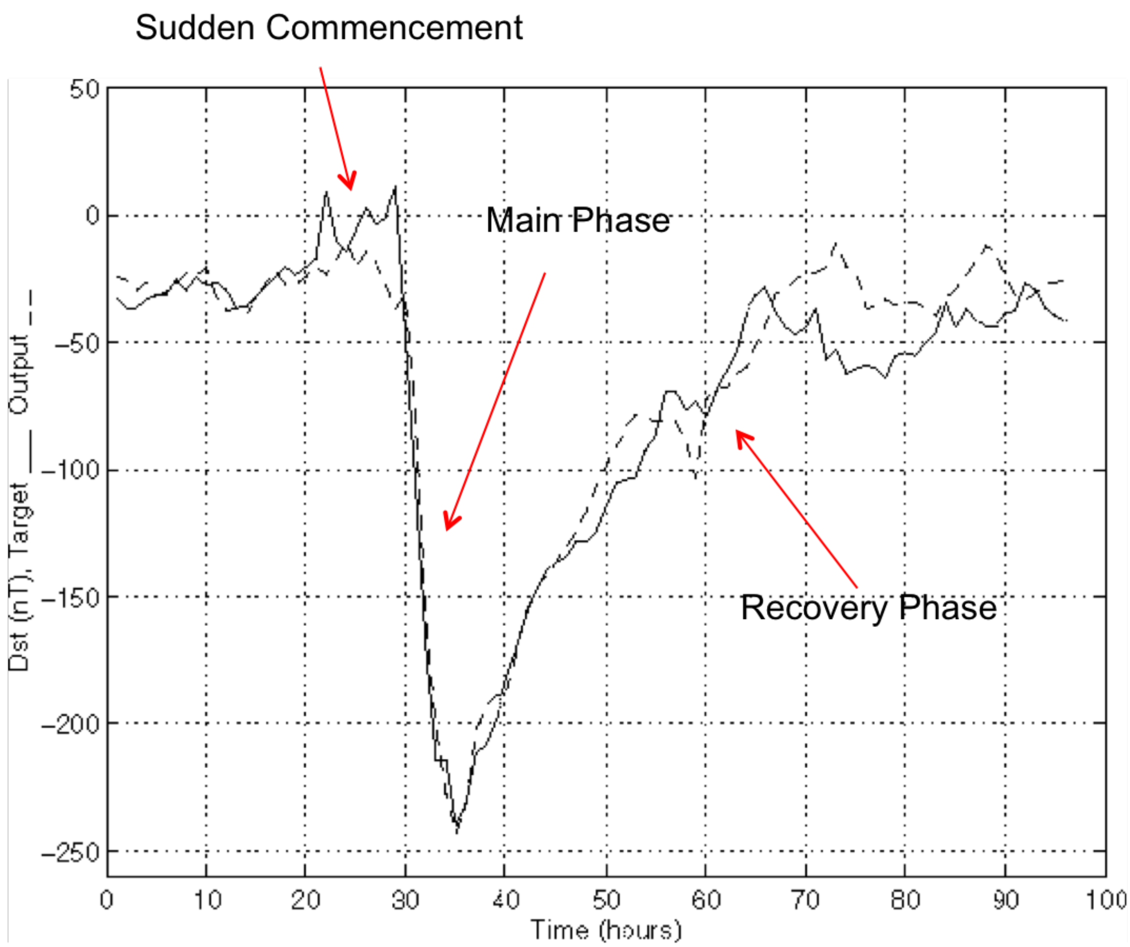

Figure 1-4: A magnetic storm featured by Dst index (http://education.gsfc.nasa.gov/experimental/all98invproject.site/Media/slide6-2.gif).

This is illustrated in Figure 1-5 (taken from Birn and Priest [2007]). The top panel shows the growth phase where reconnection is occurring on the dayside and magnetic flux is being transported to the nightside (see open arrow in panel 1). As a consequence, the tail field becomes more stretched. After this, reconnection takes place in the nightside near-tail. The start of near-tail reconnection is called the substorm onset. After this, the field becomes more dipolar (contrast panels 2 with 3). During the expansion phase a plasma sheet structure called a plasmoid is ejected down the tail. Plasmoids were shown to be magnetic flux ropes.

McPherron et al. [1973] showed that the geomagnetic tail suffers a large change at substorm onset. This change affects the current forming for dawn to dark across the tail. This current is disrupted and made to flow into the ionosphere. The closure current in the ionosphere is called the westward electrojet (WEJ). After WEJ, this is called the substorm current wedge. This current causes magnetic perturbations on ground magnetometers underneath. Taking a few such magnetometers, an auroral index is formed, the auroral electrojet index (AE). AL is defined as the lower envelopes of AE index. Thus, the AE/AL indices measure the strength of the substorm as reflected in the electrojet caused by the substorm current wedge, which is activated at substorm onset.

1.4 Instruments and Datasets

A number of satellites have been launched to study the inner heliosphere, such as Wind, ACE, STEREO. We use the data from Wind and STEREO spacecraft in our thesis.

In our work, we use data from the STEREO IMPACT (Luhmann et al. [2008]) and PLASTIC (Galvin et al. [2008]) instrument suites at 1 min resolution for the years 2007-2014. (The data is obtained from: fiji.sr.unh.edu, and aten.igpp.ucla.edu/forms/stereo/level2_plasma_and_magnetic_field.html.) We also use Wind key parameter data for the time period 1995 to 2014 acquired by the Magnetic Fields Investigation (MFI) (Lepping et al. [1995]) and Solar Wind Experiment (SWE) (Ogilvie et al. [1995]) (cdaweb.gsfc.nasa.gov/istp_public/). The magnetic field and proton data are at 1 min and 92 s time resolutions, respectively. The electron data is also obtained from the SWE instrument, and they have a resolution of 6-12 s before May 2001, and 9 s after August 2002.

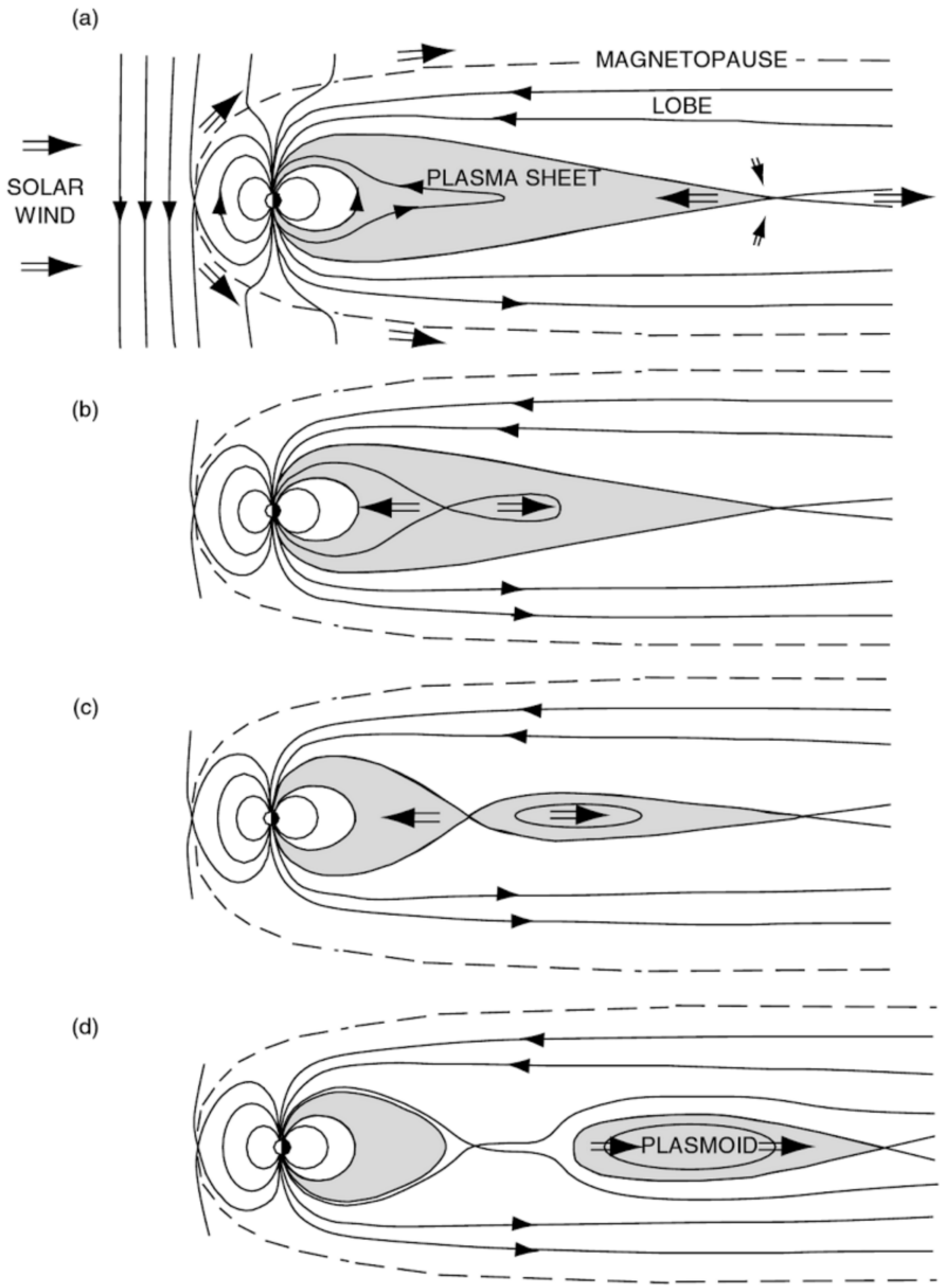

Figure 1-5: The schematic of the topological changes during a magnetic substorm (Figure 1.6 from Book - Reconnection of Magnetic Fields, Joachim Birn and Eric Priest, 2007).

1.4.1 Wind

The Wind spacecraft was launched in November 1994. Since 2004 it has been in orbit around the L1 Lagrange point. Previous to that it made many maneuvers but also was for long times collecting date in the solar wind. When in the solar wind it monitors the interplanetary conditions which will affect the Earth.

Wind spacecraft has a group of instruments on board (pwg.gsfc.nasa.gov/wind_inst.shtml).

(i) WAVES. It measures the waves emitted from the Sun, and studies how these waves affect the interplanetary plasma. This furthers our understanding of the plasma processes in the solar wind.

(ii) EPACT. It studies energetic particles, understands how they are accelerated and transported from, e.g., solar flares.

(iii) SWE. It measures the ions and electrons in the solar wind. Our study used the deduced moments (velocity, density, temperature) from this instrument.

(iv) SMS. This observes the suprathermal ions, determine the abundance, composition, and charge state of them.

(v) MFI. It investigates the interplanetary magnetic field. Our study used the magnetic field magnitude and components from this instrument.

(vi) 3D PLASMA. It also studies the ions and electrons in the interplanetary space, but with energies that include both the solar wind and energetic particle range.

(vii) TGRS. It provides the high-resolution spectroscopy of solar flares, and also high resolution of cosmic gamma-ray bursts.

(viii) KONUS. It also provides measurements on gamma-ray burst. It has lower resolution than TGRS, but with broader energy range.

In our study, we mostly use the plasma and magnetic data from Wind during the year 1994 to 2014. We use the key parameter data from the MFI (Lepping et al. [1995]) and SWE (Ogilvie et al. [1995]) instruments.

1.4.2 STEREO

STEREO consists of two spacecraft, which were launched in 2006. The ahead spacecraft (STA) was ejected to the heliocentric orbit inside the Earth's orbit, and the behind spacecraft (STB) was launched in a higher Earth orbit. These two spacecraft depart from each other at around 44 degrees per year (see Figure 1-5). In Feburary, 2011, the two spacecraft were 180 degrees apart from each other, which allowed us to study the sides of the Sun. And from then on, the two STEREO spacecraft continued to separate from each other and reached the farside of the Sun. This configuration allows us to observe the Sun along with the Earth's orbit in three points.

A visualization tool is available at (WHERE IS STEREO website). Figure 1-5 shows the spacecraft configuration on 1 Jan 2010 as an example. The positions of the STEREO spacecraft are shown. HEE coordinates are used. Spacecraft Wind is near the Earth. Also shown is the Parker-spiral orientation of the interplanetary field lines.

Each STEREO spacecraft contains four instruments.

(i) SECCHI. It has five cameras with overlapping field of view. It could observe the 3D evolution of the CMEs from the Sun to the interplanetary space.

(ii) IMPACT. It provides the magnetic field data, and also studies the energetic particles. We use the magnetic field and its components data from this instrument.

(iii) PLASTIC. It studies the plasma properties. In our work, we use the plasma moments (proton temperature, velocity, density) and iron charge states from it.

(iv) SWAVES. It tracks the radio disturbances from the Sun to Earth.

The STs in this thesis observed by the STEREO are selected by using the 1 min resolution data from IMPACT (Luhmann et al. [2008]) and PLASTIC (Galvin et al. [2008]) instrument suites.

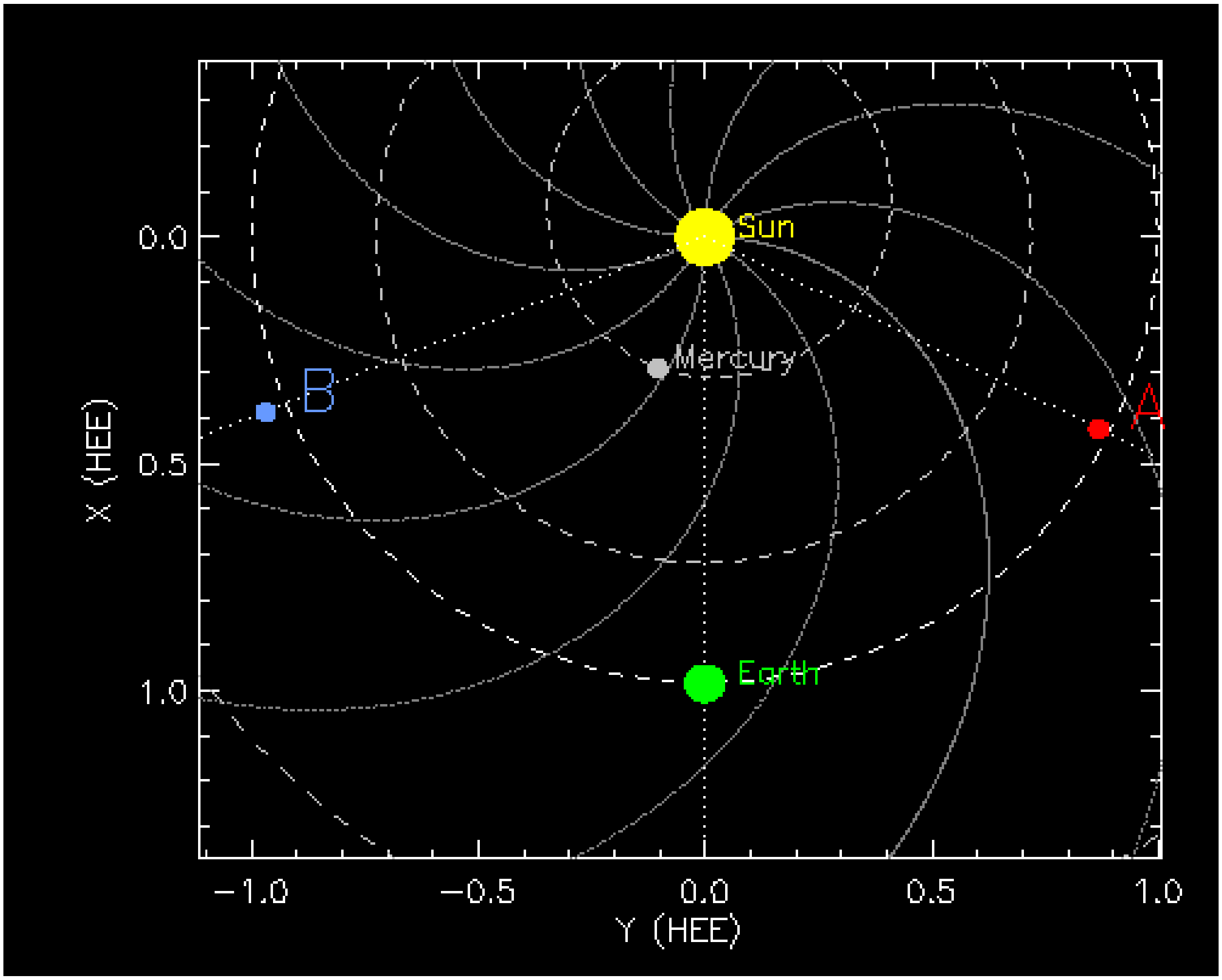

Figure 1-6: The positions of the STEREO spacecraft on Jan 1, 2010 (https://stereo-ssc.nascom.nasa.gov/cgi-bin/make_where_gif).

1.5 Objectives and Questions

The goals of this thesis are the following.

We first propose a definition of STs, which is based on an extension of previous work. This definition also includes STs which are not flux ropes. We then perform a dedicated study of STs in the solar wind and their modeling. We also address aspects of geomagnetic activity they caused. As noted above, the data set is from Wind in 1995 - 2014, when the spacecraft is in the solar wind, and from the STEREO probes (2007 - 2014). This gives a large data base of STs, much larger than in any previous work. This data base allows for both case studies and statistical analysis. Throughout we compare statistical results obtained for STs with those of ICMEs/MCs.

We discuss the dependence of ST occurrence rate on solar cycle phase and on the speed of solar wind. We also give statistics of the distribution of their sizes, duration etc. To obtain these statistics we develop an automated algorithm to search for STs.

We then discuss their radial expansion in terms of a normalized quantity described by Démoulin and compare with the results obtained earlier for magnetic clouds.

Our work suggests that the model to use for flux rope STs (force free or non-force free) depends also on solar cycle phase. We thus discuss results of using both force free and non-force free models. We employ three analytical models (force free model with Lundquist's solution, non-force free model with circular cross-section, non-force free model with elliptical cross-section). We also reconstruct the geometry of flux rope STs with a Grad-Shafranov reconstruction.

In a final chapter we discuss the geoeffects caused by STs. For this we study STs of duration from 1-4 hours, which are the most common in our statistics. The geomagnetic disturbances we focus on are magnetic substorms and storms.

1.6 Thesis layout

In this introductory chapter, we introduced the studies on the large and small transients. We also introduced the instruments and the datasets which we use in our thesis. We explained why we are interested in study the small transients, and the questions we would like to solve in the thesis.

In chapter 2, we present a comprehensive statistical analysis of the STs from 2007 to 2009 made by the Wind spacecraft. The properties of the STs in this deep and long solar minimum years are discussed.

In chapter 3, we extend our work to two solar cycles (solar cycle 23 and 24). We use the automated routine to get the event list from Wind in 1995 to 2014 (listed in Appendix A), and the lists from STEREO in 2007 to 2014 (Appendix B and C). We examine the dependence of their frequency distribution on solar activity and solar wind speed. Further, we compare the properties of the STs with those of ICMEs. The expansion velocity of STs will be discussed by using the formula from Démoulin.

In chapter 4, we use 3 different non-force free approaches to model small transients. The first is an analytical model which assumes a cylindrically symmetric structure with circular cross-section; the second is an analytical model which assumes a cylindrical symmetric with elliptical cross-section; and the third is a numerical model (the Grad-Shafranov reconstruction method). The details of the two analytical solutions are shown in Appendix D and E. We compared the fitting results by non-force free models with the force free model (Lundquist solution). The shape of the cross-section from the GS-reconstruction has been compared with the analytical methods. The orientations and the current density from the models are also studied in this chapter.

In chapter 5, we discuss the geoeffectiveness of STs. In this chapter, we examine whether STs cause magnetic storms or substorms.

In chapter 6, we summarize the key results of this thesis.

Chapter 2

STs in 2007 - 2009: STEREO and Wind Observations

Small Transients (STs) were observed in the solar minimum, and are frequently in the slow solar wind (Kilpua et al. [2009]). We present a comprehensive statistical analysis of small solar wind transients (STs) in 2007-2009. Extending work on STs by Kilpua et al. (2009) to a three-year period (2007 - 2009). We searched for STs using Wind (2007 - 2009) and STEREO (STA, 2009) data. We exclude Alfvénic fluctuations. Case studies illustrate features of these configurations. In total, we find 126 examples from Wind spacecraft, ~81% of which lie in the slow solar wind ($\leq$ 450 km s^{-1}). Many start or end with sharp field and flow gradients/discontinuities. Year 2009 had the largest number of STs, in which year there was 53 STs from Wind, and 45 STs from STEREO-A. The average ST duration is ~4.3 hours, 75% $<$ 6 hours. Comparing with ICMEs in the same solar minimum, we find the major difference to be that T_p in STs is not significantly less than the expected T_p. Thus, whereas a low T_p is generally considered a very reliable signature of ICMEs, it is not a robust signature of STs. Finally, since the total thermal pressure is comparable to the magnetic pressure (plasma $\beta \sim 1$) force-free modeling of those STs having a magnetic flux rope geometry may be inappropriate.

2.1 Introduction

A major work on STs in the slow solar wind is that of Kilpua et al. [2009], who presented examples seen by the STEREO-A/B (STA/STB) and Wind probes during Carrington rotations 2054, 2055 (March - April, 2007). To search for STs the authors focused on the following features: (i) decreased magnetic field variability; (ii) smooth rotation of the magnetic field; (iii) clear decreases in T_p and β_p. They found 17 cases in all, some seen at more than one spacecraft. (At this stage of the STEREO mission, the heliographic longitude separation between STA and STB increased from 1.2 to 5.0°, small enough to permit some multiple observations). Examples were included where not all of these criteria were simultaneously fulfilled; sometimes only one was satisfied (e.g. see Event 7 in Kilpua et al. [2009], and further below). Some had very few of the signatures we associate with large ICMEs and MCs (Neugebauer and Goldstein [1997], Zurbuchen and Richardson [2006], Richardson and Cane [2010]). Using the Global Oscillation Network Group (GONG) magnetogram-based coronal field source surface model map, they found that most of these transients map back to the vicinity of the model sector boundaries. Later, Kilpua et al. [2012] studied STs and ICMEs and found that STs occur more often close to SIRs and in the declining phase of fast streams than large ICMEs.

The high frequency of the STs in the slow solar wind attracted our attention. We first studied Kilpua et al. [2009]'s paper with the aim of adding other acknowledged ICME/MC signatures also present in their data sets. Essential for this is to compare against the average solar wind properties measured specifically in 2007-2009. From this we find the candidate set of parameters for our survey, i.e. those signatures which recur most frequently in the *in situ* data of these STs over the two Carrington rotations. These are: (i) duration of events between 0.5 and 12 hours; (ii) low proton temperature (T_p); (iii) enhanced magnetic field strength (B); (iv) decreased magnetic field variability; (v) coherent field rotations; (vi) low proton beta (β_p); (vii) low Alfvén Mach number (M_A); (viii) T_e/T_p higher than the average value over the 3 years.

Our definition of STs emerges from this study. We require STs to have durations between 0.5 and 12 hours; low T_p and/or low β_p; and an enhanced magnetic field strength relative to the three-year average. In addition, they must have at least one of the following: (a) decreased magnetic field variability; (b) large, coherent rotation of the field vector; (c) low Alfvén Mach number (M_A); and (d) T_e/T_p higher than the three-year average. We note that this definition includes small magnetic flux ropes but is not restricted to them.

We extended Kilpua et al.'s work to the years 2007 - 2009 by using the data from Wind and STA spacecraft. We survey by eye, and the above selection method yielded 126 STs from Wind spacecraft from 2007 to 2009 (Yu et al. [2014]), and 53 STs from STA in the year 2009 (Yu et al. [2013]). Our STs list not only includes the small flux rope structures, but also contains other STs.

We use Wind key parameter data from the MFI (Lepping et al. [1995]) and SWE (Ogilvie et al. [1995]) instruments. The key parameter data have a temporal resolution of 92 s (plasma) and 1 min (magnetic field). The electron temperature T_e is obtained from the SWE instrument at 9 sec resolution. For the STA, the data are from the PLASTIC and IMPACT instrument suites with 1 min resolution.

We present six events as case studies which we believe to be representative of various features seen in these STs, e.g. where they occur, typical durations, etc. We then present our statistical results, grouping by slow/fast winds. Finally, in the discussion section, we compare ST properties with those of ICMEs seen during the same period after the tabulation of Richardson and Cane [2010].

We stress again that when comparing ST properties to those of the "normal" solar wind we use as reference the solar wind during 2007-2009, which was in many respects (e.g. low magnetic field strength and low plasma density) different from solar winds during minima of other solar cycles (Smith and Balogh [2008], and McComas et al. [2008], Farrugia et al. [2012]). This information is given in Table 2.1, which includes the average values and the standard deviations of the ((i) magnetic field, B; (ii) β_p; (iii) M_A; (iv) proton density, N_p; (v) proton bulk speed, V_p; (vi) T_p; (vii) T_e/T_p of the solar wind. The average magnetic field strength in these three years was only 4.2 nT (Wind), while 4.34 nT and 3.92 nT were obtained from the STA and STB data sets, respectively. The expected proton temperature for normal solar wind expansion, however, depends on the solar wind bulk flow speed. Empirical formulas obtained from statistics were given by Lopez [1987]. However, we do this from first principles. The reason for doing so is that the period under study had special properties and we want to be sure that these be adequately reflected in the statistics.

2.2 Methodology

In this section we motivate our selection criteria for STs by extending the work of Kilpua et al. [2009], isolating other indicators which appear frequently in the data sets. We give one example to illustrate the approach. We also discuss the expected proton temperature of the solar wind during 2007-2009, useful for comparison purposes.

We begin with the latter. We derive the expected T_{exp} of the solar wind in 2007-2009 as a function of V_p. The statistical formula obtained by Lopez [1987] is

- $T_{exp} = (0.031 \times V_p - 5.1)^2 \times 1000$ for V_p <500 km s^{-1};

- T_{exp} = (0.51×V_p - 142)×1000 for V_p ≥500 km s^{-1}.

We shall assume a similar functional form for T_{exp} in terms of V_p, and also use the same demarcation line at V_p = 500 km s^{-1}. The key parameter data from the Wind/SWE instrument results in over 9×10^5 data points in the three-year period (720271 in slow, and 209379 in fast wind). We used the IDL least-squares fitting routine "curvefit", and the initial parameters were set very different from those of Lopez [1987]. The routine then converges to:

- T'_{exp} = (0.027×V_p - 3.665)^2×1000 for V_p <500 km s^{-1};

- T'_{exp} = (0.323×V_p - 58.277)×1000 for V_p ≥500 km s^{-1}.

Figure 2-1 shows these results in blue. The red trace shows the Lopez [1987] values. The goodness-of-fit parameter χ^2 is shown in table 2.2. As can be seen, the results we obtain are close to those of Lopez and, particularly for the slow solar wind, the fits almost coincide.

We looked at the 17 events listed by Kilpua et al. [2009], which occurred in March - April, 2007. We added the following quantities in search of possible further candidate signatures of ST: (i) T_e/T_p and (ii) Alfvén Mach number, M_A. The reason for including (i) is that in various studies it has been shown that in large transients $T_e >> T_p$ (Fainberg et al. [1996], Richardson et al. [1997], Sittler and Burlaga [1998]). Indeed, this ratio could reach values of ∼10 (Sittler and Burlaga [1998]). In an example using Ulysses data, Osherovich et al. [1999] showed values >20 at large heliospheric distances. The Alfvén Mach number, M_A, is typically lower in ICMEs and MCs than in the surrounding solar wind (Farrugia et al. [1995], Lavraud et al. [2007], Leitner et al. [2009]; Leitner and Farrugia [2010]). Indeed, low M_A is one reason why magnetosheath properties, and hence solar wind-magnetosphere

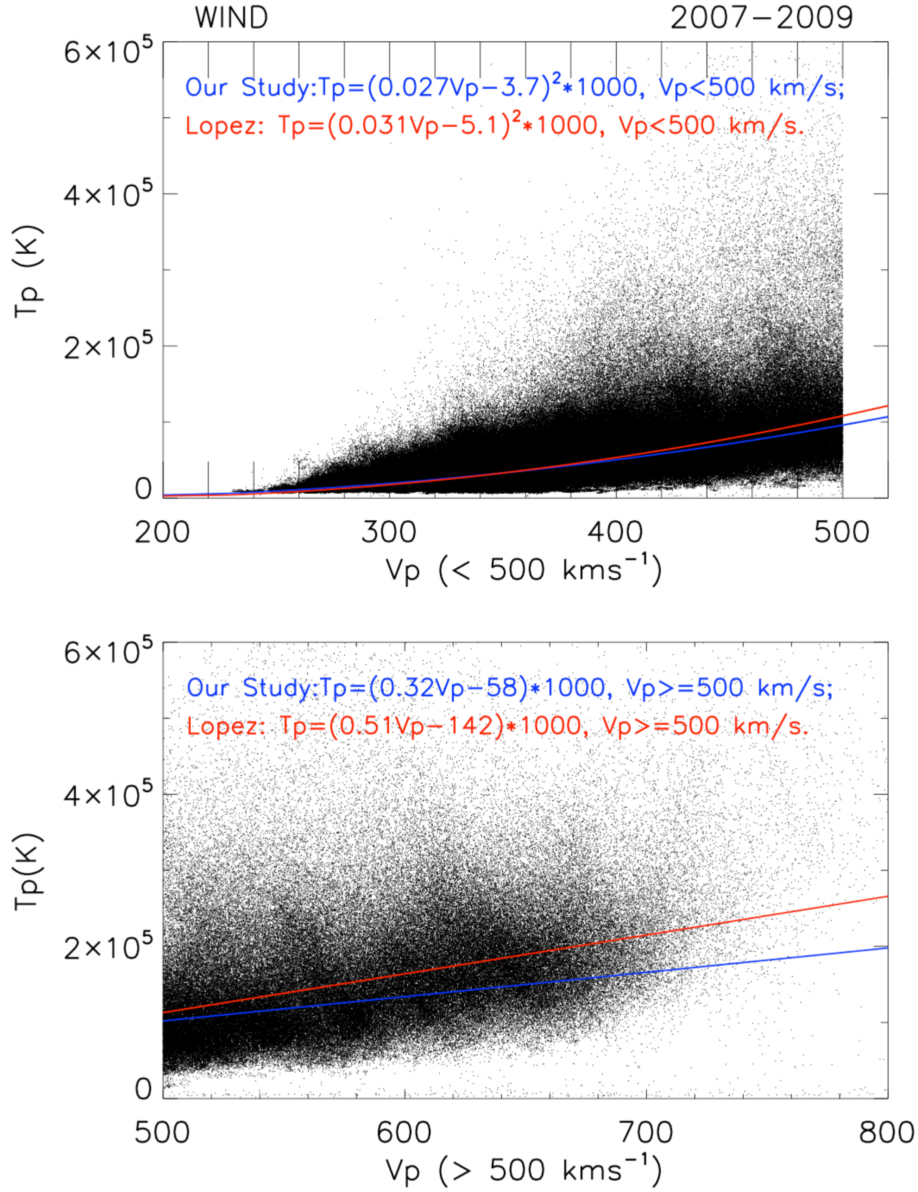

Figure 2-1: T_p versus solar wind speed V_p in 2007 - 2009 for slow (top) and fast winds. Our least - squares fit is shown in blue and the result derived by Lopez (1987) is in red.

interactions, can depart strongly from typical behavior when ICMEs pass Earth, because it implies enhanced magnetic forces acting on the sheath flow (Farrugia et al. [1995], Lavraud and Borovsky [2008]).

Table 2.1: Average values of key solar wind parameters in 2007-2009 observed by Wind and STA, STB.

2007-2009	Wind Ave	Wind Std-Dev	STA Ave	STA Std-Dev	STB Ave	STB Std-Dev
B (nT)	4.2	2.08	4.34	2.07	3.92	1.98
Proton β	0.95	1.64	0.90	5.94	1.12	1.06
M_A	11.8	6.25	10.7	6.63	11.1	3.33
N_p (cm^{-3})	5.9	4.67	5.58	4.99	4.66	2.16
V_p (km s^{-1})	419	108	410	107	407	20
T_p (K)	8 $\times 10^4$	7.6 $\times 10^4$	6.2 $\times 10^4$	9.8 $\times 10^3$	6.8 $\times 10^4$	2.0 $\times 10^3$
T_e/T_p	3.7	3.10	-	-	-	-

Table 2.2: The expected solar wind T_p as a function of V_p for 2007-2009: Our results and those of Lopez (1987)

2007-2009	V_p <500km s^{-1}		T_{exp}=(A1$\times V_p$+A2)$^2\times$1000		
	V_p $\geq$500km s^{-1}		T_{exp}=(B1$\times V_p$+B2)$\times$1000		
	A1	σ_{A1}	A2	σ_{A2}	χ^2_A
Our study	0.027	3.1$\times 10^{-7}$	-3.7	1.2$\times 10^{-4}$	13655.2
Lopez	0.031	-	-5.1	-	13982.4
	B1	σ_{B1}	B2	σ_{B2}	χ^2_B
Our study	0.32	1.3$\times 10^{-5}$	-58	7.4$\times 10^{-3}$	37498.5
Lopez	0.51	-	-142	-	43111.8

To illustrate our selection procedure, we look at a ST on April 10, 2007 (event No. 7) from Kilpua et al. [2009]'s list. Figure 2-2 shows, from top to bottom, N_p, T_p, V_p, the temperature ratio T_e/T_p, the total magnetic field strength, B, the latitude and longitude of the magnetic field (GSE coordinates), the β_p, M_A, and the pressures, P (black trace: total, red: magnetic, blue: proton, green: electron thermal pressure). The horizontal red traces in the various panels indicate the average value of the respective quantities in 2007-2009. The blue trace in panel 2 is the expected proton temperature for normal solar wind expansion as derived above.

The ST interval, lasting ~4.5 hrs, is bracketed by the vertical guidelines in Figure 2-2.

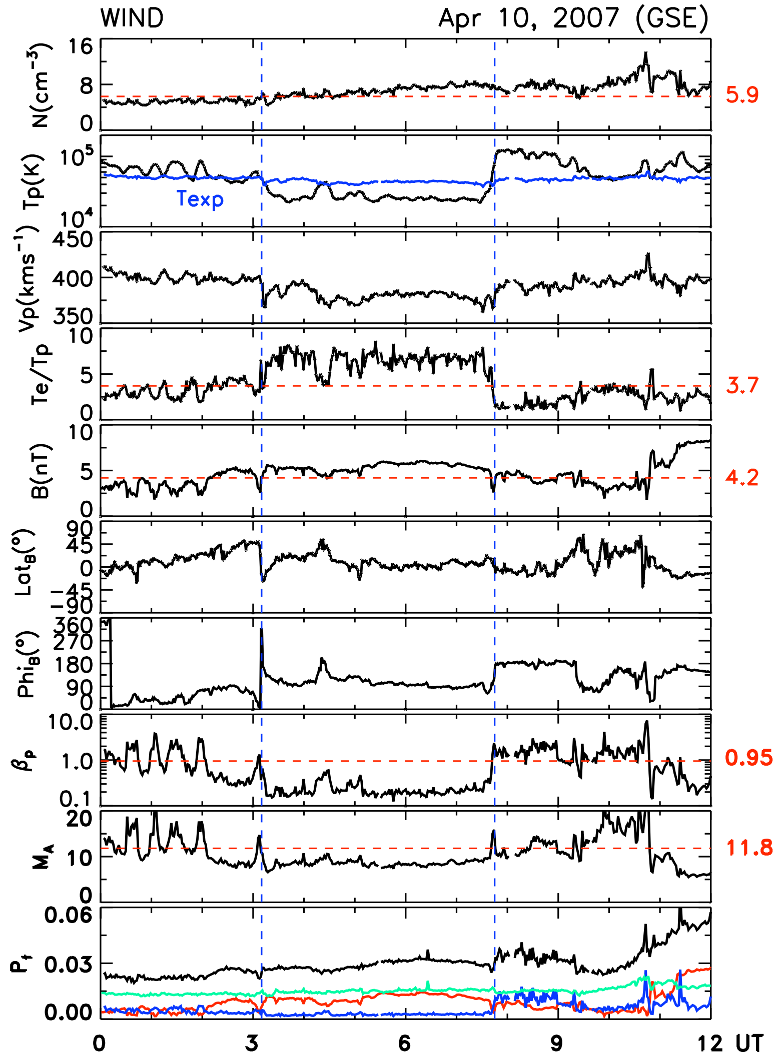

Figure 2-2: The ST on April 10, 2007, shown between vertical guidelines. For further details, see text.

From the second panel it is seen that the proton temperature T_p is well below the expected temperature. Indeed, this is the way this particular ST was identified in the original work. But there are other signatures satisfying our criteria for a ST: proton β_p is $<<$ 1 and the T_e/T_p temperature ratio clearly rose to well above average values (6.43 $\pm$ 1.13; mean and standard deviation). The total magnetic field strength was $\sim$5.3 nT $\pm$ 0.27 nT. At 1 AU 5.3 nT is not usually considered a strong solar wind field. However, the three-year average is 4.2

nT (red line). Similar arguments apply to M_A (last-but-one panel). Its average value in this ST is 8.7, while in the 2007-2009 solar wind the average value was 11.8 (Table 2.1), so it is lower than average. Except for the low T_p, which was chosen to be one of the most important criteria in Kilpua et al.'s work, there are four other properties which can distinguish this ST event from the ambient solar wind.

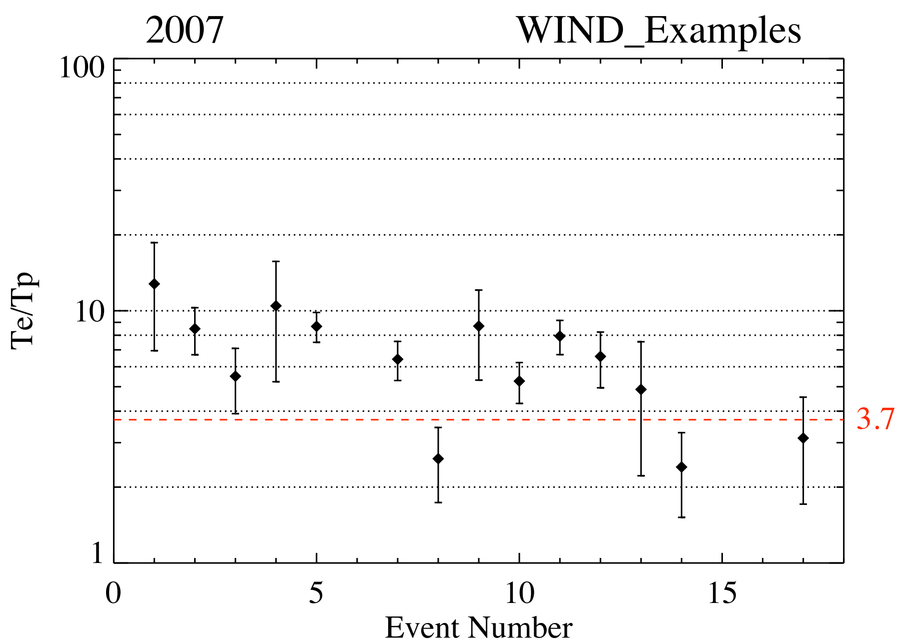

Figure 2-3: The statistical result of the temperature ratio T_e/T_p for the STs identified by Kilpua et al. (2009) from the Wind spacecraft. The dashed red line labeled 3.7 in the three - year average of quantity T_e/T_p

We now consider the total ensemble of 14 events seen at Wind during these two Carrington rotations. First we show results on the temperature ratio T_e/T_p (Figure 2-3), plotting the mean values and the standard deviations for each event. The red dashed line gives the three-year average. The range of values extends over [$\sim$2.5, $\sim$14]. It is evident that in many cases this temperature ratio exceeds the average value over 2007-2009. So this temperature ratio may be a good indicator of STs.

Figure 2-4 shows scatter plots of the results obtained for the parameters we consider. The three columns refer from left to right to Wind (14 STs), STA (10 STs), and STB (9 STs) observations, respectively. Plotted in rows from top to bottom are (i) the average field strength B, (ii) the average β_p, (iii) the average M_A, and (iv) the average T_p/T_{exp}. For the STs observed by STA and STB, we compare the proton temperature T_p with the average values. Standard deviations are shown by the vertical lines.

Wind: Concerning the average B in STs, we have values in the range [$\sim$3, $\sim$11] nT. So clearly this quantity, as noted also by Kilpua et al. [2009], is generally, but not always, above average values of the solar wind at 1 AU. When comparing with the three-year average of 4.2 nT (red dashed line), many STs (86%) have indeed higher average field strength. The average proton beta ($< \beta_p >$) in STs varies over a wide range and some have large standard deviations. However, it is clear that a $\beta_p < 1$ is a recurrent feature of these STs. The average M_A values lie in the range [4, 20]. Since the mean of the 2007-2009 measurements of this quantity is 11.8 $\pm$ 6.25 (Table 2.1; horizontal line), most STs (86%) have an average M_A which is lower than that in the solar wind in this three-year period. The average T_p/T_{exp} is with two exceptions below unity. While $T_p < T_{exp}$ for these STs, the difference is not that small. This point will be taken up again in the Discussion section.

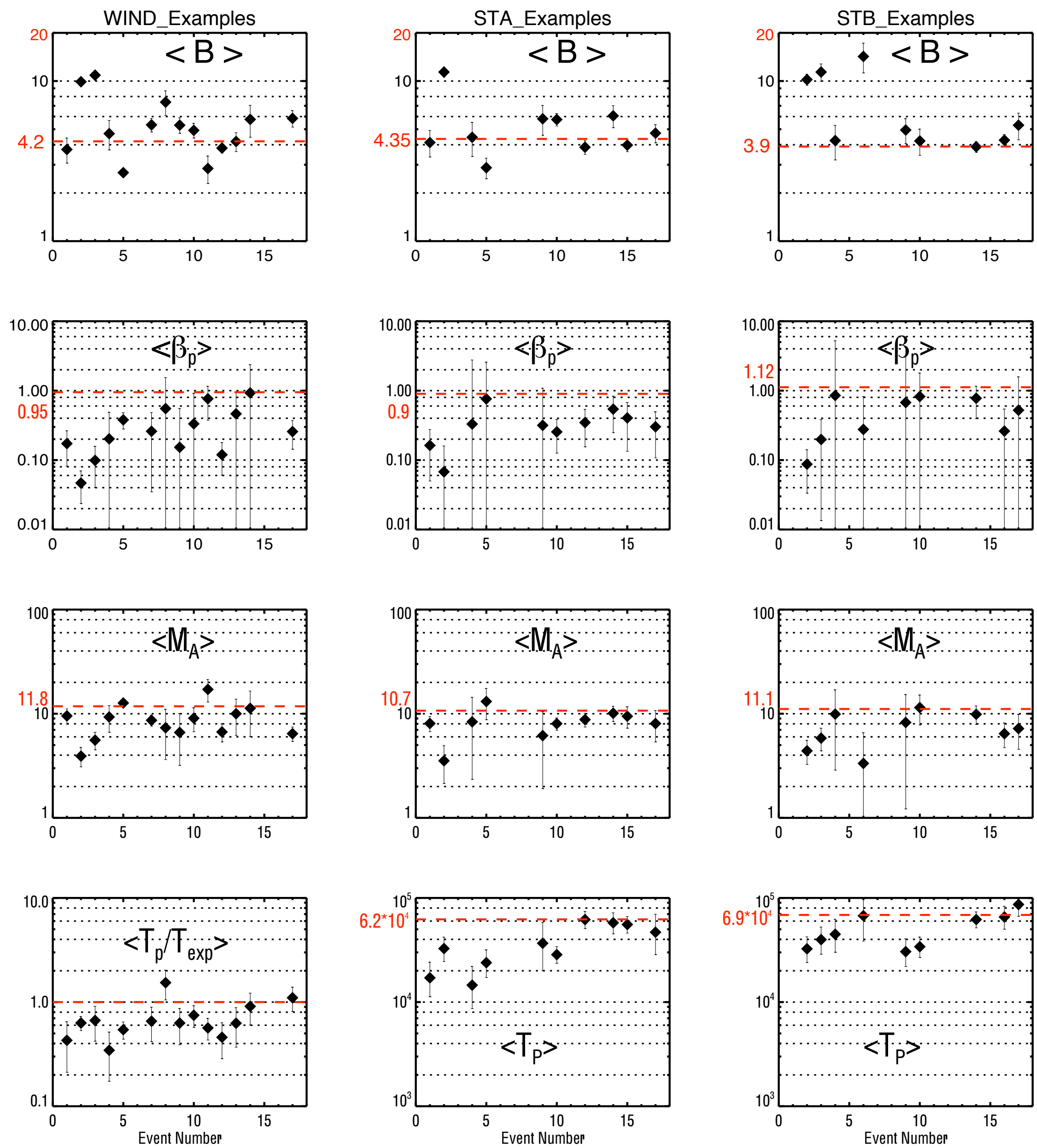

Figure 2-4: Statistical results on STs in March - April 2007: (i) average B, (ii) proton beta, β_p, (iii) Alfvén Mach number, M_A, (iv) T_p/T_{exp} as identified by Kilpua et al. (2009) from Wind, STA and STB. Note that we only plot T_p for data from STA and STB.

STA and STB: Similar trends are seen in the STA and STB examples. Most STs have a average magnetic field stronger than the average value. Quantity β_p <1 is also a reliable parameter in these examples. Most of the STs have mean M_A below the normal solar wind value. In the last panel we compare the proton temperature with the surroundings. We find that the average proton temperatures at STA and STB are 6.2 $\times 10^4$ K and 6.8 $\times 10^4$ K, respectively. In STA, all the events have $T_p <$ 6.2 $\times 10^4$ K, and most of them (8 out of 10) have $T_p >$ 2.4 $\times 10^4$ K. A similar result can be seen in STB, where almost all the STs (8/9) have T_p lower than its average value, and all T_p higher than 2.4 $\times 10^4$ K (thermal speed, v_{th} = 20 km s^{-1}). The above analysis motivated our choice of characteristics we shall use to identify STs, detailed in the Introduction.

2.3 Small Transient Events (STs)

In this section we present a number of case studies to illustrate the varieties of ST features and the ambient conditions they occur in.

2.3.1 Alfvénic Fluctuations

We start first with the kind of event we exclude. As pointed out by Marubashi et al. [2010] and Cartwright and Moldwin [2010], some solar wind Alfvénic structures can be mistaken for STs. For that reason we examined all events we identified to remove those which were evidently Alfvénic fluctuations. We give one example in Figure 2-5, which was observed by Wind on August 29, 2008. From top to bottom the panels show the proton density N_p, temperature T_p (in blue: the expected temperature for normal solar wind from the statistics discussed above); bulk speed, the T_e/T_p temperature ratio, the total field, the magnetic field vector in GSE Cartesian coordinates (B_x, B_y, B_z), and overlaid in red, the corresponding solar wind velocity components, β_p; M_A; and the total pressures (red: magnetic; blue and green: proton and electron thermal pressures, respectively; black: total).

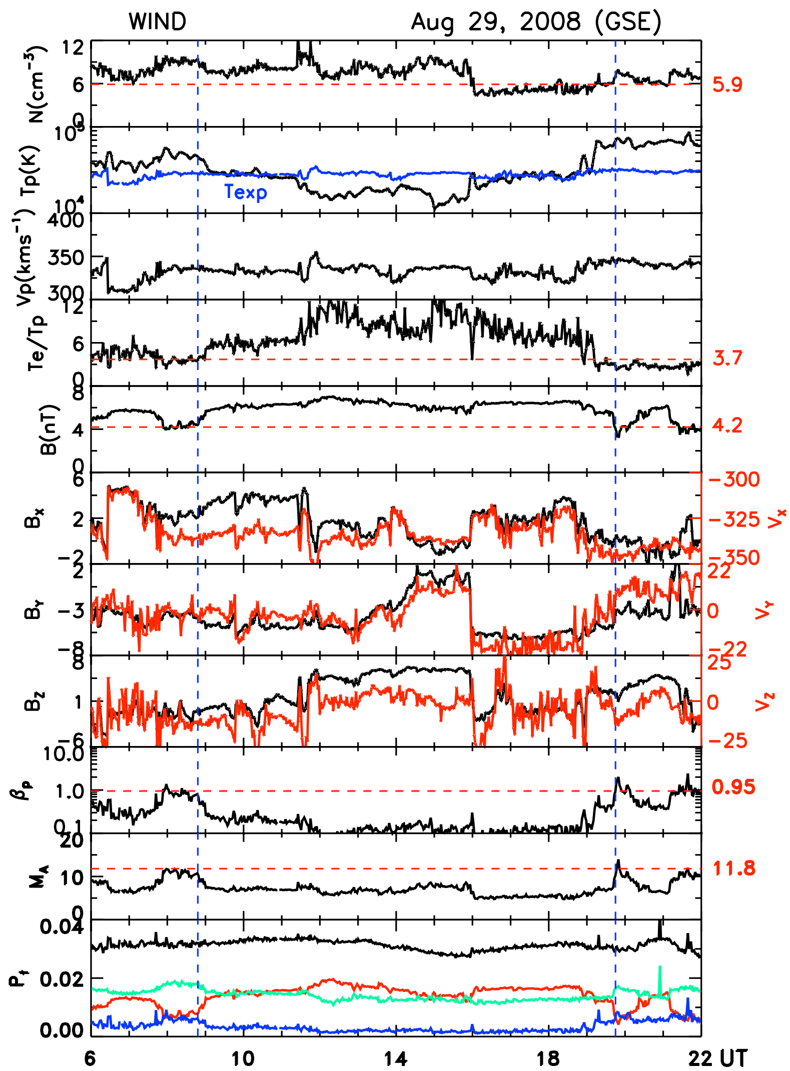

Figure 2-5: The Alfvénic event on August 29, 2008.

Part of the Alfvénic event is bracketed by two vertical guidelines and lasts from 08:48 - 19:45 UT. We find this event to have (i) decreased T_p, at least in the central part (~11:30 - 16:00 UT); (ii) enhanced T_e/T_p (> 3.7); (iii) stronger-than-average magnetic field strength;

(iv) low β_p ($\beta_p < 1$) and low M_A ($M_A < 11.8$). All these properties comply with our definition of STs. However, when we compare the components of the magnetic field and the velocity vectors (GSE coordinates; overlaid in red with scales on the right), we see a clear correlation between them. That means that the event is really an Alfvénic structure.

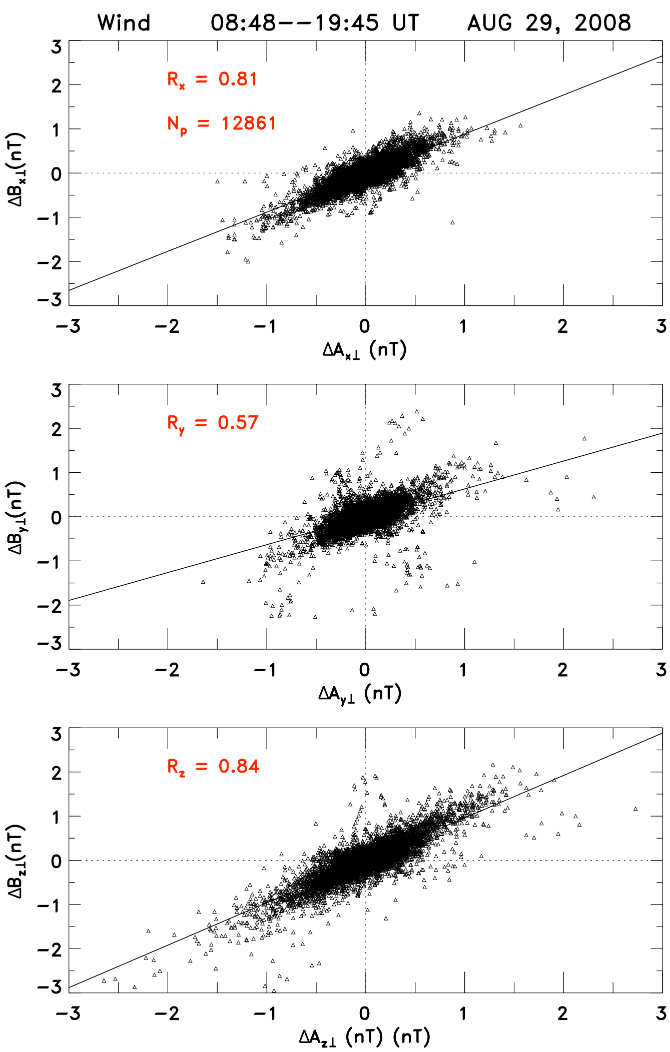

Figure 2-6: For the Alfvén event on August 29, 2008. For further details, see text.

We confirm this formally by comparing in Figure 2-6 the perturbations of the magnetic field perpendicular to the background field ($\Delta\mathbf{B}_\perp$) with the perturbations of the velocity perpendicular to the background magnetic field and modified by a function of the mass density ρ ($\Delta\mathbf{A}_\perp \equiv (\mu_0\rho)^{1/2}\Delta\mathbf{V}_\perp$). The background field is obtained from a seven-point running average of the magnetic field data. The regression lines are shown. With correlation coefficients of 0.8, 0.6, 0.8 (x, y, z), over 12861 data points, the correlation is good. These are thus Alfvén waves propagating against (positive gradient) the magnetic field. We carried out this procedure on all the events we initially identified. If the regression coefficients were larger than 0.5 for all three components, we classified them as Alfvénic events.

2.3.2 Event 1: December 27, 2007 from Wind

We now discuss six case studies to present what we think are representative features of the STs listed in this paper. The first event was observed by Wind on December 27, 2007. Figure 2-7 shows the plasma and magnetic field data. From top to bottom, the panels show the proton density, temperature T_p (in blue: the statistically expected value in 2007-2009), the proton bulk speed, the T_e/T_p temperature ratio, the total field and the latitude and longitude of the magnetic field vector in GSE coordinates, proton β_p, M_A, and the total pressures (black: total; red: magnetic; blue: proton; green: electron thermal pressure). The red horizontal lines indicate the three-year averages of the respective quantities (Table 2.1). The event is shown between the two vertical lines.

This is a very short-duration ST, lasting only 47 min. Features of this event are the low proton temperature ($< T_p > /T_{exp} = 0.65$), and the low proton β_p (~ 0.13). The average magnetic field strength ($< B >$=9.2 nT) is about twice the average value, and the average M_A (~6.0) is about one half of average (red line). The field variability is lower than in the surroundings. The T_e/T_p ratio, while it reaches above ambient values in the 12-hour interval shown, is just 1.03 times the three-year average. The event occurs within a stream -

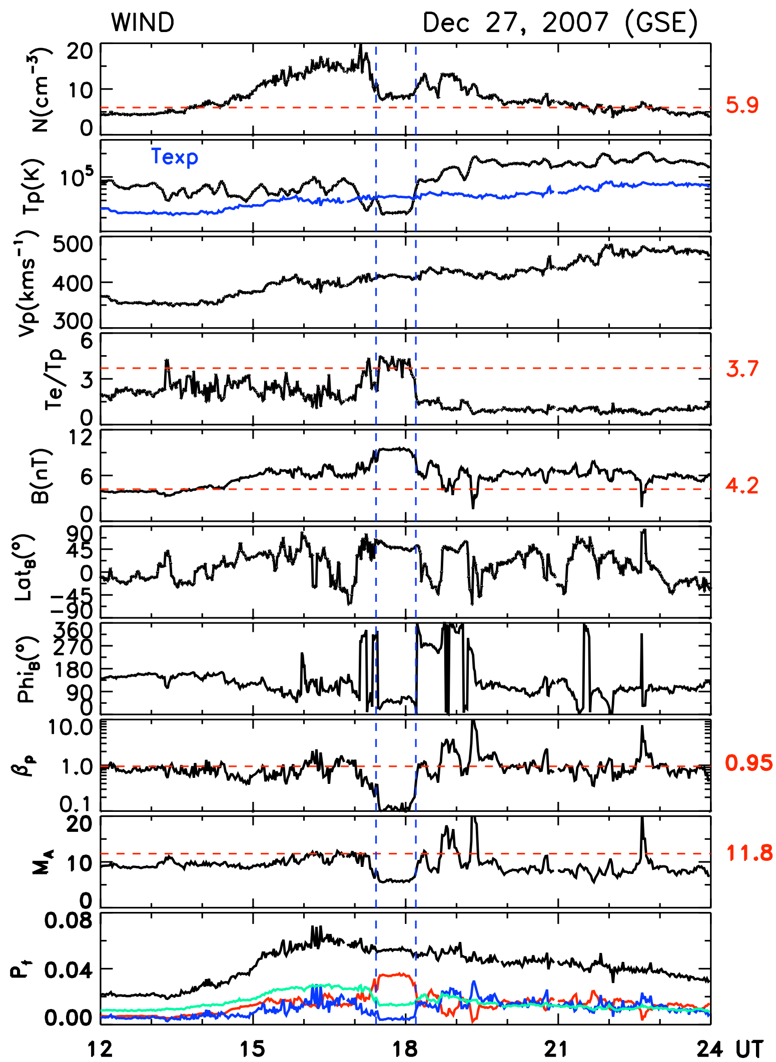

Figure 2-7: The ST on December 27, 2007 observed from Wind spacecraft, shown between vertical guidelines. From top to bottom: the proton density, temperature (in blue: the expected temperature in year 2007 - 2009), bulk speed, the T_e/T_p temperature ratio, the total field and its latitude and longitude in GSE coordinates, the β_p, the M_A and the pressures (black: total; red: magnetic; blue: proton; green: electron thermal pressure).

stream interaction region (positive gradient in V_p), but has a constant V_p, implying no radial expansion. The variations of the latitude and longitude of the magnetic field are small. It is in approximate pressure balance ($P_t = 0.053 \pm 0.001$ nPa). The event starts and ends with strong gradients in N_p, T_p, B and T_e/T_p, distinguishing it clearly from the ambient solar wind. Using the average speed of 413 km s^{-1} and the duration gives a rough estimate of the scale size in the Sun-Earth direction of 0.0078 AU (183 R_E, Earth radii).

2.3.3 Event 2: May 9, 2009 from Wind

Figure 2-8 shows the second case, which was observed on May 09, 2009. The data of this and the other four cases studies are shown in the same format as that of Figure 2-7. This ST is encountered in the time interval 03:24 to 04:48 UT (between vertical guidelines). The following properties may be seen: (i) the proton temperature, T_p/T_{exp} is 0.65, as in case 1; (ii) an average field strength which is higher the three-year average ($< B > = 5.4$ nT); (iii) low magnetic field variability; (iv) a low β_p ($\sim$0.16), and (iv) a lower M_A (6.2) than the surroundings, and about one half of its three-year average value (11.8).

The event occurs in a (borderline) fast solar wind. The decreasing trend in the flow profile indicates radial expansion, with a value for the expansion velocity of $\sim$ 15 km s^{-1}. (The expansion velocity is computed as $(V_f - V_r)/2$, where V_f (V_r) are the velocities of the front (rear) boundaries of the structure). As in event 1, there are sharp gradients in the parameters at both the front and rear boundaries, which appear to be discontinuities. The pressures reflect the increasing trends in the density and field strength. For this event, too, the T_e/T_p, while it is clearly enhanced compared to ambient values plotted in the figure and helps to distinguish it from them, does not exceed the three-year average (ratio = 3.5 $\pm$ 0.2 versus 3.7). As in the first event the proton density is depressed during the event. Its value (2.3$\pm$0.34 cm^{-3}) is lower than ambient, and it is also much lower than the average value (5.9 cm^{-3}) over these three years. This feature is similar to that of the first event.

This ST is only 1.4 hours long. Multiplying by an average speed of 486 km s^{-1} we obtain a scale size in the Sun-Earth direction of approximately 0.016 AU (2.45$\times 10^6$ km) (376 R_E).

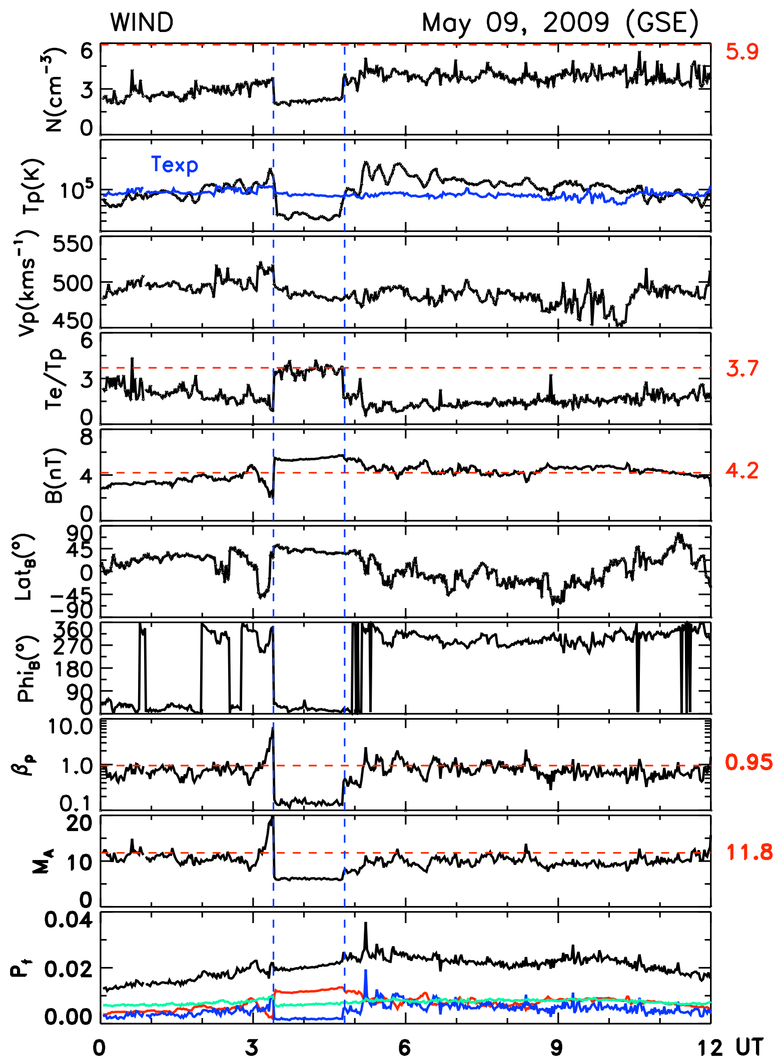

Figure 2-8: The ST on May 09, 2009 observed from Wind spacecraft. The format is the same as that of Figure 2-7.

At 5.44 ± 0.13 nT, the magnetic field B in this event is very steady. There is a decreased variability of the field compared to the surroundings. Since B is much steadier than its components, the (small) fluctuations are likely perpendicular to the background field. There is an interesting feature adjoining the front boundary of this small transient, namely, a strong double depression of the magnetic field, and a concomitant rise in M_A and β_p. This might be a signature of reconnection, but we do not discuss this further here.

2.3.4 Event 3: April 15, 2008 from Wind

In contrast to the previous two examples, the third ST observed on April 15, 2008 is a long event, lasting 11.3 hours. It lies in the slow wind (average 371 km s^{-1}). The properties of this event are (i) the proton temperature ($< T_p >=2\times10^4$K) is lower than the expected temperature, (ii) the T_e/T_p ratio is high, reaching a value of 16.4, well above the three-year average; (iii) the average magnetic field strength (6.5 nT) is higher than the three-year average (4.2 nT); (iv) the β_p is very low ($\sim$0.13 $\pm$ 0.06); and (v) low M_A ($\sim$7.02$\pm$1.29).

The smooth decrease of the proton velocity from 380 km s^{-1} to 350 km s^{-1} indicates a radial expansion speed of 15 km s^{-1}. The latitude of the magnetic field exhibits a large rotation ($\sim$70 deg), though it is not monotonic, and the longitude of the magnetic field rotates by $\sim$50 deg. Discontinuous changes in many field and plasma parameters are present, especially at the leading edge.

2.3.5 Event 4: December 03, 2008 from Wind

Another event is the one observed on December 3 - 4, 2008 (Figure 2-10). It is characterized by (i) a magnetic field strength ($\sim$8.91 $\pm$ 0.52 nT) which is about twice the three-year average; (iii) low magnetic field variance; (ii) low β_p (0.19); and (iii) low M_A (4.9). In this event, too, the proton density ($< N_p > = 4.5$ cm $^{-3}$) drops below ambient values. The T_p/T_{exp} fluctuates and is often above unity.

With an average bulk speed $\sim$447 km s^{-1}, and a duration of 3.58 hours, the scale size of this event at L1 point is about 0.039 AU (916 R_E). The event is embedded in a stream-stream interaction region (overall change in V is 35 km s^{-1}), as the solar wind flow changes from slow to fast.

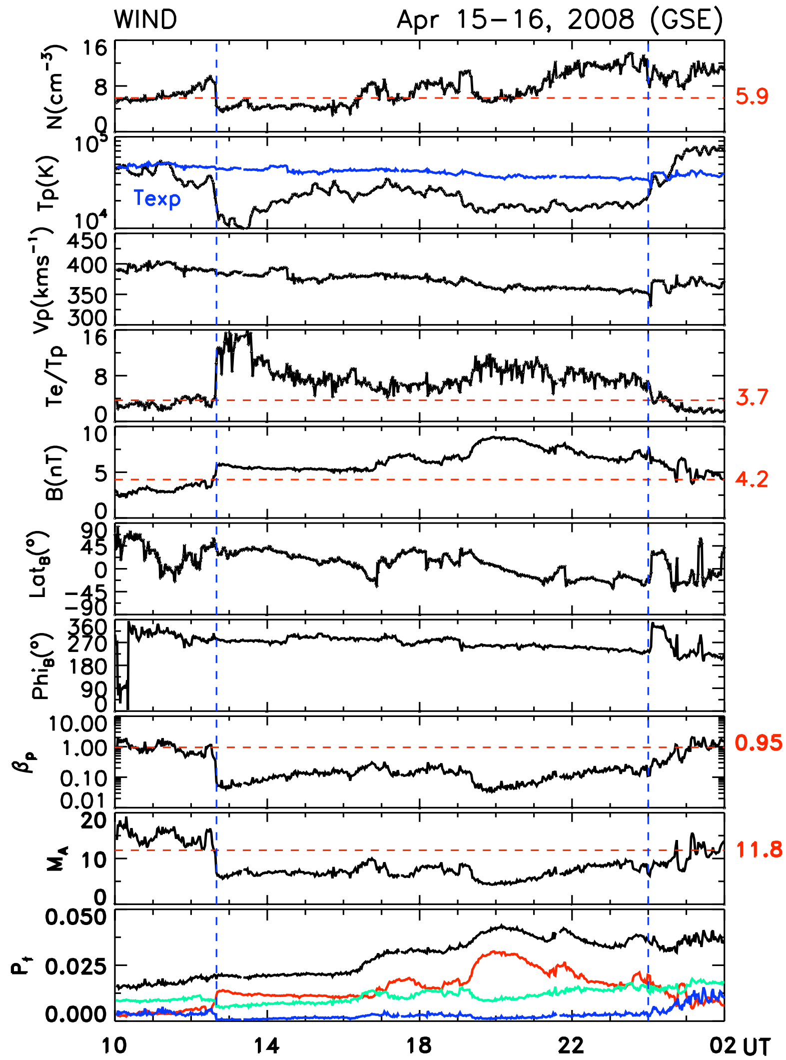

Figure 2-9: Case event 3 (April 15 - 16, 2008 observed from Wind spacecraft) with data plotted in a format similar to that of Figure 2-7.

In this event the leading speed ≤ trailing edge speed, which is indicative of radial contraction, probably the result of compression by the trailing, faster flow. Though the T_e/T_p does not generally exceed the three-year average, it has values forming a clear local enhancement. The latitude of the magnetic field changes smoothly by about 45°, while its longitude is very steady in this period. It may thus be considered as a small magnetic flux rope.

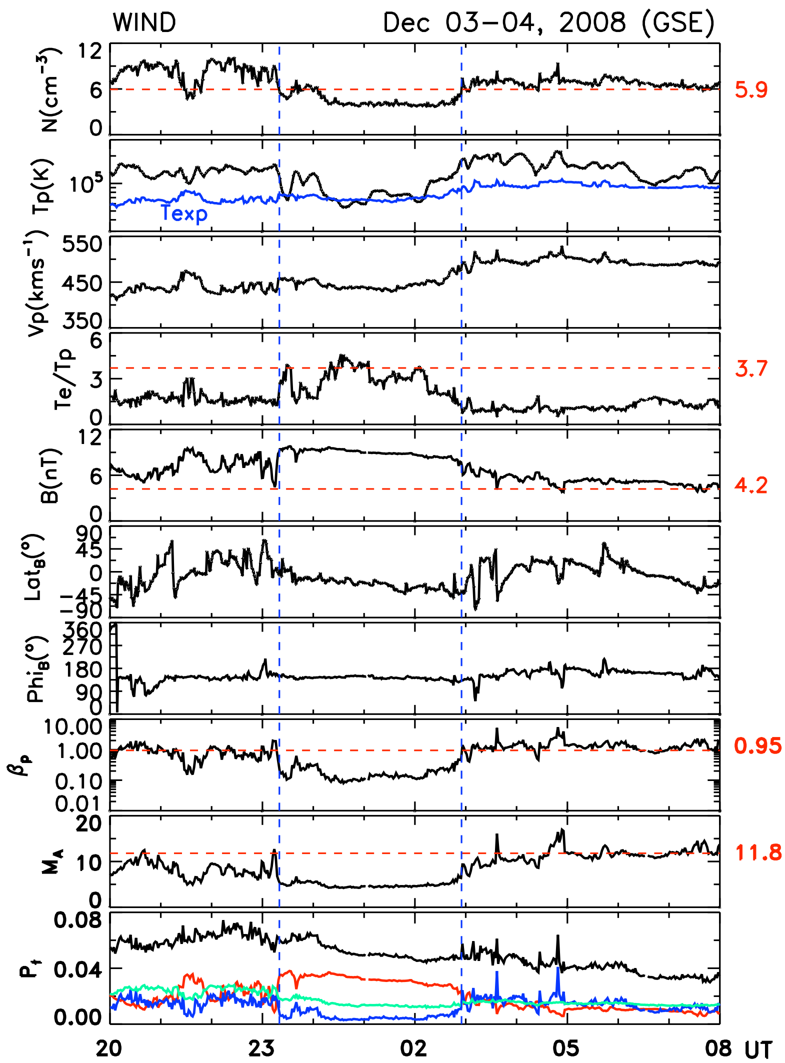

Figure 2-10: Case event 4 on December 03, 2008 observed from Wind spacecraft. Similar format as in Figure 2-7.

2.3.6 Event 5: May 18, 2008 from Wind

An example of a ST with clear magnetic flux rope features is the one observed on May 18, 2008 (Figure 2-11). Its duration is $\sim$ 2.67 hours. The magnetic field executes a large and coherent north - south rotation of 135 deg. The longitude remains relatively steady at 90°. The event occurs in the slow solar wind and is being convected with the surrounding flow. With a low proton beta ($<\beta_p>$=0.22), and a stronger-than-average magnetic field strength (5.5 vs 4.2 nT), it may be considered as a small magnetic cloud. Interestingly, however, the T_p/T_{exp} ratio fluctuates around unity as in the surrounding plasma. Further, T_e/T_p, while above the three-year average, is hardly distinguishable from the surroundings. A rough estimate of the diameter of the ST is $\sim$ 0.022 AU (517 R_E). Noteworthy are the pressure profiles, where it can be seen that the sum of the thermal pressures (electron + proton) is of the same order as the magnetic pressure. Thus it is not a priori clear that such a flux rope may be modeled as a force-free configuration.

2.3.7 Event 6: May 06, 2009 from STA

The last example was observed on May 6, 2009 from STA, data for which are shown in Figure 2-12. This ST was observed by STA on 6 May, 2009 from 04:40:00 to 06:30:00 during solar minimum activity. The duration of this event is about 1 hour 50 mins. The figure shows the total field strength (B), the field components in RTN coordinates (B_R, B_T, B_N), the proton bulk speed (V_p), density (N_p) and temperature (in red, the expected temperature, T_{exp}; in black is the proton temperature, T_p), the Alfvén Mach number (M_A), β (in black is the proton beta, β_p; in red, the plasma beta, β_{plasma} with alphas not included in its calculation), and the pressures (proton pressure in blue, magnetic pressure in red, the total pressure in black). To derive the electron contribution to the plasma pressure we use the result of Newbury et al. [1998], who gave an estimate for T_e based on data from the ISEE spacecraft. They obtained $T_e = 1.42 \times 10^5 K$. We use the same value for T_e and let $N_e = N_p$ when we calculate the β_{plasma}.

In this example, we could see that (a) the maximum B (6.84 nT) is high compared to the yearly average (4.09 nT). (b) Its temporal profile is symmetric, the value in the center being

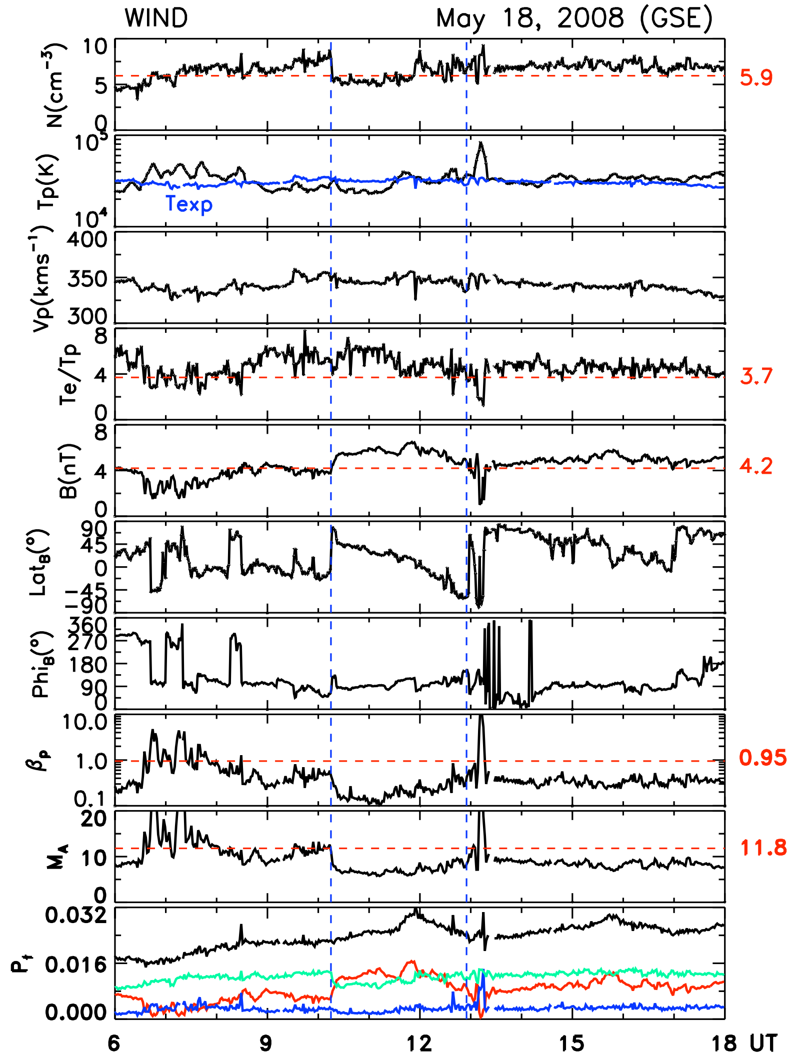

Figure 2-11: Case event 5 (May 18, 2008 observed from Wind spacecraft). Similar format as in Figure 2-7.

about twice that at the boundaries. (c) There are smooth and large rotations in the magnetic field components. The B_T component changes polarity from negative to positive. (d) V_p is very steady; the front-to-back gradient is just 1.1 km/s. The above properties identify it as a ST with a clear flux rope structure. The β_{plasma} exceeds unity near the boundaries and thus the magnetic configuration may not be force free. Force free modeling is not suitable for this ST.

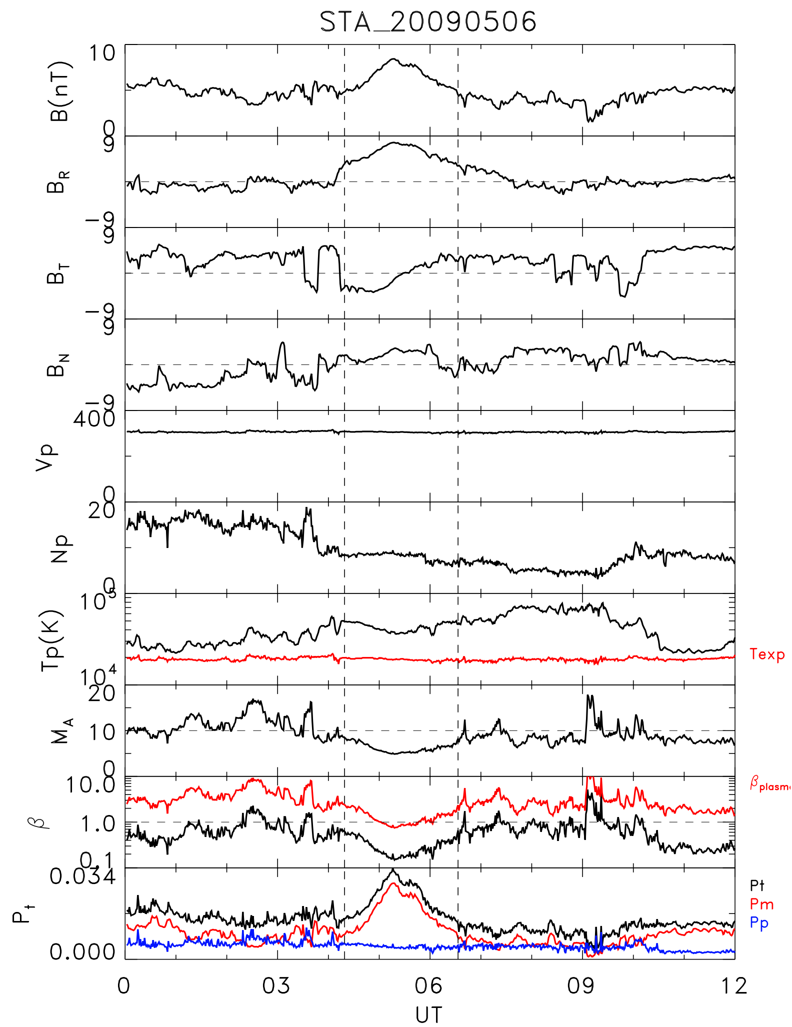

Figure 2-12: Case event 6: May 06, 2009 observed from STA spacecraft.

2.4 Statistical Survey

We now present statistical results from our survey, considering first the ST occurrence rate. Figure 2-13 shows a histogram of the number of STs per month observed by Wind as a function of time. In all we identified (by eye) 126 STs, with 33 STs in the year 2007, 40 STs in 2008 and 53 STs in 2009. On average we thus find 3.5 events/month. It appears that in 2009 the STs are more frequent. This may be due to the fact that in 2009 the slow solar wind occurred over a larger fraction of the time (89 %). The fraction of fast STs in year 2007 is much higher than in the other two years. The percentages of the slow solar wind in each year, and the percentages of the slow STs are listed in the Table 2.3.

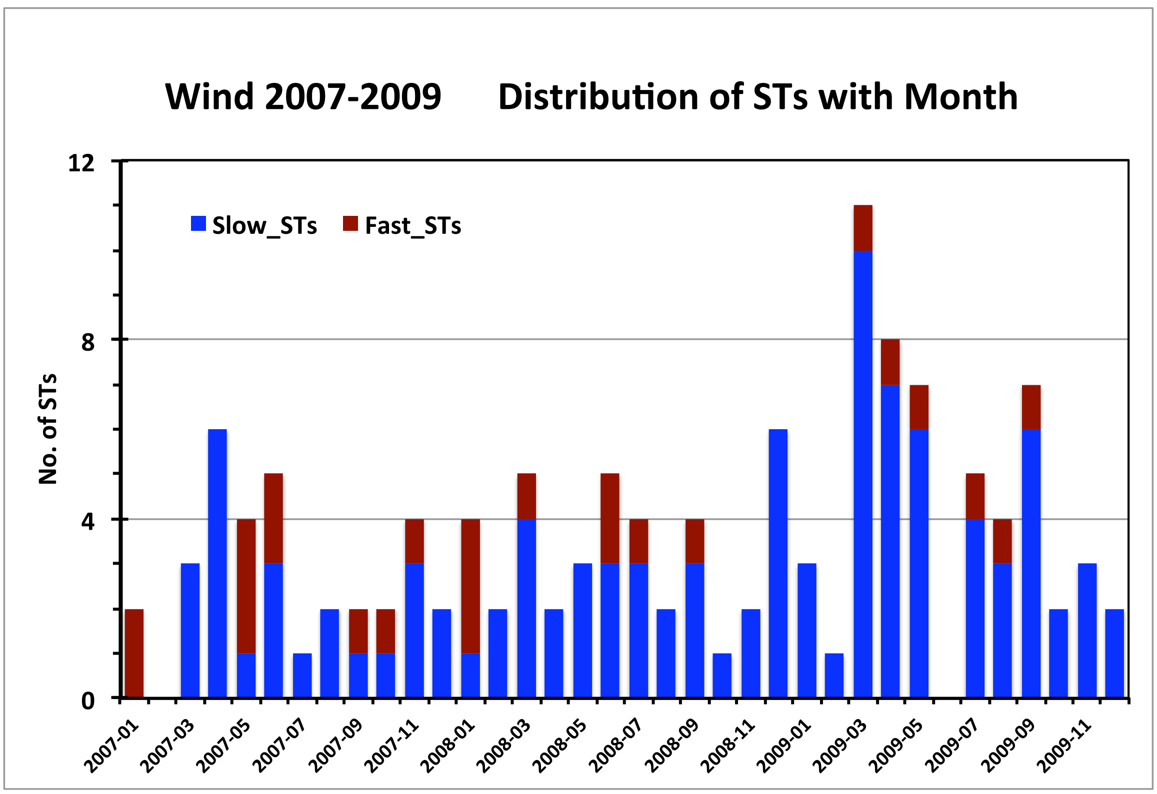

Figure 2-13: The distribution of number of STs per month observed by Wind in 2007 - 2009.

Figure 2-14 sorts these events by average speed. Most of the events have average bulk

Table 2.3: Distribution of STs in the slow solar wind.

Year	Percentage of Slow Solar Wind	Percentage of Slow ST
2007	60 %	70 %
2008	55 %	80 %
2009	89 %	87 %

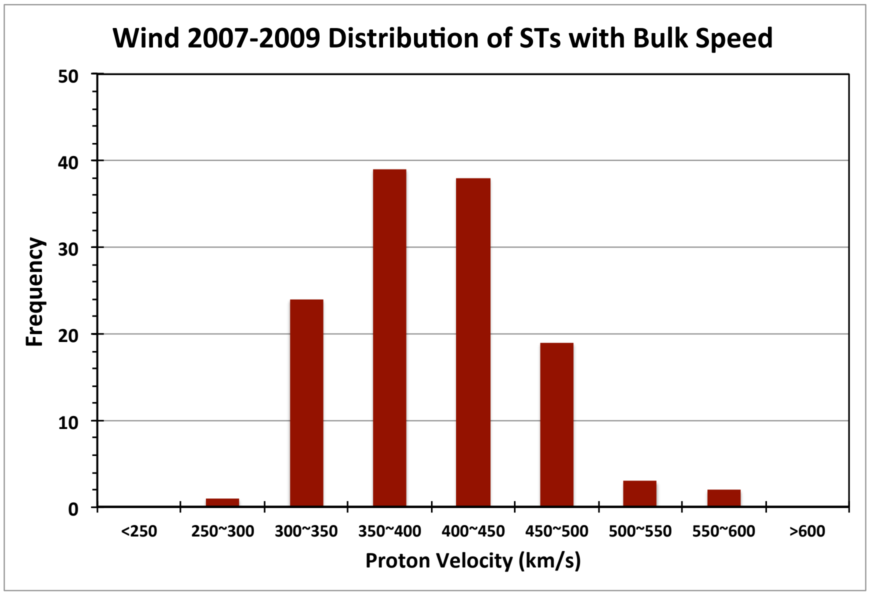

Figure 2-14: The proton velocity distribution of the observed STs.

speeds in the range [300, 500] km/s. Of the 126 STs, 102 STs (81 %) are in the slow solar wind (<450 km s^{-1}). The STs observed by STA in year 2009 also showed the similar distribution (90 % are in the slow solar wind, see Figure 3c in Yu et al. [2013]).

The distribution of the durations of STs from Wind spacecraft is shown in Figure 2-15. The most frequently observed ST duration lies between 1 and 4 hours. The average duration of the 126 STs is ∼4.3 hours, and 94 STs (75 %) last less than 6 hours. Of the 45 STs observed by STA in 2009, 36 STs (80 %) lasting less than 6 hours.

We now turn to the distribution of individual parameters (we now present the statistical results from the 126 STs observed by Wind spacecraft, while the STA's observations show the similar trends (see Figure 2 in Yu et al. [2013])). (i) Average magnetic field (Figure

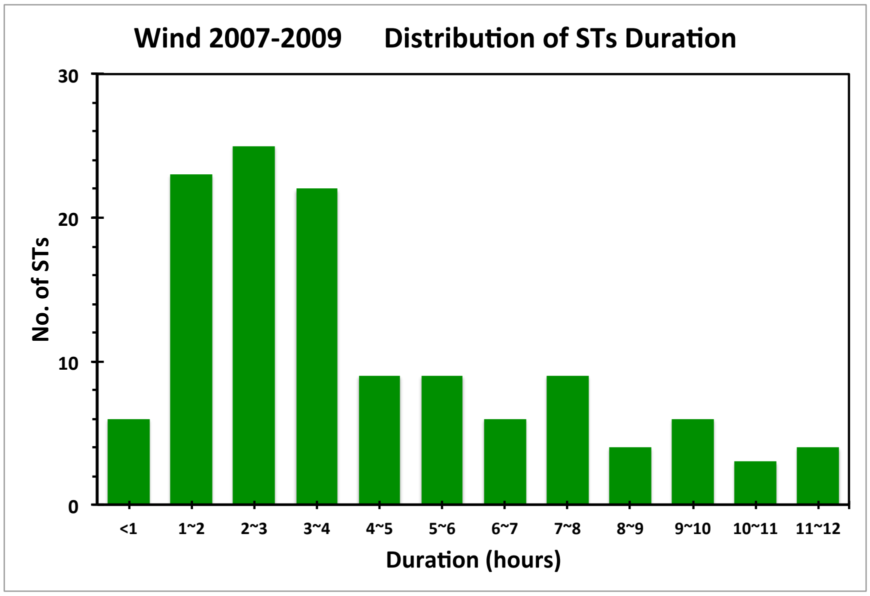

Figure 2-15: The distribution of ST duration.

2-16). In STs we find that this quantity lies in [4, 20 nT]. The ensemble average is ~7.8 nT ±3.0 nT, i.e., about twice the three-year average (4.2 nT). This conclusion can only be drawn if we compare with average properties of the solar wind in 2007-2009, as we do (see Introduction).

(ii) β_p. Figure 2-17 show average β_p per event and their standard deviations. All lie below the three-year value and are confined to the range [0.02, 0.7], albeit with large standard deviations. The ensemble average of β_p is 0.24, about four times smaller than the three-year average (0.95). Grouping by solar wind speed, the average β_p = 0.235 (slow) and 0.249 (fast), i.e., there is no significant difference between the slow and fast solar wind.

(iii) M_A. The averages of this quantity lie in [~2, 12]. The ensemble average $< M_A >$ is 6.3 (about one half of three-year average). In slow solar wind $< M_A >$ is 6.29 and in fast solar wind is 6.50.

(iv) T_e/T_p. Figure 2-19 shows that for almost all the STs, the temperature ratio $T_e/T_p >$

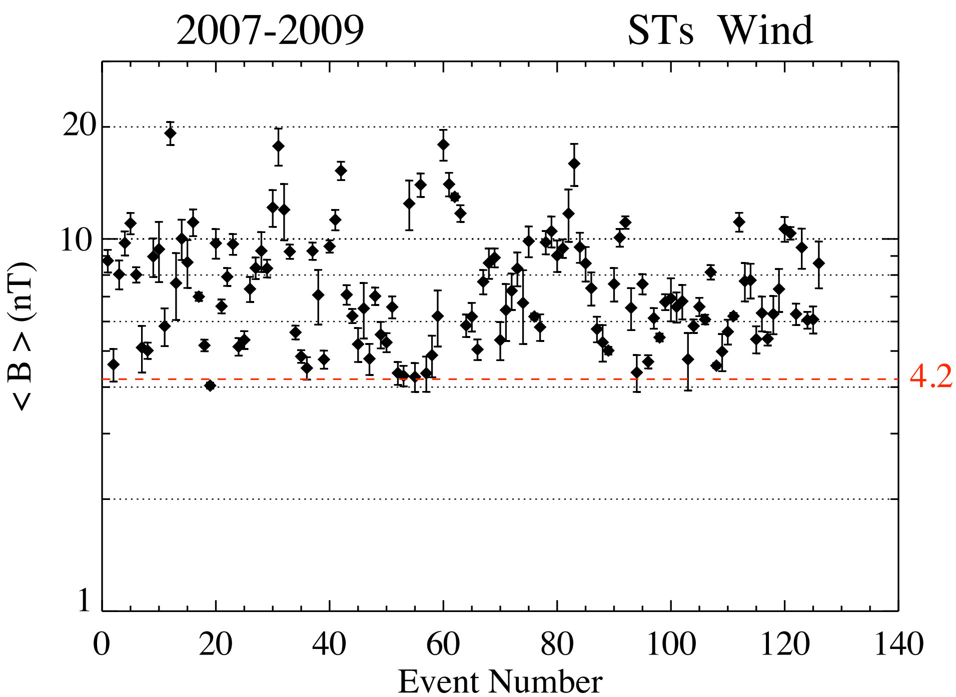

Figure 2-16: The statistical result of the average B in the 126 STs. The value 4.2 nT is the three - year average.

1, and lies in a band of [0.9, ∼20]. The ensemble average for all STs is 4.31. It is 4.64 and 3.02 for the slow and fast solar winds, respectively. The average temperature ratio in our study is only a little higher than the three-year value (3.7). The implications of (ii) and (iv) are discussed further in the last section.

(v) T_p/T_{exp}. The scatter plot of Figure 2-20 shows that this ratio straddles the three-year average. In (53%) of cases, this ratio is below, and in 47% it is above, unity. Thus, while $T_p << T_{exp}$ is often considered a very robust signature of the ICMEs (Gosling et al. [1973], Richardson and Cane [1995]), it is not a robust signature of STs. This point is considered further in the Discussion section.

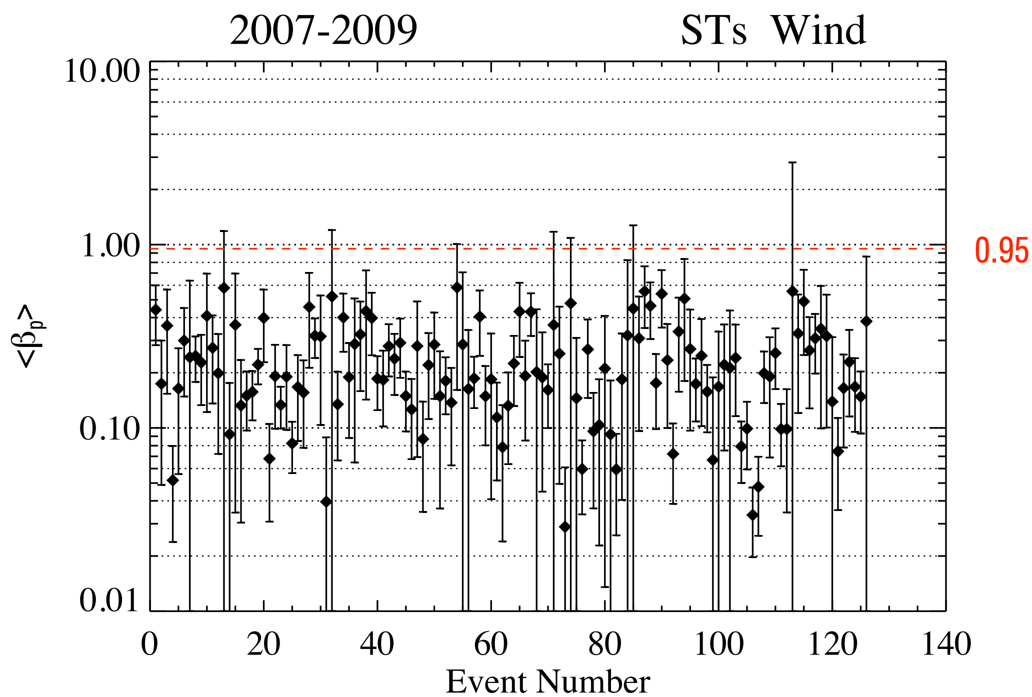

Figure 2-17: The statistical result of the average proton beta, β_p.

2.5 Results and Discussion

We have discussed properties and distributions of small solar wind transients (STs) during 2007-2009. They were monitored by the SWE and MFI instruments on Wind and PLASTIC and IMPACT instrument suites on STA. We elaborated a methodology of how to search for these events. We first extended the analysis of Kilpua et al. [2009] covering two consecutive Carrington rotations with the aim of including other parameters which may be of interest. Having identified these quantities, we arrived at a selection scheme for STs. This scheme included, but was not restricted to, magnetic flux ropes. After eliminating Alfvénic fluctuations, we found 126 examples of STs from Wind spacecraft, and 45 STs from STA spacecraft.

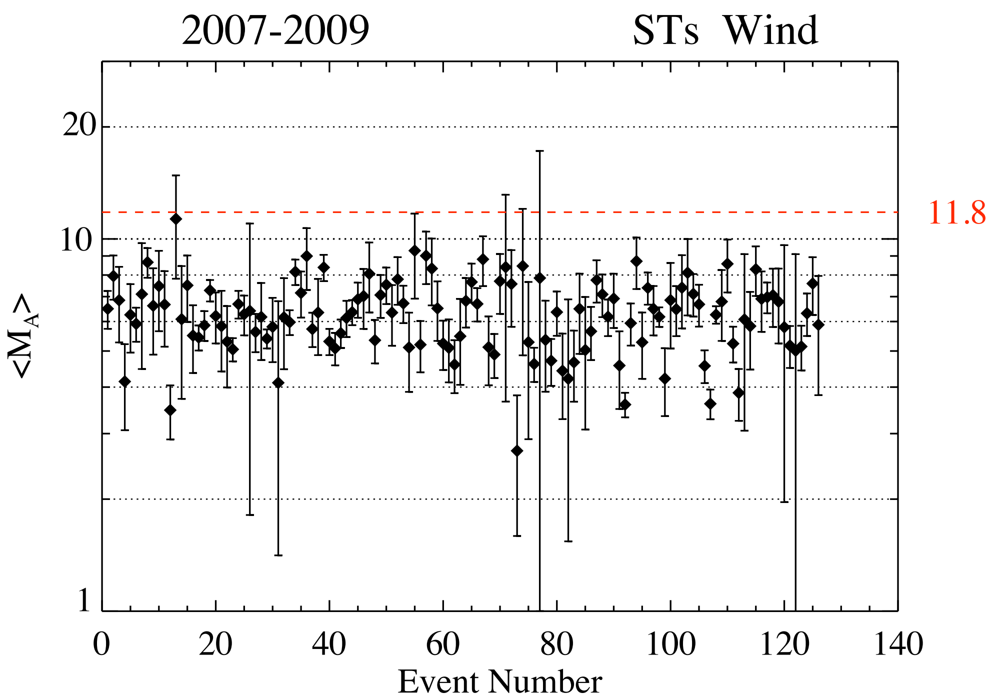

Figure 2-18: The statistical result of M_A.

They were of various durations, but mostly shorter than six hours. The majority was found in the slow solar wind and convecting with it. It was a major concern of our effort to compare ST properties with those of the background solar wind in these three years which, as has been pointed out in previous studies, had unusual properties, such as low magnetic field strengths and low proton densities.

Some caveats on the selection are in order. When searching by eye for these transients we sometimes had difficulty in locating their exact boundaries. When the boundaries were very unclear we did not include the event. Note also that by definition we excluded events which are shorter than 30 min. Thus the set of STs we arrived at is non-exclusive: it is

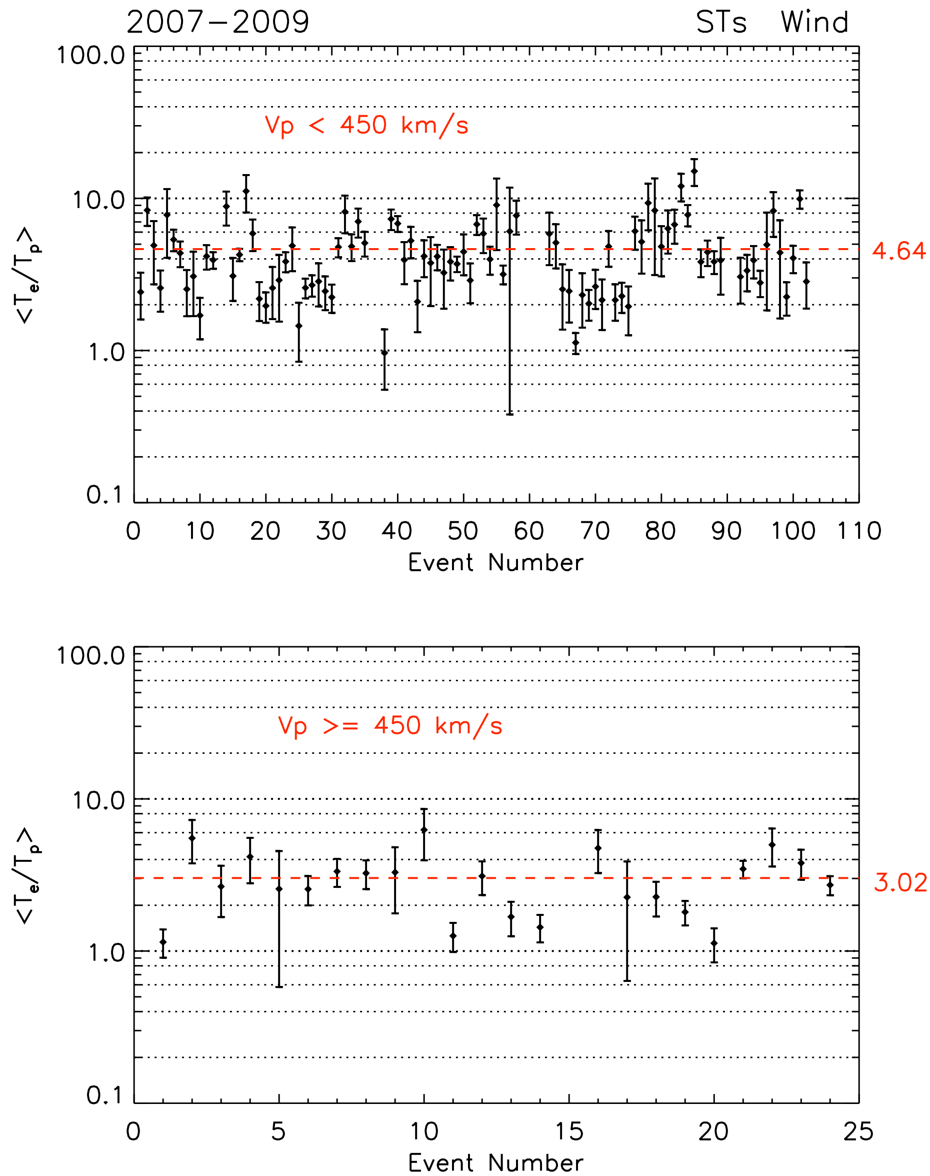

Figure 2-19: Statistical result for the temperature ratio T_e/T_p sorted by solar wind speed. Top panel: slow wind; bottom panel: fast wind. The red dashed lines are ensemble averages.

not being claimed that we found them all. Worth noting is also that identification of STs depends on the definition. We paid particular care to this, but other works may use similar

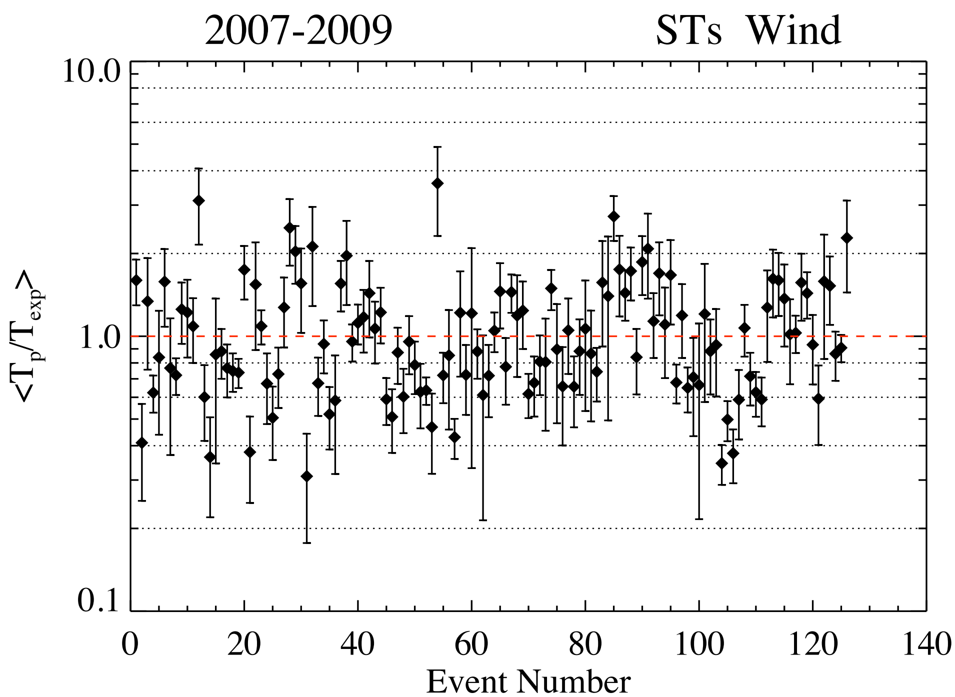

Figure 2-20: The statistical result for T_p/T_{exp}.

but not identical definitions.

Year 2009 was the last year of a long and pronounced solar activity minimum. In this year the solar wind in the inner heliosphere was for 90% of the time slow (< 450 km s^{-1}) and with a weaker magnetic field strength. We choose this year to present the results observed by both Wind and STA spacecraft. We observed 45 STs from STA in 2009 (Yu et al. [2013]), while we found 55 STs from Wind observation. The properties of the STs are similar at Wind and STA: higher magnetic field strength, lower proton beta and Alfvén Mach number. These STs observed in year 2009 tend to be predominantly shorter than 6 hours.

We now take a closer look at our results for the temperature ratio T_e/T_p. This is hardly ever discussed in connection with STs (but see Yu et al. [2013]). And yet it has been discussed in connection with large-scale ICMEs (see references in Introduction and below). Locally, T_e/T_p in STs is generally well above ambient values. Indeed, this ratio alone can often distinguish STs from their surroundings (see, for example, the case studies 2 and 4). However, overall it fluctuated around the three-year average of this ratio (Figure 2-19).

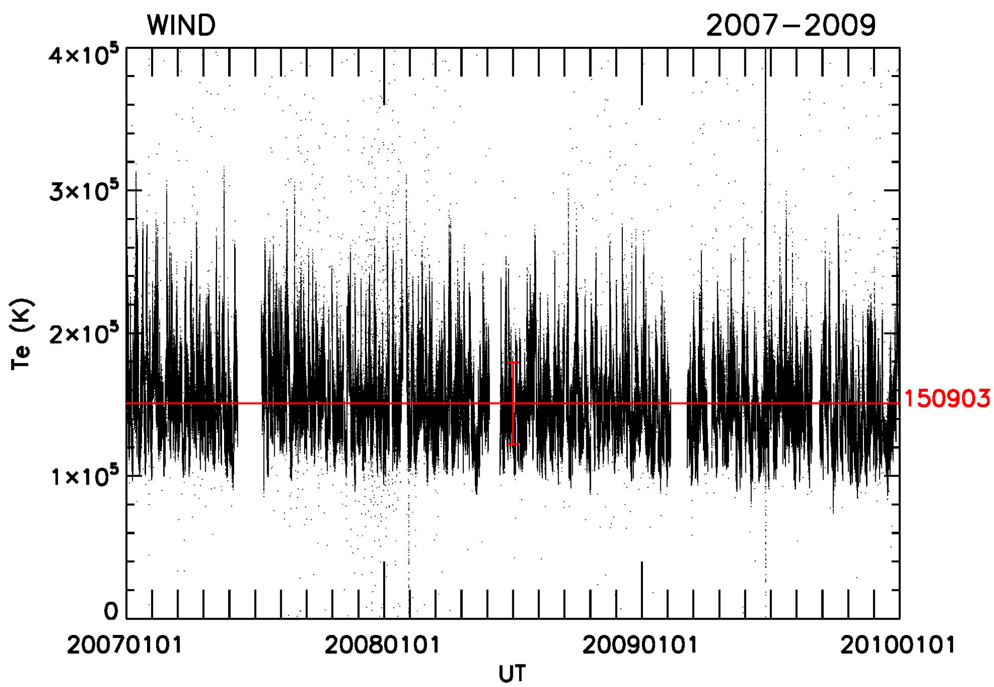

Figure 2-21: Temporal profile of the electron temperature T_e. In red, the mean value and its standard deviation.

For the normal solar wind, Newbury et al. [1998] gave a rule-of-thumb estimate for the value of T_e based on an analysis of ISEE data. They reached the conclusion that, irrespective of solar wind speed, a good estimate of T_e is $T_e = 1.42$ x 10^5 K. Figure 2-21 shows T_e for our three-year period. Its average value is 1.51×10^5 K, which is in very good agreement with

Newbury et al.'s result. This is remarkable seeing that Newbury et al.'s study covered 18 months when ISEE 3 was orbiting the L1 point during a phase approaching solar maximum of cycle 21. Below we shall compare the temperature ratio T_e/T_p in STs with that in ICMEs during the solar minimum 2007-2009.

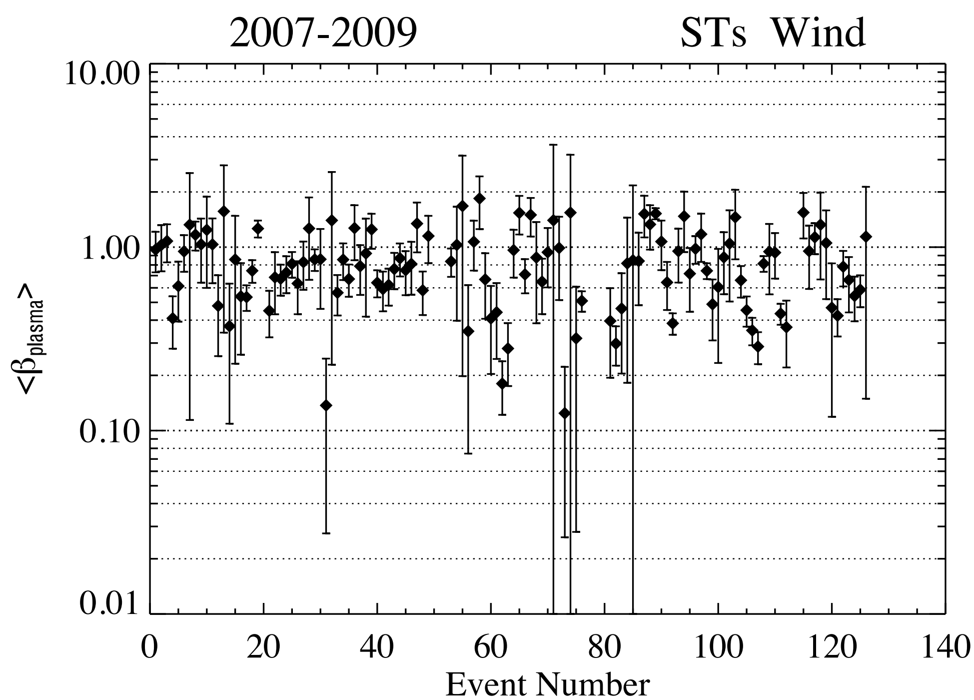

Figure 2-22: Statistics of the plasma β (electrons + protons) over the 126 STs. Values generally cluster around unity.

The local high value of T_e/T_p in STs has an important implication. It concerns force-free modeling of those STs which have the geometry of magnetic flux ropes, i.e. those which exhibit a large and coherent rotation of the magnetic field vector. When this temperature ratio is taken into account, the plasma β (electrons + protons + α particles, though we did not study the α's in this paper) will of course rise substantially. Figure 2-22 confirms this result over our assembly. At an average value of 0.85 ± 0.38, the plasma β is not small and thus the thermal pressure is comparable to the magnetic pressure. This means that force-free modeling for flux-rope STs might not be a suitable approach. Grad-Shafranov reconstruction and the elliptical model of Hidalgo et al. [2002b] could be more suited.

An interesting feature often seen in our STs were the sharp gradients at one or both boundaries. Sometimes these were abrupt enough to become discontinuities. The possibility of some of these being rotational discontinuities, implying reconnection with the ambient plasma, will be followed up in future work.

Table 2.4: Comparison of STs and ICMEs in 2007-2009.

2007-2009	STs	ICMEs
$< B >$	7.84±3.00	8.39±3.40
$< \beta_p >$	0.24±0.13	0.13±0.10
$< M_A >$	6.3±1.4	5.7±1.6
$< T_e/T_p >$	4.3±2.5	8.3±2.4
$< T_p/T_{exp} >$	1.10±0.56	0.67±0.28

Perhaps the most distinguishing feature of STs is that, generally, they do not expand but convect with the solar wind. This eliminates adiabatic cooling and yields a T_p distribution which straddles the expected T_p value (see Figure 2-20). (See below when we compare with the properties of ICMEs in this period.) It will emerge that while a low T_p has been universally considered as a very robust signature of ICMEs, it is not a robust signature of STs.

The convection with the solar wind and the general occurrence of STs in the slow wind lends support to the idea that many STs represent the plasma blobs which Sheeley Jr. et al. [1999] discovered to be emanating steadily from streamer cusps. And blobs tracked directly in the Imagers are the most direct way of associating STs with streamer transients (e.g. Rouillard et al. [2011]). See Kilpua et al. [2012] for an in-depth investigation of this issue.

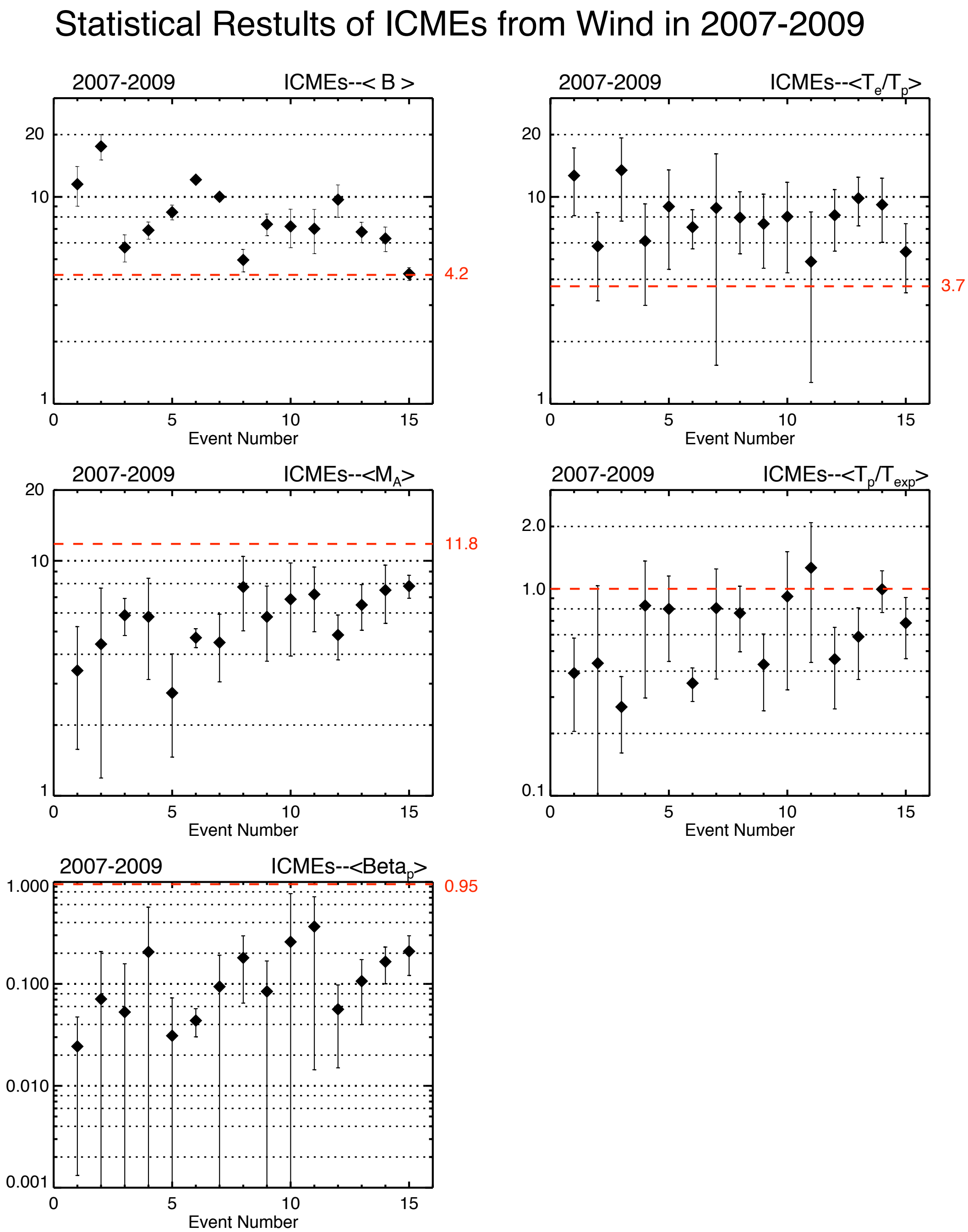

Figure 2-23: Statistical results for the ICMEs observed by Wind in 2007 - 2009 from the classification of Richardson and Cane (2010).

We now compare our results for STs with the properties of ICMEs in this same period. We use for the latter the compilation of Richardson and Cane [2010], who tabulated 15 ICMEs. Summary results are collected in Figure 2-23. Proceeding by column, this shows the average (i) B, (ii) M_A, (iii) β_p, (iv) T_e/T_p and (v) T_p/T_{exp}. Comparing with the corresponding plots for STs, it may be seen that (i) B is similar in STs and (ii) so is M_A. By contrast, (iii) β_p is lower and (iv) T_p/T_{exp} is lower (0.67 in ICMEs versus 1.1 in STs, Table 2.4) and perhaps in part as a consequence of this, (v) average T_e/T_p is higher (∼8.3) in ICMEs. Values of T_e/T_p ∼10 were also obtained in various studies on ICMEs/MCs. The strength of the resulting ion acoustic wave emissions can be seen very trenchantly in an example from Ulysses where $T_e/T_p \approx 20$ (Osherovich et al. [1999], see their Figure 4 panels b and c). In summary, it seems that the major difference between in situ observations of ICMEs and STs is the proton temperature, and its effects on other derived parameters. It is lower than T_{exp} in ICMEs but of the same order in STs.

As a last item, we consider in Figure 2-24 the distribution of the expansion velocity, V_{exp} for STs (blue) and ICMEs (red). Some STs have negative V_{exp}, implying compression. This might reflect the fact that, if encountered in SIRs, they are often compressed by the trailing faster stream. The mean and standard deviations are as follows: V_{exp}^{ST} = -3.8 ± 15.2 km s^{-1} and V_{exp}^{ICME} = 9.9 ± 17.1 km s^{-1}. Thus during the three-year minimum, the expansion speeds are not large, though the average V_{exp} for STs are significantly smaller. If we take only positive values in Figure 2-24 we obtain 17.3 km/s for ICMEs and 8.0 km/s for STs.

Recall that with only 15 ICMEs, the statistics are not so robust. So we depart from practice and consider a larger ICME data set, one that encompasses 14 years and all solar activity levels taken from Richardson and Cane [2010]. For the V_{exp} of ICMEs they find 31 km/s and 42 km/s with, and without, negative values included. (Other authors quoted in Richardson and Cane find even higher values). It seems that indeed ICMEs expand considerably more than STs. Currently this is only based on a limited data set, but we intend to extend to a larger data set in the next chapter.

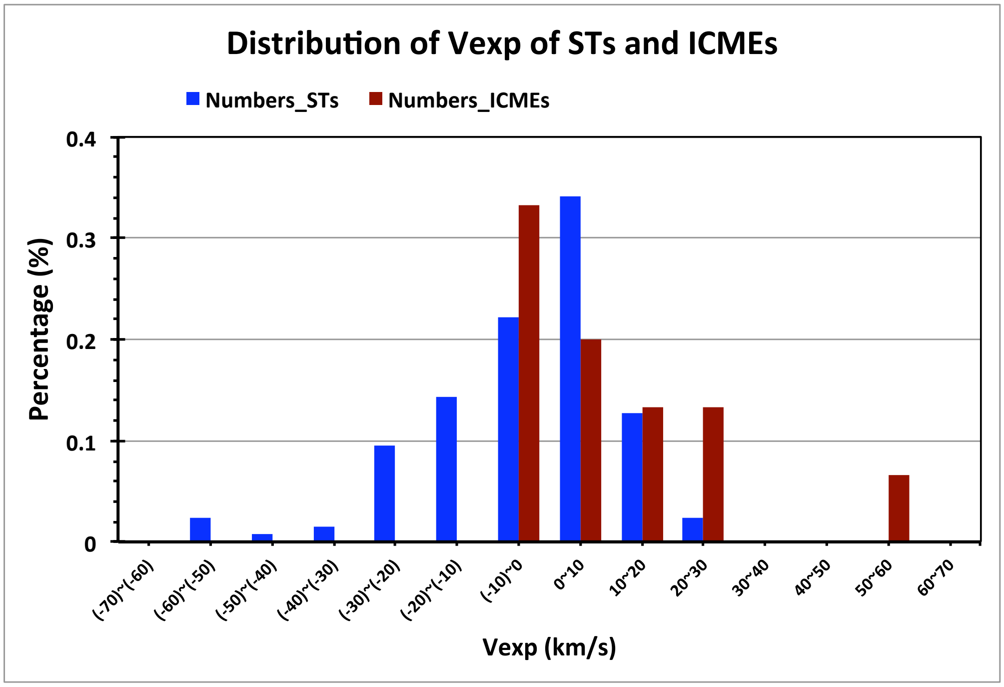

Figure 2-24: Normalized distribution of the expansion velocity for STs (in blue: 126 cases) and ICMEs (in red: 15 cases).

Chapter 3

Small Solar Wind Transients at 1 AU: STEREO Observations (2007-2014) and Comparison with Near-Earth Wind Results (1995 - 2014)

This chapter discusses small solar wind transients (STs) from 1995 to 2014. Using STEREO data, we have more sites from which to study STs near 1 AU. STEREO measurements are compared with Wind observations near the Sun-Earth line. We examined statistically the dependence of ST occurrence frequency on (i) solar cycle phase, as monitored by the sunspot number (SSN), and (ii) solar wind speed. We find dependencies on both: an anti-correlation with SSN, an opposite trend to that of ICMEs, and correlation with slow solar wind (over 80 % in the slow wind). We compare ST distributions during solar maximum year 2003, which had the lowest percentage of slow wind, and minimum year 2009, which had the highest percentage thereof, and show evidence of both dependencies. We give a statistical overview of ST parameters: field strength, B, Alfvén Mach number, M_A, and proton beta, β_p. They show the same temporal trends as the ambient solar wind, but have twice (B) or one half (M_A, β_p) of its average values. In STs, the proton temperature is not below the temperature expected from corotating solar wind expansion. Non-force free models should be used in solar minimum years where $\beta_{plasma} \approx 1$, while the force free models could be used in solar maximum when $\beta_{plasma} << 1$. We find that only ~ 5 % of STs show enhanced values of iron charge states. Our work further supports the 2-source origin of STs, i.e., the solar corona and the interplanetary medium.

3.1 Introduction

In former chapter, we studied the STs observed by Wind spacecraft from the year 2007 to 2009, and by STA spacecraft in the year 2009. The STs showed the tendency to occur in the slow solar wind (∼81% lie in the slow solar wind). The speed of the ambient solar wind may be an important factor in ST occurrence frequency. An aspect of this emerges from the work of Sheeley Jr. et al. [1997] and Wang et al. [2000], who suggested that the streamer cusps, which are one major source location of the slow wind, often contain small flux ropes convecting with the surrounding solar wind. According to these authors, these small flux ropes form an integral constituent of the slow solar wind. Also, Feng et al. [2008] found that the speed of many of the flux ropes was in the range 300-500 km/s, although they insisted that these small flux ropes were similar to small magnetic clouds and, like them, produced near the Sun. Since a high percentage of STs were in the slow solar wind during these solar minimum years. Do STs also occur preferably in the slow solar wind during the entire solar cycle?

In our previous work we investigated 126 STs observed by the Wind spacecraft in the years 2007 to 2009 Yu et al. [2014] and 45 STs from STA spacecraft Yu et al. [2013] during the year 2009. All events were identified by eye. The high occurrence frequency during these solar minimum years prompted the questions whether the occurrence frequency depends on the solar cycle, and how STs are created.

In this chapter, we have a much more extensive database from observations at three different spacecraft – STEREO-A (STA), STEREO-B (STB), and Wind – situated at different azimuthal locations around 1 AU. The period we survey is from 1995 to 2014, which covers almost 2 solar cycles (numbers 23 and 24). The STEREO probes make measurements near 1 AU but at different azimuthal angles from the Sun-Earth line, separating themselves by 22.5 deg/year, while Wind makes measurements near the Sun-Earth line. From April 2011 onward the STEREO probes were on the far side of the Sun, reaching superior conjunction in March 2015. This allows us to obtain as broad a view as currently possible of the distribution and properties of these small transients near 1 AU. (The lists of the identified STs are given in the Appendix-A, Appendix-B and Appendix-C.)

The database comprises over a thousand STs. Further, we do not restrict ourselves to flux ropes. We aim at understanding the dependence of ST occurrence frequency on (i) the solar cycle phase and (ii) solar wind speed. In addition, we give statistical results on the average properties of STs, and their radial expansion. Finally, we examined if STs have any of the compositional signatures generally found in ICMEs, specifically high iron charge states.

The layout of this chapter is as follows. We first describe our automated identification method. Quantity T_{exp}, which we need in our definition (see below), is derived from first principles, using the same functional forms found by Lopez and Freeman [1986]; Lopez [1987]. We then present statistical results of ST properties, comparing their values with the yearly averages. We give the distributions of duration of STs at STA, STB and Wind. We also discuss the expansion parameter and relate it to the non-dimensional expansion factor for MCs introduced by Démoulin. We then address the dependence of ST occurrence on solar cycle phase, while their dependence on solar wind speed is addressed in the following section. Furthermore, a study on the iron charge states has been done on the STs from STA. Finally, we examine the ICME-like STs in our list, and compare their occurrence frequency and expansion property with the above results. We finish with a summary and discussion.

3.2 Methodology

In our work, we use data from the STEREO IMPACT Luhmann et al. [2008] and PLASTIC Galvin et al. [2008] instrument suites at 1 min resolution for the years 2007 - 2014. We also use Wind key parameter data for the time period 1995 to 2014 acquired by the Magnetic Fields Investigation (MFI) Lepping et al. [1995] and Solar Wind Experiment (SWE) Ogilvie et al. [1995]. The magnetic field and proton data are at 1 min and 92 s time resolutions, respectively. The electron data are also obtained from the SWE instrument, and they have a resolution of 6-12 s before May 2001, and 9 s after August 2002.

We apply a numerical algorithm to search for structures satisfying the following criteria: (i) Duration between [0.5, 12] hours. (ii) Magnetic field strength (B) which is higher than the yearly average. To nail down what we mean by "higher" we specifically take a factor of 1.3 times the yearly average B. (iii) Low proton beta (β_p less than 0.7 times yearly average) or low proton temperature, where by "low" we mean T_p/T_{exp} less than 0.7. T_{exp} is the expected proton temperature for solar wind expansion which we derive for each year. The factors 0.7 and 1.3 are, of course, arbitrary but meant to quantify 'larger than' and 'smaller than'. (iv) Low Alfvén Mach Number (M_A less than 0.7 yearly average), i.e. magnetically-dominated structures, or large rotations of magnetic field components. The latter criterion implies flux rope structures. More systematically, we identify flux rope STs by the use of a minimum variance analysis on the magnetic field Sonnerup and Cahill Jr. [1967]; Sonnerup and Scheible [1998] (which we calculate the eigenvalues of the three magnetic field components, the maximum, medium and minimum eigenvalues are related to the maximum, medium and minimum variance directions. For the flux-rope type structures, where the axis of the flux rope is associated with the medium direction, usually have ratio of the medium and minimum eigenvalues large). We require that the intermediate-to-minimum eigenvalue ratio be greater than 5, so that an invariant axis is reliably determined (part of the automated selection code is shown in the Appendix F).

We now address the issue about how to determine T_{exp} for the solar wind. T_{exp} emerges from a correlation that exists between T_p and V_p in the expanding solar wind from the hot solar corona (see e.g. Démoulin [2009]). For each year and for each spacecraft we obtain the scatter plot of T_p vs. V_p after removing the ICMEs using tabulations. We then do least-squares fits to these scatter plots, first subdividing into slow and fast wind – in this context usually taken as 500 km/s – and then using the same functional relations as Lopez [1987]. The functions we used are as follows (the same with the last chapter):

$$T_{exp} = (A_0 \times V_p + A_1)^2 \times 1000, for V_p < 500 km/s \quad (3.1)$$

$$T_{exp} = (B_0 \times V_p + B_1) \times 1000, for V_p > 500 km/s \quad (3.2)$$

The results are given in Tables 3.1 and 3.2. Note that when we compare the coefficients at the various spacecraft we anticipate that there will be variations due to the different heliocentric distances of the probes. There may also be some differences arising from the data processing used, which we do not explore in this paper.

Table 3.1: The relationship of Tp vs. Vp for each year for STA and STB

STA	A0	A1	B0	B1	STB	A0	A1	B0	B1
2007	0.020	-1.13	0.525	-184	2007	0.034	-5.66	0.224	21.1
2008	0.023	-2.13	0.47	-145	2008	0.034	-5.62	0.19	36.8
2009	0.025	-2.62	0.465	-133	2009	0.038	-6.84	0.043	122
2010	0.023	-1.88	0.424	-118	2010	0.034	-5.40	0.205	31.4
2011	0.023	-1.97	0.307	-62.7	2011	0.030	-4.08	0.111	62.5
2012	0.024	-2.24	0.191	-2.28	2012	0.033	-4.82	0.027	119
2013	0.022	-1.67	0.487	-154	2013	0.035	-5.60	-0.04	159
2014	0.016	+0.68	0.152	-0.717	2014	0.030	-4.06	-0.282	263

Table 3.2: The relationship of Tp vs. Vp for each year for Wind

Wind	A0	A1	B0	B1	Wind	A0	A1	B0	B1
1995	0.030	-4.38	0.658	-217	2005	0.020	-0.78	0.647	-240
1996	0.036	-6.59	0.499	-122	2006	0.029	-4.58	0.473	-135
1997	0.033	-5.43	0.548	-152	2007	0.027	-3.71	0.521	-168
1998	0.033	-5.56	0.829	-296	2008	0.028	-4.05	0.511	-156
1999	0.028	-3.75	0.713	-246	2009	0.028	-3.81	0.574	-188
2000	0.026	-2.98	0.498	-148	2010	0.029	-4.15	0.397	-95.1
2001	0.027	-3.43	0.778	-283	2011	0.029	-4.07	0.577	-183
2002	0.030	-4.45	0.518	-143	2012	0.025	-2.89	0.546	-181
2003	0.032	-5.57	0.497	-137	2013	0.026	-3.22	0.584	-197
2004	0.031	-4.91	0.582	-177	2014	0.029	-3.95	0.547	-162

Having thus obtained a set of candidate STs, we then remove those which are really Alfvénic fluctuations. We do this by checking if the relation $\Delta \mathbf{V}_\perp = \frac{\Delta \mathbf{B}_\perp}{\sqrt{\mu_0 \rho}}$ is satisfied, where Δ represents the perturbation of the flow and field vectors relative to background (average obtained by smoothing), and $\perp$ means perpendicular to the background field. For it to be classified as Alfvénic, we require all three correlations to be greater than 0.5, or two greater than 0.6 and the other greater than 0.3, which is similar to the criterion in Cartwright and Moldwin [2008]. Examples were given in Yu et al. [2014] (we also showed these pictures in last chapter - Figures 2-5, 2-6).

Having derived our set of STs, we looked carefully at public tabulations of ICMEs Richardson and Cane [2010], www.srl.caltech.edu/ACE/ASC/DATA/level3/icmetable2.htm; Jian et al. [2006], www-ssc.igpp.ucla.edu/∼ jlan/STEREO/Level3/STEREO_Level3_ICME .pdf. Both of them are continually updated and cover our period completely.) We found that a subset of our STs were listed in these time ranges. Specifically, 107 STs from STA (16%), 68 STs from STB (11%), 142 STs from Wind (13 %) were in the published ICMEs time range. To proceed in an orderly manner, we shall first discuss the other STs in our list and then reserve a special section (see below 3.3.8) to discuss these 'ICME-like STs' and how their inclusion affects the statistical results obtained. Having removed these ICME-like STs, we finally arrive at 549 STs from STA, 557 STs from STB, 925 STs from Wind.

3.3 Results

3.3.1 Distribution of STs at 1 AU

We first look at the distribution of the number of STs at 1 AU. We show in Figure 3-1 the numbers of STs from 3 different spacecraft plotted year by year from the 2007 to 2014 (STA - red; STB - blue; Wind - green). The positions of STEREO in the month of July of each year have also been shown in this picture (STA - red, STB - blue), while that of Wind is plotted in green. STA is advancing ahead of Earth and STB is receding from Earth, increasing their azimuthal separation from Earth by 22.5 deg per year. These 8 years of observations cover practically the whole orbit near 1 AU and most of solar cycle 24. This includes farside observations and observations during the minimum and maximum phase of cycle 24.

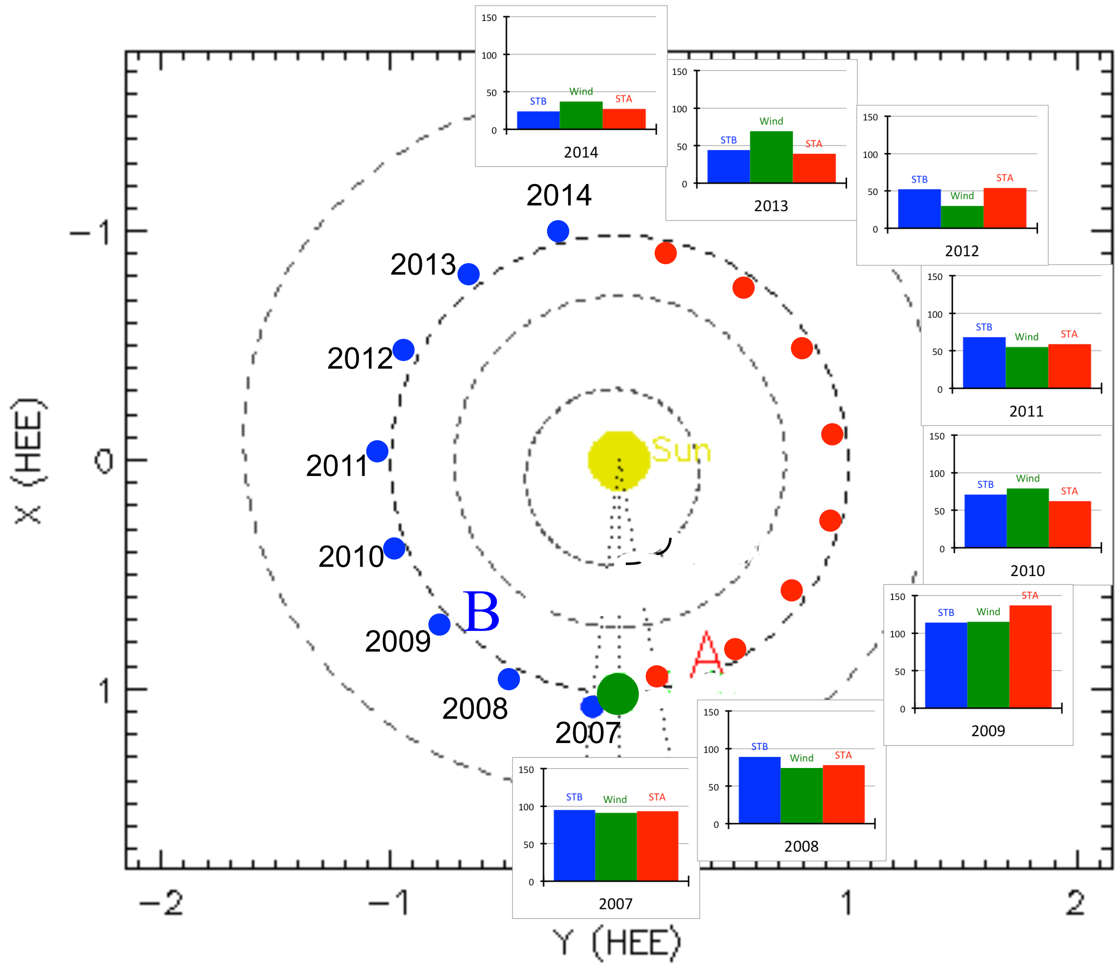

Figure 3-1: The trajectories of the STEREO spacecraft (-A and -B) from July, 2007 to July, 2014 (red - STA, blue - STB). The number of the STs per year is also shown in this picture (red - STA, blue - STB, green - Wind).

The ST frequency peaks in the minimum years 2007-2009 and reaches a clear maximum in 2009, at the depth of the unusual and prolonged solar minimum of cycle 24 (e.g. Farrugia et al. [2012], and references therein). Note that year 2009 is not only at solar minimum but is also a year where the incidence of slow wind was the highest in the period (92%, 89% and 90% at STB, Wind and STA, respectively). This point is taken up further below. The minimum in ST occurrence frequency occurs in year 2014 at all spacecraft.

The distribution of ST frequency does not change much with different positions in the solar minimum/ascending phases (2007 - 2011), while the numbers of STs from Wind are different from STEREO's in the solar maximum years (2012 - 2014). The details on the number of STs for the years 1995 to 2014 are shown in the Table 3.3.

Table 3.3: The STs' numbers from STEREO and Wind per year

Year	STA	STB	Wind		Year	STA	STB	Wind
1995	-	-	38		2005	-	-	41
1996	-	-	54		2006	-	-	57
1997	-	-	44		2007	93	95	91
1998	-	-	30		2008	78	89	74
1999	-	-	16		2009	137	114	115
2000	-	-	16		2010	62	71	79
2001	-	-	22		2011	59	68	55
2002	-	-	19		2012	54	52	30
2003	-	-	18		2013	39	44	69
2004	-	-	20		2014	27	24	37

3.3.2 Statistical Overview of ST Properties

Figures 3-2 - 3-4 show statistical results on key ST parameters from STA (Figure 3-2), STB (Figure 3-3) and Wind (Figure 3-4). The results are presented in the form of scatter plots. The parameters in question are (i) $< B >$; (ii) $< \beta_p >$, (iii) $< M_A >$ and (iv) the temperature ratio $< T_p/T_{exp} >$, where $<>$ denotes the average of the respective quantities. In all three plots, the black traces are the yearly averages of the solar wind (with ICME-like STs removed).

Figure 3-2 gives the results from STA. For each parameter we have shown by the red traces the average of that parameter in STs. Concerning (a), we see that the $< B >$ in STs (red) tends to increase as we move from solar minimum (left) to solar maximum. This is the same tendency as in the solar wind, but the values in STs are about twice those of the ambient solar wind. Concerning (b), we note the large variability and that β_p in STs has

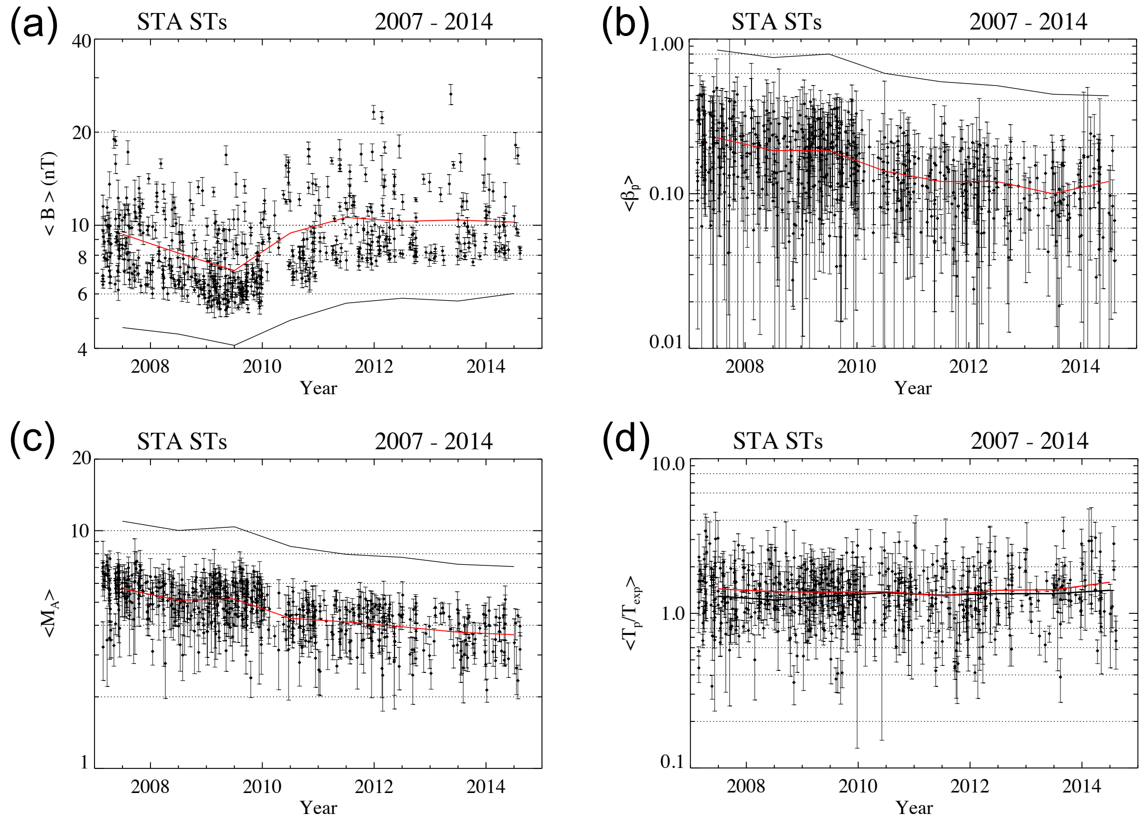

Figure 3-2: The average values of four key parameters in STs from STA. (a) Average magnetic field strength, $< B >$; (b) Average proton β, $< \beta_p >$; (c) Average Alfvén Mach number, $< M_A >$; (d) Average T_p/T_{exp}, $< T_p/T_{exp} >$. (Red lines - the yearly averages of the STs from STA. Black lines - the yearly averages of the solar wind.)

a tendency to decrease as the solar activity increases (same tendency as in the solar wind, and the values are about half as much). Panel (c) shows that M_A in STs is lower by a factor of ~2 that in the solar wind. In panel (d) the black and red traces are almost on top of each other, showing that STs are not cold structures. (The yearly averages of the above parameters are listed in Table 3.4.) Similar trends are seen at STB (Figure 3-3, Table 3.5). Note that the average of the parameters in the STs have been shown by the blue traces.

Now we discuss results near the Sun-Earth line for about 2 solar cycles in Figure 3-4.

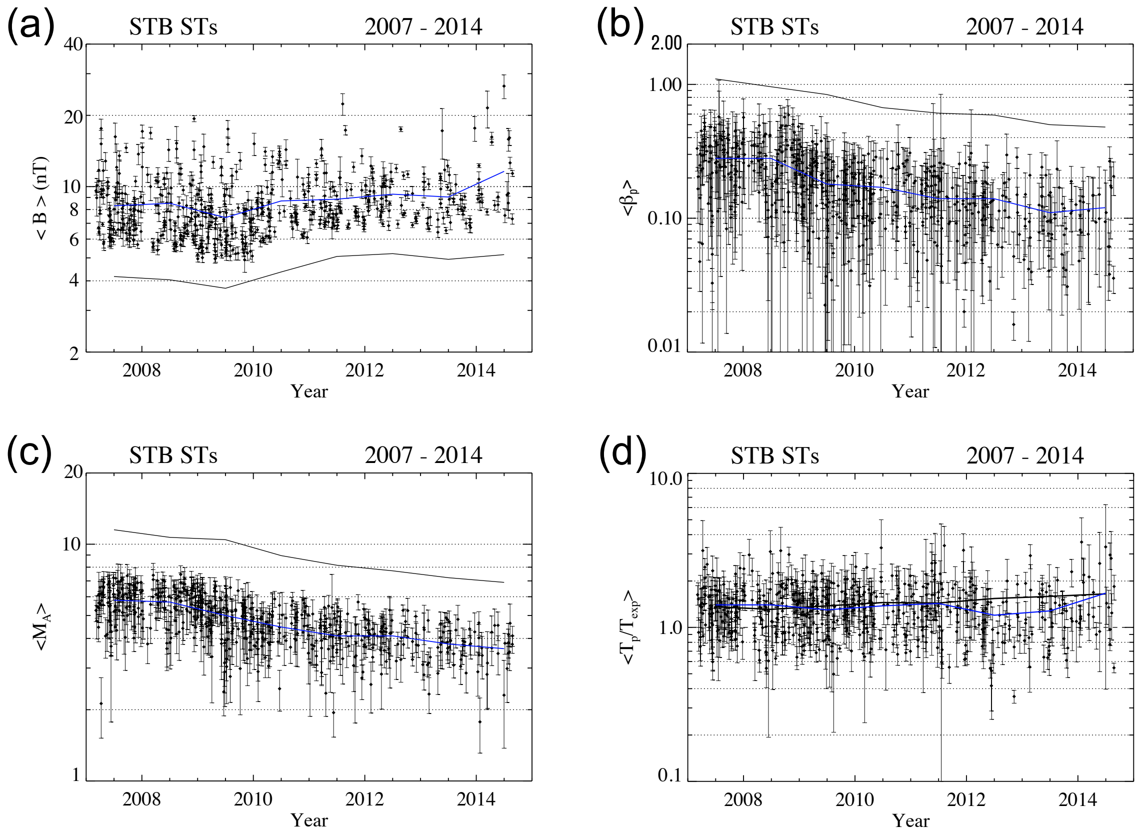

Figure 3-3: Similar statistics as in previous figure, but for STB. The blue lines join the yearly averages for the STs.

Table 3.4: The average values of the STs and the solar wind from STEREO-A

STs	B	β_p	M_A	T_p/T_{exp}		SW	B	β_p	M_A	T_p/T_{exp}
2007	9.36	0.23	5.7	1.44		2007	4.67	0.85	10.96	1.29
2008	8.13	0.19	5.1	1.38		2008	4.45	0.76	10.02	1.22
2009	7.14	0.19	5.16	1.37		2009	4.09	0.8	10.38	1.29
2010	9.44	0.14	4.28	1.38		2010	4.93	0.6	8.59	1.36
2011	10.6	0.12	4.13	1.3		2011	5.6	0.53	7.95	1.31
2012	10.3	0.12	3.94	1.41		2012	5.81	0.5	7.72	1.34
2013	10.4	0.1	3.74	1.42		2013	5.69	0.44	7.22	1.34
2014	10.24	0.12	3.65	1.59		2014	6.02	0.43	7.06	1.41

The same vertical scales are used. The dependence of $< B >$ on solar cycle, which we found at STA and STB, is confirmed, with the additional information that $< B >$ has now a two-

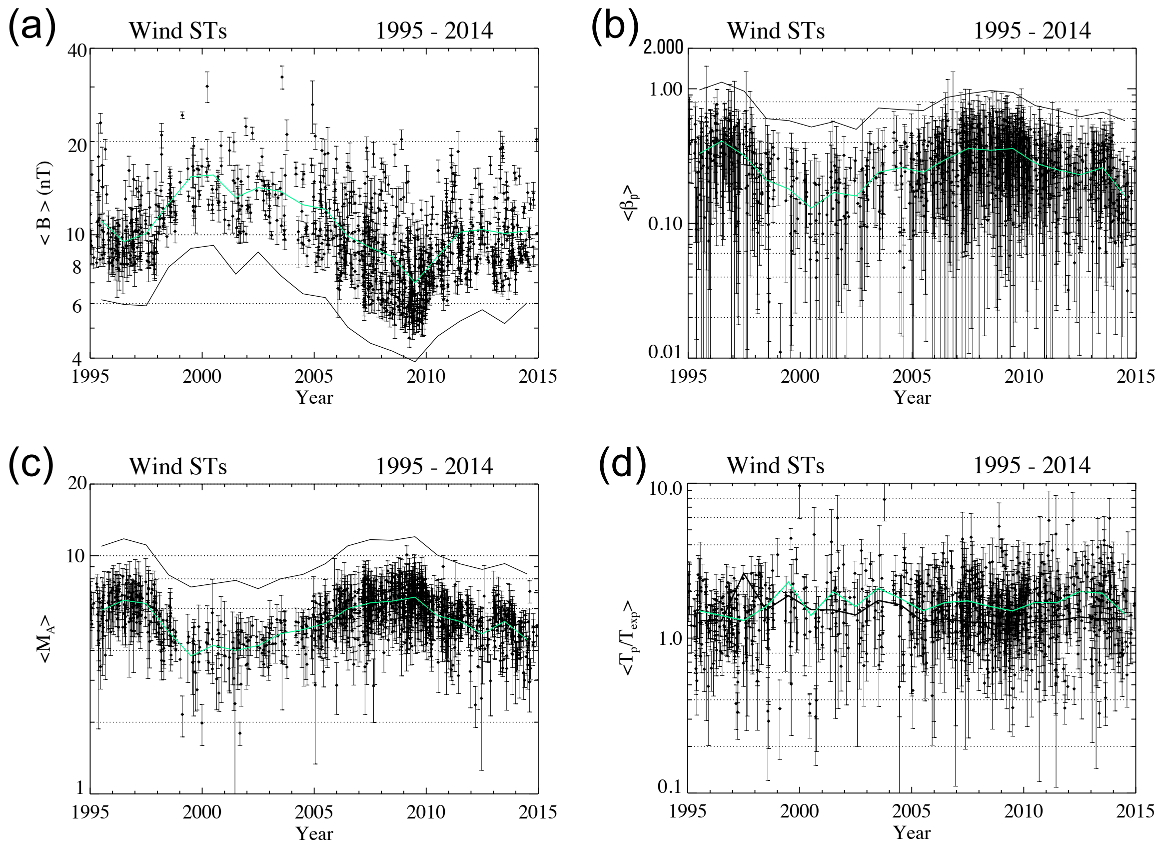

Figure 3-4: Same as previous but this time for Wind over a longer period. The green lines join the yearly averages for the STs.

Table 3.5: The average values of the STs and the solar wind from STEREO-B

STs	B	β_p	M_A	T_p/T_{exp}		SW	B	β_p	M_A	T_p/T_{exp}
2007	8.3	0.28	5.8	1.4		2007	4.17	1.1	11.51	1.36
2008	8.5	0.28	5.7	1.4		2008	4.04	0.96	10.69	1.31
2009	7.4	0.18	5	1.3		2009	3.72	0.84	10.45	1.38
2010	8.7	0.17	4.47	1.38		2010	4.36	0.67	8.95	1.45
2011	8.85	0.14	4.1	1.43		2011	5.07	0.61	8.15	1.44
2012	9.29	0.14	4.1	1.2		2012	5.21	0.59	7.72	1.54
2013	9.04	0.11	3.79	1.28		2013	4.93	0.5	7.22	1.59
2014	11.6	0.12	3.62	1.67		2014	5.16	0.48	6.9	1.65

humped profile and the rise in $< B >$ in solar cycle 23 is markedly higher than that in cycle 24. Similarly, the drop in $< B >$ in 2007-2009 is deeper than that in the previous minimum

Table 3.6: The average values of the STs and the solar wind from Wind

STs	B	β_p	M_A	T_p/T_{exp}	β_{plasma}	SW	B	β_p	M_A	T_p/T_{exp}	β_{plasma}
1995	11.1	0.33	5.9	1.5	0.98	1995	6.17	0.98	10.96	1.3	3.43
1996	9.5	0.41	6.5	1.4	1.14	1996	5.96	1.12	11.78	1.29	4.58
1997	10.1	0.32	6.3	1.3	0.91	1997	5.9	0.96	11.1	2.62	3.51
1998	12.6	0.21	4.8	1.6	0.5	1998	7.86	0.6	8.31	1.52	1.71
1999	15.4	0.18	3.8	2.3	0.43	1999	9.04	0.58	7.39	1.88	1.62
2000	15.6	0.13	4.2	1.4	0.32	2000	9.25	0.52	7.63	1.53	1.44
2001	13.2	0.17	4	2	0.42	2001	7.47	0.57	7.88	1.52	1.6
2002	14.2	0.16	4.2	1.6	0.49	2002	8.8	0.5	7.27	1.41	1.34
2003	13.8	0.24	4.7	2.1	0.67	2003	7.39	0.72	8	1.75	1.73
2004	12.5	0.26	4.9	1.8	0.78	2004	6.45	0.7	8.35	1.64	2.67
2005	12.1	0.24	5.2	1.5	0.77	2005	6.27	0.69	9.26	1.28	2.26
2006	9.9	0.3	6	1.7	0.99	2006	5.03	0.86	11	1.33	3.15
2007	9.1	0.36	6.34	1.74	1.23	2007	4.47	0.92	11.69	1.27	5.24
2008	8.5	0.35	6.45	1.6	1	2008	4.21	0.97	11.61	1.26	3.01
2009	7	0.36	6.7	1.5	1.07	2009	3.89	0.94	12.02	1.2	3.68
2010	8.5	0.28	5.6	1.7	0.85	2010	4.7	0.75	10.06	1.27	2.65
2011	10.2	0.25	5.3	1.7	0.77	2011	5.26	0.69	9.25	1.3	2.27
2012	10.4	0.23	4.7	2	0.63	2012	5.73	0.62	8.76	1.37	2.16
2013	10.1	0.26	5.3	1.95	0.77	2013	5.17	0.67	9.27	1.33	2.61
2014	10.3	0.16	4.45	1.44	0.55	2014	6.03	0.58	8.39	1.33	2.23

(1995-1996). Quantity $< B >$ in STs is about twice that in the ambient solar wind. The average β_p in STs (Figure 3-4b), which is less than unity, is one-half that in the ambient solar wind (Table 3.6). On top of this we also see a clear solar cycle variation of β_p and M_A, the respective values reaching a minimum at peak solar activity and this minimum is more pronounced at the stronger cycle maximum. Near Earth, too, the T_p of STs is typically higher than T_{exp} for solar wind expansion, in contrast to ICMEs (Figure 3-4d).

Figure 3-5 now shows statistical results for β_{plasma} (protons + electrons) from Wind. The T_e is taken here from measured SWE values. Note that there is a gap from June 2001 to August 2002, which is an artifact due to lack of SWE electron data in this period. In STs the β_{plasma} is smaller than in the solar wind throughout the 20-year period. The average values are about one-half of the ambient solar wind. The value of β_{plasma} in STs clearly depends on

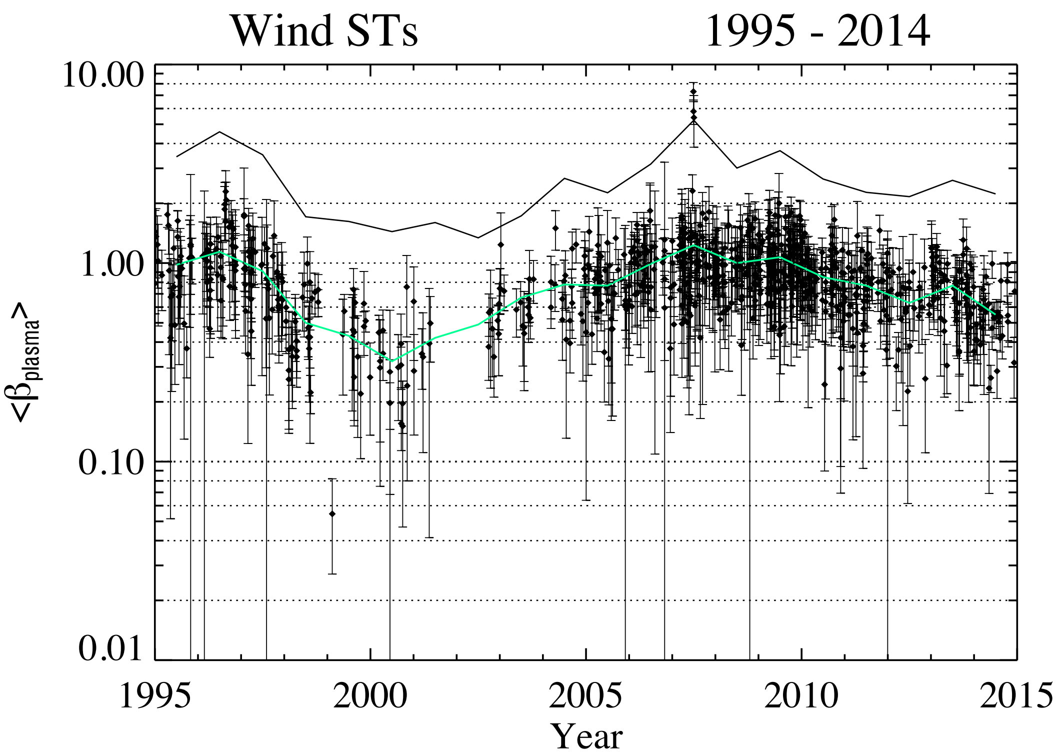

Figure 3-5: The average β_{plasma} from Wind data.

solar activity level. In the solar minimum years, the β_{plasma} is close to unity. This confirms the result reached by Yu et al. [2014] for 2007-2009. However, in the solar maximum years, β_{plasma} in STs is less than 1. The implication for analytical modeling of these structures is that non-force free models should be used in the solar minimum years, while force free models could be appropriate to events near solar maximum when β_{plasma} is less than unity.

3.3.3 ST Duration

Figure 3-6 shows the spread of the ST durations at the three spacecraft (red - STA, blue - STB, green - Wind). The distribution of the durations peaks in the [1, 2] hour range at all spacecraft. The distribution has a long tail. The majority of the STs are shorter than 6 hours (88 % for STA, 88 % for STB, 84 % for Wind). The median value of the duration is 2.3 hours for STA, 2.4 hours for STB, and 2.9 hours for Wind. We also obtained the median values of the velocity, which is 369 km/s for STA, 352 km/s for STB, and 393 km/s for Wind. (We show the velocity distribution below.) Multiplying the median duration by the median velocity, we obtain 0.022 AU ($\sim 4.7R_{\odot}$, solar radii) as an approximate size of STs in the solar radial direction near 1 AU.

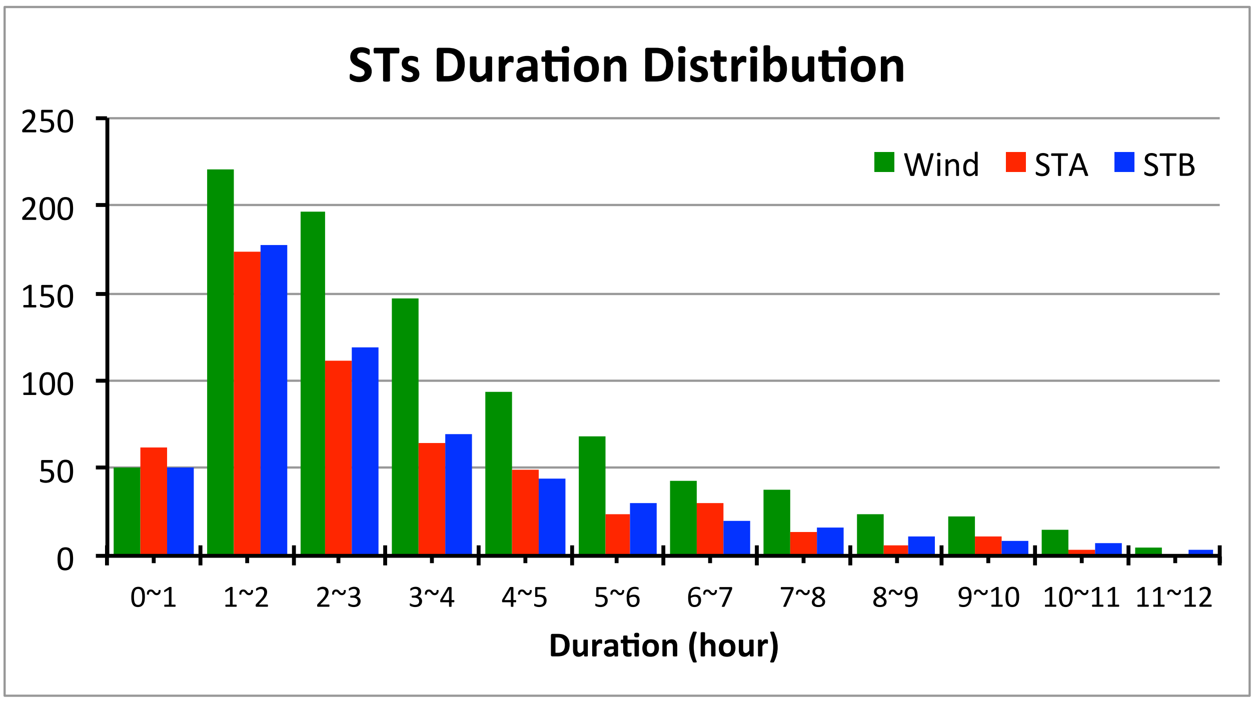

Figure 3-6: The distribution of the ST durations. (Red - STA, blue - STB, green - Wind).

3.3.4 Radial Expansion of STs

Interaction of transients with the ambient solar wind is often inferred from their speed relative to the surrounding wind. The expansion velocity is half the difference between the velocities at the leading and trailing edges. The expansion clearly impacts the way they are modeled (static versus non-stationary structures), with various complications arising for the latter (e.g. Farrugia et al. [1992]). With this in mind, we now study the expansion velocity of STs (V_{exp}) from STA, STB and Wind. This is shown in Figure 3-7 (the distribution combines all the STs from three spacecraft). The values of V_{exp} are small; almost all the STs have radial velocity between the [-50, 30] km/s. And the narrower range [-20, 20] km/s encompasses 82 % of them. Thus STs tend to effectively convect with the surrounding solar wind and may be modeled by static methods. Other researchers have also noted this behavior in STs Moldwin et al. [2000]; Kilpua et al. [2009].

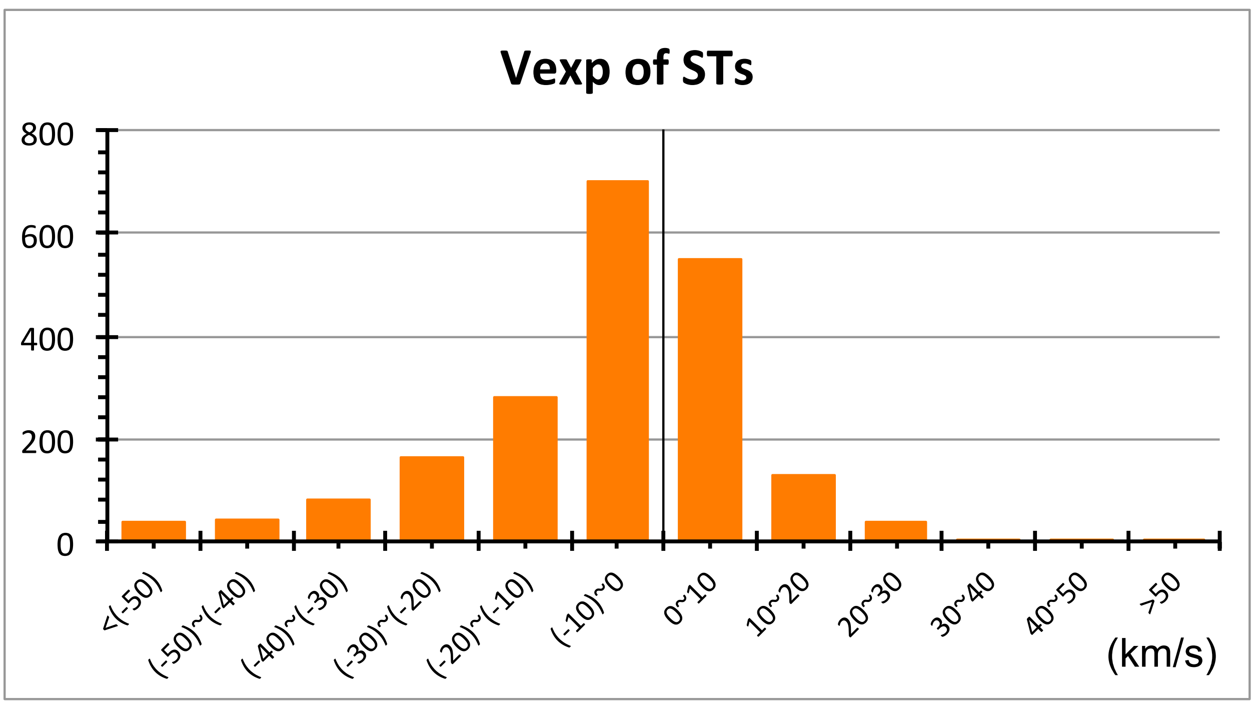

Figure 3-7: The distribution of the expansion velocities of STs ($V_{exp} = (V_{in} - V_{out})/2$).

A further important point arising from Figure 3-7 is that many – indeed, more than one-half – of the radial velocities are, in fact, negative, implying radially contracting structures. This is consistent with their frequent occurrence in stream - stream interaction regions where they are compressed by the faster, trailing stream.

A non-dimensional expansion parameter was introduced by Démoulin (their Figure 5b). This quantity is defined as $\zeta = (\Delta V_x/\Delta t) \cdot D \cdot V_c^{-2}$, where ΔV_x is the radial expansion velocity, Δt is the duration of the transient, D is the heliocentric distance, V_c is the velocity of the structure's center. For magnetic clouds the author found that this orders the data very nicely. The expansion velocities of MCs range approximately from 0 to 300 km/s. When the normalization is applied, the values of ζ now lie in the narrow range [0.2, 1.2].

In the discussion section we pursue this issue further. We consider this for the subset of STs which are (a) expanding and (b) which are also flux ropes (FRs) in order to better be able to compare it with Démoulin's result for non-perturbed MCs, which are also FRs, albeit large ones. We do not, of course, expect any such simplification for compressed STs (what Démoulin called "perturbed") since the ensuing contraction depends on external circumstances. So we discuss what Démoulin called "unperturbed" cases only.

Show the main results from this chapter. Our results are the same with Moldwin et al. [2000]'s, in most of the STs, they do not have expansion property.

3.3.5 Dependence of ST Occurrence Frequency on Solar Cycle Phase

We now address more explicitly the effect of solar cycle variation on ST occurrence frequency. Figures 3-8 and 3-9 show in the same format the relation between the solar cycle phase, as gauged by the SSN, and the occurrence frequency of STs, as observed by STA (Figure 3-8) and STB (Figure 3-9) during the period 2007-2014. The top panel gives a histogram of yearly numbers of ICMEs. The SSN variation is shown in black in yearly (solid black trace) and monthly averages (lighter black traces). The yearly ST numbers are in red (blue for STB) symbols plotted at mid-year. Noteworthy features are (i) higher values during solar activity minimum, encompassing the years 2007-2009, with a clear peak in 2009; (ii) the steady decrease during rising SSN (and possibly passing maximum in 2013, as inferred from the peak in ICMEs). STB sees more or less the same picture although fewer STs are seen in 2009, and the number of ICMEs at STB peak in the year 2012. (Note that the data from STB stops in October 2014.) Clearly both figures show that there is an anti-correlation of ST occurrence frequency with SSN.

This point is illustrated more trenchantly with Wind where the period covered is longer. Figure 3-10 shows now a 20-year interval (1995-2014). The format is the same as in the previous figure. The anti-correlated behavior of ST frequency with solar activity extends over the whole interval. Note that the STs during the maximum solar activity years 2000-2002 are significantly less than during the current maximum solar activity year. Correspondingly, the ST numbers during the solar minimum years of cycle 23 (1995-1996) are less than those in 2007-2009. These factors reflect the unusual nature of not only the minimum, but also the maximum, phase of cycle 24.

We return to the histogram of the listed ICMEs (yellow) during the same interval (Jian et al. [2006]; Richardson and Cane [2010] updated as indicated in Introduction). (At the time of writing, the ICME list stopped in 2014.) The known correlation of the ICME occurrence rate with solar cycle is well illustrated: Their numbers peak with solar activity, in sharp contrast to STs. Note that the monthly sunspot number has a depression after reaching a

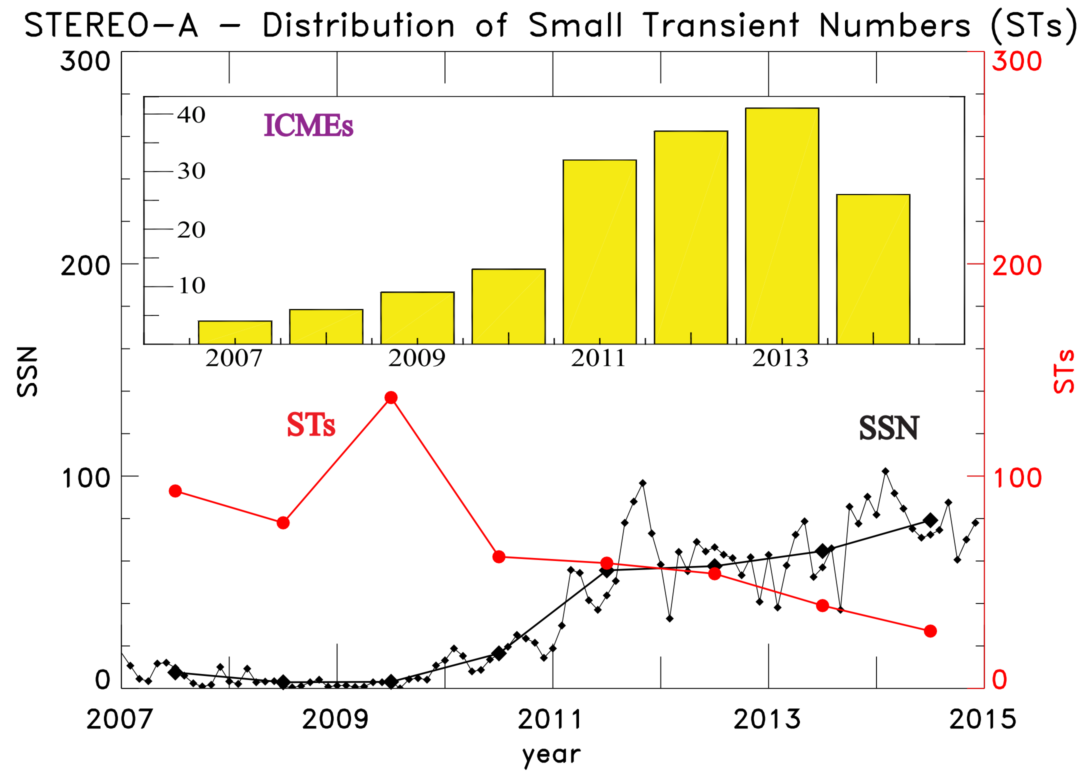

Figure 3-8: Distribution of yearly numbers of small transients (STs) observed by STA (red) from year 2007 to 2014. The sunspot numbers (SSN) are shown in black. The top panel gives a histogram of the ICMEs (yellow). (The STEREO ICMEs list is obtained from: http://www-ssc.igpp.ucla.edu/∼ jlan/STEREO/ Level3/STEREO_Level3_ICME.pdf.)

first peak in 2000. This is the so-called Gnevyshev gap Gnevyshev [1977], and it straddles the peak in ICME numbers. In the distribution observed by Wind, there are more ICMEs in cycle 23 maximum than in the maximum of cycle. In solar cycle 24, the ICMEs show a peak around the year 2012, which coincides with a valley in the distribution of STs. In summary, we have established a clear anticorrelation between the ST occurrence frequency with the solar cycle as monitored by the SSN, which is opposite to that of ICMEs.

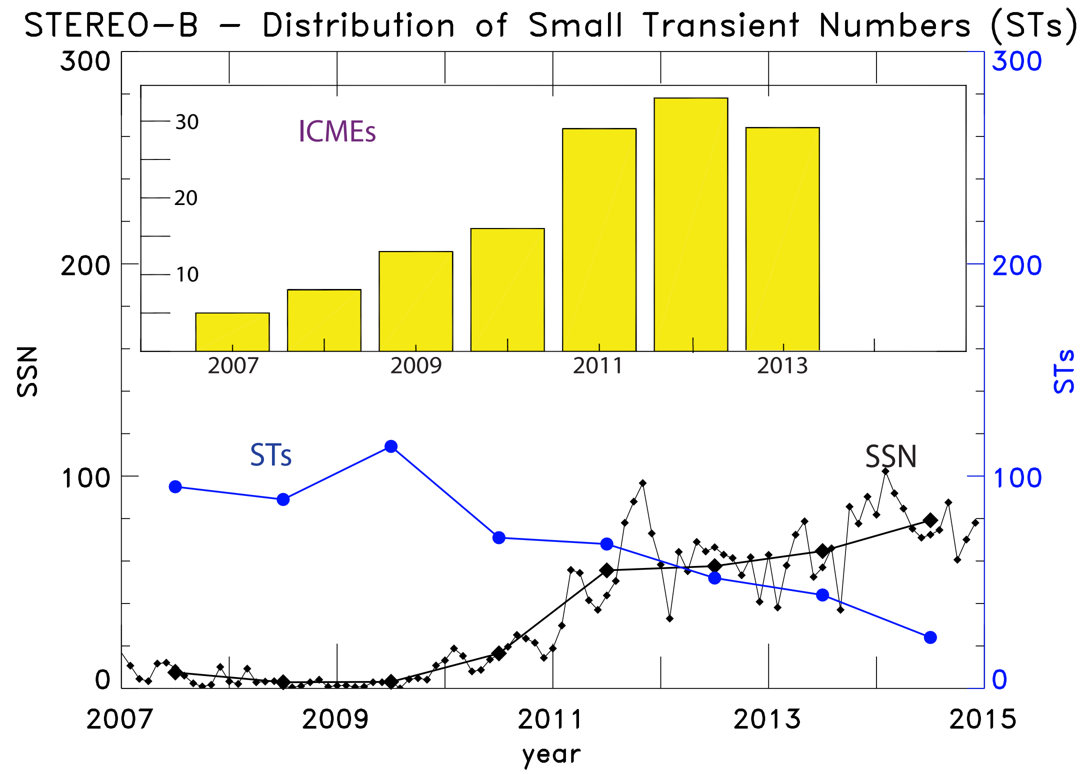

Figure 3-9: Distribution of yearly STs observed by STB (blue) from year 2007 to 2014. Same format with Figure 8.

3.3.6 Dependence of ST Occurrence Frequency on Solar Wind Speed

We now investigate any dependence that ST occurrence frequency may have on solar wind speed. This is an important issue because it gives further clues as to their origin (see Introduction). Figure 3-11 plots the velocity distribution of STs at STA, STB, and Wind, all covering the same time intervals as in the previous figures. Note that since the STs tend to convect with the ambient wind (see section 3.3), this velocity reflects the velocity of the

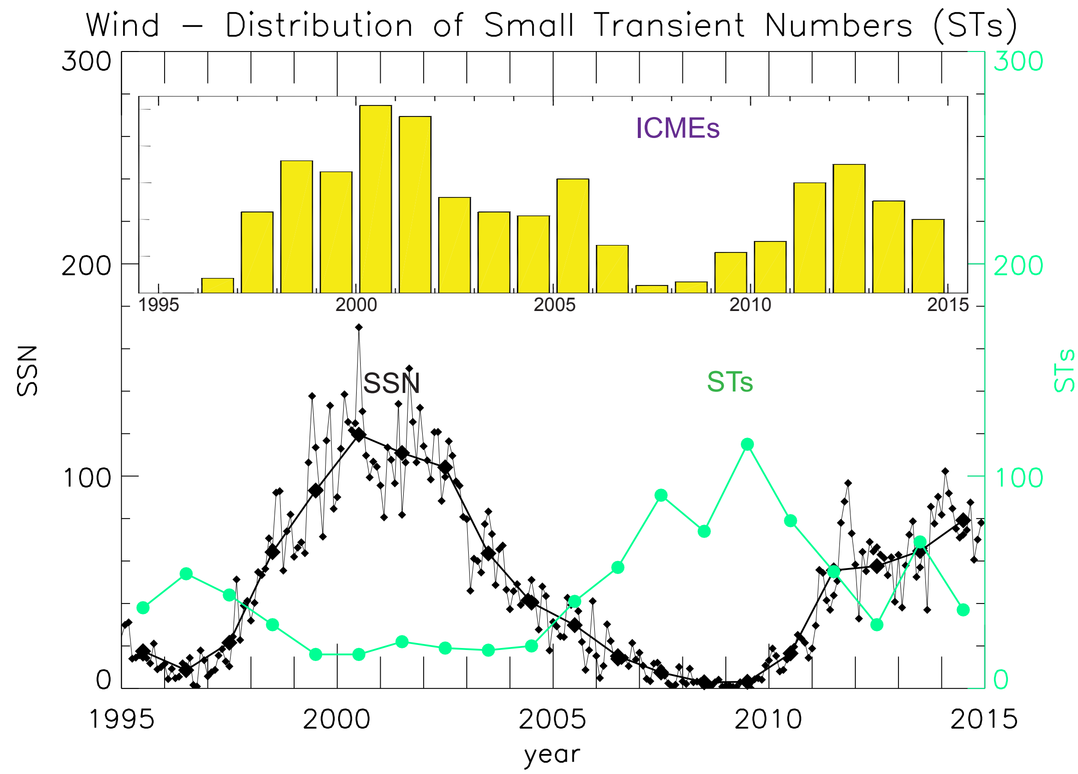

Figure 3-10: Distribution of yearly STs observed by Wind (green) from year 1995 to 2014. (The Wind's ICMEs list is obtained from: http://www.srl.caltech.edu/ACE/ASC/DATA/level3/icmetable2.htm.)

solar wind in which they occur. A vertical line has been drawn at V = 450 km/s to indicate the separation between slow and fast winds. (Recall that 500 km/s was only used as a value separating slow from fast solar winds in the context of T_{exp} to agree with convention.) The clear message from this figure is that the huge majority of STs tend to occur in the slow wind. The numbers are: Wind (726 vs. 199 in fast), STA (473 vs. 76), STB (500 vs. 57). In addition, at all three spacecraft the velocity distribution peaks at 300 - 400 km/s. So this velocity dependence is over and above that on solar cycle.

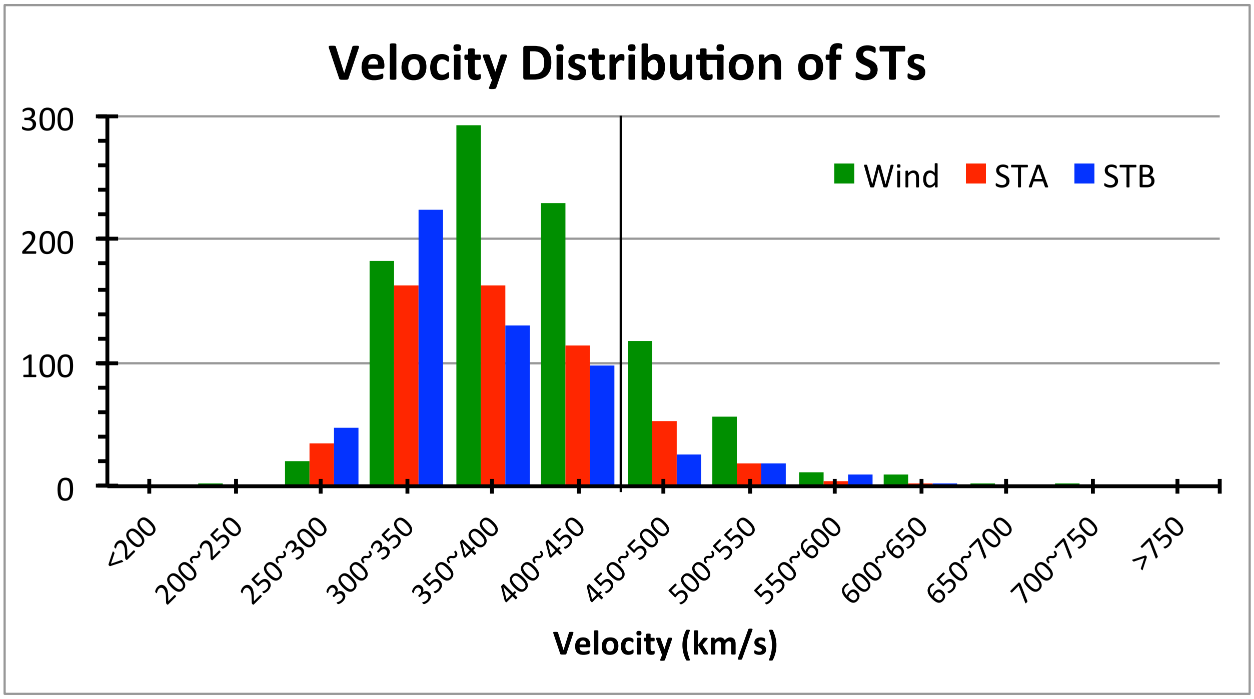

Figure 3-11: The distribution of ST velocities (red - STA, blue - STB, green - Wind).

As an example of this, we contrast the ST occurrence in 2009 with that in year 2003. Year 2003 had 27% of slow solar wind, while year 2009 had 89% (from Wind statistics), i.e. a factor of 3.3 more. Thus, if the speed of the solar wind were the only determining factor, then we would expect year 2009 to have on average about 3.3 times as many STs as year 2003. But in fact in year 2003 we identified 18 while in year 2009 we identified 115 (see Table 3.3), which is approximately 6.4 times as much. Thus to the speed of the wind has been added another contributor, namely, the solar cycle phase (minimum). So in a sense the number of the STs in 2009 represents a sort of upper limit to ST frequency occurrence around 1 AU. See also the clear peak in the Figure 3-10. All three spacecraft show the highest number in this year (Table 3.3).

3.3.7 Compositional Signatures

We now search for compositional signatures, using data from STA. Specifically, we shall concentrate on iron charge states. As described in Lepri et al. [2001] and Richardson and Cane [2010] (and references therein) one frequent signature of ICMEs is an enhanced value of iron charge states.

Figure 3-12 shows in panels (a) and (b) two examples of this. The data are 1 hour averages and are shown as spectrograms. The horizontal axis represents 1 day. Average values are shown by the red trace in the middle panel. The bottom panel shows the speed of the solar wind where these transients occur. The ST interval is bracketed by the vertical guidelines.

Figure 3-12a actually shows two neighboring STs which may be coalescing. In both there is a significant increase in Fe charge states reaching up to 23. The ST pair is observed in a borderline fast wind (bulk speed about 500 km/s). Figure 3-12b shows an event which lasts $\sim$ 4 hrs and which is encountered in the slow wind ($\sim$ 400 km/s). It, too, has an enhanced Fe charge state abundance. So these STs have signatures in common with large ICMEs. By contrast, the STs shown in the bottom two figures (3-12c and 3-12d) do not show any enhanced values of the Fe charge state. Figure 3-12c occurs in the very slow solar wind ($\sim$ 300 km/s). The time series for this ST was 06 May, 2009, 04:40:00 - 06:30:00. This example was shown in previous chapter (Figure 2-12), where it was described as a small flux rope. Finally, Figure 3-12d shows a short ($\sim$ 2 hours) ST which is entrained in a stream-stream interaction region (bottom panel). This example corresponds to the flux rope observed at STA at 14 May, 2012, 08:38:00 - 10:38:00.

Since the published iron charge states data only cover STA from Feb, 2007 to August,

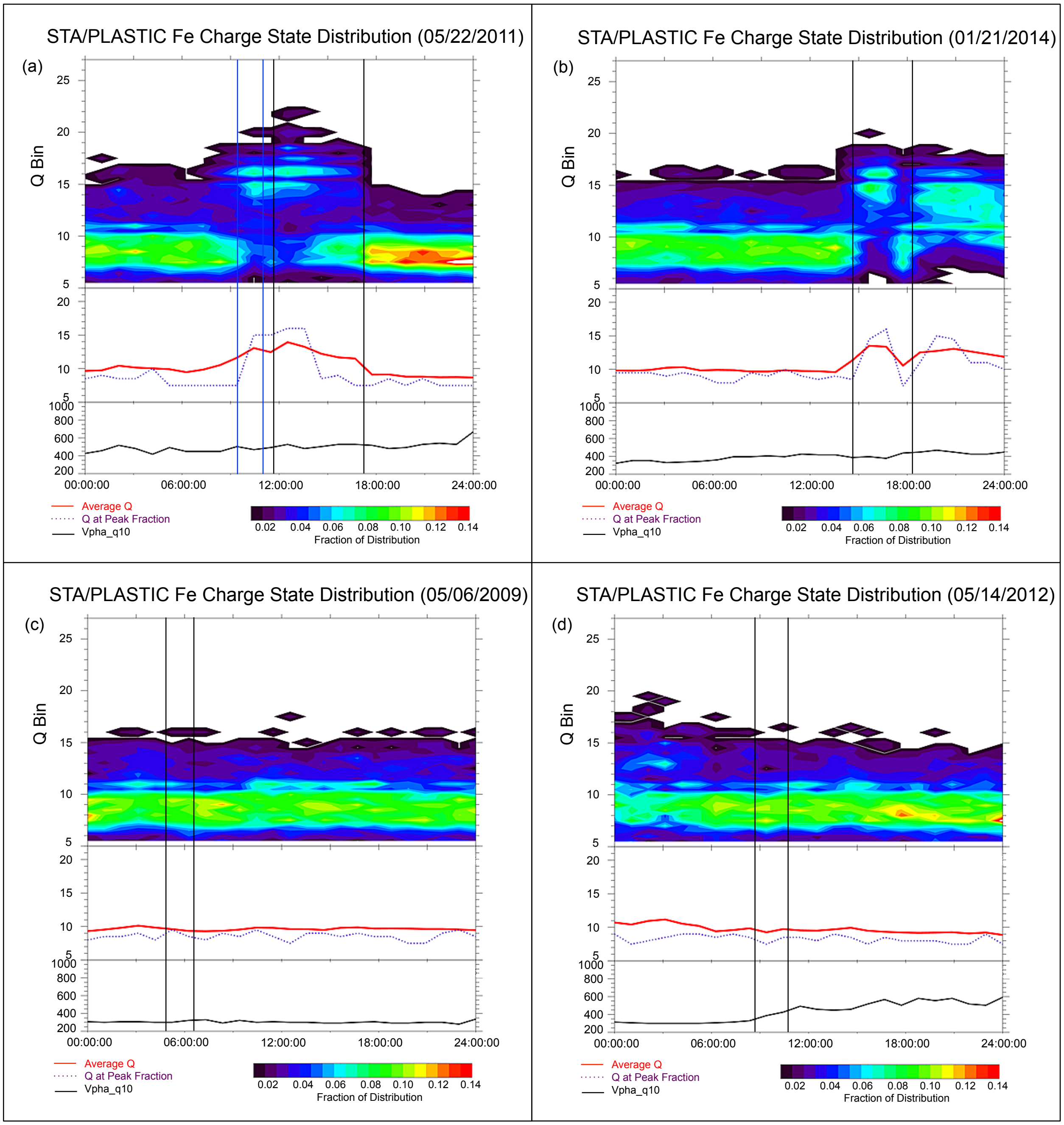

Figure 3-12: The Fe charge state distribution from STA. (a) Two neighboring STs observed on 22 May, 2011. (i) 09:32:00 - 10:58:00; (ii) 11:45:00 - 17:10:00. (b) 21 Jan, 2014, 14:40:00 - 18:25:00. (c) 06 May, 2009, 04:40:00 - 06:30:00. (d) 14 May, 2012, 08:38:00 - 10:38:00. (The pictures are downloaded from: $fiji.sr.unh.edu/cgi-bin/fe\_qstates\_daily.cgi$)

2014, we looked only at STs from STA in this time range. In our ST event list from STA very few have the signature of increasing Fe charge states (less than 5 %). We conclude that high iron charge states occur only occasionally in STs at 1 AU.

3.3.8 Consideration of the ICME-like STs

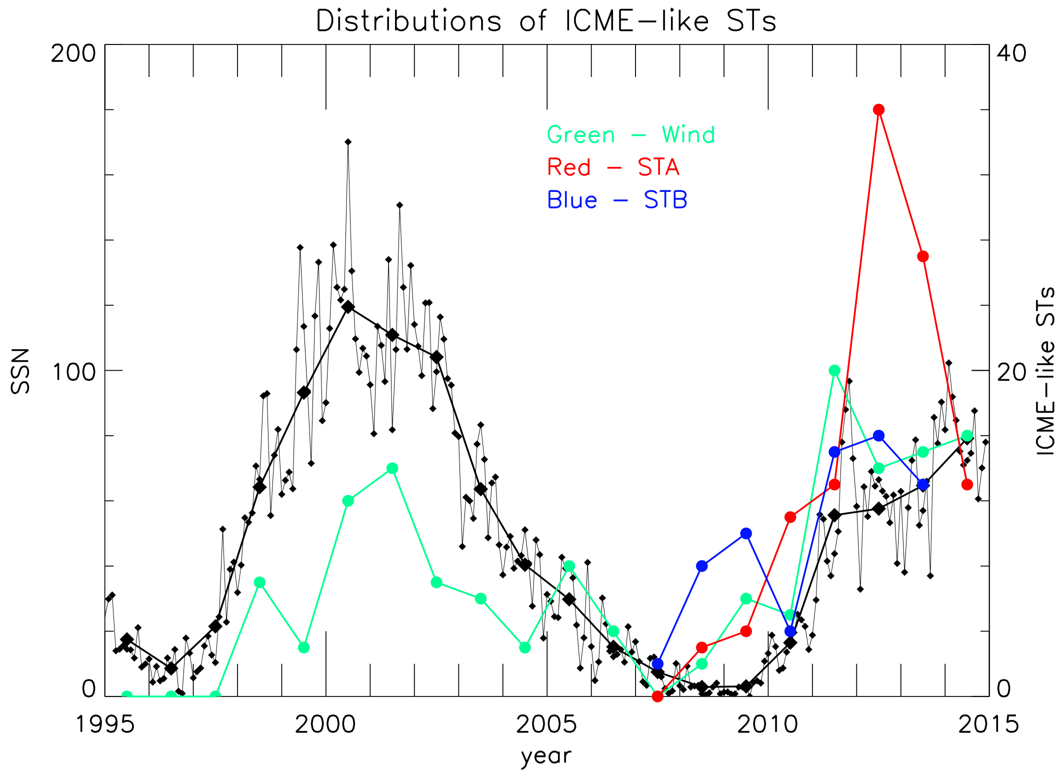

Figure 3-13: Distribution of yearly number of STs observed by Wind (green), including the ICME-like STs for 1995 to 2014.

In the above sections, the ICME-like STs were removed from the discussion, as described in the Introduction. We now direct our attention to these. In our list, we found 107 ICME-like STs from STA (16%), 68 from STB (11%), and 142 from Wind (13 %). In this section we treat these ICME-like STs separately and discuss their statistics. We then compare the results in this section with those reported above, which do not include this subset.

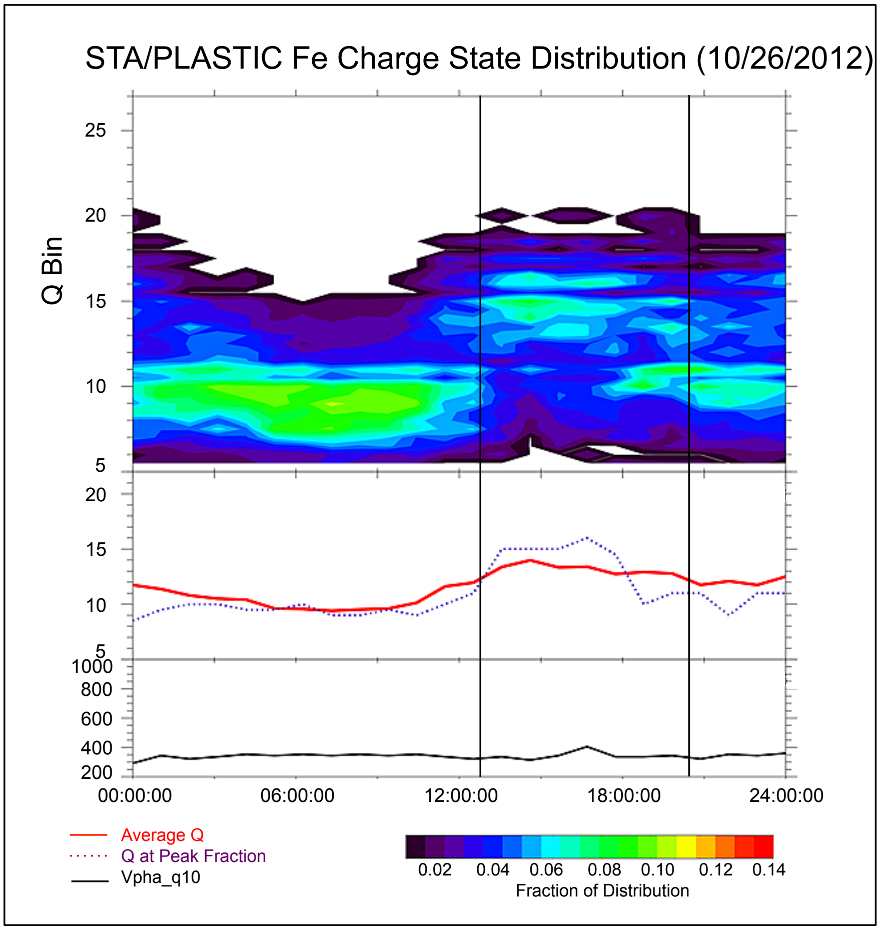

Figure 3-14: The Fe charge state of an ICME-like ST. It was observed on 26 Oct, 2012 between 12:50:00 to 20:22:00. (The picture is downloaded from: fiji.sr.unh.edu/ cgi-bin/fe_qstates_daily.cgi).

In Figure 3-13 we discuss ICME-like STs and compare them with Figures 3-8 - 3-10. One noticeable difference is there is a peak in year 2001, right at the Gnevyshev gap, which was absent in Figure 3-10. Furthermore there is a rise in occurrence frequency with solar cycle 24. The ICME-like STs occur mostly at solar maximum and exhibit the same behavior as large ICMEs, whose occurrence frequency is correlated with the solar cycle. Thus there are two peaks in the ST distributions. One is the same distribution as the large ICMEs (Figure 3-13), whereas one is anti-correlated with that of the large ICMEs (first panel, Figure 3-10). In Figure 3-14, we look at the iron charge states of an ICME-like ST. This event is bracketed by the two vertical guidelines. Fe charge states extending to or above the often used ICME level of Q=16 (Lepri and Zurbuchen [2004b,a]) are present.

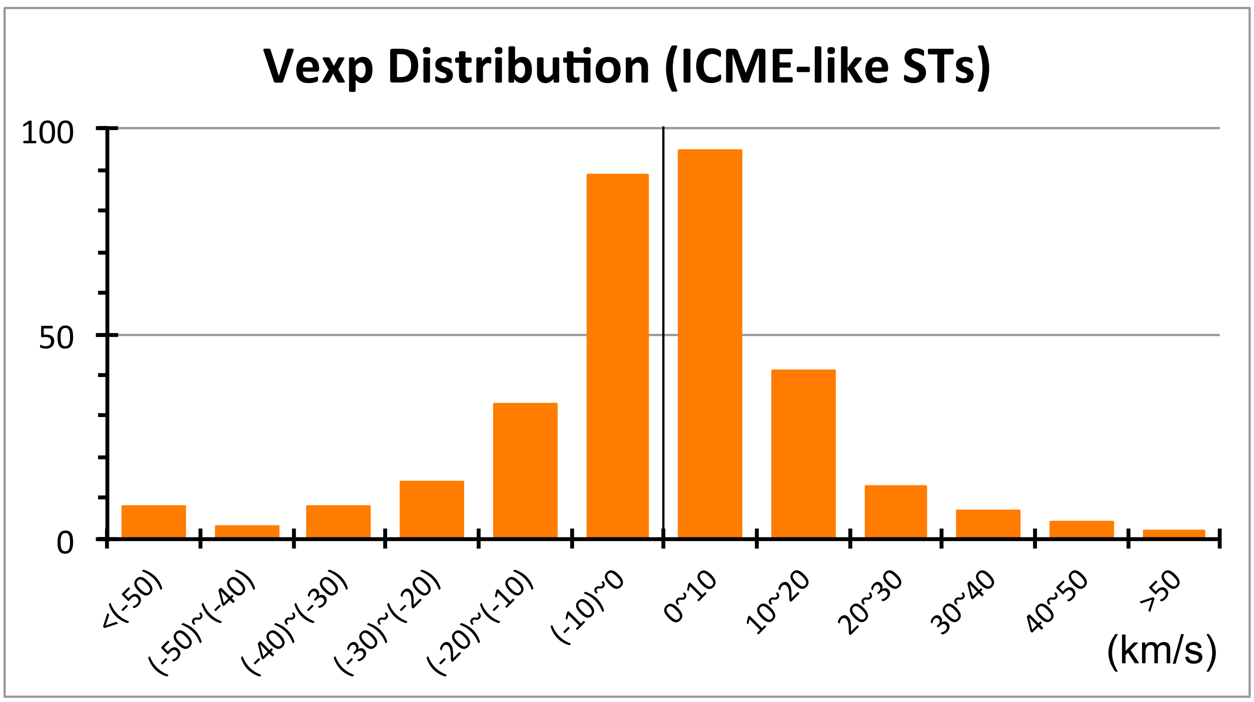

Figure 3-15: The distribution of the expansion velocities of STs (including ICME-like STs).

Figure 3-15 addresses the radial expansion of only ICME-like STs. We combined data on these from all three spacecraft. The expansion velocity distribution does not change much from that in Figure 3-7. Compared with Démoulin's results on MCs, the distribution of the expansion velocities is narrow and confined mostly to the [-20, 20] km/s range.

3.4 Summary and Discussion

3.4.1 Summary

In this chapter we have used data from the STEREO and Wind probes at different angular positions around the Sun at ∼1 AU to examine statistically the properties of solar wind STs. We developed an automated method for identifying these small transients, which is an extension of that used by chapter 2 (Yu et al. [2014]). The event list covers solar cycles 23 and 24 (1995 - 2014). We then removed all the Alfvénic fluctuations. We derived T_{exp} year by year for the 3 spacecraft separately using the same functional relationship as that of Lopez [1987], and used the derived yearly trend when comparing T_p with T_{exp}. Also, those ICME-like STs whose time was coincident with those of published ICMEs were treated separately. Note that the ICME tabulations which we consulted listed transients longer than ∼5 hrs. This duration may be, however, an arbitrary one. We finally obtained 549 STs from STA, 557 STs from STB, 925 STs from Wind.

The ST occurrence frequency does not change with different positions in solar minimum years, but is different during solar maximum years of cycle 24 at different positions along the Earth's orbit. The distribution of the ST duration is wide but has a clear peak at [1, 2] hours. We presented statistical results on ST properties. In STs, quantity $< B >$ is about twice that in the ambient solar wind, while quantities $< \beta_p >$ and $< M_A >$ are about one half as much. Quantity $< T_p >$ is generally higher than T_{exp}. The statistical β_{plasma} is obtained for the Wind measurements, in which the electron contribution is included. The

β_{plasma} is close to 1 during the solar minimum years, while it is much less than unity when as we go to solar maximum years. We conclude that force free modeling is appropriate for the solar maximum years, but may be unreliable during solar minimum years. This expands on the previous results given in Yu et al. [2014].

In addition, STs expand little into the surrounding solar wind. Most values for radial expansion velocity lie in the range [-20, 20] km/s. The frequent occurrence of negative radial velocities implies that STs tend to also occur in stream - stream interaction regions where they are being compressed by the faster stream behind.

The occurrence frequency of STs has two clear dependencies. One is an anti-correlated relation with phase of the solar cycle; the other is that STs tend to occur predominantly in the slow solar wind, suggesting that they may form an important constituent of the slow wind. Many of these characteristics are in sharp contrast to those of large-scale transients (ICMEs and magnetic clouds), suggesting that many STs may not originate from near the Sun.

We then analyzed separately the ICME-like STs that we identified independently but which had been previously noted in the two published ICMEs time ranges. Doing so, we addressed 2 issues: (i) Is there any impact on the solar cycle dependence?, and (ii) do they change the expansion speed statistics?. As regards (i) we find that there is a rising peak at solar maximum year 2001 which is indeed ICME-like and opposite to that of other STs. For (ii) we find no significant dependence.

3.4.2 Discussion

A clear correlation between the T_p and V_p of the expanding solar wind has been shown by Lopez and Freeman [1986]; Lopez [1987] from in-situ measurements. They also obtained functions to calculate the T_{exp}. Later, Neugebauer et al. [2003] and Elliott et al. [2005] also found other functions to describe the relationship between T_p and V_p. In Démoulin [2009], the physics behind this relationship was discussed based on the momentum and the internal energy equations. He proposed that the main cause of this correlation is the increase of V_p with heliospheric distance, occurring mostly close to the Sun. This means that the distance to the Sun and the positions in the ecliptic plane might affect this relationship. In most of the above observational studies, the relation between T_p and V_p was derived with small databases near the Sun-Earth line. In our study, we covered about 20 years of data and with 3 different spacecraft (STA, STB and Wind). They have different distances to the Sun (∼0.95 AU for STA, ∼1.05 AU for STB, and ∼1 AU for most of the Wind's period). Therefore we decided to determine the exact relationship between T_p and V_p for each spacecraft in each year.

The preference of STs for the slow solar wind ties in well with Wang et al. [2000] model of small flux ropes (called ”streamer blobs”) emanating from the cusps of helmet streamers into the slow solar wind. A further consideration on this is the following. If, for example, we take a 2-hour-long ST propagating at, say, 300 km/s, we would have a structure of about 3 solar radii at 1 AU (vs. $\sim$ 45 solar radii for a MC). The ζ parameter of Démoulin describes more or less how the radial size increases with distance, so that we are most likely dealing with structures of 0.2-1 solar radii in a coronagraph field-of-view. The blobs discussed by Wang et al. [2000] are about 1-2 solar radii in width, i.e., they lie at the higher end of this range.

The expansion speed of STs (Figure 3-7) appears to be in sharp contrast with that quoted for MCs. Thus Démoulin (his figure 5a) shows expansion velocities in the range [0, 300]. This difference is, in part, connected to the relative sizes. Take 0.02 AU versus 0.2 AU as a rough approximation for ST and MC average sizes, respectively. Thus a 2-hour-long ST which has a $V_{exp} = 15$ km/s would have one equal to ∼150 km/s if it were as large as a MC. This would be in the typical V_{exp} range of MCs. However, we must keep in mind that there are many STs whose V_{exp} is only of order 1-2 km/s. (One example was given in Figure 2-12.) This would correspond to 10-20 km/s for a typical 20-hour MC duration, which would still be considered low. So in such cases the front-to-back velocity gradient is not low because the event is of short duration; it is intrinsically low.

We now look at this issue in a more detailed manner. We take the subset of flux rope STs and exclude those we found to be ICME-like STs. The events are from all three spacecraft and total number of events we arrive at is 246. We calculate the ζ function for this subset and compare it with the result that Démoulin found for large flux ropes. Recall that in section 3.2 we defined a flux rope by minimum variance analysis on the magnetic field, requiring the ratio of intermediate-to-minimum eigenvalues to be larger than 5.

The result is shown in Figure 3-16, top panel. The ζ function giving the normalized expansion velocities lies mainly in the range [0, 1.5]. The mean and median values of the distribution are 0.74 and 0.49. The range and mean values agree well with those for MCs (Démoulin, his Figure 5b). Further, for FR-STs the peak of the ζ lies in the range [0, 0.1], while the MC-normalized distribution peaks near 0.8. In short, many FR-STs do not expand at all. The bottom panel shows results for the non-flux ropes STs. They are similar except that ζ peaks around 0.2-0.3 as opposed to 0-0.1.

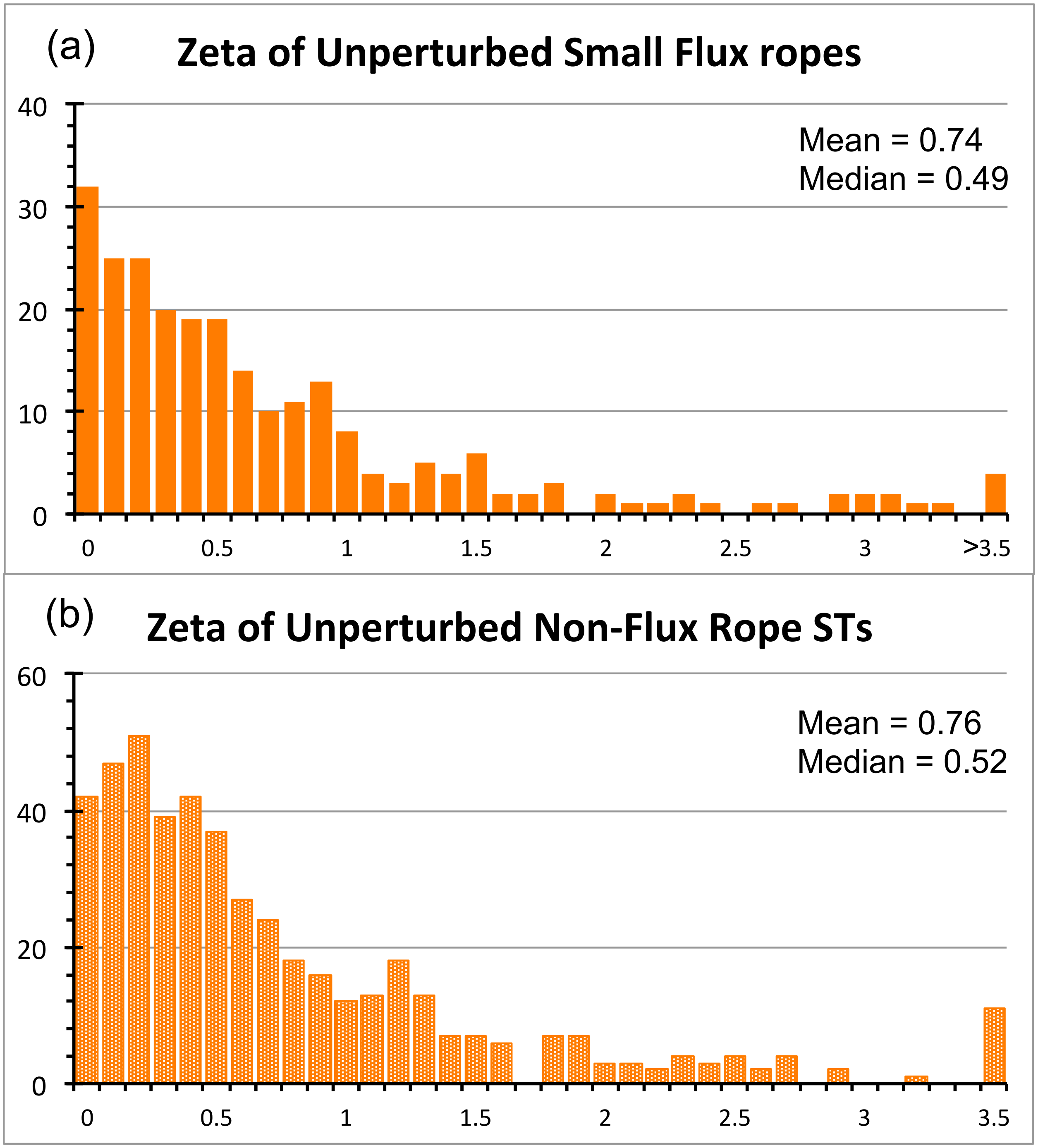

Figure 3-16: (a) The non-dimensional expansion factor (ζ) of the unperturbed small flux ropes. (b) ζ of the unperturbed non-flux rope STs.

Janvier et al. [2014a] also studied the normalized expansion rate (ζ) for small FRs, and compared them with MCs. They proposed that the ζ of small FRs is half that of MCs. So the ordering introduced by Démoulin is still present for FR-STs, but the value is smaller than MCs. Janvier et al. [2014a] explained that this smaller ζ may be due to a smaller total pressure decrease, and is proposed to be one of the reasons why T_p in small FRs is generally not less than T_{exp}.

We now turn to modeling. In many of the studies of magnetic clouds and flux rope-type STs, the linear force free cylindrical model of Lundquist [1950] has been used (Lepping et al. [2006]; Cartwright and Moldwin [2008]; Feng et al. [2007]; et al.). However, in our study of the β_{plasma} in STs, we found that this parameter depends on the solar activity level. Especially during solar minimum activity, many of the STs have β_{plasma} close to 1. Therefore, non-force free models would be more appropriate. As practically static structures, they are particularly well suited for testing models, whether they are force free or not.

In next chapter, we will consider the non-force free models, and compare our results with the force free fittings.

Chapter 4

Models

Some STs have the small flux rope type structure, and the most used model for the small flux ropes is the Lundquist's solution of the cylindrically symmetric force free configurations with constant alpha (Lundquist's force free solution, Lundquist [1950], Lepping et al. [1990]). However, in our study, β_{plasma} (protons + electrons) of the STs depends on solar activity level. The β_{plasma} is close to unity in the solar minimum years, while it is less than 1 in the solar maximum years. Therefore, the non-force free models should be used in the solar minimum years, while the force free models could be appropriate to the small flux ropes near solar maximum when $\beta_{plasma} < 1$. In this chapter, we use 3 non-force free models to study the small flux ropes. These are: (i) the analytical model assume a cylindrically symmetric with circular cross-section (our own solution by following Hidalgo et al. [2002a]); (ii) the analytical model assume a cylindrically symmetric with elliptical cross-section (our own solution by following Hidalgo et al. [2002b]; Hidalgo [2003, 2005]); (iii) the numerical model (GS-reconstruction method Hu and Sonnerup [2002]). We studied several small flux ropes observed from Wind and STEREO spacecraft. And our results show that our non-force free models could also fit very well as or even better than the force free model. The GS-reconstruction shows the small flux ropes tend to have elliptical cross-section.

4.1 Introduction

Magnetic clouds (MCs) have smooth rotations on their magnetic field components. They are often the sources for strong southward interplanetary magnetic fields (IMF), in which condition the plasma entry into the magnetosphere via magnetic reconnection. The MCs are believed to be generated by processes at the Sun. Sometimes they could last over period of days, and are considered as the sources of the magnetic storms or substorms near the Earth.

The small flux ropes were identified by Moldwin et al. [2000], they have some common features with magnetic clouds but smaller size observed at 1 AU (usually last about several hours). They also have smooth rotations in the magnetic components and low proton beta. Later, a large number of small flux ropes be observed at 1 AU (Cartwright and Moldwin [2008, 2010]; Feng et al. [2007, 2008]), these small structures also attract many scientists' attention since their high occurrence frequency and the stable property. The studies on their orientations with respect to the elliptic plane, the current densities inside of these small structures, and also the shape of them, the geomagnetic effectiveness have been proposed.

Because of the smooth rotations on the magnetic components, and the geomagnetic effectiveness, scientists created models (analytical and numerical) to study them, in order to find more information (which could not be measured directly) about this kind of structures (e.g., the origins, orientations, shapes, and variations with time, and so on).

In the past 20 years, the most frequently used model is the Lundquist's solution of the cylindrically symmetric force free configurations with constant alpha (Lundquist's force free solution, Lundquist [1950]). Goldstein [1983] first proposed that the MCs are cylindrically symmetric force free configurations with variable alpha, and the magnetic fields in MCs are a family of helices. However, Goldstein did not suggest a solution to describe the observations.

Burlaga [1988] provided that the solutions obtained from Lundquist [1950] for a cylindrically symmetric force free configuration with constant alpha could be used to describe the signatures of MCs at 1 AU (we call it Lundquist's force free solution). The Lundquist's analytical solution expressed in cylindrical coordinates, are as follows:

$$\begin{cases} B_r = 0 & \text{radial component,} \\ B_\varphi \propto J_1(\alpha r) & \text{azimuthal component,} \\ B_z \propto J_0(\alpha r) & \text{axial component.} \end{cases} \tag{4.1}$$

J_0 and J_1 are zeroth- and first-order Bessel functions. By using this solution, the magnetic field lines in the MCs are a family of helices, the pitch angle increasing from the axis of the MC to the boundary. Figure 4-1 (Burlaga [1988], Figure 1) shows these helices in a plane.

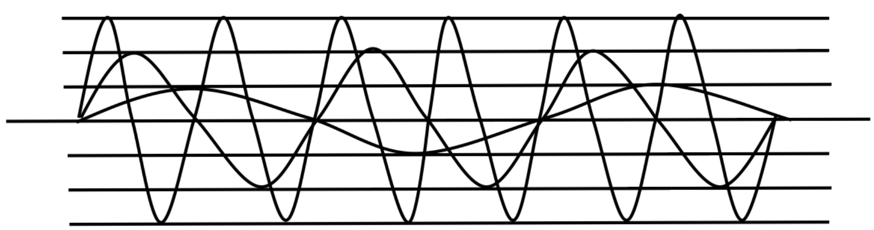

Figure 4-1: The magnetic field lines for a cylindrically symmetric constant alpha force free magnetic field.

Burlaga [1988] showed that the Lundquist's force free solution could describe the magnetic field direction in MCs very well, but it is less successful on the magnetic field strength. Since Lundquist's force free solution is very simple, and could work very well on the magnetic field components of many MCs and small flux ropes, it is mostly used in modeling symmetric flux rope type structures (Lepping et al. [1990]; Cartwright and Moldwin [2008]). However, for the magnetic field strength, it does not work so well, especially when it is asymmetric.

And the Lundquist's solution is a static structure, while the MCs are usually expand as they move away from the Sun. In addition, in some of the MCs, the thermal pressure is not small. Which means that we should study a more general condition (non-force free solution) to observe these flux rope type structures.

In Moldwin et al. [2000] and Kilpua et al. [2009], they found that small flux ropes do not expand too much as the magnetic clouds. Yu et al. [2014] also studied the velocity expansion of over 100 STs, and found that most of them do not expand. In Yu et al. [2016], they studied over 1000 STs from Wind and STEREO spacecraft, most values for radial expansion velocity lie in the range [-20, 20] km/s. That is, many of the small flux ropes are static. In this case, the flux rope models are appropriate to be used in these small structures since most of these models are static.

Since more and more MCs and small flux ropes are observed non-force free, numerous non-force free models have been provided. Mulligan and Russell [2001] proposed the non-force free flux rope model with kinematic expansion, Hidalgo et al. [2002a,b]; Hidalgo [2003, 2005] studied the cylindrical symmetric non-force free model with circular cross-section or elliptical cross-section, Hu and Sonnerup [2001, 2002] created the numerical simulations on the flux rope type structures (GS-reconstruction), Owens et al. [2006] discussed the kinematically distorted model, Marubashi and Lepping [2007] provided a cylinder and torus model, et al. All of these models fit the in-situ experiment data to an assumed structure, and could get the orientation, shape, and size.

In our study, while most of the STs have β_{plasma} close to 1, only some STs in the solar maximum years have $\beta_{plasma} < 1$, we use the non-force free models in general study the structures of them. We followed Hidalgo et al. [2002a,b]; Hidalgo [2003, 2005] cylindrical symmetric non-force free models with circular cross-section or elliptical cross-section, and derived these two solutions by ourselves(see Appendix-D and Appendix-E for the details). In order to make the elliptical solution under the circular limitation the same with the circular solution, our elliptical solution is different with Hidalgo et al. [2002b]; Hidalgo [2003]'s. However, our two solutions (circular cross-section and elliptical cross-section) are more consistent.

In this chapter, we chose 8 small flux ropes from STEREO and Wind spacecraft. And we fit these observed data by using 3 non-force free models we mentioned above: (i) the analytical model assume a cylindrically symmetric with circular cross-section (our own solution by following Hidalgo et al. [2002a]); (ii) the analytical model assume a cylindrically symmetric with elliptical cross-section (our own solution by following Hidalgo et al. [2002b]; Hidalgo [2003, 2005]); (iii) the numerical model (GS-reconstruction method Hu and Sonnerup [2002]). We compare the fitted results obtained from analytical models with the numerical model's, and also compared them with the results obtained from the Lundquist's force free solution. Then we discussed the size, shape, current densities, and the orientations of these small flux ropes. Finally we finish with a summary and discussion.

4.2 Flux rope models

4.2.1 Analytical model with circular cross-section (Analytical Circular)

A detailed and well-based theoretical model was presented in Hidalgo et al. [2002a]. In this model, they assumed that the MC is locally a cylinder with circular cross-section. They describe it with a toroidal reference system, there is no radial component, and the toroidal and poloidal components of the magnetic field only relate to the poloidal and the toroidal components of the current density, respectively. And by simplicity, they assumed the current distributions are uniform. Under these conditions the solutions of the Maxwell equations are:

$$\begin{cases} B_r = 0 & \text{radial component,} \\ B_\varphi = \frac{\mu_0 j_z r}{2} & \text{azimuthal component,} \\ B_z = \mu_0 j_\varphi (R - r) & \text{axial component.} \end{cases} \tag{4.2}$$

, where μ_0 is the vacuum permeability, r is the distance to the cloud axis, and R is the radius of the cloud.

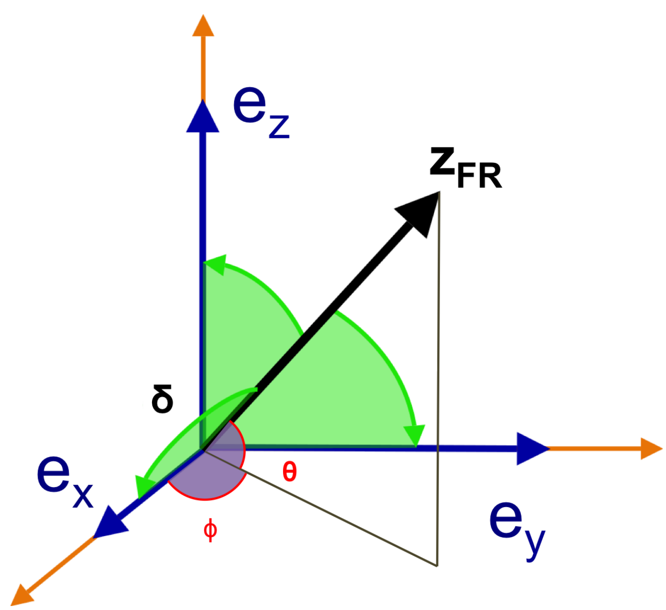

Figure 4-2: The flux-rope axis in the GSE coordinate.

When the cloud is observed at 1 AU, its axis has an angle θ (latitude) with respect to the ecliptic plane, and an angle ϕ (longitude) in the ecliptic plane (see Figure 4-2). The relationship between the magnetic field components observed in the MC coordinate and the magnetic field components observed in the GSE system is:

$$\begin{cases} B_x^{GSE} = NB_\varphi cos\varphi_{sat} + B_z cos\theta cos\phi \\ B_y^{GSE} = \frac{1}{N} B_\varphi sin\varphi_{sat} sin\theta - \frac{1}{N} B_\varphi cos\varphi_{sat} (cos\theta)^2 sin\phi cos\phi + B_z cos\theta sin\phi \\ B_z^{GSE} = -\frac{1}{N} B_\varphi sin\varphi_{sat} cos\theta sin\phi - \frac{1}{N} B_\varphi cos\varphi_{sat} sin\theta cos\theta cos\phi + B_z sin\theta \end{cases} \tag{4.3}$$

, where we define

$$N^2 = (sin\theta)^2 + (cos\theta sin\phi)^2 \tag{4.4}$$

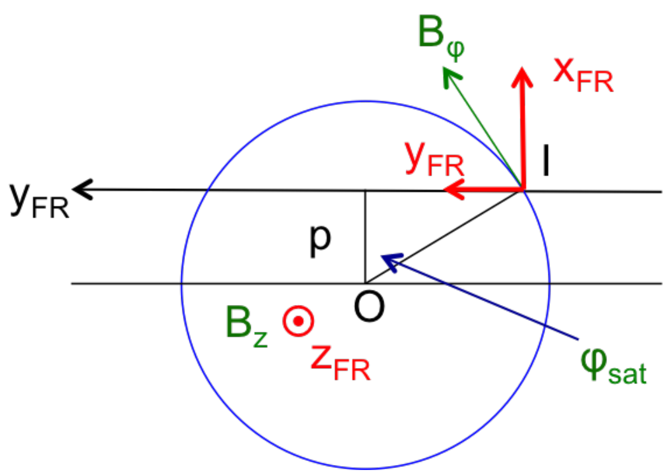

Figure 4-3: The trajectory of the spacecraft in the flux-rope coordinate.

Assume the spacecraft passes along the x-GSE direction, and the position of it at any time t is (x, 0, 0), where $x = V_{SW}(t - t_0)$. Consider the spacecraft removes out of the cloud at time t_1, and the distance between the cloud axis and the spacecraft trajectory is p, the position of the spacecraft at time t on the cloud's cross-section plane is (see Figure 4-3):

$$r_{sat} = \sqrt{p^2 + [NV_{SW}(t-t_0) - \frac{NV_{SW}(t_1-t_0)}{2}]^2} \quad (4.5)$$

$$sin\varphi_{sat} = \frac{NV_{SW}(t-t_0) - NV_{SW}(t_1-t_0)/2}{r_{sat}} \quad (4.6)$$

$$cos\varphi_{sat} = \frac{p}{r_{sat}} \quad (4.7)$$

Therefore, at $t = t_0$, the radius of the MC is

$$R = \sqrt{p^2 + \frac{N^2(V_{SW})^2(t_1-t_0)^2}{4}} \quad (4.8)$$

So, with the above equations, we could fit the theoretical magnetic field vector (B_x^{GSE}, B_y^{GSE}, B_z^{GSE}) to the observed magnetic field data in GSE coordinate system (B_x^{obs}, B_y^{obs}, B_z^{obs}). This model has five free parameters: (i) the latitude, θ; (ii) the longitude, ϕ; (iii) the closest approach distance, p; (v) j_φ; (vii) j_z are corresponding components of the plasma current density.

The equations and the relationships obtained above have shown in the Appendix-D. We also presented the details on the solutions in RTN coordinate system in the Appendix-D. And the fitting code of the non-force free model with circular cross-section is shown in the Appendix-F.

4.2.2 Analytical model with elliptical cross-section (Analytical Elliptical)

Some flux ropes have unsymmetrical structures in the total magnetic field strength, so the fitting by using the analytical model with circular cross-section does not work properly. The main reason of this asymmetric is probably the interaction of the flux ropes with the solar wind, which distorts the local shape of the cloud.

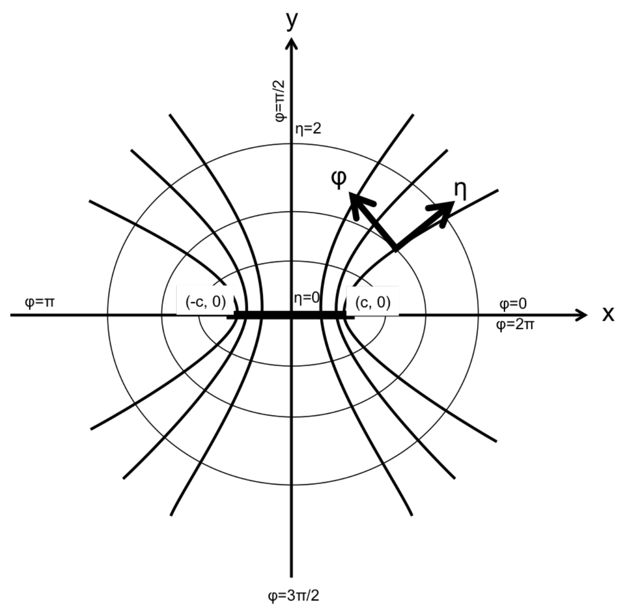

Figure 4-4: The elliptical coordinate system.

In this section, we assume the flux ropes are locally have a cylindrical structure with elliptical cross-section. We start with solving the Maxwell equations and the continuity equation in the elliptical cylindrical coordinate. The elliptical cylindrical coordinate is defined (see Figure 4-4):

$$\begin{cases} x = ccosh\eta cos\varphi \\ y = csinh\eta sin\varphi \\ z = z \end{cases} \tag{4.9}$$

, where two foci F1 and F2 are fixed at -c and +c, η is a nonnegative real number and $\varphi \in (0, 2\pi)$.

We assume the magnetic field has only two components: $(B_\eta = 0, B_\varphi, B_z)$. And also we take j_η is constant, and $\frac{\partial}{\partial z} = 0$. In elliptic cylindrical coordinates, the scale factor is:

$$
\begin{aligned}
h = h_\eta = h_\varphi &= c\sqrt{(cosh\eta)^2 - (cos\varphi)^2} = c\sqrt{(sinh\eta)^2 + (sin\varphi)^2} && (4.10)\\
h_z &= 1 && (4.11)
\end{aligned}
$$

Solving the Maxwell equations and the continuity equation in the elliptical cylindrical coordinate, the solutions of j and B are:

$$
\begin{aligned}
j_\eta &= constant && (4.12)\\
j_\varphi &= \frac{j_\eta c sinh\eta S cos\varphi}{h} + \frac{j^0_\varphi c sinh\eta}{h} && (4.13)\\
j_z &= \frac{j^0_z c^2 (sinh\eta)^2}{h^2} && (4.14)\\
B_\eta &= 0 && (4.15)\\
B_\varphi &= \frac{\mu_0 j^0_z c^2 sinh\eta cosh\eta}{2h} - \frac{\mu_0 j^0_z c^2 \eta}{2h} && (4.16)\\
B_z &= -\mu_0 j_\eta c cosh\eta S cos\varphi - \mu_0 j^0_\varphi c cosh\eta + \mu_0 j^0_\varphi R_0 && (4.17)
\end{aligned}
$$

, where j^0_φ and j^0_z are constant, $S = \frac{\sqrt{(sin\varphi)^2}}{sin\varphi}$, and R_0 is the distance of the spacecraft to the axis of flux rope at time t_0.

When the flux rope is observed at 1 AU, we assume the axis has angle θ with respect to the ecliptic plane, and ϕ in the ecliptic plane. The mapping of the trajectory has an angle ξ with respect to the minor-axis of the elliptical cross-section (see Figure 4-5). The relationship between the magnetic field components observed in the flux rope coordinate and

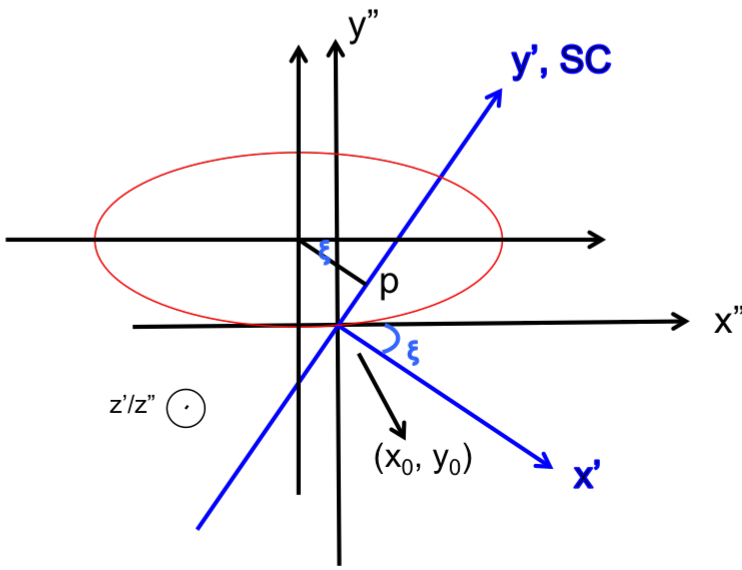

Figure 4-5: The mapping of the spacecraft's trajectory on the elliptical cross plane.

the components observed in the GSE system is:

$$\begin{cases} B_{xGSE} = N sin\xi B_x^{''} + N cos\xi B_y^{''} + cos\theta cos\phi B_z^{''} \\ B_{yGSE} = -\frac{1}{N}(sin\theta cos\xi + (cos\theta)^2 sin\phi cos\phi sin\xi) B_x^{''} + \frac{1}{N}(sin\theta sin\xi - (cos\theta)^2 sin\phi cos\phi cos\xi) B_y^{''} \\ + cos\theta sin\phi B_z^{''} \\ B_{zGSE} = \frac{1}{N}(cos\theta sin\phi cos\xi - sin\theta cos\theta cos\phi sin\xi) B_x^{''} - \frac{1}{N}(sin\theta cos\theta cos\phi cos\xi + cos\theta sin\phi sin\xi) B_y^{''} \\ + sin\theta B_z^{''} \end{cases} \tag{4.18}$$

, where $N = \sqrt{(sin\theta)^2 + (cos\theta sin\phi)^2}$. And $(B_x^{''}, B_y^{''}, B_z^{''})$ are determined by the expressions

$$\begin{cases} B_x^{''} = -\frac{c}{h} cosh\eta sin\varphi B_\varphi \\ B_y^{''} = \frac{c}{h} sinh\eta cos\varphi B_\varphi \\ B_z^{''} = B_z \end{cases} \tag{4.19}$$

We assume the spacecraft passes along the x-GSE direction. At any time t, the position of it is $x = V_{SW}(t - t_0)$. The minimum distance between the spacecraft trajectory and the axis is p. Inside the flux rope, the position of the spacecraft to the axis is

$$\begin{cases} x = V_{SW}(t - t_0)Nsin\xi + x_0 \\ y = V_{SW}(t - t_0)Ncos\xi + y_0 \end{cases} \tag{4.20}$$

, where (x_0, y_0) is the position of the spacecraft to the axis at time t_0. And they are determined by

$$\begin{cases} x_0 = -\frac{Lsin\xi}{2} + \frac{pcos\xi(cosh\eta)^2}{(cos\xi)^2+(sinh\eta)^2} \\ y_0 = -\frac{Lcos\xi}{2} - \frac{psin\xi(sinh\eta)^2}{(cos\xi)^2+(sinh\eta)^2} \end{cases} \tag{4.21}$$

, where $L = V_{SW}(t_1 - t_0)N$.

Therefore, at any time t, the distance of spacecraft to the axis is determined by

$$r_{sat} = \sqrt{[V_{SW}(t - t_0)Nsin\xi + x_0]^2 + [V_{SW}(t - t_0)Ncos\xi + y_0]^2} \tag{4.22}$$

and,

$$\varphi_{sat} = tan^{-1}(\frac{y}{x} \cdot \frac{cosh\eta}{sinh\eta}) \tag{4.23}$$

$$c = \sqrt{\frac{x^2 + y^2}{(cos\varphi_{sat})^2 + (sinh\eta)^2}} \tag{4.24}$$

At time t_0, the distance of the spacecraft to the axis is $R_0 = \sqrt{(\frac{L}{2} - \frac{pcos\xi sin\xi}{(cos\xi)^2+(sinh\eta)^2})^2 + p^2}$.

So with the above equations, we could fit the observed magnetic field components by using this elliptical model. This model has eight free parameters: (i) the latitude, θ; (ii) the longitude, ϕ; (iii) the orientation of the elliptical cross section, ξ; (iv) the closest approach distance, p; (v) the parameter associated with the eccentricity, η; (vi) $j_\eta; (vii) j_\varphi^0; (viii) j_z^0$ are corresponding components of the plasma current density.

The details of getting this analytical elliptical model have shown in the Appendix-E.

4.2.3 Numerical model: GS-reconstruction (Numerical GS)

Sonnerup and Guo [1996] made the first attempt to recover the internal magnetopause structure from magnetic and plasma data measured by a single spacecraft as it penetrated the magnetopause current layer. The technique was improved and more magnetopause traversals were studied by Hau and Sonnerup [1999]. Hu and Sonnerup [2000] recovered structures from a partial magnetopause traversal by the pair of spacecraft Active Magnetospheric Particle Tracer Explorers (AMPTE)/Ion Release Module (IRM) and UKS. The final output of the technique is a contour plot of recovered transverse field lines in a rectangular domain surrounding the spacecraft trajectory, together with the distributions of axial field, axial current density, plasma pressure, etc.

Their cross sections consist of nested irregular loops of transverse field lines rather than the concentric circles of an axially symmetric model.

GS-reconstruction model uses a number of assumptions. (i) Assume the observation is in magnetohydrostatic equilibrium: $\nabla p = j \times B$. (ii) The magnetic field is assumed to have translation symmetry with respect to an invariant-axis direction, i.e. the flux rope is assumed to have 2.5-dimensional structure, where the approximation $\frac{\partial}{\partial z} = 0$ can be used. (iii)The whole analysis is carried in the deHoffmann-Teller (HT) frame, in which the electric field vanishes and thus the magnetic structure can be treated as time-stationary: $\frac{\partial B}{\partial t} = 0$.

Under these assumptions, the magnetic field vector can be written as $B = [\frac{\partial A}{\partial y}, -\frac{\partial A}{\partial x}, B_z(A)]$. Where $A = A(x, y)$ is the magnetic vector potential, and can be given by the Grad-Shafranov equation: $\frac{\partial^2 A}{\partial x^2} + \frac{\partial^2 A}{\partial y^2} = -\mu_0 \frac{d}{dA}(p + \frac{B_z^2}{2\mu_0})$. In this case, the plasma pressure, the axial magnetic-field component and thus the transverse pressure $P_t = p + \frac{B_z^2}{2\mu_0}$ are functions of A alone.

The numerical GS solver is implemented using the Taylor expansions:

$$A(x, y \pm \Delta y) \approx A(x, y) + (\frac{\partial A}{\partial y})_{x,y}(\pm\Delta y) + \frac{1}{2}(\frac{\partial^2 A}{\partial y^2})_{x,y}(\pm\Delta y)^2 \quad (4.25)$$

$$B_x(x, y \pm \Delta y) \approx B_x(x, y) + (\frac{\partial^2 A}{\partial y^2})_{x,y}(\pm\Delta y) \quad (4.26)$$

The data collected by a spacecraft along its trajectory, i.e. at y=0 are used (at y=0 the physical quantities come directly from the spacecraft measurements).

Most of the flux-rope models are able to give reasonable results only for small impact parameters. The GSR possesses this disadvantage too. The Grad-Shafranov reconstruction (GSR) technique was originally developed for reconstruction of flux ropes embedded in the magnetopause (Hau and Sonnerup [1999]), and later applied to magnetic clouds (Hu and Sonnerup [2002]). An extended version of GSR useful for multiple-spacecraft observations was derived by Möstl et al. [2008]). In Isavnin et al. [2011], they present improvements to the GSR technique, show examples of its usage, and discuss main constraints of the method.

In this chapter, we used the Hu and Sonnerup [2002] model, and considered both force free condition and non-force free condition.

4.3 Methodology

In our work, we use data from the STEREO IMPACT (Luhmann et al. [2008]) and PLASTIC (Galvin et al. [2008]) instrument suites at 1 min resolution for the small flux ropes obtained from STEREO. We also use Wind key parameter data acquired by the Magnetic Fields Investigation (MFI) (Lepping et al. [1995]) and Solar Wind Experiment (SWE) (Ogilvie et al. [1995]) for the small flux ropes from Wind. The magnetic field and proton data are at 1 min and 92 s time resolutions, respectively. The electron data is also obtained from the SWE instrument, and they have a resolution of 6-12 s before May 2001, and 9 s after August 2002.

We chose 8 small flux ropes at random from the lists we published in Chapter 3, which have the eigenvalue ratio (medium eigenvalue / minimum eigenvalue got from minimum variance analysis) larger than 5. Then we fit them by using the two non-force free analytical models (with circular cross-section and elliptical cross-section) and numerical model (GS-reconstruction, considered no pressure and with pressure conditions) we talk about above. The output magnetic field contour and the fitting residue could tell us the fitting quality.

In addition, we fit these 8 small flux ropes by the Lundquist's force free solutions, and compared the results with the non-force free solutions' outputs.

Then the orientations obtained from all of the above models are compared with the minimum variance analysis. We discussed the sizes, shapes and also the impact parameters we received from different models.

4.4 Data Examples

There are many small flux ropes which are observed convecting with the ambient solar wind (very typical feature). Most of the analytical models assume a circular cross-section, which assume the symmetric structure in the total magnetic field. Nevertheless, many of the small flux ropes were observed with asymmetric structure. In this case, the analytical model with elliptical cross-section is much more general.

We choose 8 small flux ropes from STEREO and Wind spacecraft. And fit them by using

(i) the analytical model with circular cross-section, (ii) the analytical model with elliptical cross-section, (iii) numerical model (GS-reconstruction), and (iv) the Lundquist's force free model with circular cross-section. For the small flux ropes observed by Wind spacecraft, the orientations obtained from the fitting are in the GSE coordinate. And for the events observed by STEREO spacecraft, the orientations are in the RTN coordinate.

4.4.1 Event 1: STA - 20090221

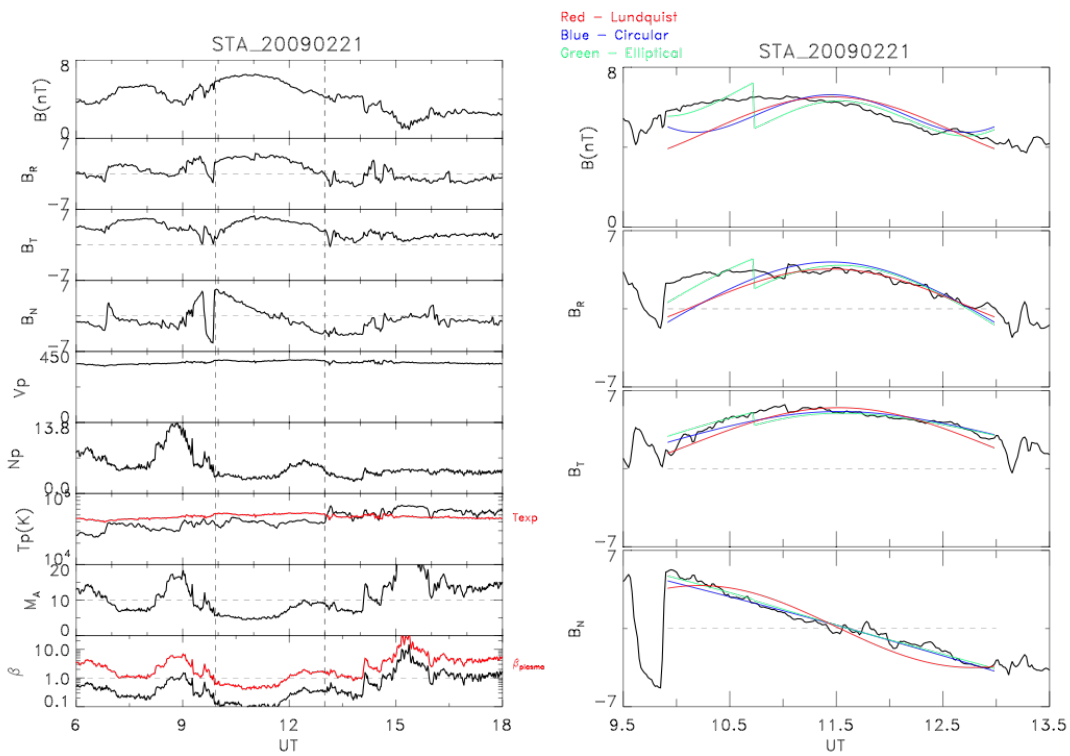

Figure 4-6: Event 1: Fitting the small flux rope observed by STEREO-A on Feb 21, 2009 by analytical models. (a) The small flux rope is between the two vertical lines, 09:55:00 13:00:00. (b) Fit this small flux rope by (i) Blue: analytical model with circular cross-section; (ii) Green: analytical model with elliptical cross-section; (iii) Red: analytical force free model with Lundquist's solution.

The first small flux rope was observed by STEREO-A on Feb 21, 2009 from 09:55:00 to 13:00:00. It is marked in the figure 4-6a by two vertical lines. In this picture, from the top

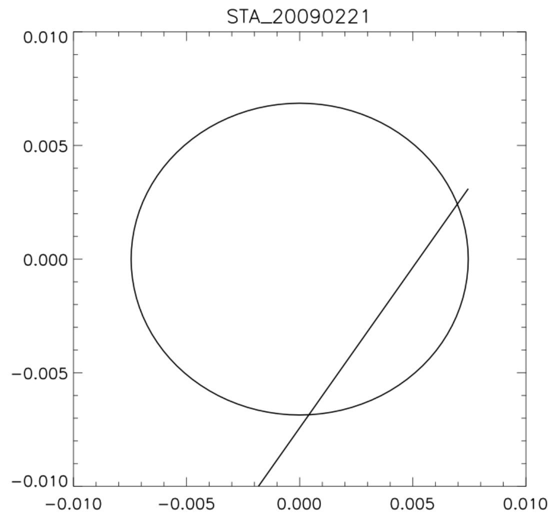

Figure 4-7: Event 1: The spacecraft's trajectory on the elliptical cross-section plane of the event observed by STEREO-A on Feb 21, 2009 (obtained from the analytical model with elliptical cross-section).

to bottom, it is (i) total magnetic field strength B,(ii) the magnetic field component in the RTN coordinate, B_R, (iii) B_T, (iv) B_N, (v) proton velocity, V_P, (vi) proton density, N_P, (vii) proton temperature, T_P (black - observed data; red - expected temperature T_{exp}), (viii) Alfv$\acute{e}$n Mach number, M_A, (ix) beta (black - β_{proton}, red - β_{plasma}).

This event is convect with the background solar wind, which shows that the proton velocity is stable. And $V_P = 391 km/s$, which lies in the slow solar wind. And the observed T_P is clearly lower than T_{exp}. This event, the B_N changed from the positive to negative.

The fittings of this event are shown in the figure 4-6b. From top to bottom are total magnetic field and its components in RTN coordinates (black - observed data; blue - analytical model with circular cross-section; green - analytical model with elliptical cross-section; red - analytical force free model with Lundquist's solution). The fitting with elliptical cross-section has the least normalized chi-square ($\chi^2_{elliptical} = 0.01, \chi^2_{circular} = 0.021, \chi^2_{Lundquist} = 0.027$). However, the non-force free model with elliptical cross-section fitting has a clear discontinuity (especially in the total magnetic field).

The analytical non-force free fitting with circular cross-section obtained the orientation of this small flux rope is: $\theta = 2.0°, \phi = 24.1°$ (the details of the fitting are shown in the Table 4.1). The elliptical cross-section model obtained orientation is: $\theta = 2.0°, \phi = 23.1°$ (see Table 4.2). And the Lundquist's solution obtained the orientation is: $\theta = 1.6°, \phi = 24.1°$ (see Table 4.3). These three orientations are very close. Compared with the orientation from the minimum variance analysis (MVA), which obtained the orientation: $\theta = 11.3°, \phi = 54.1°$ (see Table 4.4), all the three analytical models (no matter non-force free or not) have 32° angle difference.

The spacecraft's trajectory on the elliptical cross-section plane has been plotted in the figure 4-7. The eccentricity is 0.39. The straight line cross the ellipse is the trajectory of the spacecraft mapped on this plane.

Figure 4-8 are the GS-reconstruction results of the event 1, the details of the GS-reconstruction results are shown in the Table 4.5 (without plasma pressure) and Table 4.6 (with plasma pressure). The left two pictures are the magnetic field contour and the fitting residue obtained by considering there is no plasma pressure during the reconstruction ($\beta_{plasma} = 0$). Without the plasma pressure, this reconstruction could be considered as the force-free condition. The orientation here is: $\theta = 14.4°, \phi = 252.2°$.

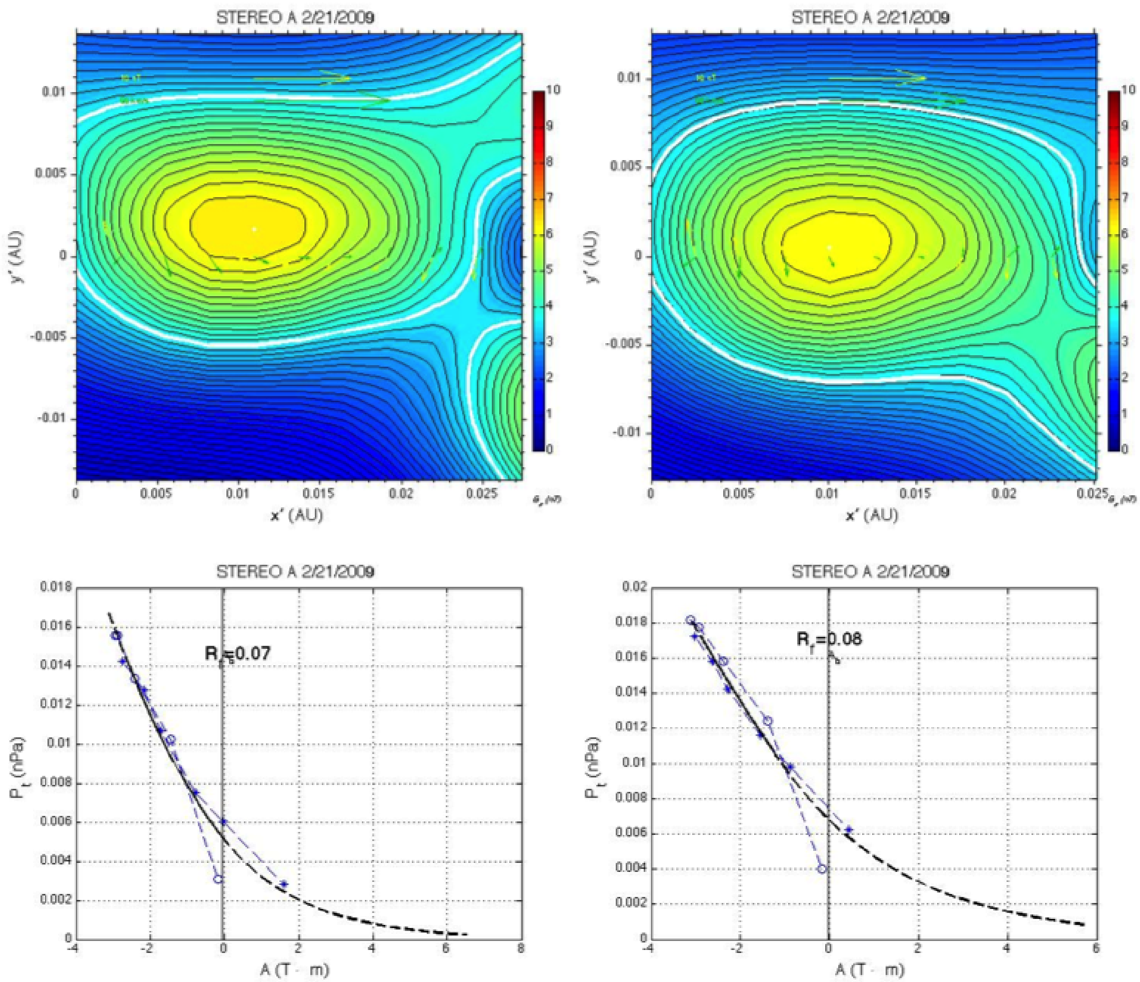

Figure 4-8: Event 1: Fitting the small flux rope observed by STEREO-A on Feb 21, 2009 by numerical model. Left: do not include the plasma pressure in the reconstruction; Right: include the plasma pressure in the reconstruction.

And the right two panels are the results include the plasma pressure into reconstruction. For the small flux ropes observed by the STEREO spacecraft, only the proton pressure is included in the plasma pressure. In the events observed by STEREO spacecraft, we only include the proton into the plasma pressure, that is plasma pressure = proton pressure. In this case, the β_{proton} is 0.191. It is much smaller than 1, so the output results obtained by considering the plasma pressure are close to the results obtained without plasma pressure. The orientation now is: $\theta = 10.3°, \phi = 241.9°$ (32° away from the no pressure condition). Compared with the MVA orientation, they have 157° difference.

Both of the magnetic field contours show elliptical cross-section. And the fitting residue with plasma pressure is 0.076, a little larger than the result without plasma pressure (0.068). While the plasma pressure is small in this case, the GS-reconstruction without it shows a better fitting quality.

Table 4.1: The output results of analytical non-force free model with circular cross-section

Events	θ	ϕ	p	j_φ	j_z	Radius	χ^2
STA-20090221	2.0	24.1	0.0043	10.5	-7.3	0.0073	0.021
STA-20090314	49.1	108	0.0067	-2.8	-4.0	0.0183	0.036
STA-20090506	-52.8	176.9	0.0057	-12.6	6.6	0.0086	0.023
STB-20120614	-1.5	88.8	0.02	-13.5	3	0.024	0.033
Wind-19980716	8.3	118.8	0.00095	-25	-30.5	0.004	0.041
Wind-20060309	-7.2	114.3	0.006	7.2	-6.7	0.014	0.021
Wind-20090115	-12.9	102.8	0.017	4.1	2.9	0.024	0.045
Wind-20100225	28.9	44.7	0.006	6.5	5.1	0.012	0.041

Note: $\theta(°)$ - latitude angle in GSE/RTN coordinate system; $\phi(°)$ - longitude angle in GSE/RTN coordinate system; p (AU) - impact parameter; $j_\varphi(10^{-12}Cm^{-2}s^{-1})$ - poloidal flux; $j_z(10^{-12}Cm^{-2}s^{-1})$ - axial flux; χ^2 - normalized chi-square.

4.4.2 Event 2: STA - 20090314

The event 2 was observed by STEREO-A on March 14, 2009 from 15:05:00 to 19:30:00. It is marked in the figure 4-9 by the vertical lines. The panels in the picture are the same as the event 1. This event is convect with the background solar wind, which shows that the proton

Table 4.2: The output results of analytical non-force free model with elliptical cross-section

Events	θ	ϕ	ξ	p	η	j_η	j_φ	j_z	χ^2
STA-20090221	2.0	23.1	35.3	0.0043	1.59	-1.5	11.7	-10.3	0.01
STA-20090314	-49.2	288	3.2e-11	0.0067	28.5	0.0087	2.8	4.0	0.036
STA-20090506	-54.8	177	38	0.0064	1.43	0.24	-12.1	9.2	0.02
STB-20120614	0.84	268.8	5.2e-11	0.02	11.4	0.09	13.5	3	0.033
Wind-19980716	6.2	134.5	0.0049	2.7e-7	0.37	0.17	-6.87	446.8	0.039
Wind-20060309	-5.3	141.3	0	2.3e-7	247.3	4375.8	5.58	-9.83	0.025
Wind-20090115	-2.7	156.2	0.0001	1.8e-6	0.03	2793.5	0.08	11721.9	0.032
Wind-20100225	39.2	72.5	0.00066	3.6e-7	4.08	-8413.6	1.8	-4.2	0.035

Note: $\theta(^\circ)$ - latitude angle in GSE/RTN coordinate system; $\phi(^\circ)$ - longitude angle in GSE/RTN coordinate system; ξ - tilt angle in the cross-section plane; p (AU) - impact parameter; η - the parameter associated with the eccentricity of the cross-section of the cloud; j_η - the radial component of the plasma current density in the elliptical coordinate system; $j_\varphi(10^{-12}Cm^{-2}s^{-1})$ - poloidal flux; $j_z(10^{-12}Cm^{-2}s^{-1})$ - axial flux; χ^2 - normalized chi-square.

Table 4.3: The output results of analytical force free model with Lundquist's solution

Events	θ	ϕ	p	B_0	H	Radius	χ^2
STA-20090221	1.6	24.1	0.003	7.6	-	0.0066	0.027
STA-20090314	-50.2	284.3	0.0073	8.2	+	0.0187	0.033
STA-20090506	73.6	352.3	0.0069	9.96	-	0.01	0.018
STB-20120614	2.5	268.8	0.0079	12.6	-	0.0155	0.062
Wind-19980716	-9.5	288.7	0.0014	15.1	+	0.0044	0.041
Wind-20060309	-7.8	95.4	0.0087	13.2	-	0.016	0.025
Wind-20090115	-11.6	102.8	0.013	9.9	+	0.022	0.039
Wind-20100225	28.5	44.7	0.004	8.6	+	0.011	0.052

Note: $\theta(^\circ)$ - latitude angle in GSE/RTN coordinate system; $\phi(^\circ)$ - longitude angle in GSE/RTN coordinate system; p (AU) - impact parameter; B_0 - the maximum magnetic field magnitude on the axis; H - helicity of the magnetic field lines; χ^2 - normalized chi-square.

Table 4.4: The output results of minimum variance analysis (MVA)

Events	Ratio	θ	ϕ
STA-20090221	11.3	-9.8	54.1
STA-20090314	11.1	38.5	138
STA-20090506	6.3	43.6	21.7
STB-20120614	7.5	-17.2	118.8
Wind-19980716	25.8	28.4	124.6
Wind-20060309	7.2	-4	120.4
Wind-20090115	5.2	-12.8	132.8
Wind-20100225	11.4	20.2	74.7

Note: Ratio - the ratio of the medium eigenvalue to the minimum eigenvalue; $\theta(^\circ)$ - latitude angle obtained by MVA; $\phi(^\circ)$ - longitude angle obtained by MVA.

velocity is stable. And $V_P = 328km/s$, which lies in the slow solar wind. The observed T_P is higher than T_{exp}. The β_{plasma} is around 1. This event, the B_z changed from the positive to negative.

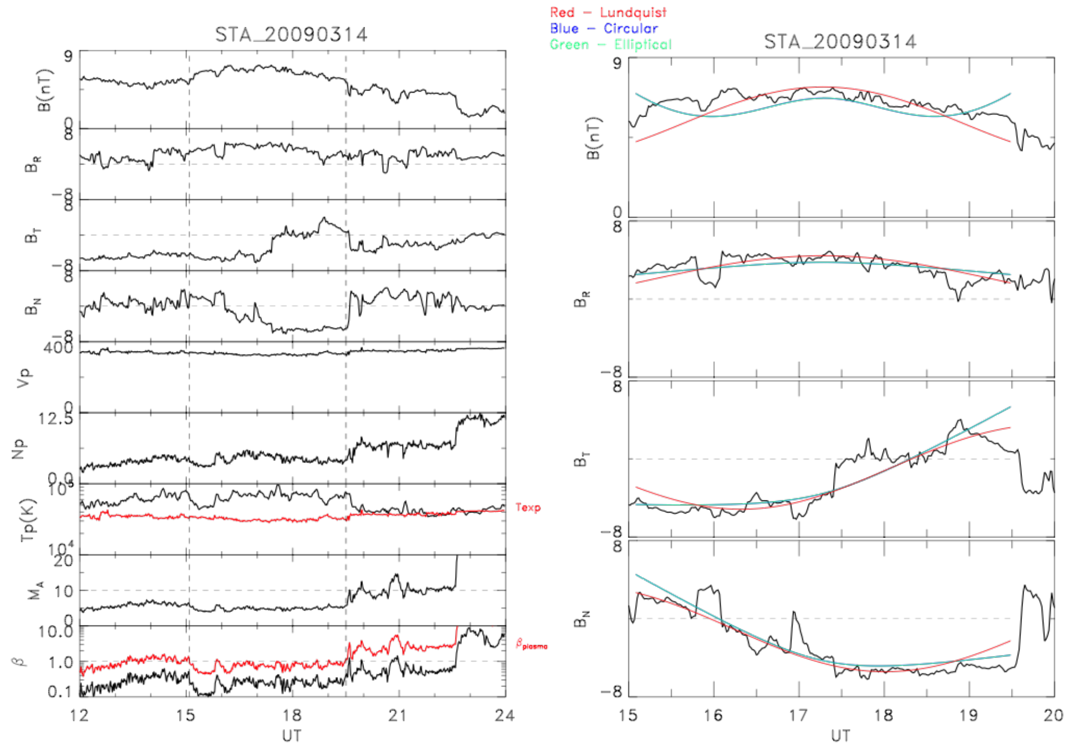

Figure 4-9: Event 2: Fitting the small flux rope observed by STEREO-A on Mar 14, 2009 by analytical models. (a) The small flux rope is between the two vertical lines, 15:05:00 19:30:00. (b) Fit this small flux rope by (i) Blue: analytical model with circular cross-section; (ii) Green: analytical model with elliptical cross-section; (iii) Red: analytical force free model with Lundquist's solution.

From the fittings of this event, the fitted magnetic fields from non-force free model with elliptical cross-section coincident with the fittings with circular cross-section. They have the same normalized chi-square values (0.036). The shape of the cross-section fitted by elliptical modeling also supported the results (see Figure 4-10, the cross-section shows to be the circular shape).

The analytical non-force free fitting with circular cross-section obtained the orientation of this small flux rope is: $\theta = 49.1°, \phi = 108°$. While the elliptical cross-section model obtained orientation is: $\theta = -49.2°, \phi = 288°$. They have 180° angle difference, which still show that their orientations are on the same line. Both of the orientations have 24° angle difference

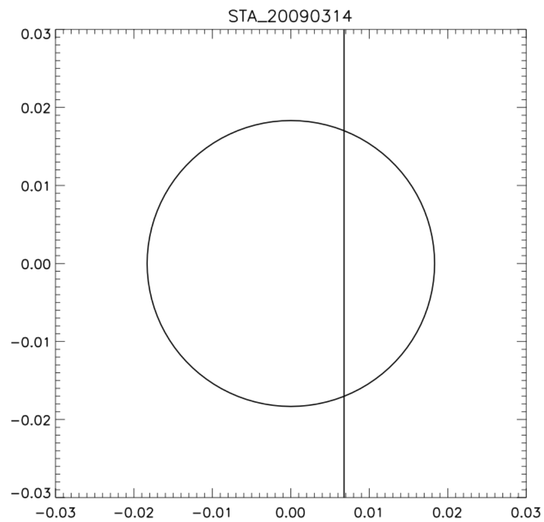

Figure 4-10: Event 2: The spacecraft's trajectory on the elliptical cross-section plane of the event observed by STEREO-A on Mar 14, 2009 (obtained from the analytical model with elliptical cross-section).

with the MVA orientations.

Compared with the fittings by Lundquist's force free solution. Which we obtained $\theta = -50.2°, \phi = 284.3°$. The orientations by the non-force free fittings have $2.6°$ angle difference with Lundquist's orientations. In this case, the normalized chi-square value of Lundquist's solution is smaller (0.033).

Figure 4-11 are results obtained by using the GS-reconstruction on the event 2. Both of the magnetic field contours present the similar shapes of the cross-section (tend to elliptical cross-section). In this case, when considered the condition with pressure, only proton pressure was added into the GS-reconstruction ($\beta_{proton} \sim 0.24$ ¡¡ 1). Therefore the output results obtained by considering the proton pressure are close to the results obtained without proton pressure. The orientation without pressure here is: $\theta = -53.8°, \phi = 168.4°$. And the orientations with proton pressure is: $\theta = -62.4°, \phi = 164.1°$. The angle difference away from the analytical fittings are $\sim 65°$.

All the three analytical models obtained the similar orientations for this event, but the GS-reconstructions show different results.

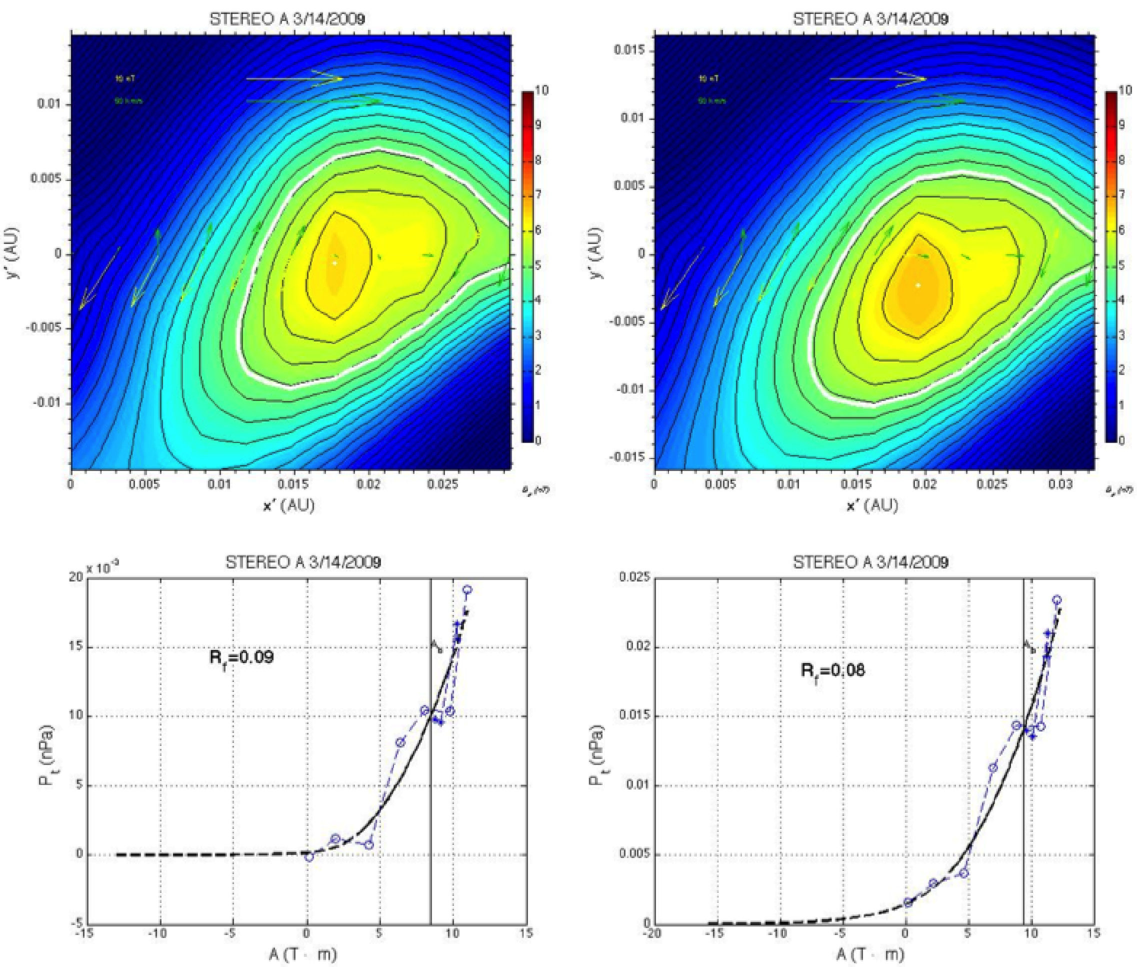

Figure 4-11: Event 2: Fitting the small flux rope observed by STEREO-A on Mar 14, 2009 by numerical model. Left: do not include the plasma pressure in the reconstruction; Right: include the plasma pressure in the reconstruction.

4.4.3 Event 3: STA - 20090506

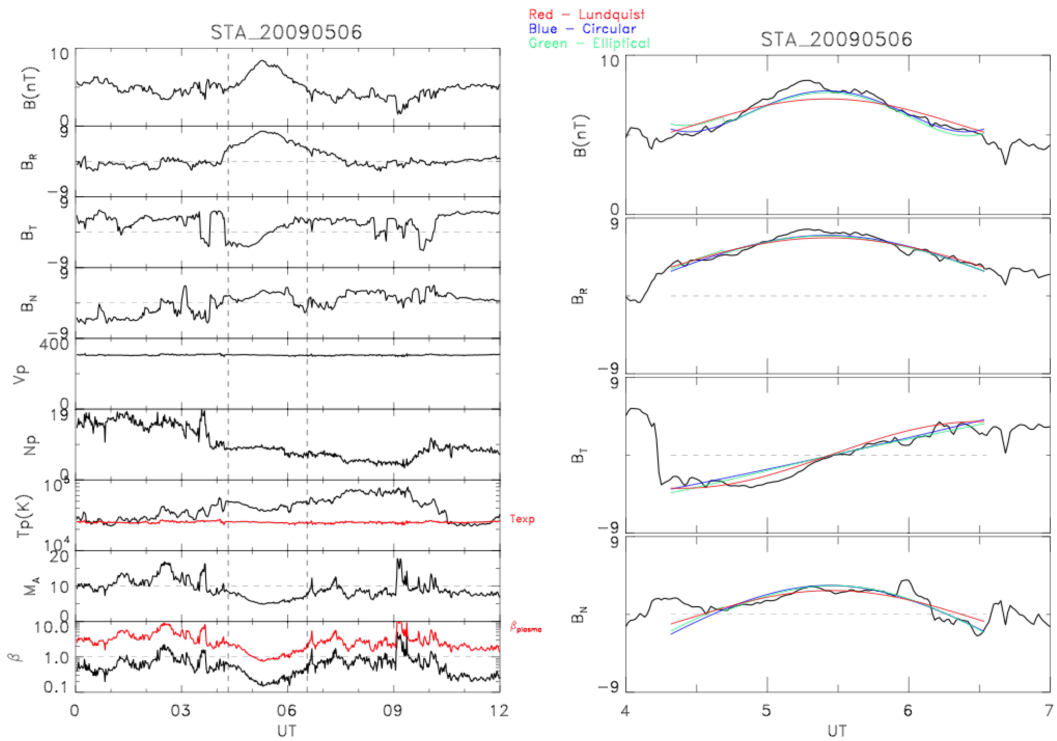

Figure 4-12: Event 3: Fitting the small flux rope observed by STEREO-A on May 06, 2009 by analytical models. (a) The small flux rope is between the two vertical lines, 04:19:00 06:33:00. (b) Fit this small flux rope by (i) Blue: analytical model with circular cross-section; (ii) Green: analytical model with elliptical cross-section; (iii) Red: analytical force free model with Lundquist's solution.

The event 3 was observed by STEREO-A on May 06, 2009 from 04:19:00 to 06:33:00. It is marked in the figure 4-12 by the vertical lines. The panels in the picture are the same as the event 1. This event also has static proton velocity, $V_P = 303km/s$. The observed T_P is higher than T_{exp}. The β_{plasma} is larger than 1. This event, the B_N is positive.

From the fittings of this event, it looks like the non-force free model with elliptical cross-section is better, however, the normalized chi-square shows that the force free model with Lundquist's solution has the minimum value ($\chi^2_{Lundquist} = 0.018, \chi^2_{circular} = 0.023, \chi^2_{elliptical} = 0.02$).

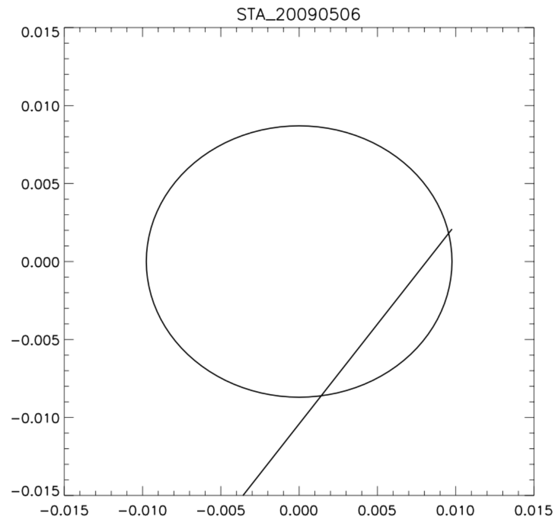

Figure 4-13: Event 3: The spacecraft's trajectory on the elliptical cross-section plane of the event observed by STEREO-A on May 06, 2009 (obtained from the analytical model with elliptical cross-section).

The shape of the cross-section fitted by elliptical non-force free model is plotted in the figure 4-13. The eccentricity is 0.46.

The orientations of the 3 analytical models are: (i) the non-force free model with circular cross-section: $\theta = -52.8°, \phi = 176.9°$; (ii) the non-force free model with elliptical cross-section: $\theta = -54.8°, \phi = 177°$; (iii) the force-free model with Lundquist's solution: $\theta = 73.6°, \phi = 352.3°$. Both non-force free models have orientations close to each other, while the force free model have orientation 160° away from them.

Figure 4-14 is the GS-reconstruction of the event 3, the details of the GS-reconstruction results are shown in the Table 4.3 (without plasma pressure) and Table 4.4 (with plasma pressure). Since $\beta_{proton} \sim 0.32$ ¡ 1 in this event, the magnetic field contours and the fitting residues in both conditions are very close. Both contours present elliptical cross-sections.

The orientations of both GS-reconstruction results are also the same ($\theta = 35.1°, \phi = 143.4°$), however, they are 92.6° away from the analytical modelings, and 85.1° away from the MVA orientations.

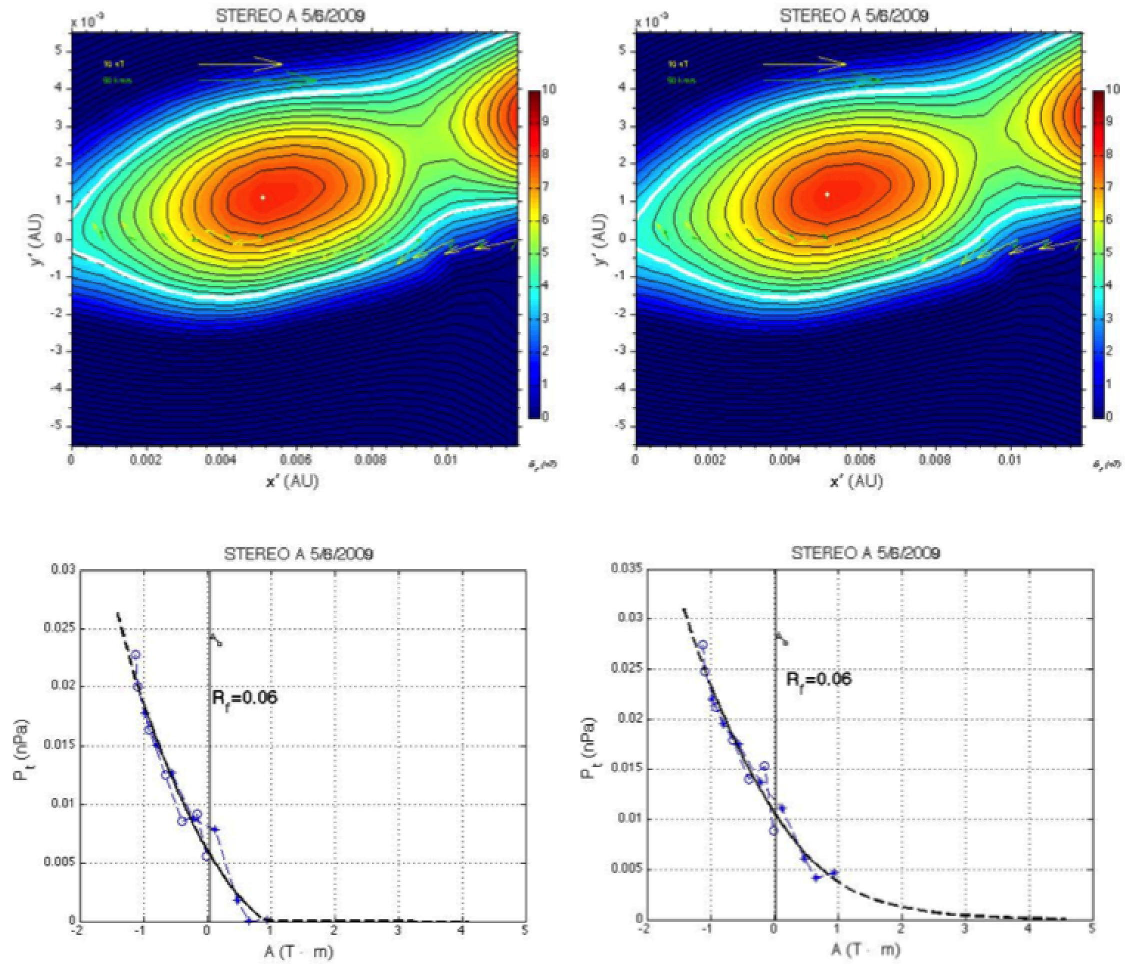

Figure 4-14: Event 3: Fitting the small flux rope observed by STEREO-A on May 06, 2009 by numerical model. Left: do not include the plasma pressure in the reconstruction; Right: include the plasma pressure in the reconstruction.

4.4.4 Event 4: STB - 20120614

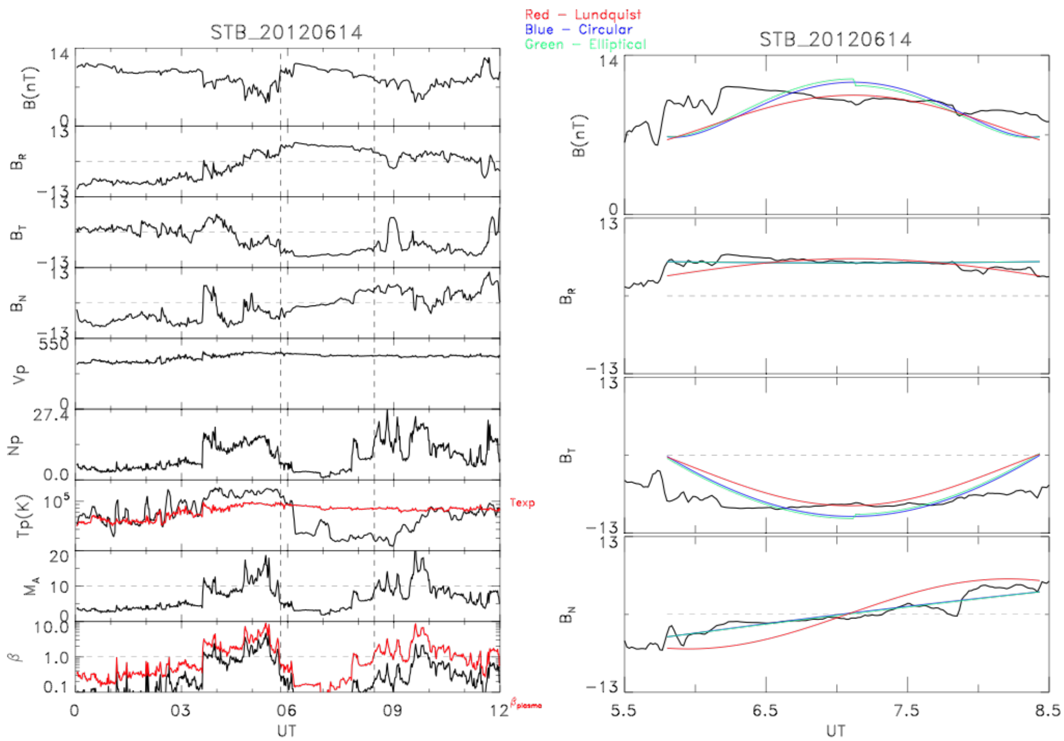

Figure 4-15: Event 4: Fitting the small flux rope observed by STEREO-B on Jun 14, 2012 by analytical models. (a) The small flux rope is between the two vertical lines, 05:48:00 08:27:00. (b) Fit this small flux rope by (i) Blue: analytical model with circular cross-section; (ii) Green: analytical model with elliptical cross-section; (iii) Red: analytical force free model with Lundquist's solution.

The event 4 was observed by STEREO-B on June 14, 2012 from 05:48:00 to 08:27:00. It is marked in the figure 4-15 by the vertical lines. The panels in the picture are the same as the event 1. This event also has stable proton velocity ($V_P = 420km/s$), which lies in the slow solar wind. And the observed T_P is lower than T_{exp}. The β_{plasma} is much smaller than 1. This event, the B_N is from negative to positive.

From the fitting of this event with elliptical cross-section is similar as the fitting with circular cross-section. They have the same normalized chi-square values, and their orientations are on the same line (179.4° away from each other). The shape of the cross-section

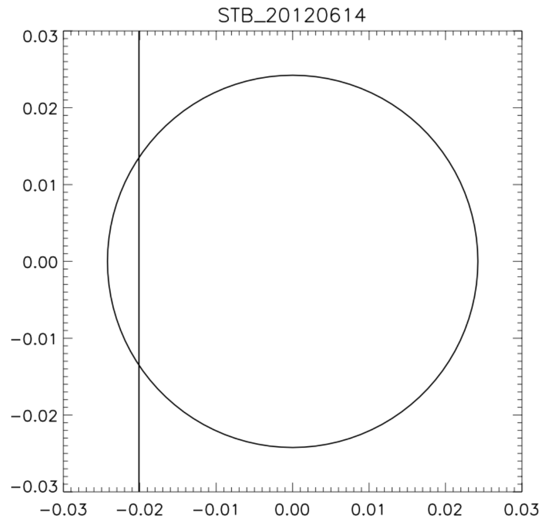

Figure 4-16: Event 4: The spacecraft's trajectory on the elliptical cross-section plane of the event observed by STEREO-B on Jun 14, 2012 (obtained from the analytical model with elliptical cross-section).

from elliptical model is plotted in the Figure 4-16. Compared with the force free model. Both of the non-force free models have smaller normalized chi-square (0.033 compared with 0.062). They have very close orientations (the force free model obtained the orientation: $\theta = 2.5°, \phi = 268.8°$, which is only 1.7° away from the non-force free models). While in this case, the impact parameter obtained from the force free model is smaller than obtained from the non-force free model (0.51 to 0.84).

Figure 4-17 is the GS-reconstruction of the event 4, the details of the GS-reconstruction results are shown in the Table 4.3 and 4.4. Both of the magnetic field contours show elliptical cross-section. And the fitting residue with plasma pressure is 0.154, a little larger than the result without plasma pressure (0.144). While the plasma pressure is small in this case, the GS-reconstruction without it shows a better fitting quality. And the output orientations with pressure are different with the results without pressure (44.5° difference). The orientations also have a large angle difference with the analytical models.

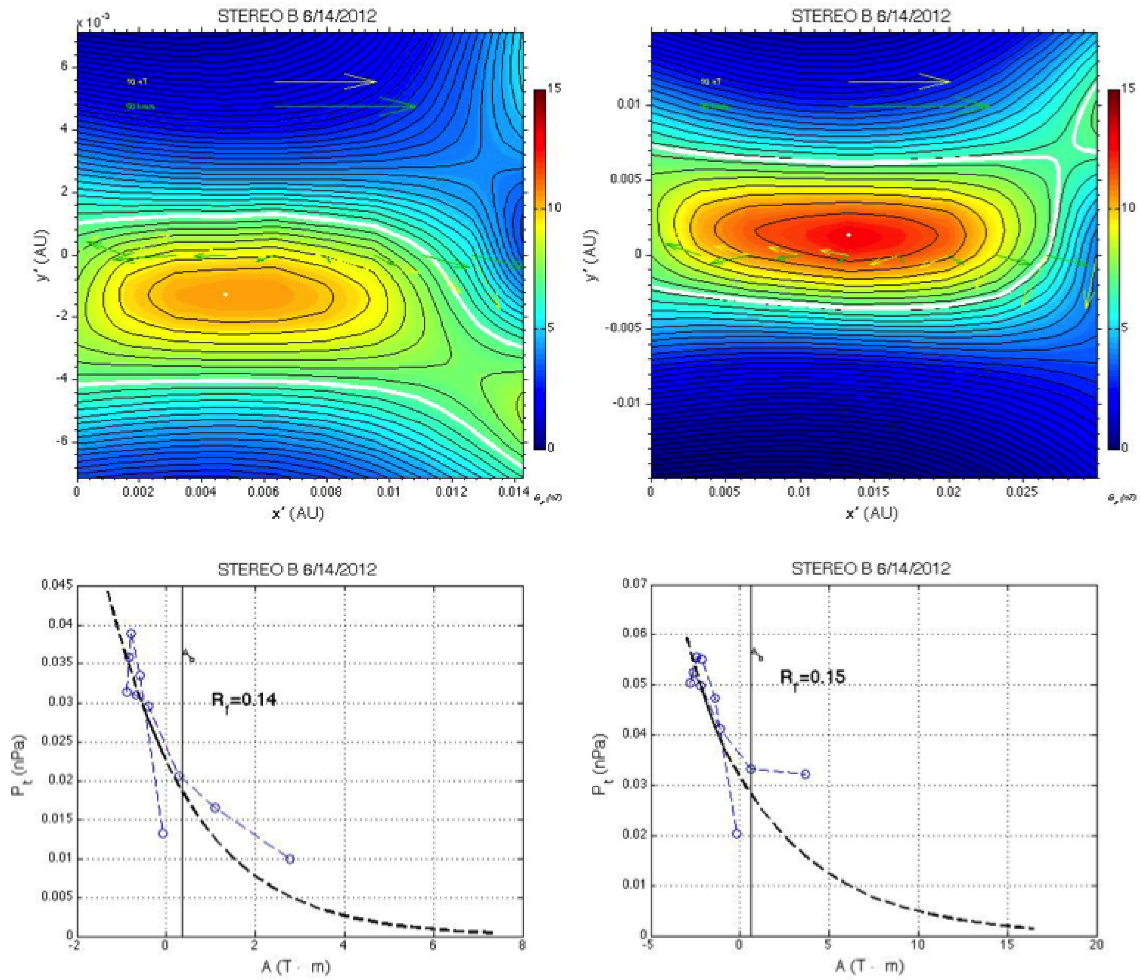

Figure 4-17: Event 4: Fitting the small flux rope observed by STEREO-B on Jun 14, 2012 by numerical model. Left: do not include the plasma pressure in the reconstruction; Right: include the plasma pressure in the reconstruction.

4.4.5 Event 5: Wind - 19980716

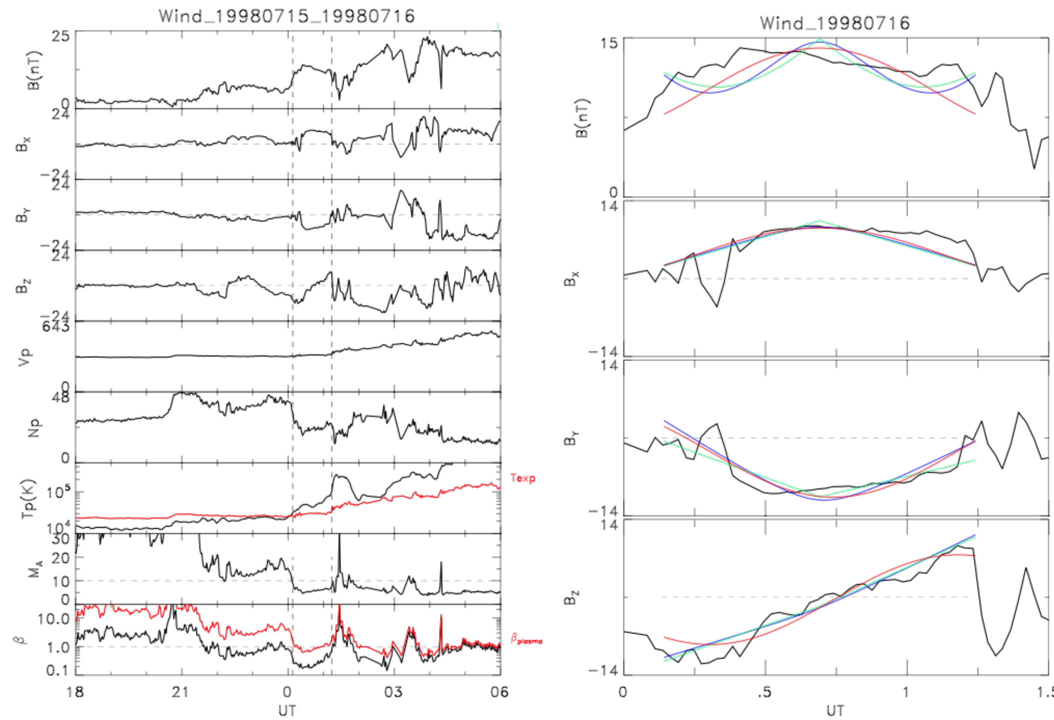

Figure 4-18: Event 5: Fitting the small flux rope observed by Wind on Jul 16, 1998 by analytical models. (a) The small flux rope is between the two vertical lines, 00:08:00 01:14:00. (b) Fit this small flux rope by (i) Blue: analytical model with circular cross-section; (ii) Green: analytical model with elliptical cross-section; (iii) Red: analytical force free model with Lundquist's solution.

The event 5 was observed by Wind on July 16, 1998 from 00:08:00 to 01:14:00. It is marked in the figure 4-18 by the vertical lines. The panels in the picture are the same as the event 1, but the magnetic field components are in the GSE coordinate system. This event is in the stream-stream interaction region, the average $V_P = 334km/s$, which lies in the slow solar wind. The observed T_P is higher than T_{exp}. The β_{plasma} is larger than 1 ($\beta_{plasma} = 1.53$, the events observed by Wind considered both proton and electron into the β_{plasma}). This event, the B_z is from negative to positive.

From the fittings of this event, the elliptical cross-section has the smallest normalized

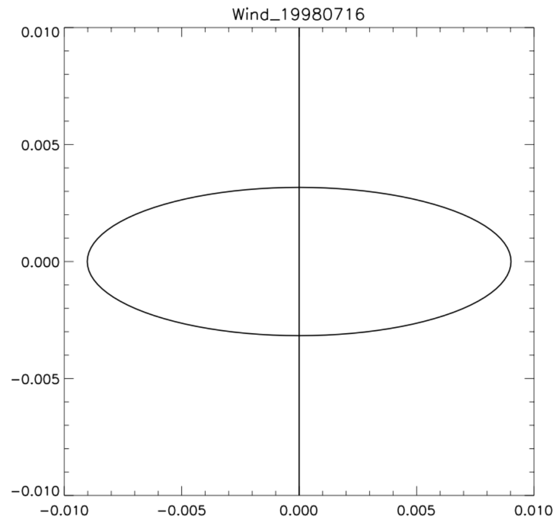

Figure 4-19: Event 5: The spacecraft's trajectory on the elliptical cross-section plane of the event observed by Wind on Jul 16, 1998 (obtained from the analytical model with elliptical cross-section).

chi-square ($\chi^2_{elliptical} = 0.039, \chi^2_{circular} = 0.041, \chi^2_{circular} = 0.041$). The orientations of these three analytical models are close, the angle differences between them are between 10° to 15°. They have 20° to 25° angle way from the MVA orientations. The shape of the cross-section obtained by elliptical model is shown in Figure 4-19. The eccentricity is 0.94.

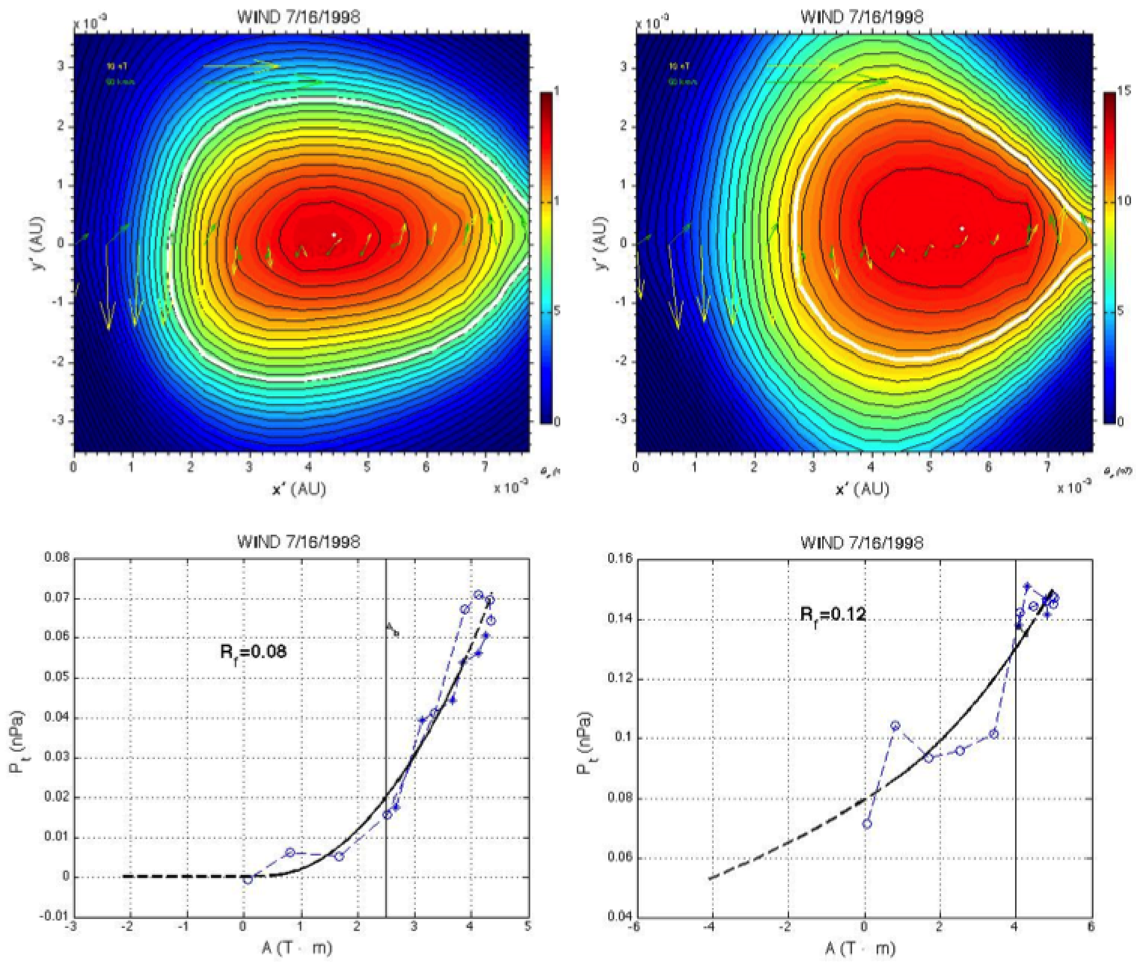

Figure 4-20: Event 5: Fitting the small flux rope observed by Wind on Jul 16, 1998 by numerical model. Left: do not include the plasma pressure in the reconstruction; Right: include the plasma pressure in the reconstruction.

Figure 4-20 is the GS-reconstruction of the event 5. Since in this case, the $\beta_{plasma} > 1$, the magnetic field contour with pressure is different with the magnetic field contour without pressure. The contour with pressure exhibits bigger and unsymmetrical cross-section, while the contour without pressure tend to close to a circular cross-section.

The orientations of both conditions are close to each other (8° angle difference). The GS-reconstruction without pressure has a smaller fitting residue in this case, which means the without pressure condition shows a better fitting quality. The orientations of the GS-reconstructions have a large angle difference with the analytical models ($\sim 120°$).

Table 4.5: The output results of GS-reconstruction model without plasma pressure

Events	θ	ϕ	β	R_f	B_{zmax}	y_0	j_z	j_φ
STA-20090221	14.4	252.2	0	0.0677	6.5	0.0016	0.007	0.046
STA-20090314	-53.8	168.4	0	0.0934	6.7	0.0006	0.006	0.037
STA-20090506	35.1	143.4	0	0.0555	8.2	0.0011	0.001	0.022
STB-20120614	-2.6	152	0	0.1443	10.6	0.0013	0.003	0.025
Wind-19980716	0.21	311.7	0	0.0781	13.4	0.0002	0.001	0.028
Wind-20060309	-9.4	145.5	0	0.0945	10.5	0.0007	0.003	0.057
Wind-20090115	2.6	145.2	0	0.0645	10.3	0.0078	0.005	0.06
Wind-20100225	47.6	85.5	0	0.0651	8.6	0.0135	0.009	0.134

Note: $\theta(°)$ - latitude angle in GS coordinate system; $\phi(°)$ - longitude angle in GS coordinate system; β - average proton beta for STEREO and plasma beta (proton + electron) for Wind's events; R_f - fitting residue; B_{zmax} - maximum B along the axis; y_0 (AU) - minimum distance to the flux rope axis; $j_z(10^{21}Mx)$ - axial flux; $j_\varphi(10^{21}Mx)$ - poloidal flux.

Table 4.6: The output results of GS-reconstruction model with plasma pressure

Events	θ	ϕ	β	R_f	B_{zmax}	y_0	j_z	j_φ
STA-20090221	10.3	241.9	0.191	0.0762	6.3	0.0005	0.006	0.046
STA-20090314	-62.4	164.1	0.24	0.0814	6.8	0.0023	0.008	0.044
STA-20090506	35.1	143.4	0.317	0.0574	8.2	0.0012	0.001	0.022
STB-20120614	-2.3	107.5	0.404	0.1537	12.7	0.0013	0.011	0.054
Wind-19980716	8.1	311.8	1.531	0.1174	13.4	0.0003	0.001	0.015
Wind-20060309	-0.22	145.6	1.564	0.084	10.6	0.0014	0.003	0.045
Wind-20090115	-6.6	148.8	0.914	0.0956	10.8	0.0003	0.004	0.046
Wind-20100225	34.6	100.8	0.768	0.0618	7.2	0.0027	0.009	0.043

Note: $\theta(°)$ - latitude angle in GS coordinate system; $\phi(°)$ - longitude angle in GS coordinate system; β - average proton beta for STEREO and plasma beta (proton + electron) for Wind's events; R_f - fitting residue; B_{zmax} - maximum B along the axis; y_0 (AU) - minimum distance to the flux rope axis; $j_z(10^{21}Mx)$ - axial flux; $j_\varphi(10^{21}Mx)$ - poloidal flux.

4.4.6 Event 6: Wind - 20060309

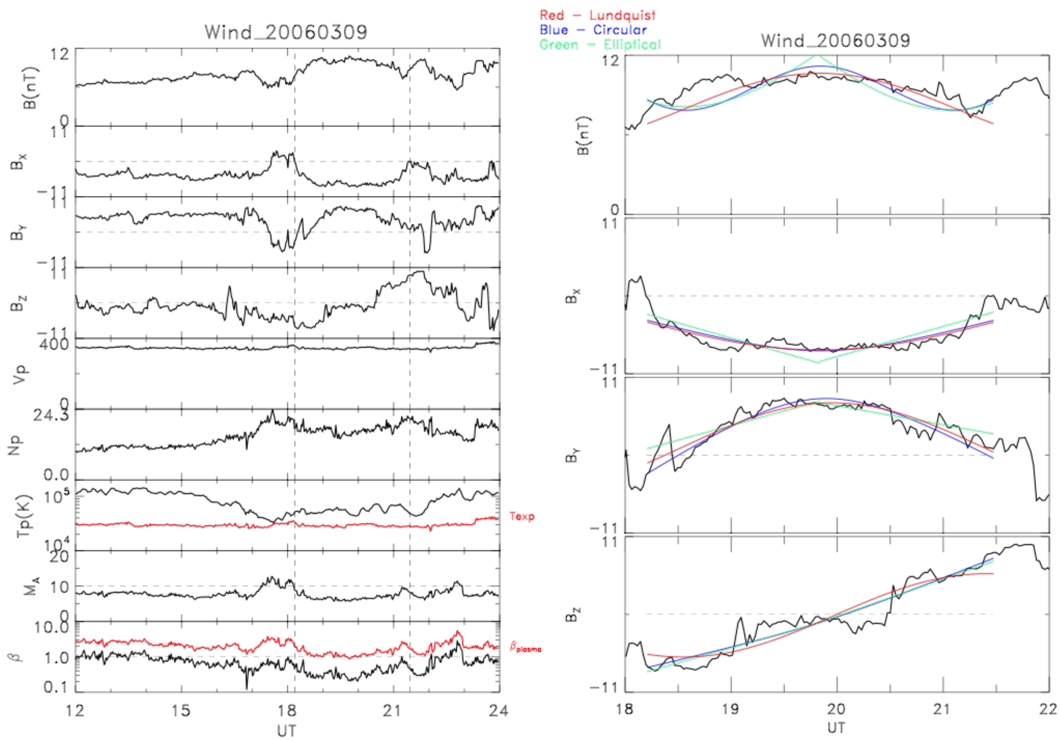

Figure 4-21: Event 6: Fitting the small flux rope observed by Wind on Mar 09, 2006 by analytical models. (a) The small flux rope is between the two vertical lines, 18:12:00 21:28:00. (b) Fit this small flux rope by (i) Blue: analytical model with circular cross-section; (ii) Green: analytical model with elliptical cross-section; (iii) Red: analytical force free model with Lundquist's solution.

The event 6 was observed by Wind on March 09, 2006 from 18:12:00 to 21:28:00. It is marked in the figure 4-21 by the vertical lines. The panels in the picture are the same as the event 5. This event also has stable proton velocity ($V_P = 343km/s$), which lies in the slow solar wind. And the observed T_P is higher than T_{exp}. The β_{plasma} is larger than 1 ($\beta_{proton} = 1.56$). This event, the B_z is from negative to positive.

From the fittings of this event, the modeling with circular cross-section shows the smallest normalized chi-square ($\chi^2_{circular} = 0.021$, while the other two are both 0.025). The modeling with elliptical cross-section also output the shape of the cross-section close to the circle (see

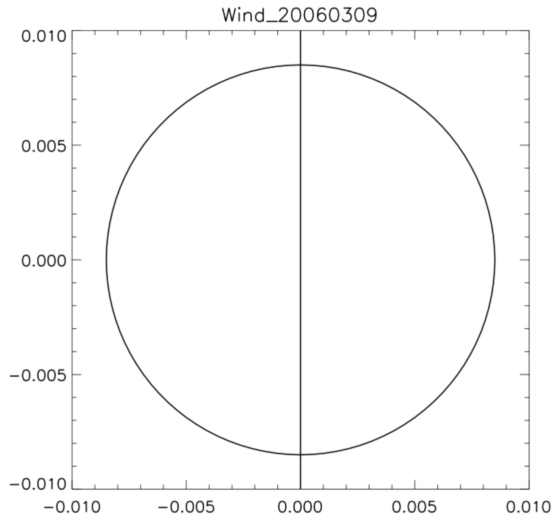

Figure 4-22: Event 6: The spacecraft's trajectory on the elliptical cross-section plane of the event observed by Wind on Mar 09, 2006 (obtained from the analytical model with elliptical cross-section).

the Figure 4-22). The orientations from the non-force free model with circular cross-section is very close to the MVA results ($\sim 6.8°$), while the Lundquist's and non-force free model with elliptical cross-section's orientations have $\sim 25°$ angle difference.

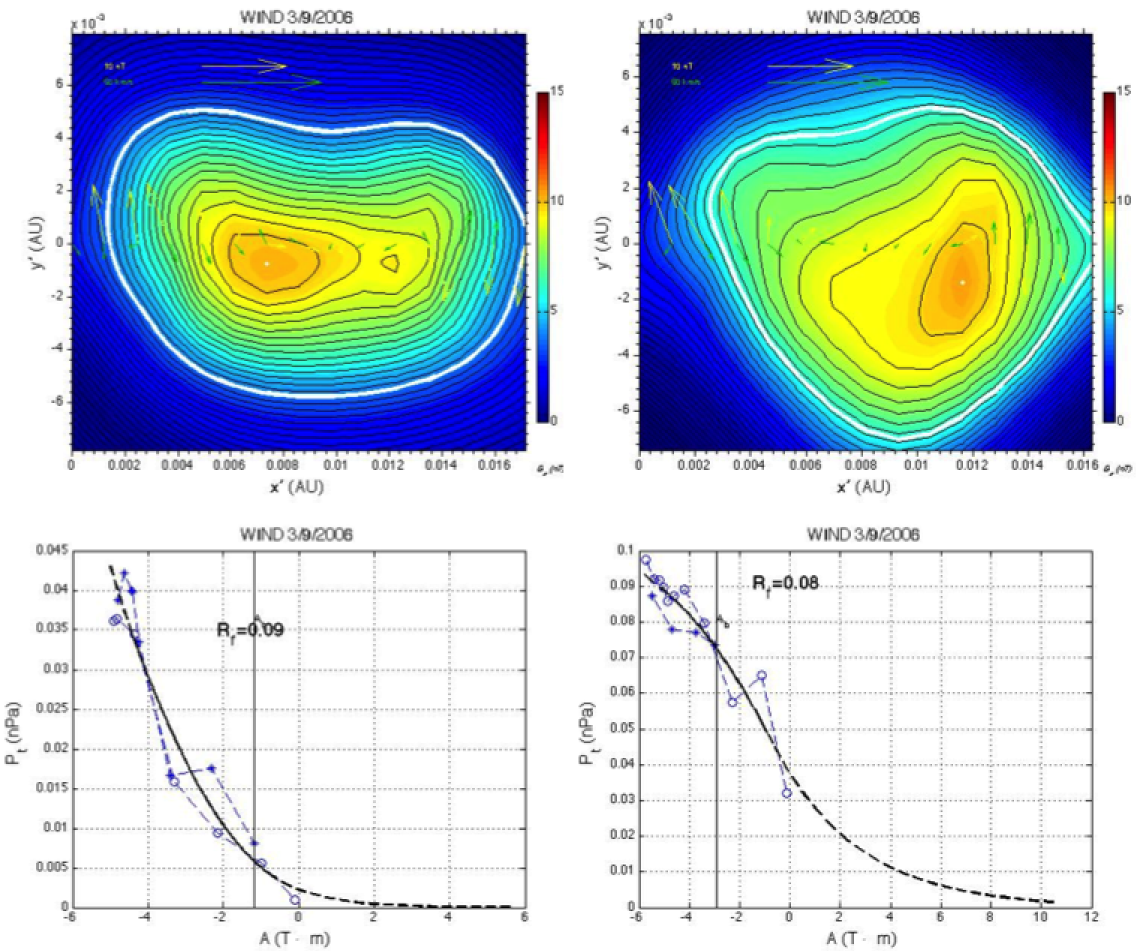

Figure 4-23: Event 6: Fitting the small flux rope observed by Wind on Mar 09, 2006 by numerical model. Left: do not include the plasma pressure in the reconstruction; Right: include the plasma pressure in the reconstruction.

Figure 4-23 is the GS-reconstruction of the event 6. Since the β_{plasma} is larger than 1 in this case, the output magnetic field contour with pressure is different with the contour without pressure, but both present elliptical shape. And the fitting residue with pressure is a little smaller. These two conditions obtained the orientations close to each other. And they have $\sim 30^\circ$ angle difference with the orientations obtained by the analytical models.

4.4.7 Event 7: Wind - 20090115

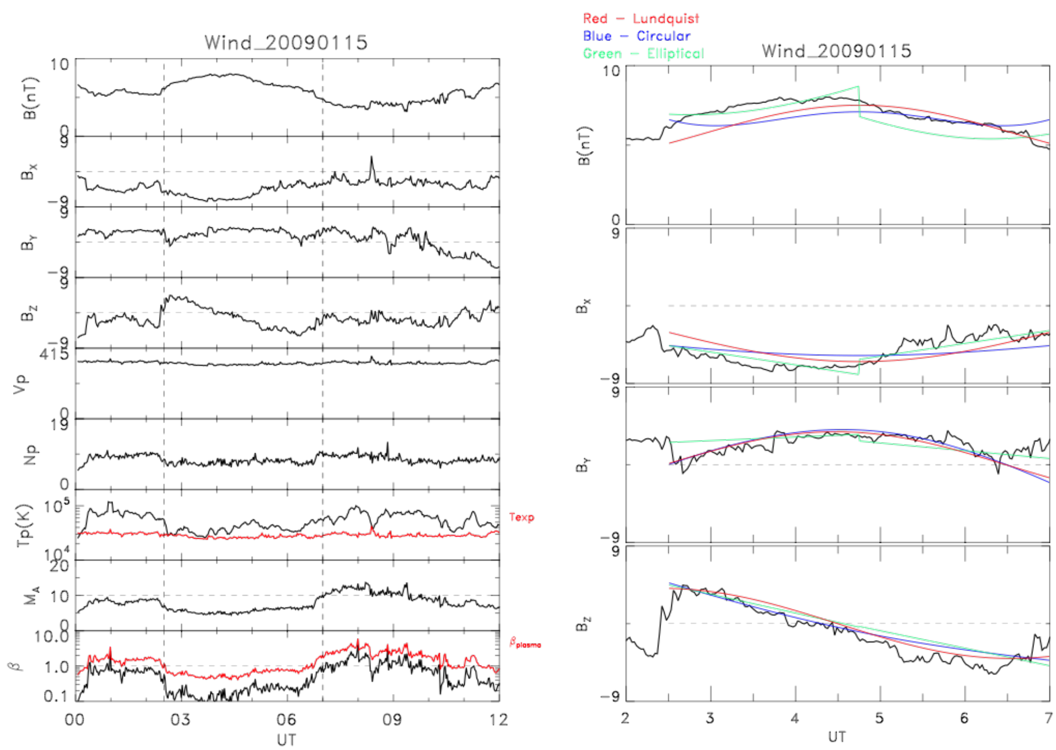

Figure 4-24: Event 7: Fitting the small flux rope observed by Wind on Jan 15, 2009 by analytical models. (a) The small flux rope is between the two vertical lines, 02:30:00   07:00:00. (b) Fit this small flux rope by (i) Blue: analytical model with circular cross-section; (ii) Green: analytical model with elliptical cross-section; (iii) Red: analytical force free model with Lundquist's solution.

The event 7 was observed by Wind on January 15, 2009 from 02:30:00 to 07:00:00. It is marked in the figure 4-24 by the vertical lines. The panels in the picture are the same as the

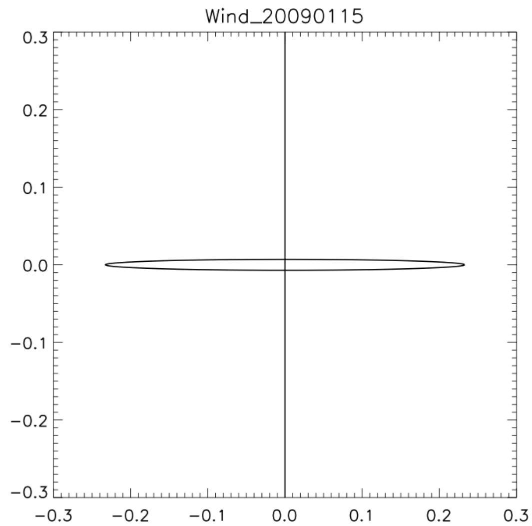

Figure 4-25: Event 7: The spacecraft's trajectory on the elliptical cross-section plane of the event observed by Wind on Jan 15, 2009 (obtained from the analytical model with elliptical cross-section).

event 5. This event has stable proton velocity ($V_P = 321km/s$), which lies in the slow solar wind. And the observed T_P is higher than T_{exp}. The β_{plasma} is close to 1 (~ 0.91). This event, the B_z is from positive to negative.

From the fittings of this event with elliptical cross-section model has the smallest normalized chi-square. There are clear discontinuities in the fittings. The shape of the cross-section shows a very narrow elliptical structure, the eccentricity is 0.9995. The orientations of these three analytical models are close, they have $25° - 30°$ angle differences with MVA's results.

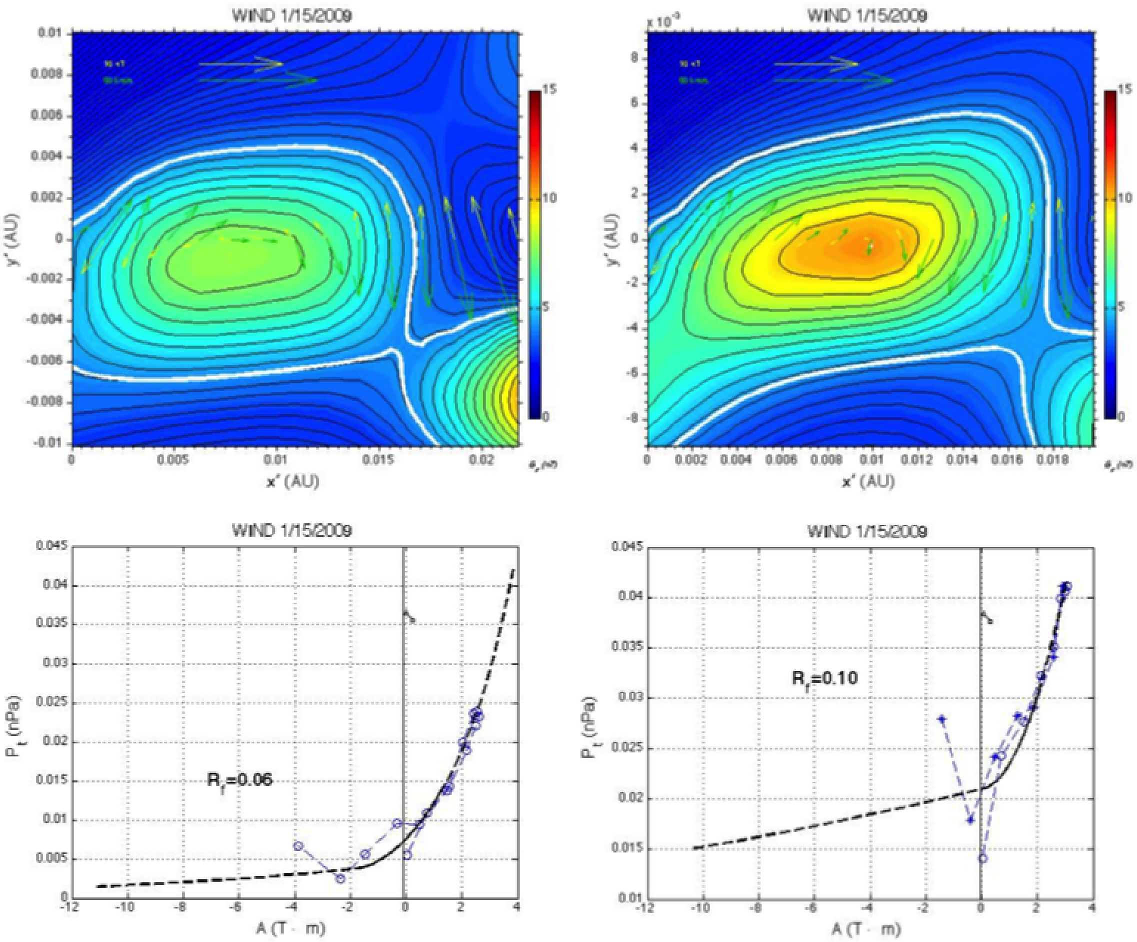

Figure 4-26: Event 7: Fitting the small flux rope observed by Wind on Jan 15, 2009 by numerical model. Left: do not include the plasma pressure in the reconstruction; Right: include the plasma pressure in the reconstruction.

Figure 4-26 is the GS-reconstruction of the event 7. Both of the magnetic field contours show elliptical cross-section. And the fitting residue with plasma pressure is 0.096, a little larger than the result without plasma pressure (0.065). While the plasma pressure is smaller than 1 in this case, the GS-reconstruction without it shows a better fitting quality.

The orientations with pressure are close to the without pressure's. And both orientations are close to the analytical models' results (there is only 8.3° angle difference between the orientations obtained from GS-reconstruction with pressure and the analytical non-force free model with elliptical cross-section).

4.4.8 Event 8: Wind - 20100225

The event 8 was observed by Wind on February 25, 2010 from 15:18:00 to 18:28:00. It is marked in the figure 4-27 by the vertical lines. The panels in the picture are the same as the event 5. This event shows that the proton velocity is stable ($V_P = 360 km/s$), which lies in the slow solar wind. And the observed T_P is lower than T_{exp}. The β_{plasma} is less than 1 (~ 0.77). This event, the B_z is positive.

From the fittings of this event, the non-force free model with elliptical cross-section has the smallest normalized chi-square ($\chi^2_{elliptical} = 0.035, \chi^2_{circular} = 0.041, \chi^2_{Lundquist} = 0.052$). There are clear discontinuities on the fittings with elliptical cross-section, and the output shape of the cross-section tend to be circular (see Figure 4-28). The orientations obtained from the elliptical model are close to the MVA's results, while the other two models (which obtained the same orientations) are a little further away.

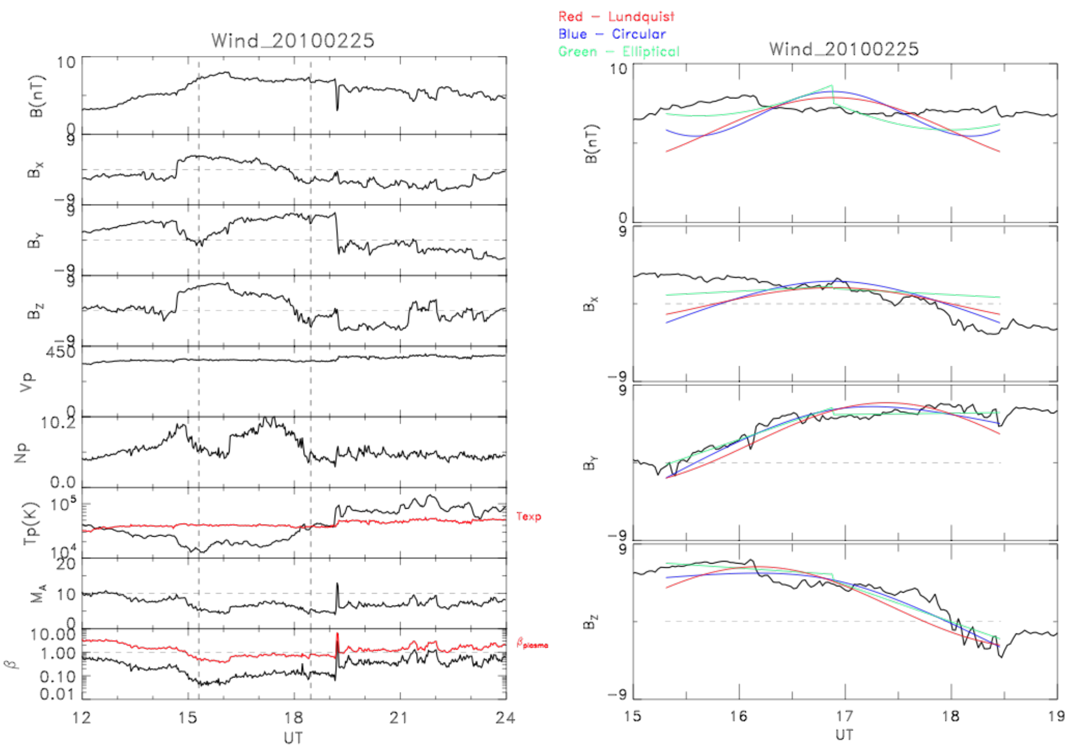

Figure 4-27: Event 8: Fitting the small flux rope observed by Wind on Feb 25, 2010 by analytical models. (a) The small flux rope is between the two vertical lines, 15:18:00 18:28:00. (b) Fit this small flux rope by (i) Blue: analytical model with circular cross-section; (ii) Green: analytical model with elliptical cross-section; (iii) Red: analytical force free model with Lundquist's solution.

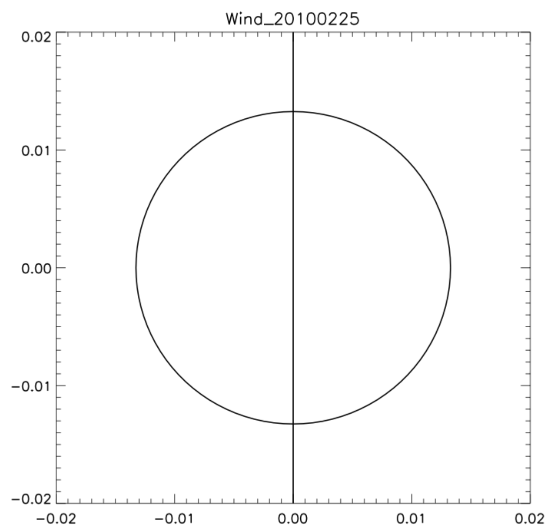

Figure 4-28: Event 8: The spacecraft's trajectory on the elliptical cross-section plane of the event observed by Wind on Feb 25, 2010 (obtained from the analytical model with elliptical cross-section).

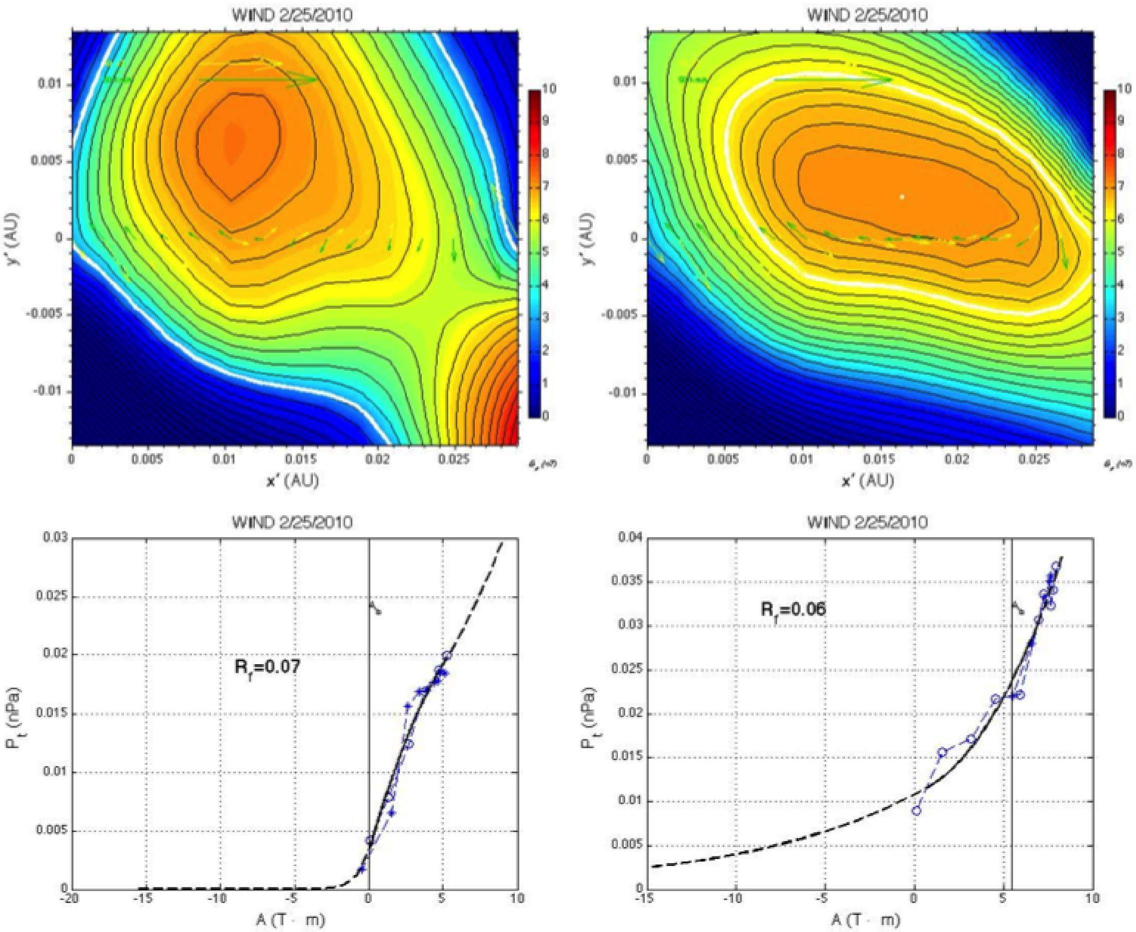

Figure 4-29: Event 8: Fitting the small flux rope observed by Wind on Feb 25, 2010 by numerical model. Left: do not include the plasma pressure in the reconstruction; Right: include the plasma pressure in the reconstruction.

Figure 4-29 is the GS-reconstruction of the event 8. The magnetic field contour without plasma pressure is very different with the other. The contour without pressure tends to be circular, while the contour with pressure is elliptical. The fitting residue with plasma pressure is 0.062, a little smaller than the result without plasma pressure (0.065). While the plasma pressure is not small in this case, the GS-reconstruction with it shows a better fitting quality.

The orientations from the GS-reconstructions under the two conditions are close ($\sim 17°$ angle difference). The orientations are also close to the analytical models' (only 12° away from the non-force free model with elliptical cross-section).

4.5 Results and Discussion

4.5.1 Results

We modeled the small flux ropes by two non-force free methods (one with circular cross-section, the other with elliptical cross-section).

The non-force free model with circular cross-section also has a simple solution as the force free model with Lundquist's solution. It could also fit the observed magnetic field components as well as and sometimes better than the Lundquist's model. However, for the total magnetic field, sometimes it still has some differences with the observed data.

The non-force free model with elliptical cross-section is a more general condition. In some of our examples, it could get the smallest normalized chi-square. And the fitting results are also very good; the orientations are close to the MVA results. All the three analytical models (no matter force free or non-force free), their orientations are close (the angle differences are no more than 30°).

From the GS-reconstruction, the small flux ropes tend to have elliptical cross-section. In this case, the elliptical cross-section model will be better than the circular cross-section model. The orientations obtained from the GS-reconstruction are mostly different with the analytical models' results.

4.5.2 Discussion

Lundquist's force free model with circular cross-section is used by a large number of researchers in the past 20 years. One reason is because this model could fit the flux ropes very well. This force free model could fit very well on the magnetic field components, especially for the events with symmetric structures. Another reason is because the Lundquist's solution is very simple, and could be used easily. However, when more and more flux ropes were observed, some of them have very high β_{plasma} (see the results in last chapter). Therefore in this case, the force free model does not work anymore. And also there are some events they do not have symmetric structures, where the symmetric circular cross-section could not fit these conditions.

In this chapter, we studied two non-force free models. One with circular cross-section, the other is elliptical cross-section. The circular cross-section model also has a very simple solution. In most of the cases, the non-force free model with circular cross-section could also fit the flux ropes components very well. However, for the total magnetic field, they sometimes have a little difference with the observed data. Since this model considered the plasma pressure, it could be more reliable than the force free model. And in almost all of the 8 fittings, it could get the similar or even better fitting quality than the force free model. And this model also output the current densities information. While this model is a symmetric one, therefore for some conditions, it still could not fit very well.

The other model is the non-force free model with elliptical cross-section. This one is more general than the circular cross-section. And in some of the conditions, it could fit better than the other two analytical models. However, this solution also has some disadvantages. For example, in some events, this model has discontinuities on the fittings.

From the 8 examples fittings, the GS-reconstruction shows that the cross-sections of these small flux ropes tend to elliptical. The orientations obtained from the GS-reconstruction are usually different with the analytical fitting results (especially on the events observed by STEREO spacecraft). One main reason is because when we use the GS-reconstructions on the events at STEREO, we only include the proton pressure into the reconstruction, while the plasma pressure is much larger than the proton pressure. Another reason is because the fitting residues with plasma pressure are not better than the fitting residues without plasma pressure. Therefore, in some of the GS-reconstructions with plasma pressure, we did not get better fittings.

Therefore, if we want to improve our non-force free models. We have to consider the more general situations. E.g., the current densities are not constant; they could be changed with time and distance to the center of the flux ropes. Since in both of the models, we assumed the magnetic fields have only two components (that is, $B_r = 0$ in both of the models). We could improve our models by adding more general situations. In addition, when we solve the Maxwell equations, we could try to find another solutions which maybe even better than this one we used right now. Or we could follow other people's idea, consider the flux ropes have neither circular nor elliptical cross-section, but rather a convex-outward, "pancake" shape (Riley et al. [2004]; Riley and Crooker [2004]).

Chapter 5

Geoeffectiveness of STs

It is known that substorms can be caused by a southward interplanetary magnetic field. In our studies we have observed thousands of STs. Many of them have intervals of southward magnetic field. This motivates us to study if STs can be associated with magnetic substorms or even storms. In this chapter, we studied 615 STs (not just limited to the small flux ropes) which have durations between [1, 5] h by using OMNI's 1-min data. We showed that not only the small flux ropes, but also the other STs could be associated with magnetic storms and substorms. There are 47 % of them associated with magnetic substorms (288 events). In our statistical studies, most of them have B_y, B_z bipolar signatures and a southward B_z signature (in which $B_z <$ -3 nT for more than 1h). In these 615 STs, we find that 21 STs are associated with moderate magnetic storms (3.4 %) and 5 STs are associated with intense magnetic storms ($\sim$ 1 %). All those STs related with magnetic storms have low B_z values ($<$ -10 nT) lasting for more than 1h.

5.1 Introduction

Magnetic storms and substorms are two main appearances of geomagnetic activity (Chapman and Bartels [1940]; Akasofu [1964]). The magnetic storm is a temporary disturbance of the

Earth's magnetosphere. It usually has a strong decrease in the horizontal component of the earth's magnetic field (Chapman and Bartels [1940]). The essential feature of a magnetic storm is a significant development and energization of the ring current Kamide et al. [1998]. It can be monitored by the Dst index (disturbance - storm time index). A magnetic storm has three phases: initial, main and recovery. It is classified as moderate (minimum Dst is between -100 nT and -50 nT), intense (minimum Dst is between -250 nT and -100 nT) and super-storm (minimum Dst $<$ -250 nT).

The magnetic substorm is also called auroral substorm. Substorms were first seen in auroral displays by Akasofu in the 1960's (Akasofu [1964]). The dayside merging of the magnetic fields of the Earth and the solar wind followed by reconnection in the near-magnetotail causes energy to be released from the tail of the magnetosphere and injected into the high latitude ionosphere and plasma sheet. The magnetic substorm has been called "The flare on Earth", and this is because it has the similar energy transfers at a fast rate that occur in flares and with the same physical mechanisms (mainly reconnection).

Substorms include growth phase, expansion phase and recovery phase. The growth phase is related to the loading process in the tail lobe, which is created by the magnetic reconnection on the dayside. The growth phase is usually a 60 min long process with the magnetic energy accumulation in the tail lobes. The energy accumulation leads to a 30 min long expansion phase of energy dissipation in the plasma sheet (PS) - ionosphere system, which we call the unloading process (Akasofu [2013]). Then the recovery phase sets in and usually lasting for 90 min (Feldstein et al. [2011]).

Feng et al. [2010] studied 26 small magnetic flux ropes which were observed by Wind from year 2000 to 2002. 18 small flux ropes gave rise to magnetospheric substorms. 14/18 substorm expansion phases were triggered by a northward turning of the interplanetary magnetic field in the small magnetic flux ropes. 4/18 expansion phases were triggered by sudden changes in the solar wind dynamic pressure. Both triggers were related to magnetic directional discontinuities. Based on these results, the authors suggested that substorms have 2 external triggers: (1) sudden enhancements or drops in solar wind dynamic pressure (Schieldge and Siscoe [1970]; Kawasaki et al. [1971]; Burch [1972]; Kokubun et al. [1977]; Liou [2007]). (2) A northward turning of the IMF (Burch [1972]; Caan et al. [1975]; Rostoker [1983]; Samson and Yeung [1986]). Because of their short duration, SIMFRs should be more effective for substorm triggering.

Zhang et al. [2013] studied 141 small flux ropes, and found that bipolar B_y, B_z variations are associated with substorms. They studied the small flux ropes, duration between [0.5, 4] h. They demonstrated that the B_z bipolar signatures from south to north (SN) and from north to south (NS) are associated with different substorm activities, and the B_z bipolar signatures only drive substorms, and not magnetic storms.

In our study, we extended this work to the small transients (not only small flux ropes). We focus on the STs which have duration between [1, 5]h, which we showed to be the most common (see Chapter 3). We are interested in searching if the STs could associated with magnetic substorms or storms.

5.2 Methodology

In this chapter, we use the STs events observed by Wind spacecraft. The OMNI website (omniweb.gsfc.nasa.gov/from/omni_min.html) is used to examine the solar wind data and the STs arrival time at L1. The 1-min data resolution has been used to plot the magnetic fields and other substorm indices (AE, AL, SYM-H). According to the above duration criteria and the OMNI data check, we finally obtained 615 STs.

AE and AL indices are good indicators of magnetic substorms. In Zhang et al. [2013]'s study, they used the magnitudes of AE/AL > 100 nT as a criterion to select substorms (they suggested the values of AE/AL larger than 100 nT occurred during the interval from 1h before the small flux rope and 1 h after it is considered to be associated with the substorm). In our study, we use the magnitudes of AE/AL > 150 nT as the criterion to select the substorms. And we require the values to be larger than 150 nT during the intervals of the STs. That is, we do not study the substorms before/after the STs.

The 1-min SYM-H index has also been examined. We ask the question: Is there a magnetic storm associated with ST passage at Earth?. WE first show 6 substorm events and then present our statistical studies of the AE/AL indices.

5.3 Substorm Events

We chose 6 STs examples which have clear substorms signatures. They are discussed below. We use the 1-min OMNI data to plot these events (all the time showed below are all recorded by OMNI website). They are all plotted in 6h time windows. From the top to bottom of the pictures, they are the total magnetic field, its three components in the GSM coordinate system, the dynamic pressure, the AE Index, AL Index, SYM-H index. The STs are between the two black vertical lines. The red lines indicate the start of the expansion phases.

The first event is shown in the Figure 5-1. It was observed on July 16, 1995 from 13:54:00 to 18:17:00 UT. This event has a duration of about 4.38 h. It has increased total magnetic field ($\sim$ 20 nT), and clear bipolar signature in the B_y component, southward B_z in the first half part of the ST, and the flow pressure is increased. The expansion phase starts at

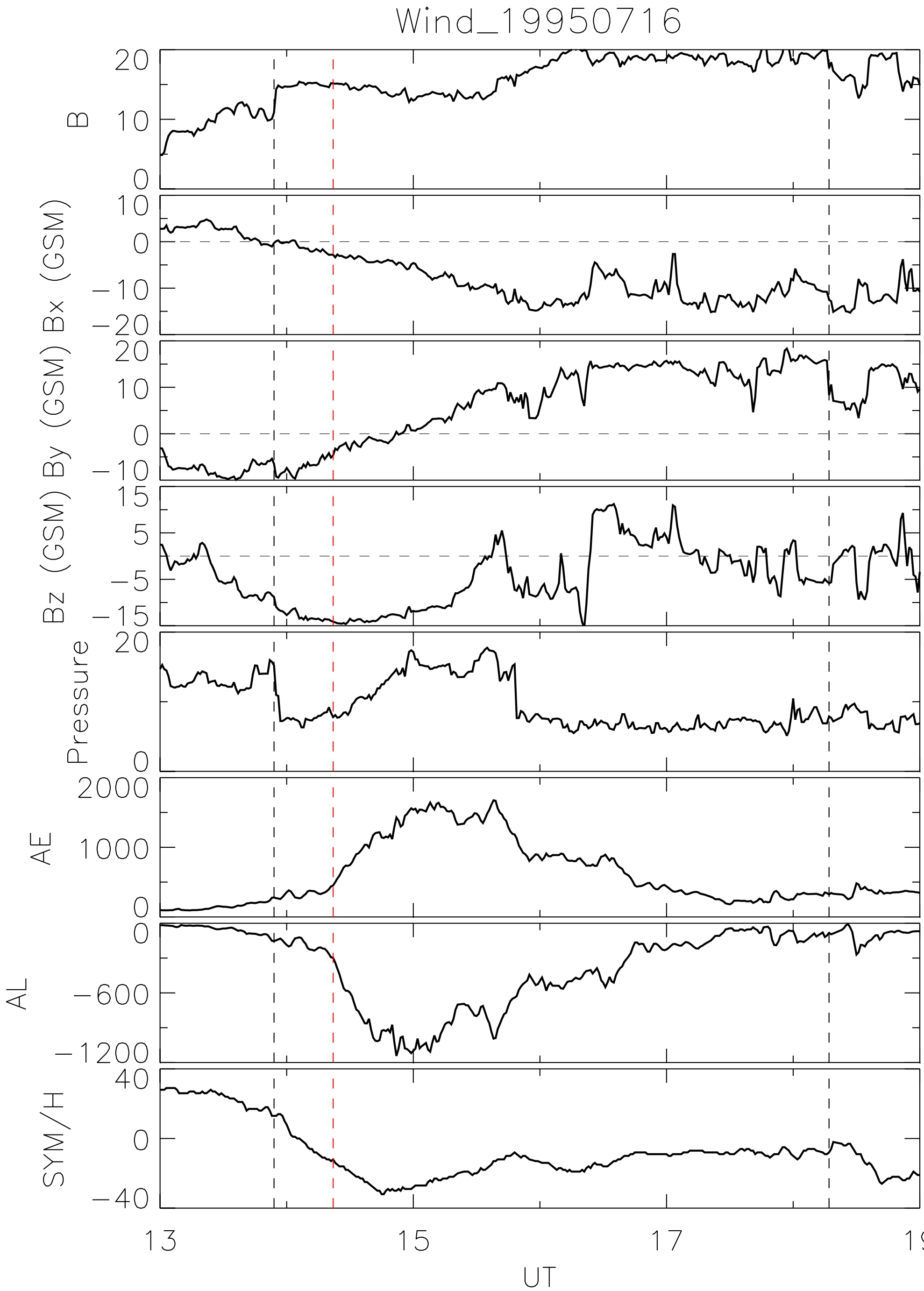

Figure 5-1: Event 1: The magnetic substorm related with the ST on July 16, 1995 from 13:54:00 to 18:17:00.

14:22:00 where the AL index develops a sharp negative gradient as an effect of the enhanced WEJ. In this event, the flow pressure starts to increase when the expansion phase starts. When the flow pressure reaches the maximum, the AE index reaches the maximum ($\sim$ 1600 nT), and the AL index reaches to the minimum ($\sim$ -1100 nT). The ST associated with the substorm is related to increased pressure and southward B_z. It is however not related to (i) a sudden change in dynamic pressure or (2) a northward IMF turning.

The SYM-H is also examined in this event, the minimum of which is $\sim$ -36 nT. That is, this event does not drive a magnetic storm.

Figure 5-2 presents the second ST event. It was observed on May 18, 2006 from 10:05:00 to 11:42:00 UT. This event has a duration of 1.62 h. The B_z component is southward between the 10:55:00 to 11:15:00. At 11:15:00, B_z changed from south to north suddenly and the flow pressure decreased a little, the AE increased (the maximum reaches to $\sim$ 310 nT) and AL decreased (the minimum reaches $\sim$ -150 nT). This ST is associated with a substorm which is triggered by the northward turning of B_z. However, it does not associated with the magnetic storm.

Figure 5-3 presents the third ST event. It was observed on Jan 28, 2010 from 15:38:00 to 19:15:00 UT. This event last for 3.62 h. There is no bipolar signature in B_y component, and the flow pressure is stable. At 16:44:00 UT B_z changed from north to south, the AE started to increase (the maximum reaches to $\sim$ 300 nT) and AL started to decrease (the minimum reaches $\sim$ -300 nT). This ST is associated with a substorm which is related to the southward turning of B_z. It is not associated with a magnetic storm.

Figure 5-4 presents the fourth ST event. It was observed on Feb 27, 2003 from 01:14:00 to 03:45:00 UT. This event has a duration of 2.52 h. There is no bipolar signature on the B_y component, and the flow pressure is stable. At 02:04:00, the expansion phase starts, the AE

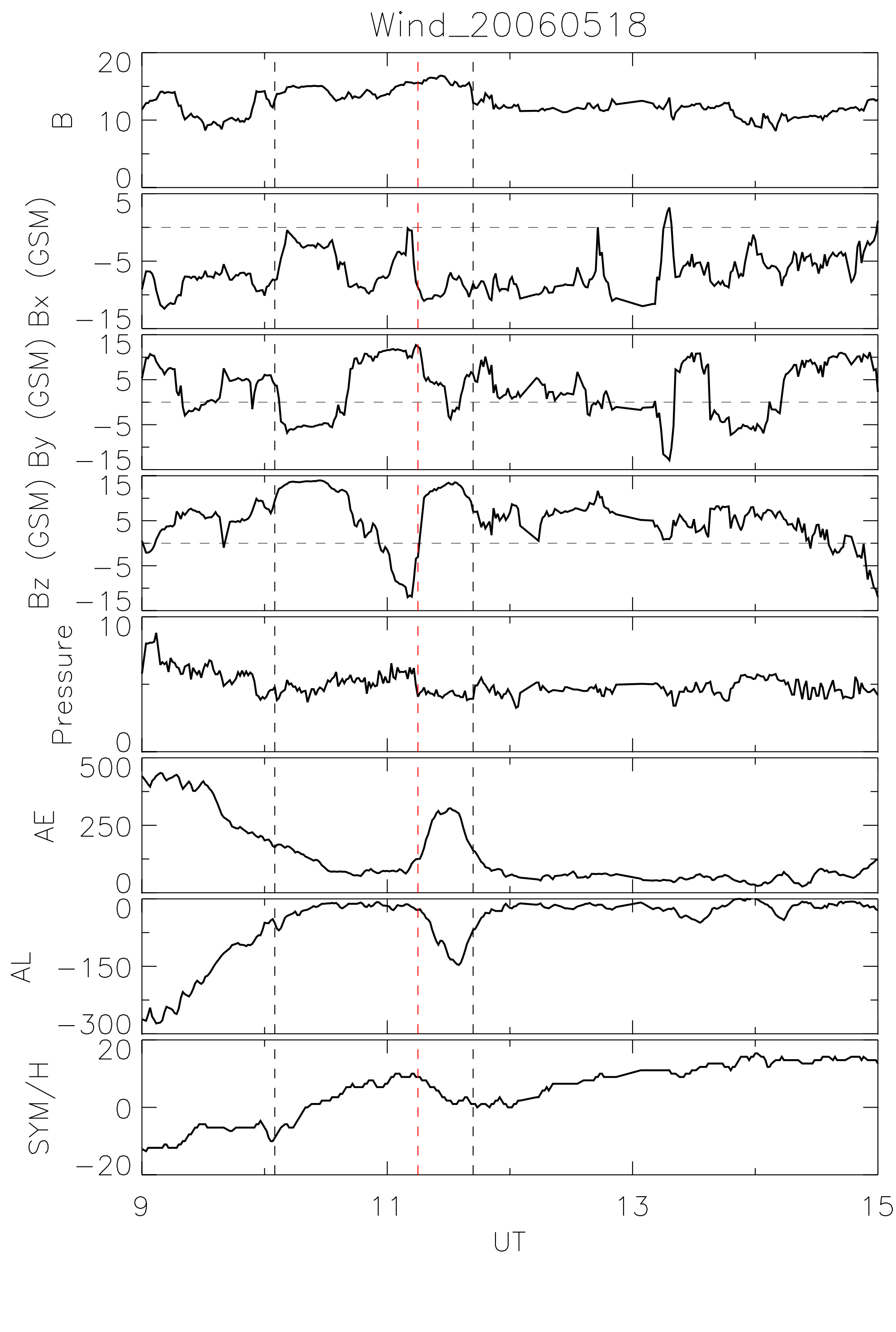

Figure 5-2: Event 2: The magnetic substorm related with the ST on May 18, 2006 from 10:05:00 to 11:42:00.

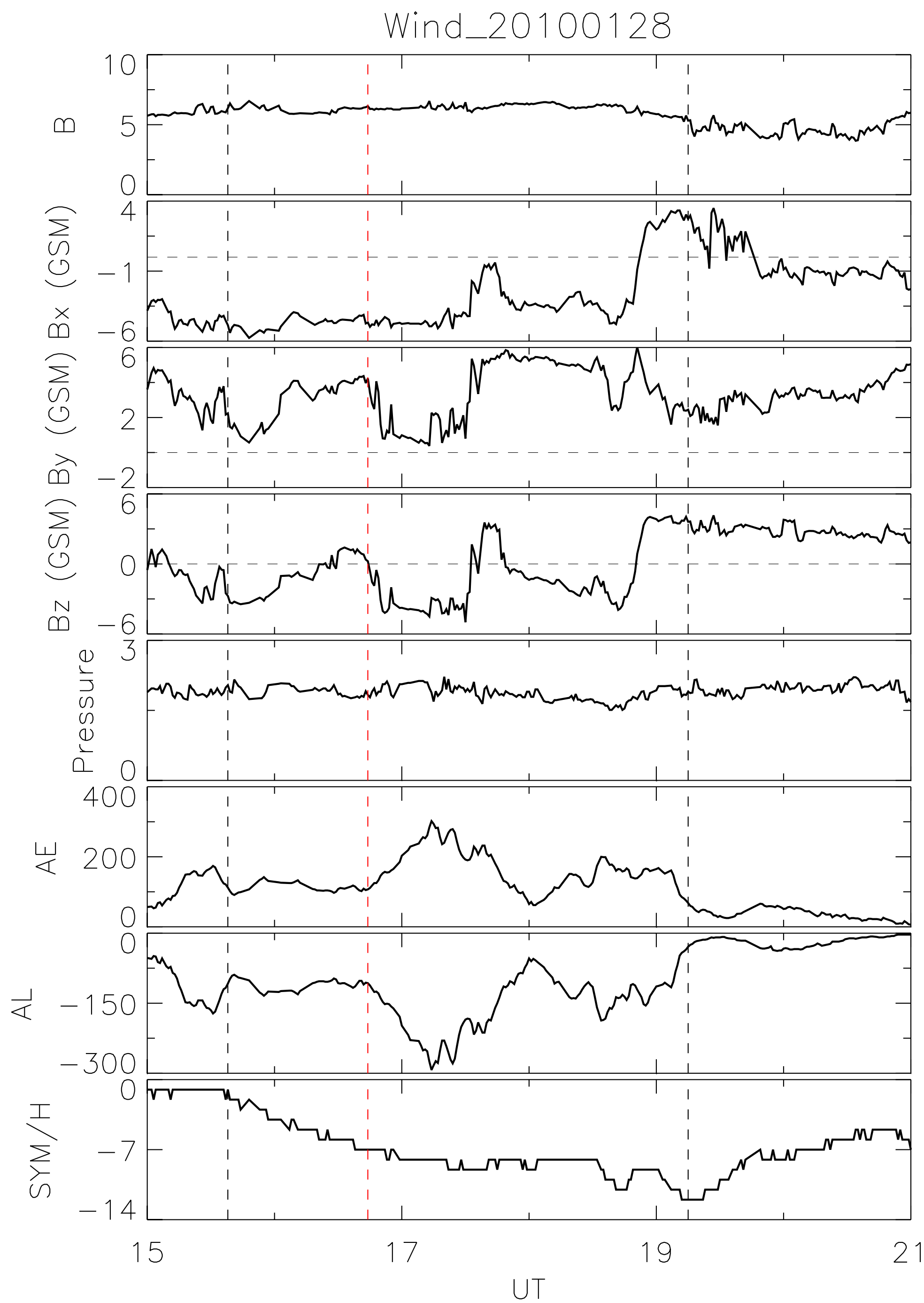

Figure 5-3: Event 3: The magnetic substorm related with the ST on Jan 28, 2010 from 15:38:00 to 19:15:00.

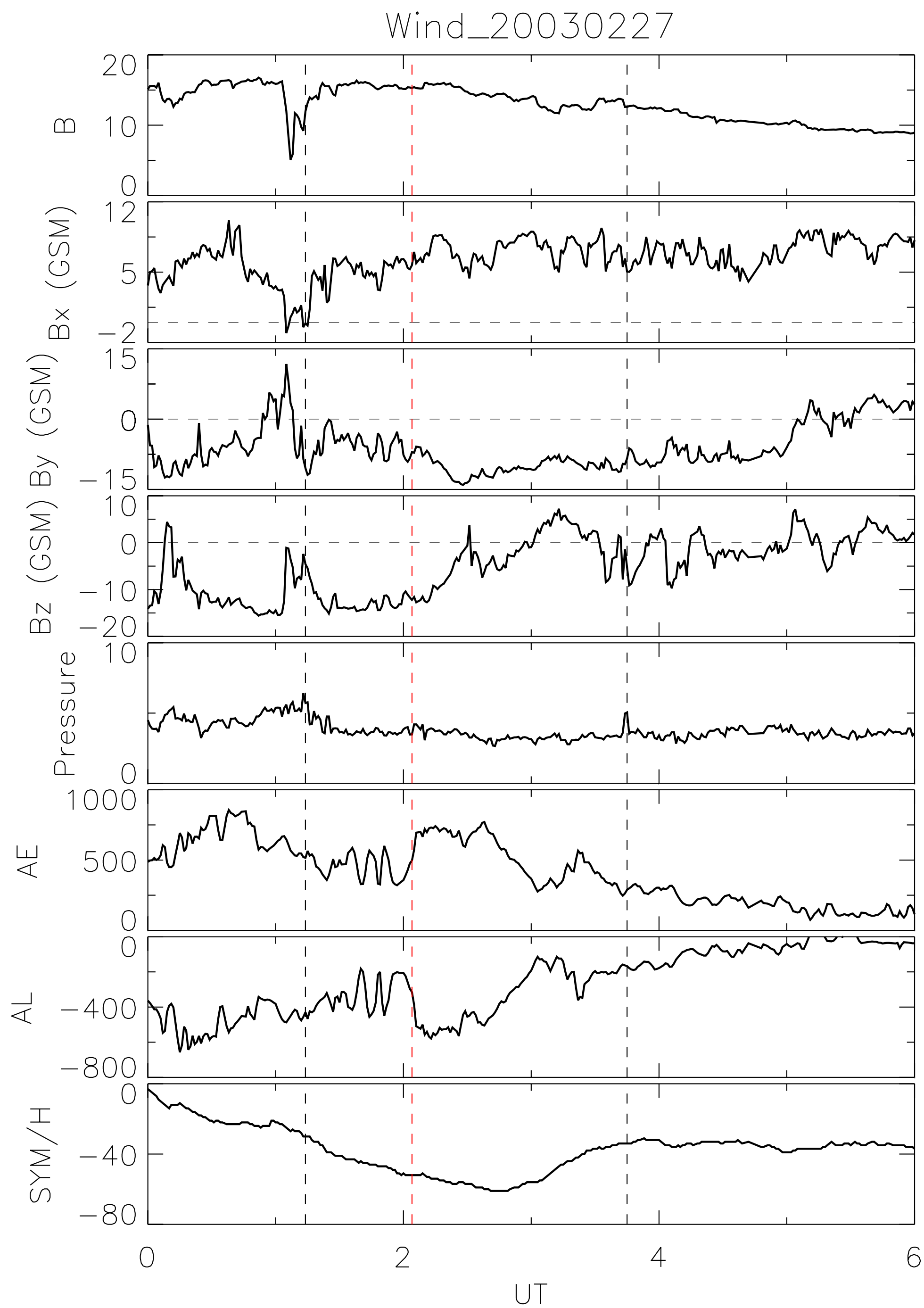

Figure 5-4: Event 4: The magnetic substorm related with the ST on Feb 27, 2003 from 01:14:00 to 03:45:00.

increased (the maximum reaches to $\sim$ 700 nT) and AL decreased (the minimum reaches to $\sim$ -580 nT). In this event, the B_z component lis ess than -10 nT for about 2 hours before the expansion phase starts, i.e. during the growth phase. When we examine the SYM-H index, this event was on part of the main phase and recovery phase of a magnetic storm. It has the minimum value $\sim$ -60 nT, which is related with a moderate storm. This magnetic storm was associated with the low B_z ($<$ -10 nT during and before this ST for about 2h). This ST is associated with a substorm and a moderate storm which triggered by the southward B_z ($<$ -10 nT).

The fifth event is shown in Figure 5-5. It was observed on Aug 06, 1998 from 19:52:00 to 23:33:00 UT. This event has a duration of 3.68 h. At time 22:17:00 UT, the B_y changed from positive to negative, and the flow pressure increased sharply. Then the AE index started to increase (the maximum reaches to $\sim$ 1300 nT) and AL index started to decrease (the minimum reaches to $\sim$ -1100 nT). In this event, B_z changed from north to south, and starting around 21:55:00, it is less than -10 nT, and then the SYM-H started to decrease at time 22:35:00, and reached to a minimum value $\sim$ -60 nT. This ST was on the recovery phase of a intense magnetic storm before it. And with the B_z change from north to south, to less than -10 nT, the value of the SYM-H decreased. When the ST ended, the B_z moved rotated back northward which made the SYM-H increase again.

This ST is associated with a substorm which maybe was triggered by the bipolar signature of the B_y component or increased flow pressure. And it also associated with a moderate magnetic storm which was triggered by the southward B_z ($<$ -10 nT).

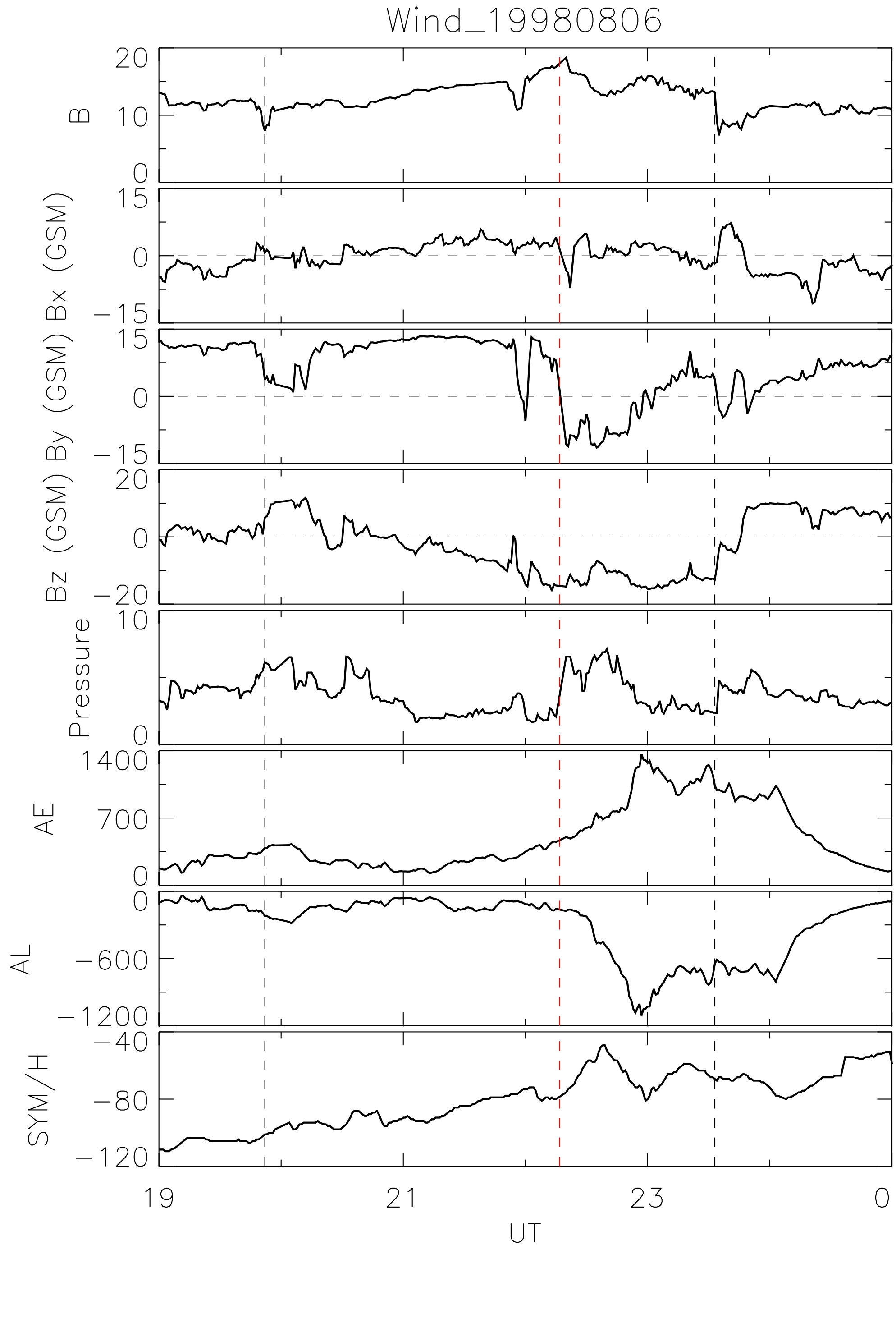

Figure 5-5: Event 5: The magnetic substorm related with the ST on Aug 06, 1998 from 19:52:00 to 23:33:00.

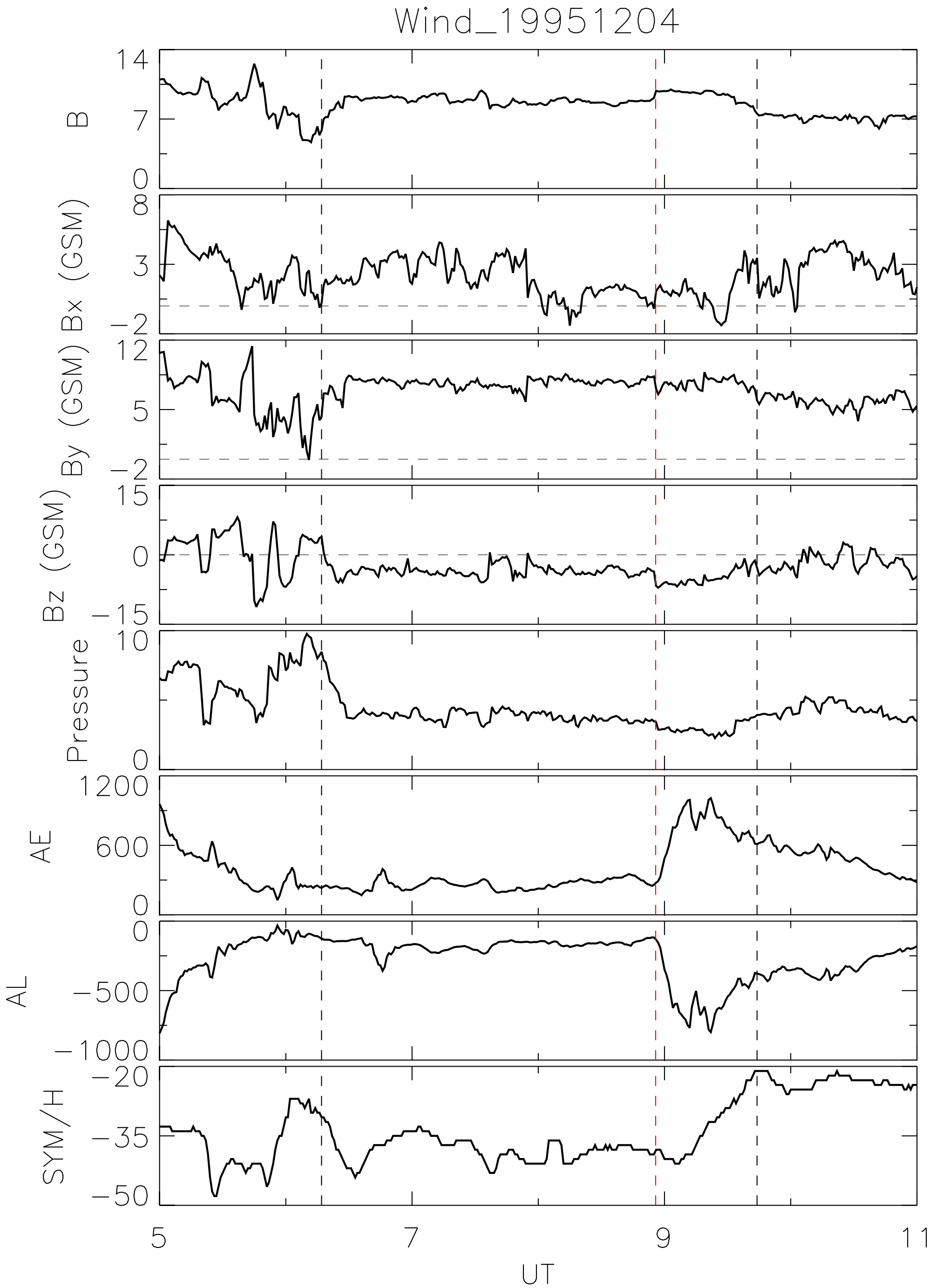

Figure 5-6: Event 6: The magnetic substorm related with the ST on Dec 04, 1995 from 06:17:00 to 09:44:00.

The last event is presented in Figure 5-6. It was observed on Dec 04, 1995 from 06:17:00 to 09:44:00 UT. This event has a duration of 3.45 h. This event does not have bipolar signatures on B_y and B_z, and the flow pressure is also stable. At time 08:56:00 UT, the expansion phase of the substorm started, the AE index started to increase (the maximum value reaches to $\sim$ 1000 nT) while the AL index started to decrease (the minimum value reaches to $\sim$ -750 nT). This ST is associated with a substorm which may have been triggered by the $B_z <$ -3 nT lasting more than 2 h. It is not associated with a magnetic storm.

5.4 Results

We examined 615 STs which have a duration between [1, 5] h. 47 % (288/615) of them were associated with magnetic substorms. Of the 288 substorms, there are 111 with SN turning (16 events also have pressure increase, and 31 event also have B_y bipolar signature), 28 events are associated with NS turning (4 events have pressure increase, and 5 event also have B_y bipolar signature), 50 events only associated with B_y bipolar signatures, 8 events only associated with pressure increase, and 91 events only have B_z southward signature.

In our statistical studies, we found that most of the magnetic substorms are related to B_y and B_z bipolar signatures or a southward B_z lasting for more than 2 h.

In our events, there are 21 STs associate with moderate magnetic storms (3.4%), and 5 STs associate with intense magnetic storms ($\sim$1 %).

The distributions of the AE and AL indices are shown in the Figure 5-7 and 5-8. From figure 5-7, the peak of the AE index is between [200, 600] nT, and the AL index has peak at [-200, -600] nT (see Figure 5-8).

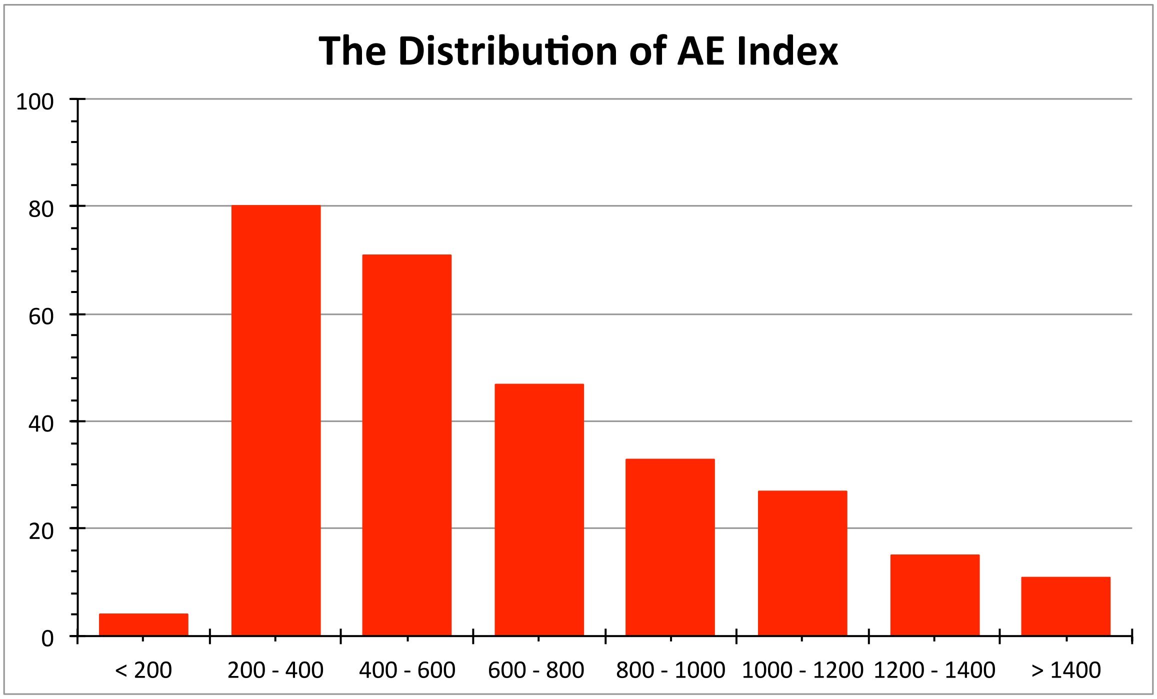

Figure 5-7: The distribution of the substorms' AE index.

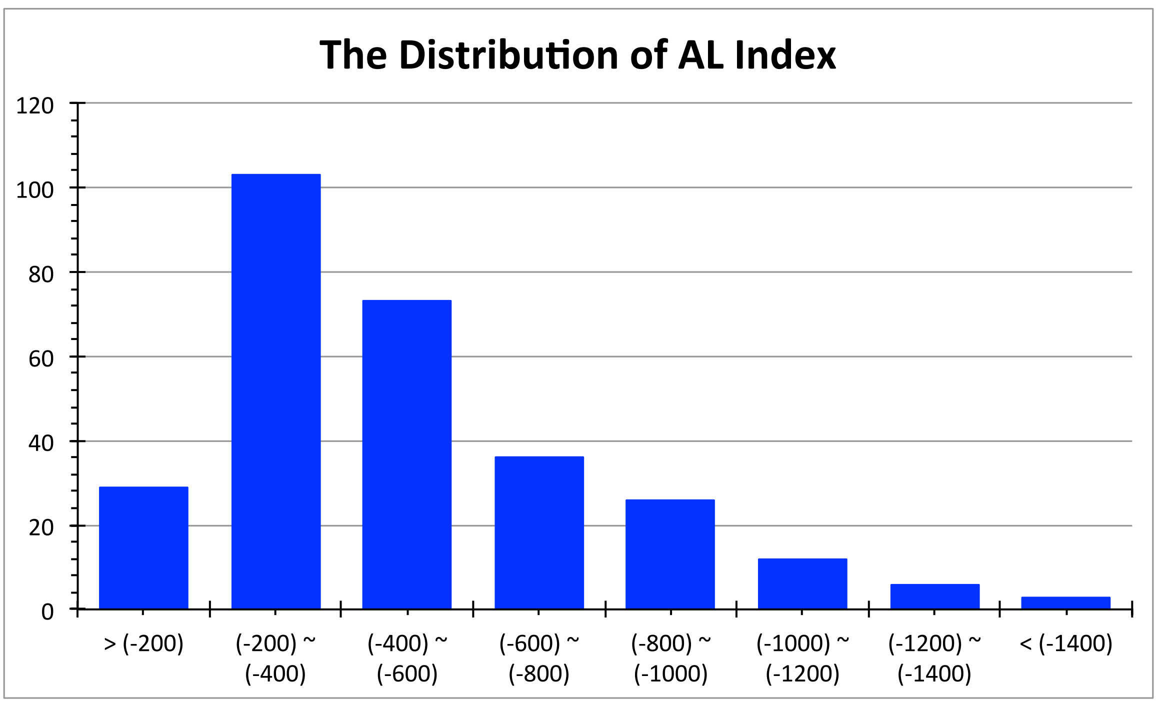

Figure 5-8: The distribution of the substorms' AL index.

5.5 Discussion

In this chapter, we studied 615 STs which have durations between [1, 5] h by using OMNI's 1-min data. There are 47 % of them associated with magnetic substorms (288 events). In our statistical studies, most of them are related with B_y, B_z bipolar signatures or southward B_z for more than 2 h. In these 615 STs, there are 21 STs associated with moderate magnetic storms (3.4 %) and 5 STs associated with intense magnetic storms ($\sim$ 1 %).

In Zhang et al. [2013], the authors concluded that the small flux ropes which are associated with substorms have bipolar signatures in B_y or B_z. They also explained that for the small flux ropes which were not related with substorms, their duration was less than 1.5 h, or the southward IMF component is short, or substorm occurred before this small flux rope arrived at Earth. They did not observed magnetic storm related any of their small flux ropes. In our study, we are not limited to the small flux ropes, but all the small transients observed by Wind spacecraft which have durations between [1, 5] h. We confirm one of Zhang et al. [2013]'s conclusions that the substorms could be associated with B_y or B_z bipolar signatures. In addition, we have 91 events which only have B_z southward signatures; they do not have any B_y or B_z bipolar signatures, nor sudden increased flow pressure. This kind of STs also related with magnetic substorms. The common signature of these events is they have $B_z <$ -3 nT for more than 1 h. Which showed the result from Kamide et al. [1977].

In our studies, we have very few STs associated with substorms which are clearly related with sharp flow pressure increases. One main reason is because typically a sudden proton density increase is not common in STs boundaries, so that we have very few STs have sudden increased flow pressure.

We also observed 26 STs associated with magnetic storms (21 with moderate storms, and 5 with intense storms). All these STs related with magnetic storms have large, negative B_z values (< -10 nT) for more than 1h or there were intense magnetic storms occurring before them. In Gonzalez and Tsurutani [1987]'s study, they suggested that events which have more than 3h with (B_z < -10 nT, GSM) could cause intense (Dst < -100 nT / SYM-H < -100 nT) magnetic storms. Our STs do not have so long durations. Therefore, most of the magnetic storms associated with the STs are moderate storms (21/26).

In Feng et al. [2010], they suggested that there are 2 triggers for the magnetic substorms. One is the B_z component turning from south to north; the other is an increase of the flow pressure. In our study, we have not looked at which features of the STs triggered the magnetic substorms. In some of our examples, there are clear bipolar signatures of B_y or B_z or the sharp increase of the flow pressure when the substorm onset occurred. Most of the STs associated with the magnetic substorms do not have clear features at the onset of the expansion phase.

In this chapter, we showed that not only the small flux ropes, but also the other small transients could be associated with magnetic substorms and magnetic storms. The B_y and B_z bipolar signatures and southward B_z which less than -3 nT and last more than 1 h are the main signatures of the substorms. A B_z < -10 nT lasting for more than 1 h has a strong possibility of being related to a magnetic storm.

Chapter 6

Summary and Conclusion

In this thesis, we studied the properties of STs observed by the Wind spacecraft (from year 1995 to 2014) and STEREO spacecraft (from year 2007 to 2014) in both case studies and statistical analyses. We applied an automated method, and found over 2000 STs which satisfied the following criteria: (i) Duration between [0.5, 12] hours. (ii) Magnetic field strength (B) which is 1.3 times higher than the yearly average value. (iii) Low proton beta (β_p less than 0.7 times yearly average) or low proton temperature ($T_p/T_{exp} < 0.7$). (iv) Low Alfvén Mach Number ($M_A < 0.7*$ yearly average) or large rotations of magnetic field components.

We discussed first the properties and distributions of STs during the solar minimum years 2007-2009. The majority ($\sim 81\%$) were found in the slow solar wind ($< 450 km/s$) and convecting with it. Many start or end with sharp field and flow gradients/discontinuities. Year 2009 had the largest number of STs since in this year there are the largest percent of slow solar wind. The average duration of STs is $\sim$ 4.3 hours, 75 % $<$ 6 hours. Compared with the large transients (ICMEs) in the same solar minimum, we found that the T_p is not significantly less than the expected temperature, which is different with the ICMEs. Since during the solar minimum years, the β_{plasma} of the STs ~ 1, the force-free modeling is inappropriate.

We then examined our large ST data base observed by the Wind and STEREO spacecraft. The event list covers solar cycles 23 and 24 (1995 - 2014). We removed the ICME-like STs whose time was coincident with those of published ICMEs (which we treated separately). Finally we obtained 549 STs from STA, 557 STs from STB, 925 STs from Wind. We obtained so many STs partly because we used three distant spacecraft. The ST occurrence frequency does not change with different positions in solar minimum years, but is different during solar maximum years of cycle 24 at different positions along the Earth's orbit. The distribution of the ST duration is wide but has a clear peak at [1, 2] hours. We presented statistical results on ST properties. In STs, quantity $< B >$ is about twice that in the ambient solar wind, while quantities $< \beta_p >$ and $< M_A >$ are about one half as much. Quantity $< T_p >$ is generally higher than T_{exp}. Only about 5% of STs have the increased iron charge states signature. The statistical β_{plasma} is obtained for the Wind measurements, in which the electron contribution is included. The β_{plasma} is close to 1 during the solar minimum years, while it is much less than unity when as we go to solar maximum years. We conclude that force free modeling is appropriate for the solar maximum years, but may be unreliable during solar minimum years. This expands on the previous results. Thus also in the modeling part we discuss both force free and non-force free methods.

In addition, STs expand little into the surrounding solar wind. Most values for radial expansion velocity lie in the range [-20, 20] km/s. There are many STs whose V_{exp} is only of order 1-2 km/s. This would correspond to 10-20 km/s for a typical 20-hour MC duration, which would still be considered low. So in such cases the front-to-back velocity gradient is not low because the event is of short duration; it is intrinsically low. The frequent occurrence of negative radial velocities implies that STs tend to also occur in stream - stream interaction regions where they are being compressed by the faster stream behind.

The normalized expansion velocities lie mainly in the range [0, 1.5]. The mean and median values of the distribution are 0.74 and 0.49. The range and mean values agree well with those for MCs (Démoulin, his Figure 5b). Further, for FR-STs the peak of the ζ lies in the range [0, 0.1], while the MC-normalized distribution peaks near 0.8. In short, many FR-STs do not expand at all. The non-flux ropes STs have similar normalized expansion velocities distribution except that ζ peaks around 0.2-0.3 as opposed to 0-0.1.

The occurrence frequency of STs has two clear dependencies. One is an anti-correlation with the phase of the solar cycle; the other is that STs tend to occur predominantly in the slow solar wind, suggesting that they may form an important constituent of the slow wind. Many of these characteristics are in sharp contrast to those of large-scale transients (ICMEs and magnetic clouds).

We then analyzed separately the ICME-like STs that we identified independently but which had been previously noted in the two published ICMEs time ranges. Doing so, we addressed 2 issues: (i) Is there any impact on the solar cycle dependence?, and (ii) do they change the expansion speed statistics?. As regards (i) we find that there is a rising peak at solar maximum year 2001 which is indeed ICME-like and opposite to that of other STs. For (ii) we find no significant dependence.

We modeled the small flux ropes by two non-force free methods (one with circular cross-section, the other with elliptical cross-section) and also by the Lundquist linear force free method. The non-force free model with circular cross-section also has a simple solution as the force free model with Lundquist's solution. It could also fit the observed magnetic field components as well as and sometimes better than the Lundquist's model. However, for the total magnetic field, sometimes it still has some differences with the observed data.

The non-force free model with elliptical cross-section is a more general condition. In some of our examples, it could get the smallest normalized chi-square. And the fitting results are also very good; the orientations are close to the MVA results. All three analytical models (force free or non-force free) give consistent orientations (the angle differences are no more than 30°).

We also compared the fitting results from analytical models with the numerical model (GS-reconstruction). From the GS-reconstruction, the small flux ropes tend to have elliptical cross-section. In this case, the elliptical cross-section model will be better than the circular cross-section model. However, the orientations obtained from the GS-reconstruction are mostly different with the analytical models' results.

Finally, we studied the disturbances in the magnetosphere (i.e. substorms and storms) of 615 STs which have durations between [1, 5] h by using OMNI's 1-min data. We showed that not only the small flux ropes, but also the other STs could be associated with magnetic storms and substorms. There are 47 % of them associated with magnetic substorms (288 events). In our statistical studies, most of them are related with B_y, B_z bipolar signatures and southward B_z signature (in which $B_z <$ -3 nT for more than 1h).

In these 615 STs, there are 21 STs which are associated with moderate magnetic storms (3.4 %) and 5 STs associate with intense magnetic storms ($\sim$ 1 %). All those STs associated with magnetic storms have low B_z values ($<$ -10 nT) more than 1h.

Appendices

Appendix A
The STs from Wind

We observed 1067 STs from Wind from the year 1995 to 2014. The event number with "*" means this ST was in the time ranges which ICMEs have been observed. We call them "ICME-like STs" in this paper. The lists of the ICMEs observed by Wind which have been used in this paper are got from: *Richardson and Cane*, 2010, www.srl.caltech.edu/ACE/ASC/DATA/level3/icmetable2.htm. The list is continually updated and cover our period completely.

The list of the STs observed by Wind has been shown in the table below. We present the start time and end time of the STs, the average magnetic field strength ($< B >$), the average proton beta (β_p), the average Alfvén Mach number ($< M_A >$), the average proton velocity ($< V_p >$), the velocity expansion ($V_{exp} = \frac{V_{front}-V_{end}}{2}$).

Table A.1: STs list from Wind Observation

No.	Start	End	B	β_p	M_A	V_p	V_{exp}
1995							
1	1995-01-02/04:55:00	1995-01-02/06:35:00	12.6	0.37	6.8	346	-2.7
2	1995-01-03/00:25:00	1995-01-03/02:10:00	11.6	0.42	5.7	522	-22.2
3	1995-01-10/21:00:00	1995-01-11/03:50:00	9.6	0.56	6.6	429	-20.7
4	1995-01-22/15:15:00	1995-01-22/22:40:00	9.2	0.6	6.1	415	-0.7
5	1995-01-29/01:40:00	1995-01-29/09:00:00	15.6	0.39	5.2	380	-64.9
6	1995-03-01/01:20:00	1995-03-01/07:15:00	8.4	0.41	6.3	609	-60.1
7	1995-04-17/02:10:00	1995-04-17/03:35:00	8.1	0.33	7.6	335	0.8
8	1995-04-26/11:10:00	1995-04-26/13:48:00	9.9	0.55	7.4	426	-9.3
9	1995-05-02/08:40:00	1995-05-02/13:15:00	11.0	0.4	5.7	522	30.0
10	1995-05-13/10:25:00	1995-05-13/15:45:00	11.1	0.09	4.4	329	4.7
11	1995-05-16/01:18:00	1995-05-16/07:55:00	17.9	0.1	4.8	394	-21.0
12	1995-05-23/14:00:00	1995-05-23/17:22:00	15.0	0.13	4.3	423	-68.4
13	1995-05-29/05:10:00	1995-05-29/12:55:00	11.3	0.15	6.6	427	-4.0
14	1995-06-09/18:32:00	1995-06-09/23:50:00	8.3	0.43	6.4	380	-33.9
15	1995-06-10/05:05:00	1995-06-10/09:40:00	10.7	0.24	5.1	382	2.6
16	1995-06-19/08:28:00	1995-06-19/10:40:00	23.0	0.24	3.4	463	-87.2
17	1995-07-12/23:10:00	1995-07-13/09:20:00	10.4	0.29	5.4	299	-12.1
18	1995-07-13/18:30:00	1995-07-13/23:00:00	8.6	0.16	5.6	309	-4.3
19	1995-07-16/13:22:00	1995-07-16/17:48:00	16.8	0.33	6.1	447	-53.9
20	1995-07-24/06:45:00	1995-07-24/17:15:00	14.2	0.32	4.8	427	-6.0
21	1995-07-30/17:50:00	1995-07-31/00:25:00	8.4	0.15	6.7	315	4.2

Table A.1: STs list from Wind Observation

No.	Start	End	B	β_p	M_A	V_p	V_{exp}
22	1995-08-03/06:22:00	1995-08-03/07:30:00	9.6	0.26	5.0	352	-0.01
23	1995-08-08/00:35:00	1995-08-08/04:55:00	10.2	0.51	5.8	494	7.2
24	1995-08-08/12:00:00	1995-08-08/13:00:00	9.1	0.48	6.8	532	-16.6
25	1995-08-17/20:32:00	1995-08-18/04:18:00	8.7	0.31	7.5	401	-4.5
26	1995-09-05/15:00:00	1995-09-05/17:20:00	18.9	0.27	3.8	434	-62.1
27	1995-09-27/13:50:00	1995-09-27/20:55:00	13.5	0.11	5.3	404	-1.5
28	1995-10-20/07:35:00	1995-10-20/11:30:00	10.1	0.61	6.3	481	-38.4
29	1995-10-30/10:40:00	1995-10-30/16:35:00	10.5	0.3	6.8	369	-42.4
30	1995-10-30/21:45:00	1995-10-31/02:58:00	9.6	0.53	5.8	390	-12.2
31	1995-10-31/04:00:00	1995-10-31/07:40:00	8.2	0.45	6.5	433	8.2
32	1995-11-04/14:10:00	1995-11-04/17:35:00	8.1	0.42	7.0	423	-4.2
33	1995-11-12/16:00:00	1995-11-12/20:00:00	8.1	0.26	6.2	356	18.7
34	1995-12-02/11:05:00	1995-12-02/20:45:00	9.8	0.07	4.8	369	1.3
35	1995-12-04/06:10:00	1995-12-04/09:30:00	9.0	0.34	7.0	382	1.7
36	1995-12-12/14:22:00	1995-12-12/15:15:00	8.1	0.21	6.2	328	-0.1
37	1995-12-31/06:35:00	1995-12-31/10:10:00	10.2	0.3	6.0	372	7.4
38	1995-12-31/14:35:00	1995-12-31/16:00:00	8.3	0.33	6.1	416	-18.5
1996							
39	1996-01-02/17:00:00	1996-01-02/20:32:00	8.7	0.47	7.3	412	-40.6
40	1996-01-03/04:20:00	1996-01-03/10:12:00	7.9	0.48	7.2	489	-35.0
41	1996-01-20/04:05:00	1996-01-20/08:25:00	10.5	0.49	6.2	502	27.5
42	1996-01-20/13:15:00	1996-01-20/21:05:00	8.4	0.29	7.8	429	-2.7
43	1996-02-10/13:25:00	1996-02-10/22:45:00	8.9	0.41	6.7	420	-41.4
44	1996-02-24/01:02:00	1996-02-24/02:18:00	9.8	0.29	7.1	447	4.4
45	1996-03-03/05:40:00	1996-03-03/06:50:00	9.2	0.32	6.7	340	3.9
46	1996-03-13/09:25:00	1996-03-13/10:42:00	8.3	0.63	7.1	571	9.3
47	1996-03-16/13:35:00	1996-03-16/16:05:00	10.9	0.28	6.9	360	-7.9
48	1996-03-17/08:45:00	1996-03-17/09:45:00	8.7	0.32	5.4	461	-19.0
49	1996-03-20/02:18:00	1996-03-20/03:45:00	8.3	0.32	6.5	432	-12.7
50	1996-03-20/17:00:00	1996-03-20/19:15:00	9.6	0.55	6.2	457	-8.6
51	1996-03-21/01:25:00	1996-03-21/04:25:00	8.9	0.56	6.7	502	-12.8
52	1996-04-08/13:15:00	1996-04-08/21:10:00	9.5	0.28	6.3	322	0.7
53	1996-04-09/09:15:00	1996-04-09/09:55:00	10.7	0.17	5.0	417	-4.8
54	1996-04-11/13:22:00	1996-04-11/17:42:00	7.8	0.55	7.5	454	-19.1
55	1996-04-14/11:00:00	1996-04-14/12:22:00	8.5	0.77	7.2	484	5.9
56	1996-04-14/12:45:00	1996-04-14/17:15:00	8.6	0.49	6.4	490	9.4
57	1996-04-14/18:30:00	1996-04-14/23:25:00	10.7	0.42	6.2	523	-84.5
58	1996-04-17/02:15:00	1996-04-17/03:55:00	9.3	0.42	7.7	449	10.5
59	1996-04-17/05:50:00	1996-04-17/12:20:00	7.7	0.65	7.1	497	-40.5
60	1996-05-21/15:00:00	1996-05-21/18:05:00	8.0	0.41	6.5	424	3.5
61	1996-06-05/18:35:00	1996-06-06/04:32:00	9.8	0.31	6.8	376	-30.7
62	1996-06-16/04:20:00	1996-06-16/07:32:00	9.1	0.33	5.0	419	-5.2

Table A.1: STs list from Wind Observation

No.	Start	End	B	β_p	M_A	V_p	V_{exp}
63	1996-06-18/20:35:00	1996-06-19/00:25:00	8.9	0.37	8.2	413	-37.6
64	1996-07-12/01:40:00	1996-07-12/05:15:00	8.0	0.27	6.3	332	-11.9
65	1996-07-12/09:45:00	1996-07-12/17:50:00	8.7	0.38	5.7	395	7.1
66	1996-07-14/05:05:00	1996-07-14/08:35:00	8.5	0.16	5.8	371	-0.98
67	1996-07-28/15:30:00	1996-07-28/22:05:00	10.3	0.27	5.5	358	-18.2
68	1996-07-31/00:40:00	1996-07-31/04:38:00	13.0	0.33	5.2	407	4.2
69	1996-08-14/09:40:00	1996-08-14/12:20:00	9.2	0.42	7.6	388	-15.4
70	1996-08-16/07:45:00	1996-08-16/12:45:00	9.2	0.51	7.3	420	-12.2
71	1996-08-23/02:45:00	1996-08-23/05:10:00	10.6	0.6	7.9	409	3.6
72	1996-08-23/09:32:00	1996-08-23/11:50:00	8.0	0.46	6.7	499	2.7
73	1996-08-28/15:00:00	1996-08-28/18:48:00	8.0	0.33	6.7	399	-15.97
74	1996-09-19/18:05:00	1996-09-19/19:30:00	9.6	0.45	7.0	474	4.5
75	1996-09-26/17:05:00	1996-09-26/18:38:00	16.1	0.41	5.3	498	-0.1
76	1996-10-08/17:45:00	1996-10-08/19:20:00	8.3	0.39	8.2	385	10.9
77	1996-10-17/21:10:00	1996-10-17/22:15:00	10.9	0.58	5.4	454	-15.1
78	1996-10-22/06:50:00	1996-10-22/12:35:00	8.6	0.37	6.5	484	-8.5
79	1996-10-27/11:42:00	1996-10-27/15:45:00	9.4	0.32	6.4	378	2.3
80	1996-10-27/20:05:00	1996-10-27/22:00:00	8.1	0.5	6.7	375	-10.3
81	1996-11-04/02:40:00	1996-11-04/04:30:00	11.1	0.25	4.9	441	-9.9
82	1996-11-13/17:40:00	1996-11-13/20:00:00	12.1	0.42	6.1	401	-0.3
83	1996-11-14/00:30:00	1996-11-14/01:45:00	11.2	0.58	6.5	441	-5.9
84	1996-11-14/02:50:00	1996-11-14/04:10:00	9.1	0.66	6.6	464	-13.8
85	1996-11-14/19:05:00	1996-11-14/23:30:00	9.3	0.39	6.1	447	-14.4
86	1996-11-24/09:40:00	1996-11-24/11:45:00	10.2	0.47	7.0	356	-0.7
87	1996-12-07/11:10:00	1996-12-07/15:32:00	9.0	0.29	5.7	330	-23.9
88	1996-12-09/22:00:00	1996-12-09/23:20:00	15.1	0.2	5.5	392	-12.5
89	1996-12-10/04:20:00	1996-12-10/09:18:00	9.2	0.45	6.4	489	-42.2
90	1996-12-10/12:25:00	1996-12-10/14:25:00	9.5	0.43	6.1	524	8.5
91	1996-12-15/03:28:00	1996-12-15/08:15:00	8.1	0.41	6.4	480	-46.1
92	1996-12-26/16:15:00	1996-12-26/22:10:00	8.1	0.28	6.2	337	-2.4
1997							
93	1997-01-07/03:30:00	1997-01-07/04:20:00	10.3	0.34	7.4	377	12.8
94	1997-01-07/04:50:00	1997-01-07/08:35:00	8.1	0.36	7.6	385	-19.1
95	1997-01-26/00:28:00	1997-01-26/02:45:00	11.2	0.49	6.9	353	-11.99
96	1997-01-26/08:00:00	1997-01-26/09:10:00	11.3	0.51	7.1	374	-20.9
97	1997-01-26/12:25:00	1997-01-26/14:45:00	14.1	0.52	5.2	477	-13.4
98	1997-02-05/15:22:00	1997-02-05/22:00:00	10.2	0.2	6.7	356	-1.3
99	1997-02-05/22:25:00	1997-02-05/23:45:00	10.3	0.16	6.3	361	2.5
100	1997-02-06/00:10:00	1997-02-06/02:30:00	9.1	0.37	6.1	403	-22.9
101	1997-02-08/03:35:00	1997-02-08/04:50:00	8.3	0.18	5.5	394	4.0
102	1997-02-27/20:05:00	1997-02-27/22:45:00	13.8	0.1	5.6	511	-6.1
103	1997-03-05/13:28:00	1997-03-05/15:10:00	9.9	0.53	7.7	344	-3.8

Table A.1: STs list from Wind Observation

No.	Start	End	B	β_p	M_A	V_p	V_{exp}
104	1997-03-05/15:45:00	1997-03-05/17:35:00	10.3	0.34	7.5	378	-4.7
105	1997-03-12/03:25:00	1997-03-12/05:25:00	11.9	0.35	5.7	391	-58.8
106	1997-03-22/05:40:00	1997-03-22/07:00:00	8.4	0.29	5.7	418	-13.4
107	1997-03-25/13:28:00	1997-03-25/16:35:00	8.5	0.1	6.6	415	3.2
108	1997-03-28/13:15:00	1997-03-28/15:25:00	10.0	0.1	5.2	411	-23.2
109	1997-03-29/08:10:00	1997-03-29/11:05:00	8.6	0.29	6.8	428	-4.4
110	1997-03-31/22:32:00	1997-04-01/05:30:00	12.5	0.2	6.9	412	-3.9
111	1997-04-01/09:25:00	1997-04-01/11:45:00	8.7	0.55	6.8	396	1.9
112	1997-04-10/13:45:00	1997-04-10/16:10:00	10.5	0.17	5.6	337	-13.6
113	1997-04-16/16:05:00	1997-04-16/21:45:00	13.4	0.39	6.7	390	-2.4
114	1997-04-30/18:20:00	1997-04-30/22:22:00	10.2	0.32	6.6	373	6.6
115	1997-06-22/06:40:00	1997-06-22/13:40:00	11.1	0.39	5.5	360	-33.2
116	1997-06-27/09:10:00	1997-06-27/10:20:00	10.8	0.33	7.8	412	-2.8
117	1997-07-18/02:25:00	1997-07-18/05:35:00	8.2	0.52	6.9	425	-26.8
118	1997-07-31/01:30:00	1997-07-31/06:40:00	15.2	0.18	4.8	379	-13.9
119	1997-08-04/09:15:00	1997-08-04/10:15:00	10.1	0.45	6.4	390	6.6
120	1997-08-09/16:00:00	1997-08-09/19:35:00	8.2	0.48	7.3	424	-32.7
121	1997-08-14/05:40:00	1997-08-14/07:28:00	8.7	0.35	7.2	495	-6.4
122	1997-08-19/05:50:00	1997-08-19/07:45:00	8.2	0.12	5.1	372	-9.1
123	1997-08-28/06:22:00	1997-08-28/07:50:00	12.3	0.19	4.4	369	-8.0
124	1997-09-21/09:35:00	1997-09-21/14:35:00	10.7	0.23	5.3	366	9.2
125	1997-09-27/13:30:00	1997-06-27/16:50:00	8.8	0.37	7.0	391	-1.5
126	1997-10-07/18:15:00	1997-10-07/22:15:00	8.7	0.5	7.2	363	-21.2
127	1997-11-01/10:00:00	1997-11-01/12:25:00	8.4	0.47	5.5	377	2.3
128	1997-11-10/00:30:00	1997-11-10/05:18:00	8.8	0.47	7.6	375	9.3
129	1997-11-10/20:18:00	1997-11-10/22:15:00	8.6	0.34	6.4	355	5.4
130	1997-11-16/11:55:00	1997-11-16/13:35:00	7.7	0.26	6.6	379	5.2
131	1997-11-16/14:35:00	1997-11-16/20:35:00	8.0	0.23	6.0	385	3.6
132	1997-11-17/18:00:00	1997-11-18/01:25:00	9.1	0.26	6.8	385	11.5
133	1997-12-10/04:35:00	1997-12-10/14:15:00	14.0	0.33	6.3	332	13.1
134	1997-12-10/15:40:00	1997-12-10/17:30:00	12.5	0.34	5.7	331	-5.4
135	1997-12-18/06:15:00	1997-12-18/10:30:00	9.7	0.17	5.3	302	-10.9
136	1997-12-18/18:50:00	1997-12-19/03:25:00	8.8	0.26	5.9	320	12.7
1998							
137*	1998-01-08/16:45:00	1998-01-08/21:10:00	10.8	0.12	5.1	366	-16.9
138	1998-01-16/16:10:00	1998-01-16/19:10:00	12.4	0.22	5.2	330	-14.0
139	1998-01-17/01:20:00	1998-01-17/03:55:00	10.1	0.28	4.8	347	0.09
140	1998-02-09/01:30:00	1998-02-09/04:15:00	11.2	0.1	5.6	378	11.0
141	1998-02-09/05:30:00	1998-02-09/08:12:00	10.6	0.09	5.0	367	9.8
142	1998-02-09/09:50:00	1998-02-09/11:25:00	11.5	0.14	5.7	371	12.1
143	1998-02-28/18:10:00	1998-02-28/20:28:00	13.9	0.22	4.0	364	3.4
144	1998-03-10/05:22:00	1998-03-10/12:00:00	18.2	0.14	5.0	358	-44.2

Table A.1: STs list from Wind Observation

No.	Start	End	B	β_p	M_A	V_p	V_{exp}
145	1998-03-10/12:30:00	1998-03-10/14:30:00	21.0	0.26	3.6	443	10.6
146	1998-04-04/14:55:00	1998-04-04/15:55:00	12.2	0.27	5.4	341	-3.0
147	1998-04-04/16:30:00	1998-04-04/19:45:00	10.7	0.26	4.3	365	1.9
148	1998-04-16/10:00:00	1998-04-16/13:18:00	11.2	0.16	4.1	369	21.8
149	1998-04-16/16:55:00	1998-04-16/20:16:00	10.9	0.17	3.6	359	16.5
150	1998-04-16/21:22:00	1998-04-17/05:30:00	11.2	0.17	4.5	372	-18.8
151*	1998-05-04/02:30:00	1998-05-04/05:00:00	37.8	0.1	2.7	799	-67.5
152	1998-06-05/12:45:00	1998-06-05/15:02:00	9.9	0.22	5.3	373	0.2
153*	1998-06-13/19:38:00	1998-06-13/21:50:00	11.3	0.12	5.4	380	-8.2
154*	1998-06-14/01:25:00	1998-06-14/06:22:00	11.1	0.2	5.5	356	17.2
155	1998-06-19/00:10:00	1998-06-19/04:00:00	12.4	0.33	5.0	376	-5.4
156*	1998-07-11/01:02:00	1998-07-11/07:32:00	13.6	0.06	3.6	358	7.6
157	1998-07-16/00:10:00	1998-07-16/01:15:00	12.5	0.33	6.1	336	-19.7
158	1998-07-22/21:45:00	1998-07-23/01:15:00	14.0	0.24	5.1	449	-20.9
159	1998-07-23/03:48:00	1998-07-23/04:45:00	15.9	0.25	4.6	540	-12.9
160	1998-07-31/08:22:00	1998-07-31/13:20:00	13.2	0.1	6.1	430	-23.6
161	1998-07-31/18:32:00	1998-07-31/21:10:00	14.5	0.19	5.6	434	10.3
162	1998-08-06/15:40:00	1998-08-06/19:30:00	12.3	0.24	5.7	359	-10.7
163	1998-08-06/19:35:00	1998-08-06/23:10:00	13.7	0.13	4.6	383	1.6
164	1998-08-06/23:35:00	1998-08-07/08:50:00	11.9	0.15	4.5	424	-34.8
165	1998-08-12/02:35:00	1998-08-12/04:50:00	11.8	0.03	3.8	397	0.7
166*	1998-08-19/20:18:00	1998-08-20/05:35:00	11.6	0.17	4.5	318	-7.8
167	1998-08-23/04:18:00	1998-08-23/06:35:00	12.9	0.28	4.4	442	-7.6
168	1998-09-18/14:55:00	1998-09-18/18:40:00	12.8	0.3	4.9	455	-0.4
169	1998-10-15/11:30:00	1998-10-15/14:35:00	11.8	0.15	4.6	343	-23.5
170	1998-10-15/19:20:00	1998-10-15/22:30:00	10.3	0.37	4.3	453	-7.4
171	1998-10-28/04:35:00	1998-10-28/09:15:00	11.7	0.32	4.8	505	-12.7
172	1998-10-28/16:30:00	1998-10-28/17:38:00	11.6	0.18	4.0	523	6.5
173*	1998-11-30/10:05:00	1998-11-30/18:20:00	12.6	0.27	5.3	1	18.2
1999							
174	1999-01-06/14:28:00	1999-01-06/19:15:00	14.8	0.3	3.7	415	-39.8
175	1999-02-11/20:22:00	1999-02-11/22:00:00	24.3	0.01	2.2	426	-12.8
176	1999-05-13/04:32:00	1999-05-13/08:55:00	16.3	0.15	4.3	412	-19.1
177	1999-05-24/22:15:00	1999-05-24/23:40:00	13.3	0.26	4.6	447	6.9
178	1999-07-30/10:25:00	1999-07-30/13:32:00	16.6	0.08	3.6	447	-28.6
179*	1999-07-30/13:50:00	1999-07-30/17:30:00	19.3	0.19	3.0	550	-83.4
180	1999-08-06/10:40:00	1999-08-06/12:15:00	12.3	0.16	4.3	368	-3.0
181	1999-08-11/01:05:00	1999-08-11/03:05:00	12.0	0.36	4.4	308	0.05
182	1999-08-15/18:32:00	1999-08-15/19:45:00	19.3	0.06	4.3	403	6.6
183	1999-08-16/02:05:00	1999-08-16/05:35:00	16.1	0.19	3.2	443	-35.4
184	1999-08-24/07:35:00	1999-08-24/08:30:00	11.9	0.28	5.0	432	-0.4
185	1999-09-15/07:45:00	1999-09-15/17:25:00	12.3	0.21	3.2	603	29.7

Table A.1: STs list from Wind Observation

No.	Start	End	B	β_p	M_A	V_p	V_{exp}
186	1999-10-10/00:22:00	1999-10-10/04:40:00	16.3	0.09	2.7	469	-35.3
187*	1999-10-21/02:25:00	1999-10-21/03:30:00	23.8	0.17	5.0	432	-6.2
188	1999-11-07/00:35:00	1999-11-07/08:40:00	13.8	0.22	5.0	386	-23.3
189	1999-11-07/17:50:00	1999-11-07/20:20:00	16.2	0.29	3.6	489	27.9
190	1999-11-21/19:05:00	1999-11-21/19:50:00	13.4	0.11	4.1	400	-1.1
191*	1999-12-27/02:35:00	1999-12-27/03:28:00	18.0	0.22	3.1	382	4.5
192	1999-12-29/00:32:00	1999-12-29/03:18:00	16.6	0.14	2.0	282	39.7
2000							
193*	2000-04-06/17:38:00	2000-04-06/23:25:00	27.4	0.18	3.9	584	2.6
194*	2000-04-06/23:45:00	2000-04-07/02:30:00	25.6	0.25	5.3	583	6.0
195	2000-04-16/07:10:00	2000-04-16/09:55:00	12.5	0.16	4.7	356	5.1
196	2000-04-16/15:15:00	2000-04-16/17:25:00	16.7	0.17	3.6	436	-6.0
197	2000-05-13/03:10:00	2000-05-13/05:25:00	16.0	0.21	4.3	361	-25.0
198	2000-05-24/00:15:00	2000-05-24/03:00:00	30.1	0.21	4.9	640	-3.8
199	2000-05-24/04:30:00	2000-05-24/10:05:00	17.6	0.2	4.3	636	-25.5
200	2000-06-14/13:05:00	2000-06-14/14:20:00	12.5	0.05	4.5	452	-1.0
201	2000-06-14/14:42:00	2000-06-14/16:25:00	12.0	0.1	5.8	446	8.7
202	2000-06-15/00:28:00	2000-06-15/01:32:00	14.0	0.08	3.3	462	-1.4
203*	2000-07-28/13:05:00	2000-07-28/14:15:00	22.2	0.05	3.7	457	4.5
204*	2000-07-28/14:40:00	2000-07-28/17:45:00	18.2	0.08	4.3	461	-2.0
205	2000-08-24/08:42:00	2000-08-24/10:28:00	14.0	0.2	3.0	320	-14.7
206	2000-09-16/20:58:00	2000-09-16/23:10:00	15.1	0.19	4.9	394	-0.03
207	2000-09-16/23:40:00	2000-09-17/00:45:00	15.4	0.11	3.9	407	-9.8
208	2000-09-18/16:22:00	2000-09-18/17:30:00	12.7	0.04	4.2	729	22.2
209	2000-09-30/10:20:00	2000-09-30/13:30:00	12.7	0.05	4.7	407	-7.3
210	2000-09-30/19:35:00	2000-09-30/23:45:00	12.8	0.06	2.6	423	-3.8
211*	2000-10-05/03:30:00	2000-10-05/06:25:00	23.8	0.13	4.0	467	-10.5
212*	2000-10-12/22:35:00	2000-10-13/01:45:00	18.8	0.13	3.8	457	-8.3
213	2000-11-04/02:30:00	2000-11-04/07:30:00	19.4	0.19	5.3	401	2.9
214*	2000-11-06/14:50:00	2000-11-06/17:40:00	14.2	0.2	4.7	614	6.5
215*	2000-11-07/20:20:00	2000-11-08/03:20:00	17.9	0.02	2.4	447	6.3
216	2000-11-08/03:35:00	2000-11-08/05:50:00	16.7	0.12	3.5	447	-18.9
217*	2000-11-26/20:40:00	2000-11-26/21:45:00	28.9	0.11	3.0	537	-17.3
218*	2000-11-26/22:00:00	2000-11-27/01:00:00	26.5	0.12	4.3	605	7.2
219*	2000-11-27/02:30:00	2000-11-27/03:45:00	20.5	0.08	3.9	624	7.6
220*	2000-12-22/22:50:00	2000-12-22/23:50:00	12.9	0.08	3.8	321	-2.2
2001							
221	2001-01-02/23:40:00	2001-01-03/00:20:00	11.2	0.15	5.1	330	9.6
222	2001-01-04/10:00:00	2001-01-04/11:15:00	12.7	0.08	3.8	404	6.5
223*	2001-03-04/16:25:00	2001-03-05/03:00:00	9.8	0.05	5.1	436	-6.7
224	2001-03-12/20:35:00	2001-03-13/02:00:00	10.7	0.12	3.4	392	1.0
225	2001-03-22/14:40:00	2001-03-22/17:10:00	18.7	0.17	3.7	352	-17.7

Table A.1: STs list from Wind Observation

No.	Start	End	B	β_p	M_A	V_p	V_{exp}
226*	2001-03-27/19:30:00	2001-03-27/21:35:00	24.3	0.2	3.9	559	-23.3
227*	2001-03-31/01:42:00	2001-03-31/02:55:00	65.6	0.09	2.0	619	-39.7
228*	2001-03-31/06:15:00	2001-03-31/12:22:00	35.6	0.09	3.6	636	45.5
229*	2001-03-31/15:00:00	2001-03-31/21:22:00	29.2	0.06	3.0	609	5.2
230*	2001-04-08/16:00:00	2001-04-08/19:50:00	16.1	0.32	5.8	794	-4.4
231*	2001-04-14/01:40:00	2001-04-14/07:05:00	10.1	0.02	3.7	695	16.7
232*	2001-05-08/12:40:00	2001-05-08/19:50:00	11.1	0.2	3.3	417.8	-24.9
233*	2001-05-09/00:58:00	2001-05-09/03:28:00	10.3	0.27	4.3	555	-34.6
234	2001-05-13/16:45:00	2001-05-13/18:10:00	11.5	0.22	4.3	454	-31.4
235	2001-05-23/04:22:00	2001-05-23/09:00:00	15.0	0.24	4.1	365	-43.6
236	2001-06-01/21:45:00	2001-06-02/03:32:00	19.9	0.18	3.1	402	-43.2
237	2001-06-18/21:30:00	2001-06-18/22:30:00	14.7	0.13	2.4	381	-3.2
238	2001-07-16/05:30:00	2001-07-16/10:00:00	10.5	0.27	4.8	402	-17.2
239	2001-08-05/12:35:00	2001-08-05/14:12:00	15.2	0.1	4.0	463	-36.2
240	2001-08-05/14:50:00	2001-08-05/16:22:00	13.2	0.21	3.7	483	-7.1
241	2001-08-10/04:32:00	2001-08-10/05:38:00	10.0	0.25	4.6	391	-10.4
242	2001-08-13/01:12:00	2001-08-13/05:30:00	12.7	0.24	4.4	395	10.7
243	2001-08-13/06:15:00	2001-08-13/07:35:00	11.3	0.15	4.7	383	-16.8
244*	2001-08-17/13:48:00	2001-08-17/19:25:00	29.6	0.23	3.6	490	-33.0
245*	2001-08-17/20:32:00	2001-08-17/22:25:00	28.4	0.09	3.9	502	-4.0
246	2001-08-26/07:35:00	2001-08-26/09:10:00	10.2	0.18	4.3	429	-13
247	2001-09-08/12:10:00	2001-09-08/15:10:00	12.1	0.06	1.8	248	1.1
248	2001-09-18/18:15:00	2001-09-19/02:15:00	10.1	0.14	4.8	426	-17.0
249	2001-09-26/10:30:00	2001-09-26/15:45:00	14.9	0.21	2.9	623	41.6
250	2001-10-08/12:30:00	2001-10-08/14:15:00	12.4	0.2	4.8	383	-23.2
251*	2001-10-21/21:22:00	2001-10-21/23:10:00	28.1	0.09	3.3	625	-14.1
252	2001-11-05/03:00:00	2001-11-05/08:30:00	10.2	0.06	4.2	363	-5.8
253*	2001-11-05/08:55:00	2001-11-05/10:30:00	10.0	0.13	5.0	358	7.3
254*	2001-11-05/16:25:00	2001-11-05/17:22:00	24.0	0.27	3.4	401	1.9
255	2001-12-15/17:00:00	2001-12-15/21:40:00	22.4	0.32	4.5	373	-11.7
256	2001-12-17/11:20:00	2001-12-17/19:40:00	10.1	0.11	3.5	471	21.0
2002							
257	2002-01-07/22:35:00	2002-01-08/03:32:00	12.4	0.11	3.5	373	-15.1
258	2002-01-08/06:35:00	2002-01-08/07:33:00	12.1	0.16	4.4	369	-6.5
259	2002-01-19/08:45:00	2002-01-19/13:12:00	15.4	0.16	4.4	343	-24.7
260	2002-02-02/01:32:00	2002-02-02/09:25:00	12.3	0.12	4.4	342	-8.1
261	2002-03-02/12:45:00	2002-03-02/17:10:00	11.8	0.11	4.6	387	9.0
262	2002-03-29/23:20:00	2002-03-30/00:30:00	21.3	0.26	5.1	375	-5.2
263*	2002-04-17/17:45:00	2002-04-17/18:25:00	23.4	0.11	4.1	529	-24.6
264*	2002-04-20/00:48:00	2002-04-20/03:35:00	19.4	0.06	3.8	574	7.6
265*	2002-05-11/12:32:00	2002-05-11/20:12:00	17.6	0.17	3.8	436	-2.1
266	2002-06-08/12:40:00	2002-06-08/15:22:00	13.9	0.21	4.6	369	-18.9

Table A.1: STs list from Wind Observation

No.	Start	End	B	β_p	M_A	V_p	V_{exp}
267	2002-06-19/06:00:00	2002-06-19/06:40:00	15.5	0.29	4.2	429	-9.4
268	2002-07-29/13:20:00	2002-07-29/15:30:00	16.1	0.14	4.1	507	-16.3
269	2002-09-03/12:00:00	2002-09-03/18:22:00	14.9	0.09	4.4	350	-7.6
270	2002-09-03/19:15:00	2002-09-04/03:50:00	17.9	0.13	3.9	373	2.5
271*	2002-09-07/20:40:00	2002-09-08/04:15:00	19.3	0.27	3.6	509	37.8
272	2002-09-29/03:58:00	2002-09-29/14:25:00	12.9	0.06	4.0	298	-6.9
273*	2002-09-30/09:00:00	2002-09-30/10:00:00	22.3	0.06	3.0	345	-4.8
274	2002-10-02/04:20:00	2002-10-02/05:25:00	14.9	0.25	3.5	374	10.3
275	2002-10-15/03:00:00	2002-10-15/07:22:00	14.4	0.26	4.2	442	-33.0
276	2002-10-30/02:15:00	2002-10-30/05:45:00	11.6	0.17	4.4	485	-7.9
277	2002-11-12/12:02:00	2002-11-12/15:25:00	13.5	0.1	4.2	566	-4.8
278	2002-12-14/17:20:00	2002-12-14/20:05:00	14.5	0.23	3.4	487	-18.7
279*	2002-12-19/11:25:00	2002-12-19/13:40:00	19.8	0.2	3.0	451	-8.7
280*	2002-12-22/10:20:00	2002-12-22/19:10:00	17.1	0.12	5.6	472	-14.7
281	2002-12-23/01:12:00	2002-12-23/04:15:00	14.0	0.16	4.0	498	-7.8
282	2002-12-26/11:45:00	2002-12-26/16:30:00	11.5	0.09	4.3	400	8.4
2003							
283	2003-01-03/01:00:00	2003-01-03/03:02:00	12.4	0.19	4.7	390	-25.7
284	2003-01-03/10:35:00	2003-01-03/13:50:00	13.6	0.29	5.0	516	-17.7
285	2003-01-09/17:35:00	2003-01-09/22:45:00	10.9	0.15	5.0	309	-7.7
286*	2003-02-02/08:45:00	2003-02-02/12:32:00	12.2	0.07	5.6	504	14.6
287	2003-02-06/14:40:00	2003-02-06/17:05:00	10.0	0.34	5.2	504	2.6
288	2003-02-27/00:40:00	2003-02-27/03:00:00	14.6	0.39	4.3	514	-21.5
289*	2003-03-19/21:30:00	2003-03-20/05:22:00	10.2	0.29	4.9	671	-31.1
290	2003-04-08/06:48:00	2003-04-08/07:35:00	13.5	0.26	4.3	419	-9.6
291	2003-05-04/17:58:00	2003-05-05/05:50:00	11.1	0.22	5.4	407	-7.8
292	2003-05-21/15:10:00	2003-05-21/19:00:00	13.2	0.22	4.6	478	-26.2
293*	2003-05-30/01:25:00	2003-05-30/10:00:00	26.1	0.23	5.5	645	53.1
294*	2003-05-30/11:15:00	2003-05-30/16:30:00	15.3	0.1	4.2	590	-140.3
295*	2003-06-16/00:15:00	2003-06-16/02:38:00	13.8	0.13	5.4	539	9.4
296*	2003-06-16/17:25:00	2003-06-16/22:25:00	10.9	0.06	2.9	535	8.9
297	2003-06-26/21:15:00	2003-06-26/22:38:00	14.1	0.36	5.4	667	-14.8
298	2003-07-14/17:55:00	2003-07-14/22:05:00	10.7	0.12	5.2	514	-4.9
299	2003-07-26/00:10:00	2003-07-26/10:45:00	13.5	0.09	4.4	337	-16.3
300	2003-07-26/18:00:00	2003-07-26/20:45:00	32.3	0.24	3.6	479	-69.8
301	2003-08-28/23:00:00	2003-08-29/00:35:00	10.0	0.16	5.3	441	-1.7
302	2003-09-01/06:35:00	2003-09-01/10:40:00	11.5	0.24	4.2	415	-0.3
303	2003-09-01/11:30:00	2003-09-01/18:40:00	10.3	0.17	4.3	431	-43.2
304	2003-09-09/02:38:00	2003-09-09/04:55:00	9.7	0.28	5.1	439	4.7
305	2003-09-16/10:25:00	2003-09-16/18:45:00	15.6	0.2	5.3	445	-27.5
306	2003-10-13/14:50:00	2003-10-13/18:58:00	21.1	0.37	3.4	340	1.9
2004							

Table A.1: STs list from Wind Observation

No.	Start	End	B	β_p	M_A	V_p	V_{exp}
307	2004-03-09/18:35:00	2004-03-09/19:28:00	16.4	0.34	4.6	564	10.3
308	2004-03-09/20:32:00	2004-03-09/22:05:00	15.7	0.47	5.3	558	-4.1
309	2004-04-12/19:18:00	2004-04-12/22:18:00	9.6	0.26	4.3	486	0.8
310	2004-04-17/02:35:00	2004-04-17/10:10:00	10.2	0.41	5.2	395	35.8
311	2004-06-13/16:00:00	2004-06-13/22:45:00	9.4	0.06	5.0	357	2.4
312	2004-06-14/05:20:00	2004-06-14/14:30:00	11.9	0.09	4.5	367	-60.6
313	2004-06-28/16:45:00	2004-06-28/20:20:00	15.1	0.28	4.9	414	-43.9
314	2004-07-10/02:22:00	2004-07-10/06:15:00	9.3	0.22	5.3	307	2.0
315	2004-07-16/22:35:00	2004-07-17/02:50:00	15.7	0.2	4.1	469	-30.8
316	2004-08-18/06:12:00	2004-08-18/07:00:00	10.3	0.09	5.1	334	-0.7
317	2004-08-18/08:02:00	2004-08-18/12:25:00	10.5	0.05	3.9	326	4.4
318	2004-08-31/07:22:00	2004-08-31/16:30:00	10.4	0.4	5.0	429	-20.6
319	2004-09-05/17:22:00	2004-09-05/22:45:00	10.6	0.24	3.5	365	-11.3
320	2004-09-05/23:30:00	2004-09-06/00:55:00	8.5	0.39	5.1	340	-4.0
321*	2004-09-14/16:02:00	2004-09-14/18:00:00	13.1	0.2	5.7	566	6.9
322*	2004-09-14/18:50:00	2004-09-14/22:16:00	10.0	0.09	5.7	572	-14.0
323	2004-10-08/13:22:00	2004-10-08/15:02:00	9.6	0.37	5.5	346	-17.5
324*	2004-11-12/08:50:00	2004-11-12/13:18:00	10.8	0.05	3.3	594	13.3
325	2004-11-19/18:28:00	2004-11-19/21:28:00	16.8	0.14	4.6	375	-23.6
326	2004-12-05/07:25:00	2004-12-05/17:10:00	26.3	0.19	4.0	438	9.6
327	2004-12-16/03:00:00	2004-12-16/12:22:00	10.1	0.3	5.7	445	-37.3
328	2004-12-21/07:02:00	2004-12-21/09:28:00	13.3	0.47	5.6	410	-7.6
329	2004-12-25/06:40:00	2004-12-25/08:12:00	10.9	0.24	6.8	418	1.8
2005							
330	2005-01-02/00:38:00	2005-01-02/02:18:00	14.8	0.19	4.5	576	-34.0
331	2005-01-17/23:28:00	2005-01-18/00:40:00	20.8	0.09	2.9	577	-3.9
332	2005-01-18/17:10:00	2005-01-18/18:30:00	10.9	0.08	4.9	711	-6.8
333	2005-01-27/22:38:00	2005-01-28/00:45:00	10.4	0.17	4.9	349	-3.9
334	2005-01-28/01:35:00	2005-01-28/07:25:00	8.2	0.3	6.4	378	-1.4
335*	2005-02-19:05:50:00	2005-02-19/08:40:00	9.0	0.07	4.3	502	-2.5
336	2005-02-20/00:10:00	2005-02-20/05:22:00	8.5	0.16	5.3	503	13.6
337	2005-03-16/14:22:00	2005-03-17/01:45:00	9.1	0.17	4.6	393	6.3
338	2005-03-17/11:25:00	2005-03-17/13:38:00	8.5	0.33	5.1	396	-12.1
339	2005-03-17/17:35:00	2005-03-18/03:50:00	8.9	0.2	4.9	403	17.5
340	2005-04-04/01:55:00	2005-04-04/04:48:00	10.3	0.21	6.2	351	-9.7
341	2005-04-04/12:35:00	2005-04-04/14:05:00	12.8	0.21	4.5	512	4.8
342	2005-04-11/16:15:00	2005-04-11/20:00:00	14.8	0.33	5.3	379	-28.7
343	2005-04-12/11:40:00	2005-04-12/19:28:00	10.4	0.32	5.2	490	-15.4
344	2005-04-20/01:25:00	2005-04-20/02:25:00	14.0	0.44	5.7	435	3.1
345	2005-04-29/23:05:00	2005-04-30/00:32:00	12.5	0.34	4.9	419	-20.6
346	2005-04-30/02:45:00	2005-04-30/06:35:00	12.3	0.3	5.4	505	-27.8
347	2005-05-07/21:22:00	2005-05-07/22:22:00	18.7	0.22	4.2	442	3.1

Table A.1: STs list from Wind Observation

No.	Start	End	B	β_p	M_A	V_p	V_{exp}
348	2005-05-08/03:25:00	2005-05-08/04:35:00	8.3	0.19	4.9	495	20.2
349	2005-05-08/05:45:00	2005-05-08/07:38:00	9.4	0.29	5.5	478	-20.6
350	2005-06-04/21:05:00	2005-06-04/22:25:00	15.5	0.16	3.3	490	-16.0
351	2005-06-11/16:00:00	2005-06-11/23:18:00	8.7	0.17	5.8	313	2.3
352*	2005-06-14/23:22:00	2005-06-15/01:35:00	11.1	0.2	6.2	518	-22.5
353	2005-06-23/04:22:00	2005-06-23/13:40:00	18.2	0.29	5.7	395	-36.0
354	2005-07-01/12:35:00	2005-07-01/16:32:00	14.2	0.39	6.6	387	-39.6
355	2005-07-09/05:00:00	2005-07-09/09:45:00	11.8	0.14	5.4	334	7.3
356*	2005-07-11/00:20:00	2005-07-11/06:15:00	9.1	0.04	4.1	420	8.1
357	2005-07-13/00:30:00	2005-07-13/04:20:00	9.9	0.11	4.4	528	27.3
358*	2005-07-17/14:00:00	2005-07-17/21:35:00	12.8	0.2	5.5	443	5.7
359	2005-07-20/10:40:00	2005-07-20/14:40:00	11.8	0.41	6.2	472	9.2
360	2005-08-02/10:15:00	2005-08-02/11:22:00	10.3	0.22	5.5	478	-1.7
361	2005-08-02/11:50:00	2005-08-02/19:15:00	9.3	0.11	4.6	495	-20.4
362*	2005-08-10/07:02:00	2005-08-10/11:25:00	8.8	0.09	4.9	448	18.1
363	2005-08-13/01:32:00	2005-08-13/09:05:00	18.3	0.15	5.0	413	-35.2
364	2005-08-21/15:40:00	2005-08-21/23:45:00	9.7	0.21	5.1	504	-59.0
365	2005-08-31/00:15:00	2005-08-31/01:48:00	9.3	0.15	6.4	365	4.1
366*	2005-09-02/20:17:00	2005-09-02/23:30:00	11.7	0.04	5.1	634	-11.9
367	2005-09-10/01:45:00	2005-09-10/04:05:00	12.2	0.38	5.4	458	24.4
368*	2005-09-12/20:05:00	2005-09-12/22:02:00	9.0	0.07	6.2	827	11.7
369*	2005-09-15/16:00:00	2005-09-15/17:22:00	18.2	0.03	2.3	843	21.2
370	2005-09-30/21:27:00	2005-09-30/23:20:00	10.3	0.4	5.2	477	-27.9
371	2005-10-25/08:55:00	2005-10-25/10:00:00	9.7	0.31	5.0	405	10.5
372	2005-11-19/13:45:00	2005-11-19/21:35:00	9.8	0.39	6.5	375	-18.5
373	2005-11-29/17:00:00	2005-11-29/21:50:00	12.7	0.19	5.6	416	-48.8
374	2005-11-29/22:15:00	2005-11-29/23:20:00	14.8	0.23	7.2	519	0.04
375	2005-11-30/01:18:00	2005-11-30/03:00:00	12.9	0.23	4.8	541	-2.3
376	2005-12-09/18:22:00	2005-12-09/21:00:00	10.6	0.18	6.0	291	-4.0
377	2005-12-09/21:40:00	2005-12-10/07:40:00	14.0	0.19	4.4	306	-9
378	2005-12-27/12:10:00	2005-12-27/14:45:00	17.6	0.2	5.9	474	-37.8
2006							
379	2006-01-01/23:25:00	2006-01-02/03:22:00	9.9	0.35	5.5	441	9.7
380	2006-01-02/06:40:00	2006-01-02/09:30:00	8.1	0.11	2.9	428	7.4
381	2006-01-16/00:10:00	2006-01-16/02:20:00	12.1	0.45	5.4	414	-7.3
382	2006-01-18/05:15:00	2006-01-18/06:35:00	7.2	0.43	7.2	484	9.9
383	2006-01-22/13:05:00	2006-01-22/14:55:00	6.7	0.31	7.3	370	4.3
384	2006-01-24/15:40:00	2006-01-24/23:38:00	7.8	0.2	5.5	467	60.9
385	2006-02-10/21:18:00	2006-02-10/23:35:00	8.7	0.44	6.6	312	2.5
386	2006-02-15/07:27:00	2006-02-15/10:00:00	9.2	0.32	6.2	388	-5.9
387	2006-02-19/04:15:00	2006-02-19/07:22:00	6.6	0.26	6.4	372	5.1
388	2006-02-20/05:00:00	2006-02-20/06:18:00	10.9	0.36	6.1	418	-4.6

Table A.1: STs list from Wind Observation

No.	Start	End	B	β_p	M_A	V_p	V_{exp}
389	2006-02-21/08:18:00	2006-02-21/09:48:00	7.1	0.27	6.2	586	-20.3
390	2006-03-09/02:35:00	2006-03-09/09:30:00	7.4	0.38	6.4	337	2.9
391	2006-03-09/18:12:00	2006-03-09/21:15:00	9.7	0.37	6.8	343	5.1
392	2006-03-10/04:35:00	2006-03-10/07:00:00	10.7	0.26	5.2	395	-12.5
393	2006-03-10/17:26:00	2006-03-10/19:32:00	8.9	0.3	5.4	483	6.5
394	2006-03-14/12:45:00	2006-03-14/23:10:00	7.6	0.27	6.0	368	-11.4
395	2006-03-15/19:28:00	2006-03-15/22:45:00	7.5	0.36	7.3	461	5.8
396	2006-03-26/22:55:00	2006-03-27/00:32:00	8.4	0.47	6.9	368	-5.3
397	2006-04-08/21:40:00	2006-04-09/07:45:00	12.3	0.2	5.1	376	-80.4
398*	2006-04-14/13:30:00	2006-04-14/22:45:00	9.1	0.2	4.8	510	4.6
399	2006-04-21/15:10:00	2006-04-21/22:18:00	9.3	0.4	5.6	458	-70.3
400	2006-05-04/11:25:00	2006-05-04/15:50:00	12.6	0.23	6.0	335	1.9
401	2006-05-04/17:10:00	2006-05-04/18:55:00	10.8	0.25	6.3	331	3.4
402	2006-05-04/19:18:00	2006-05-04/21:30:00	9.1	0.27	7.1	328	4.1
403	2006-05-04/21:55:00	2006-05-05/03:32:00	9.8	0.18	5.5	323	-0.5
404	2006-05-05/04:00:00	2006-05-05/07:45:00	8.3	0.34	6.9	342	2.0
405	2006-05-11/00:45:00	2006-05-11/02:05:00	9.5	0.46	6.9	458	-10.4
406	2006-05-17/13:50:00	2006-05-17/19:00:00	8.0	0.28	6.2	340	8.7
407	2006-05-17/21:05:00	2006-05-18/00:12:00	8.8	0.23	6.4	333	10.0
408	2006-05-18/08:45:00	2006-05-18/10:35:00	14.2	0.42	5.0	421	-23.4
409	2006-05-30/09:22:00	2006-05-30/13:00:00	8.2	0.28	7.2	320	-5.7
410	2006-05-31/00:00:00	2006-05-31/04:22:00	8.1	0.42	5.5	332	-10.3
411	2006-06-06/05:40:00	2006-06-06/08:00:00	13.5	0.21	6.1	389	-23.9
412	2006-06-14/09:25:00	2006-06-14/16:20:00	8.9	0.13	5.1	387	-10.2
413	2006-06-27/19:15:00	2006-06-27/20:20:00	9.7	0.48	7.3	350	-9.4
414	2006-06-27/22:28:00	2006-06-28/01:25:00	11.4	0.51	6.5	373	-13.3
415	2006-07-04/11:55:00	2006-07-04/12:35:00	16.6	0.14	4.5	382	-1.2
416	2006-07-04/17:30:00	2006-07-04/21:20:00	16.5	0.31	4.3	423	-7.0
417	2006-07-12/02:28:00	2006-07-12/04:00:00	10.2	0.53	6.5	449	-19.7
418	2006-07-31/03:25:00	2006-07-31/09:50:00	12.7	0.24	5.5	410	-35.8
419	2006-08-07/03:30:00	2006-08-07/08:35:00	16.4	0.58	5.6	444	-61.2
420	2006-08-18/01:15:00	2006-08-18/05:00:00	8.1	0.26	6.9	332	-16.9
421*	2006-08-20/04:45:00	2006-08-20/11:28:00	11.6	0.26	4.2	409	13.3
422	2006-08-27/10:35:00	2006-08-27/12:00:00	13.8	0.29	6.7	361	-38.7
423	2006-09-01/12:40:00	2006-09-01/18:00:00	8.0	0.23	5.8	399	-5.9
424	2006-09-03/04:00:00	2006-09-03/06:05:00	7.1	0.22	6.0	433	6.3
425	2006-09-04/00:22:00	2006-09-04/04:02:00	13.3	0.29	6.5	455	10.5
426	2006-09-10/21:30:00	2006-09-11/01:45:00	10.1	0.18	4.9	355	-12.9
427	2006-09-12/01:45:00	2006-09-12/04:55:00	7.8	0.2	5.6	356	8.8
428*	2006-09-30/02:50:00	2006-09-30/05:10:00	10.3	0.16	3.8	352	-40.9
429	2006-10-07/15:45:00	2006-10-07/16:40:00	13.8	0.2	3.5	409	-16.6
430	2006-10-13/11:30:00	2006-10-13/15:48:00	9.5	0.49	5.4	441	-23.2

Table A.1: STs list from Wind Observation

No.	Start	End	B	β_p	M_A	V_p	V_{exp}
431	2006-10-27/21:35:00	2006-10-28/01:25:00	7.6	0.33	7.1	325	-1.2
432	2006-10-28/03:00:00	2006-10-28/05:00:00	6.7	0.25	6.8	352	-5.3
433	2006-10-28/08:05:00	2006-10-28/09:48:00	8.6	0.14	5.9	360	2.3
434	2006-10-28/13:05:00	2006-10-28/14:20:00	10.2	0.39	6.3	374	-31
435	2006-10-28/14:45:00	2006-10-28/15:35:00	12.7	0.17	4.5	423	-5.1
436	2006-12-15/16:12:00	2006-12-15/19:22:00	6.8	0.13	4.4	613	12.8
437*	2006-12-16/18:30:00	2006-12-16/19:32:00	11.6	0.08	5.6	649	10.2
438	2006-12-18/12:28:00	2006-12-18/15:30:00	8.8	0.33	7.0	451	-7.5
439	2006-12-18/16:25:00	2006-12-18/19:20:00	10.7	0.22	5.7	468	-27.6
2007							
440	2007-01-01/09:27:00	2007-01-01/13:40:00	10.3	0.35	7.2	371	-3.0
441	2007-01-02/06:25:00	2007-01-02/08:02:00	8.7	0.46	6.6	562	-32.3
442	2007-01-15/11:00:00	2007-01-15/12:25:00	13.3	0.19	4.2	524	-20.8
443	2007-01-15/19:30:00	2007-01-16/03:22:00	8.3	0.23	5.8	519	11.7
444	2007-02-13/04:16:00	2007-02-13/05:16:00	8.6	0.47	6.6	516	-0.3
445	2007-03-04/22:00:00	2007-03-05/00:20:00	7.3	0.4	6.4	390	-15.8
446	2007-03-06/00:40:00	2007-03-06/02:32:00	8.6	0.43	7.0	405	1.0
447	2007-03-06/05:28:00	2007-03-06/06:30:00	10.1	0.27	4.8	440	5.3
448	2007-03-06/22:58:00	2007-03-07/01:20:00	8.3	0.6	7.0	582	16.4
449	2007-03-11/06:42:00	2007-03-11/14:50:00	8.2	0.21	6.6	343	-21.3
450	2007-03-23/03:15:00	2007-03-23/05:25:00	6.1	0.25	8.0	275	-9.2
451	2007-03-23/06:42:00	2007-03-23/09:55:00	7.0	0.31	7.9	310	-5.2
452	2007-03-23/11:00:00	2007-03-23/13:45:00	7.4	0.32	7.5	314	-8.1
453	2007-03-24/03:22:00	2007-03-24/13:28:00	9.6	0.08	4.6	363	4.9
454	2007-03-24/18:45:00	2007-03-25/04:32:00	11.0	0.16	6.2	366	-8.5
455	2007-03-25/19:55:00	2007-03-25/23:18:00	6.8	0.37	6.6	415	-5.7
456	2007-03-26/00:10:00	2007-03-26/03:40:00	6.1	0.49	8.0	445	-4.0
457	2007-03-26/14:05:00	2007-03-26/16:25:00	6.2	0.36	8.0	474	-7.8
458	2007-03-31/19:30:00	2007-03-31/22:55:00	9.1	0.26	6.4	367	-33.4
459	2007-04-01/00:02:00	2007-04-01/01:38:00	11.4	0.53	6.3	415	-8.7
460	2007-04-01/19:45:00	2007-04-01/23:25:00	8.0	0.58	6.8	549	-9.6
461	2007-04-02/12:18:00	2007-04-02/12:55:00	5.9	0.48	7.8	618	4.9
462	2007-04-09/01:00:00	2007-04-09/03:45:00	14.7	0.19	3.4	340	41.2
463	2007-04-10/11:20:00	2007-04-10/13:15:00	8.0	0.32	6.0	400	-22.5
464	2007-04-12/06:28:00	2007-04-12/08:02:00	6.1	0.53	8.1	544	8.1
465	2007-04-17/05:18:00	2007-04-17/16:48:00	8.7	0.31	5.8	339	-13.1
466	2007-04-18/16:52:00	2007-04-18/22:48:00	6.5	0.47	7.9	375	-11.4
467	2007-04-22/04:30:00	2007-04-22/07:18:00	7.6	0.41	8.0	328	-12.3
468	2007-04-22/07:30:00	2007-04-22/10:50:00	10.1	0.34	7.6	343	1.2
469	2007-04-22/21:45:00	2007-04-22/23:05:00	10.5	0.19	5.3	419	-9.7
470	2007-04-23/01:12:00	2007-04-23/04:32:00	12.3	0.54	6.7	451	-28.0
471	2007-05-07/10:25:00	2007-05-07/14:22:00	19.1	0.21	3.5	389	-26.7

Table A.1: STs list from Wind Observation

No.	Start	End	B	β_p	M_A	V_p	V_{exp}
472	2007-05-07/21:10:00	2007-05-08/01:10:00	11.5	0.48	5.0	580	-55.4
473	2007-05-18/06:05:00	2007-05-18/12:00:00	15.4	0.53	6.0	448	-89.8
474	2007-05-23/05:02:00	2007-05-23/14:20:00	9.3	0.23	6.6	490	-25.1
475	2007-05-31/21:55:00	2007-05-31/23:40:00	6.8	0.18	6.0	323	-0.9
476	2007-06-01/21:10:00	2007-06-02/05:05:00	10.6	0.22	5.2	376	-12.2
477	2007-06-02/07:02:00	2007-06-02/09:40:00	9.9	0.19	5.3	379	7.1
478	2007-06-02/15:22:00	2007-06-02/20:48:00	10.9	0.24	4.2	385	-23.8
479	2007-06-03/16:18:00	2007-06-03/18:10:00	7.5	0.34	6.5	429	-31.8
480	2007-06-03/18:28:00	2007-06-03/20:38:00	6.7	0.47	8.0	470	-15.5
481	2007-06-03/23:40:00	2007-06-04/01:18:00	6.3	0.36	7.9	477	19.4
482	2007-06-04/14:20:00	2007-06-04/17:15:00	7.0	0.15	5.5	503	4.8
483	2007-06-09/08:00:00	2007-06-09/14:15:00	6.3	0.48	7.5	437	-24.9
484	2007-06-13/15:02:00	2007-06-13/17:35:00	8.7	0.18	6.2	312	-3.3
485	2007-06-13/17:50:00	2007-06-13/21:10:00	10.0	0.25	4.3	364	-49.9
486	2007-06-14/11:25:00	2007-06-14/13:32:00	9.7	0.46	6.5	507	-20.6
487	2007-06-21/09:15:00	2007-06-21/11:40:00	9.7	0.41	6.2	432	-12.4
488	2007-06-29/08:55:00	2007-06-29/10:30:00	6.8	0.23	5.8	350	1.0
489	2007-06-30/01:00:00	2007-06-30/03:00:00	7.9	0.38	7.4	524	-3.1
490	2007-07-03/10:00:00	2007-07-03/19:00:00	9.2	0.2	6.4	366	-29.8
491	2007-07-10/17:15:00	2007-07-10/23:40:00	12.6	0.24	7.3	347	-12.2
492	2007-07-13/22:25:00	2007-07-14/08:30:00	6.9	0.13	6.3	402	-1.5
493	2007-07-14/11:48:00	2007-07-14/18:10:00	11.1	0.26	5.4	444	-15.4
494	2007-07-21/11:35:00	2007-07-21/13:50:00	6.0	0.6	7.6	474	-5.4
495	2007-07-26/18:32:00	2007-07-26/19:18:00	12.3	0.41	5.3	411	6.6
496	2007-07-27/03:00:00	2007-07-27/04:12:00	9.0	0.4	5.6	447	-7.6
497	2007-07-29/00:32:00	2007-07-29/06:42:00	13.1	0.32	6.1	408	-29.8
498	2007-07-29/12:05:00	2007-07-29/15:20:00	8.9	0.48	5.9	492	-47.8
499	2007-08-01/00:25:00	2007-08-01/03:38:00	6.8	0.46	6.2	530	25.4
500	2007-08-01/04:32:00	2007-08-01/06:58:00	7.6	0.53	7.0	575	8.8
501	2007-08-06/14:25:00	2007-08-06/15:58:00	10.4	0.41	6.9	370	-9.2
502	2007-08-15/02:00:00	2007-08-15/04:20:00	7.9	0.19	5.3	363	-11.4
503	2007-08-16/06:05:00	2007-08-16/07:38:00	6.1	0.29	6.8	455	10.3
504	2007-08-19/09:20:00	2007-08-19/13:40:00	6.7	0.3	6.4	378	-8.3
505	2007-08-25/12:40:00	2007-08-25/23:32:00	8.5	0.53	7.0	350	-15.2
506	2007-08-26/17:10:00	2007-08-26/20:48:00	18.2	0.24	2.8	396	-24.1
507	2007-09-14/14:40:00	2007-09-14/16:58:00	9.6	0.51	7.3	299	-9.9
508	2007-09-14/18:35:00	2007-09-14/23:40:00	13.6	0.28	4.7	340	-39.7
509	2007-09-15/01:28:00	2007-09-15/06:42:00	7.7	0.55	6.8	421	-7.6
510	2007-09-21/13:28:00	2007-09-21/17:00:00	9.8	0.6	6.3	471	-25.1
511	2007-10-02/21:45:00	2007-10-03/04:38:00	7.1	0.25	6.8	461	7.3
512	2007-10-12/06:30:00	2007-10-12/08:30:00	7.2	0.37	7.9	300	-0.9
513	2007-10-12/12:25:00	2007-10-12/16:00:00	8.1	0.24	6.0	308	-9.5

Table A.1: STs list from Wind Observation

No.	Start	End	B	β_p	M_A	V_p	V_{exp}
514	2007-10-18/01:02:00	2007-10-18/07:45:00	8.9	0.25	6.3	361	-31.5
515	2007-10-18/11:32:00	2007-10-18/20:50:00	10.4	0.24	5.6	448	-47.8
516	2007-11-08/14:15:00	2007-11-08/22:55:00	6.3	0.39	7.1	307	-14.8
517	2007-11-09/14:33:00	2007-11-09/21:00:00	9.4	0.42	6.0	371	-17.0
518	2007-11-09/22:22:00	2007-11-09/23:50:00	9.4	0.42	5.5	410	-15.9
519	2007-11-10/01:20:00	2007-11-10/03:20:00	8.3	0.39	5.5	414	7.9
520	2007-11-10/09:58:00	2007-11-10/14:35:00	6.2	0.42	6.5	418	-7.9
521	2007-11-12/23:30:00	2007-11-13/02:38:00	12.2	0.31	5.8	404	-15.7
522	2007-12-10/11:35:00	2007-12-10/18:30:00	12.0	0.44	6.0	385	-28.3
523	2007-12-10/19:00:00	2007-12-10/23:32:00	13.5	0.52	5.9	451	1.3
524	2007-12-11/00:28:00	2007-12-11/01:22:00	13.5	0.46	5.1	547	-34.3
525	2007-12-20/02:35:00	2007-12-20/05:30:00	7.1	0.39	7.5	565	-5.5
526	2007-12-27/02:05:00	2007-12-27/07:32:00	6.2	0.46	7.7	346	-10.2
527	2007-12-27/17:20:00	2007-12-27/18:15:00	9.0	0.2	6.3	413	-1.0
528	2007-12-28/00:48:00	2007-12-28/03:22:00	6.0	0.5	7.7	464	8.2
529	2007-12-31/02:15:00	2007-12-31/11:05:00	6.7	0.27	7.4	332	-7.6
530	2007-12-31/19:15:00	2007-12-31/21:05:00	6.9	0.39	5.9	351	5.7
2008							
531	2008-01-05/03:12:00	2008-01-05/05:55:00	13.9	0.36	5.9	407	-38.3
532	2008-01-05/06:20:00	2008-01-05/07:10:00	17.0	0.39	5.3	461	-26.8
533	2008-01-13/07:25:00	2008-01-13/09:10:00	6.2	0.55	7.0	448	-0.4
534	2008-01-13/09:25:00	2008-01-13/13:10:00	7.5	0.38	6.6	450	-16.8
535	2008-01-13/13:30:00	2008-01-13/15:05:00	8.7	0.43	6.0	473	-5.4
536	2008-01-24/12:50:00	2008-01-24/14:00:00	6.2	0.3	7.1	423	-14.3
537	2008-01-25/00:35:00	2008-01-25/02:22:00	9.3	0.32	5.7	465	-27.3
538	2008-01-29/06:02:00	2008-01-29/07:35:00	6.1	0.38	6.1	410	12.1
539	2008-01-31/21:55:00	2008-02-01/02:55:00	9.5	0.26	5.4	445	5.2
540	2008-02-10/06:22:00	2008-02-10/09:28:00	15.9	0.27	3.9	457	-40.9
541	2008-02-25/02:50:00	2008-02-25/08:35:00	5.8	0.34	7.1	420	-4.0
542	2008-02-28/03:35:00	2008-02-28/07:10:00	8.4	0.48	6.2	423	-6.2
543	2008-02-28/17:20:00	2008-02-28/23:10:00	10.0	0.49	6.3	529	-49.2
544	2008-03-08/16:12:00	2008-03-08/17:00:00	12.3	0.26	5.2	367	2.7
545	2008-03-08/17:45:00	2008-03-08/22:48:00	8.8	0.32	6.0	447	-9.6
546	2008-03-08/23:10:00	2008-03-09/00:48:00	11.3	0.17	5.0	445	3.0
547	2008-03-09/02:45:00	2008-03-09/06:05:00	15.3	0.47	5.5	512	-31.9
548	2008-03-22/11:35:00	2008-03-22/14:15:00	5.7	0.36	7.9	432	-1.9
549	2008-03-22/14:45:00	2008-03-22/22:12:00	7.0	0.25	6.3	448	3.0
550	2008-03-23/02:27:00	2008-03-23/04:00:00	6.1	0.35	6.6	445	0.8
551	2008-04-01/03:15:00	2008-04-01/04:35:00	5.7	0.11	6.4	402	-3.4
552	2008-04-16/16:00:00	2008-04-16/18:32:00	6.2	0.62	8.6	544	2.5
553	2008-04-22/21:30:00	2008-04-23/00:18:00	6.5	0.38	7.7	390	-12.5
554	2008-04-23/06:12:00	2008-04-23/07:16:00	14.5	0.38	4.4	511	-18.8

Table A.1: STs list from Wind Observation

No.	Start	End	B	β_p	M_A	V_p	V_{exp}
555	2008-05-15/23:55:00	2008-05-16/03:50:00	7.0	0.11	5.6	366	-26.0
556	2008-05-18/10:20:00	2008-05-18/13:00:00	5.5	0.23	7.1	346	-7.7
557	2008-05-19/01:45:00	2008-05-19/05:35:00	7.0	0.3	6.5	350	-8.0
558	2008-05-23/14:12:00	2008-05-23/15:22:00	5.6	0.23	6.7	471	-0.5
559	2008-06-06/08:55:00	2008-06-06/11:20:00	7.1	0.2	5.4	361	-0.3
560	2008-06-06/19:35:00	2008-06-06/23:20:00	6.1	0.46	7.8	461	-6.8
561	2008-06-06/23:38:00	2008-06-07/03:40:00	6.6	0.14	6.3	429	2.6
562	2008-06-15/18:22:00	2008-06-15/20:25:00	8.2	0.56	7.2	606	-15.5
563	2008-06-20/04:18:00	2008-06-20/06:00:00	6.4	0.65	7.7	547	4.5
564	2008-06-25/18:55:00	2008-06-25/20:32:00	13.3	0.42	4.8	463	-8.5
565	2008-07-01/08:35:00	2008-07-01/11:15:00	5.6	0.4	8.1	443	8.5
566	2008-07-05/08:16:00	2008-07-05/17:40:00	7.4	0.44	6.1	369	-29.5
567	2008-07-11/11:20:00	2008-07-11/14:32:00	8.1	0.39	6.0	386	-31.7
568	2008-07-22/10:16:00	2008-07-22/12:48:00	10.1	0.41	6.8	416	-37.3
569	2008-07-30/07:30:00	2008-07-30/11:32:00	5.8	0.28	8.1	348	-9.4
570	2008-08-01/01:30:00	2008-08-01/05:18:00	5.5	0.53	7.3	390	4.6
571	2008-08-08/14:15:00	2008-08-08/23:50:00	6.6	0.15	6.4	358	7.2
572	2008-08-09/00:22:00	2008-08-09/05:52:00	18.1	0.17	5.2	421	-15.6
573	2008-08-09/09:22:00	2008-08-09/11:20:00	9.7	0.57	5.3	445	-20.8
574	2008-08-09/12:45:00	2008-08-09/14:02:00	7.9	0.31	5.4	506	-2.1
575	2008-08-14/04:05:00	2008-08-14/04:55:00	6.0	0.24	7.4	470	-1.1
576	2008-08-18/00:12:00	2008-08-18/06:32:00	7.4	0.47	7.8	414	-57.3
577	2008-08-18/10:20:00	2008-08-18/11:30:00	10.7	0.58	6.3	537	-11.4
578	2008-09-03/04:22:00	2008-09-03/08:40:00	12.3	0.3	6.0	370	-25.8
579	2008-09-25/20:12:00	2008-09-25/22:25:00	7.5	0.16	6.4	338	7.4
580	2008-09-28/08:58:00	2008-09-28/11:00:00	5.9	0.22	6.8	348	1.0
581	2008-09-28/12:58:00	2008-09-28/17:55:00	5.9	0.18	6.8	358	-10.2
582	2008-09-30/11:32:00	2008-09-30/15:05:00	6.3	0.37	7.7	353	-6.9
583	2008-09-30/20:02:00	2008-10-01/03:32:00	7.6	0.68	7.5	474	14.0
584	2008-10-11/05:32:00	2008-10-11/08:22:00	11.5	0.43	7.5	350	-23.3
585	2008-10-19/04:12:00	2008-10-19/05:00:00	5.7	0.3	7.2	290	1.9
586	2008-10-19/07:12:00	2008-10-19/07:58:00	6.5	0.22	6.4	299	-1.1
587	2008-10-19/19:55:00	2008-10-19/23:10:00	7.4	0.33	6.1	310	-11.7
588	2008-10-22/12:15:00	2008-10-22/19:17:00	6.2	0.44	7.7	382	-32.9
589	2008-10-26/04:05:00	2008-10-26/05:30:00	7.4	0.32	6.9	332	-20.4
590	2008-11-07/02:02:00	2008-11-07/07:48:00	8.4	0.37	7.5	324	-24.6
591	2008-11-14/20:10:00	2008-11-15/04:42:00	5.5	0.27	7.7	316	4.3
592	2008-11-15/17:20:00	2008-11-15/18:25:00	9.6	0.43	7.3	354	-1.6
593	2008-11-15/19:32:00	2008-11-15/20:50:00	13.0	0.18	4.7	373	-1.4
594	2008-11-16/04:20:00	2008-11-16/07:02:00	7.1	0.5	6.5	470	-44.7
595	2008-11-25/02:35:00	2008-11-25/07:00:00	20.3	0.46	4.1	418	-68.2
596	2008-12-03/04:40:00	2008-12-03/11:00:00	6.0	0.37	8.5	319	-15.9

Table A.1: STs list from Wind Observation

No.	Start	End	B	β_p	M_A	V_p	V_{exp}
597	2008-12-03/18:32:00	2008-12-03/19:30:00	8.8	0.15	4.9	409	-4.3
598	2008-12-03/23:20:00	2008-12-04/02:55:00	8.9	0.19	4.9	447	-17.5
599*	2008-12-04/12:40:00	2008-12-04/16:32:00	6.9	0.3	6.4	427	-6.9
600	2008-12-05/13:40:00	2008-12-05/21:22:00	8.6	0.4	6.1	419	3.0
601	2008-12-10/12:55:00	2008-12-10/18:48:00	5.5	0.15	7.3	341	8.1
602	2008-12-10/20:32:00	2008-12-10/22:30:00	6.4	0.19	6.9	348	-1.3
603	2008-12-12/21:40:00	2008-12-12/23:45:00	5.6	0.3	6.5	403	3.0
604*	2008-12-16/10:45:00	2008-12-16/12:42:00	7.4	0.2	7.2	368	-2.0
605	2008-12-22/23:10:00	2008-12-23/06:30:00	7.9	0.29	6.0	431	-49.0
606	2008-12-31/00:22:00	2008-12-31/01:40:00	13.2	0.68	6.0	372	-15.3
2009							
607	2009-01-02/17:20:00	2009-01-02/22:45:00	6.1	0.41	6.2	457	-25.2
608	2009-01-03/03:00:00	2009-01-03/04:10:00	7.3	0.36	6.1	503	-16.5
609	2009-01-10/04:30:00	2009-01-10/06:10:00	5.8	0.5	7.4	379	2.9
610	2009-01-14/00:20:00	2009-01-14/05:28:00	7.2	0.35	7.4	327	9.4
611	2009-01-15/02:30:00	2009-01-15/07:00:00	6.9	0.23	5.9	321	0.04
612	2009-01-15/10:30:00	2009-01-15/14:02:00	6.5	0.33	7.0	341	-21.2
613	2009-01-15/15:35:00	2009-01-15/18:48:00	7.0	0.31	5.8	338	-1.8
614	2009-01-18/15:02:00	2009-01-18/17:00:00	5.1	0.32	6.1	350	-4.7
615*	2009-01-18/22:00:00	2009-01-18/23:28:00	7.7	0.37	8.1	438	-22.3
616	2009-01-19/06:05:00	2009-01-19/07:48:00	9.2	0.4	4.3	411	-4
617*	2009-01-26/04:42:00	2009-01-26/15:16:00	9.9	0.14	5.2	348	27.9
618	2009-01-30/16:30:00	2009-01-30/18:12:00	5.1	0.49	8.2	357	7.8
619	2009-02-05/00:30:00	2009-02-05/02:02:00	6.7	0.6	7.2	351	-12.0
620	2009-02-14/05:10:00	2009-02-14/08:05:00	14.7	0.35	4.4	416	-54.6
621	2009-02-15/06:48:00	2009-02-15/09:00:00	5.5	0.58	8.4	534	-24.3
622	2009-02-20/03:50:00	2009-02-20/04:45:00	5.4	0.37	10.1	323	-0.7
623	2009-02-24/20:50:00	2009-02-24/22:02:00	5.9	0.24	6.4	434	4.7
624	2009-02-27/07:50:00	2009-02-27/10:00:00	8.8	0.58	7.2	514	-28.4
625	2009-03-03/10:15:00	2009-03-03/15:30:00	9.8	0.1	5.4	367	-25.2
626	2009-03-03/16:05:00	2009-03-03/18:02:00	10.5	0.1	4.8	377	8.5
627	2009-03-03/19:22:00	2009-03-03/21:12:00	9.1	0.18	6.3	358	22.7
628	2009-03-13/02:00:00	2009-03-13/03:00:00	14.8	0.36	4.5	423	-7.5
629	2009-03-13/17:58:00	2009-03-13/20:30:00	5.9	0.39	7.1	544	0.1
630	2009-03-21/03:40:00	2009-03-21/08:25:00	9.6	0.27	6.4	405	-6.8
631	2009-03-21/11:00:00	2009-03-21/15:00:00	8.3	0.57	5.3	408	5.9
632	2009-03-21/20:30:00	2009-03-21/23:32:00	7.9	0.23	5.3	388	6.5
633	2009-03-24/12:10:00	2009-03-24/15:12:00	5.8	0.58	7.6	433	-29.5
634	2009-03-24/20:15:00	2009-03-24/22:30:00	5.9	0.46	7.3	489	7.6
635	2009-03-28/18:02:00	2009-03-28/21:55:00	5.2	0.51	7.4	408	-28.3
636	2009-03-30/03:10:00	2009-03-30/09:00:00	4.6	0.32	7.8	410	3.9
637	2009-04-05/04:00:00	2009-04-05/05:25:00	6.0	0.39	6.9	342	-5.8

Table A.1: STs list from Wind Observation

No.	Start	End	B	β_p	M_A	V_p	V_{exp}
638	2009-04-05/06:20:00	2009-04-05/08:22:00	5.4	0.62	8.4	352	1.5
639	2009-04-08/17:58:00	2009-04-08/19:38:00	6.4	0.23	6.0	309	-5.9
640	2009-04-08/23:32:00	2009-04-09/02:05:00	7.8	0.56	7.3	374	-16.4
641	2009-04-09/11:42:00	2009-04-09/15:12:00	7.6	0.53	6.9	467	1.5
642	2009-04-16/15:12:00	2009-04-16/20:45:00	10.1	0.23	4.5	401	-47.9
643	2009-04-16/21:45:00	2009-04-17/04:25:00	10.3	0.21	4.3	383	-5.1
644	2009-04-17/12:48:00	2009-04-17/22:00:00	6.5	0.34	5.9	406	-0.1
645	2009-04-18/03:25:00	2009-04-18/05:12:00	6.2	0.31	6.6	452	-6.7
646	2009-04-24/14:02:00	2009-04-24/17:32:00	7.5	0.29	5.3	415	-2.6
647	2009-04-26/05:02:00	2009-04-26/07:55:00	6.4	0.33	6.1	376	-6.2
648	2009-05-06/04:00:00	2009-05-06/08:02:00	6.1	0.25	6.5	355	-3.4
649	2009-05-06/14:00:00	2009-05-06/15:10:00	7.0	0.34	6.5	366	0.6
650	2009-05-06/17:42:00	2009-05-06/19:30:00	7.1	0.36	6.3	428	2.2
651	2009-05-06/23:48:00	2009-05-07/04:05:00	5.5	0.52	8.2	441	-9.3
652	2009-05-07/22:10:00	2009-05-08/00:28:00	6.2	0.4	7.7	466	-11.0
653	2009-05-08/02:38:00	2009-05-08/03:30:00	6.4	0.41	7.4	484	-12.1
654	2009-05-09/03:28:00	2009-05-09/05:10:00	5.4	0.23	6.6	485	2.8
655	2009-05-14/10:40:00	2009-05-14/15:02:00	6.8	0.06	4.2	337	-11.0
656	2009-05-14/15:15:00	2009-05-14/20:35:00	6.7	0.25	6.5	356	-27.1
657	2009-05-16/01:12:00	2009-05-16/08:42:00	6.6	0.22	6.5	335	-5.5
658	2009-05-20/14:58:00	2009-05-20/23:45:00	6.8	0.21	7.4	319	-22.5
659	2009-05-21/15:25:00	2009-05-21/17:15:00	5.2	0.48	7.7	340	6.5
660	2009-05-22/20:12:00	2009-05-22/23:25:00	5.3	0.29	6.8	388	18.2
661	2009-05-28/07:05:00	2009-05-28/08:02:00	11.7	0.19	6.6	343	3.1
662	2009-05-29/05:25:00	2009-05-29/15:50:00	6.0	0.28	6.1	385	24.7
663*	2009-06-05/06:10:00	2009-06-05/08:20:00	5.3	0.14	7.1	314	-0.6
664	2009-06-10/01:20:00	2009-06-10/03:58:00	5.4	0.35	7.5	326	-7.1
665	2009-06-14/20:45:00	2009-06-14/23:48:00	5.5	0.31	7.3	316	1.5
666	2009-06-20/05:40:00	2009-06-20/09:35:00	6.4	0.44	6.9	318	2.7
667	2009-06-20/11:00:00	2009-06-20/13:20:00	5.7	0.46	7.9	319	-3.0
668	2009-06-20/23:50:00	2009-06-21/04:15:00	6.6	0.31	7.9	351	-6.9
669	2009-06-21/08:02:00	2009-06-21/12:30:00	5.3	0.36	6.2	338	0.9
670	2009-06-24/09:40:00	2009-06-24/13:00:00	7.9	0.46	8.1	317	-27.3
671	2009-06-28/16:55:00	2009-06-28/19:32:00	9.7	0.25	6.4	384	-3.6
672	2009-07-05/14:45:00	2009-07-05/19:00:00	5.7	0.1	7.3	347	0.6
673	2009-07-05/19:55:00	2009-07-06/02:02:00	6.4	0.1	6.3	337	8.9
674	2009-07-10/02:00:00	2009-07-10/10:00:00	8.5	0.34	5.2	376	-18.7
675	2009-07-13/12:40:00	2009-07-13/13:40:00	8.3	0.39	7.9	374	-6.7
676	2009-07-27/07:00:00	2009-07-27/09:16:00	5.3	0.37	6.9	376	-3.3
677	2009-08-06/09:17:00	2009-08-06/10:45:00	10.4	0.38	5.2	488	8.6
678	2009-08-07/10:48:00	2009-08-07/14:20:00	6.1	0.13	5.5	460	3.1
679	2009-08-07/17:05:00	2009-08-07/22:00:00	5.9	0.37	7.5	445	3.0

Table A.1: STs list from Wind Observation

No.	Start	End	B	β_p	M_A	V_p	V_{exp}
680	2009-08-07/23:00:00	2009-08-08/01:55:00	6.0	0.48	7.5	478	-20.9
681	2009-08-17/22:00:00	2009-08-17/23:02:00	5.3	0.5	7.6	318	-4.6
682	2009-08-18/00:20:00	2009-08-18/01:32:00	5.8	0.46	7.3	324	1.2
683	2009-08-19/11:10:00	2009-08-19/19:12:00	9.9	0.26	5.4	354	-25.1
684	2009-08-19/23:05:00	2009-08-20/01:22:00	9.7	0.38	5.6	440	10.1
685	2009-08-22/02:30:00	2009-08-22/04:22:00	5.1	0.49	8.0	503	10.4
686	2009-09-03/20:35:00	2009-09-03/22:32:00	7.8	0.27	5.7	398	-31.1
687	2009-09-04/00:10:00	2009-09-04/02:38:00	7.8	0.29	5.7	410	12.7
688	2009-09-10/11:00:00	2009-09-10/16:38:00	5.3	0.18	6.3	305	1.7
689	2009-09-11/15:38:00	2009-09-11/18:12:00	5.4	0.24	7.0	305	2.2
690	2009-09-13/21:45:00	2009-09-14/00:15:00	6.8	0.6	6.9	348	-7.4
691	2009-09-15/08:48:00	2009-09-15/16:15:00	5.6	0.46	8.0	394	-20.2
692	2009-09-16/19:00:00	2009-09-16/21:22:00	5.6	0.45	8.4	441	-4.7
693	2009-09-21/00:45:00	2009-09-21/07:25:00	8.4	0.55	5.5	384	-21.2
694	2009-09-26/22:20:00	2009-09-27/02:42:00	8.0	0.25	6.7	321	-6.2
695	2009-09-28/05:28:00	2009-09-28/08:00:00	6.4	0.3	6.8	326	-0.6
696*	2009-09-30/01:42:00	2009-09-30/03:38:00	7.7	0.27	6.3	356	-3.0
697	2009-10-04/09:40:00	2009-10-04/12:10:00	9.0	0.47	6.0	353	-4.4
698	2009-10-04/18:12:00	2009-10-04/20:22:00	5.9	0.42	7.6	392	-1.6
699	2009-10-11/02:42:00	2009-10-11/04:02:00	12.0	0.19	6.6	298	-3.2
700	2009-10-12/11:40:00	2009-10-12/20:00:00	5.8	0.1	4.8	369	8.6
701	2009-10-13/13:22:00	2009-10-13/16:10:00	5.2	0.3	6.3	343	12.5
702	2009-10-15/07:40:00	2009-10-15/10:40:00	7.6	0.34	7.3	343	-18.6
703	2009-10-23/03:00:00	2009-10-23/04:10:00	8.6	0.33	8.1	390	0.8
704	2009-10-23/04:30:00	2009-10-23/07:58:00	7.9	0.5	7.2	375	7.3
705	2009-10-24/18:02:00	2009-10-24/21:20:00	8.4	0.59	7.3	397	-11.3
706	2009-10-30/00:30:00	2009-10-30/02:32:00	7.3	0.49	7.4	353	5.6
707	2009-10-30/04:30:00	2009-10-30/08:32:00	5.4	0.51	6.0	349	-2.4
708	2009-11-05/04:25:00	2009-11-05/07:58:00	5.2	0.43	7.8	294	2.5
709	2009-11-09/05:45:00	2009-11-09/07:50:00	7.4	0.48	6.6	387	-4.9
710*	2009-11-14/03:15:00	2009-11-14/07:40:00	7.1	0.36	8.1	323	0.5
711	2009-11-19/21:02:00	2009-11-20/06:42:00	6.2	0.19	5.2	347	-16.9
712	2009-11-20/17:40:00	2009-11-21/00:38:00	9.1	0.26	5.4	416	8.9
713	2009-11-21/03:15:00	2009-11-21/08:20:00	8.0	0.61	6.8	456	-28.7
714	2009-11-21/09:20:00	2009-11-21/13:20:00	5.8	0.57	7.5	540	-5.3
715	2009-11-26/08:02:00	2009-11-26/18:30:00	5.8	0.21	7.6	389	25.3
716	2009-11-26/19:02:00	2009-11-27/01:35:00	5.9	0.35	7.9	369	23.7
717	2009-11-27/03:10:00	2009-11-27/06:00:00	5.5	0.32	5.8	349	4.7
718	2009-12-06/07:00:00	2009-12-06/11:32:00	7.4	0.32	5.7	411	7.9
719*	2009-12-12/13:45:00	2009-12-12/18:00:00	6.3	0.3	7.5	293	-5.2
720	2009-12-16/07:27:00	2009-12-16/08:48:00	6.2	0.36	6.8	298	-2.4
721	2009-12-16/16:30:00	2009-12-16/18:35:00	5.5	0.57	7.3	322	-6.2

Table A.1: STs list from Wind Observation

No.	Start	End	B	β_p	M_A	V_p	V_{exp}
722	2009-12-17/09:02:00	2009-12-17/14:10:00	6.7	0.34	7.6	370	4.4
723	2009-12-17/15:48:00	2009-12-17/18:55:00	6.7	0.27	6.0	368	-20.3
724	2009-12-18/12:33:00	2009-12-18/18:30:00	6.0	0.43	7.6	418	2.1
725	2009-12-23/21:50:00	2009-12-23/23:12:00	5.7	0.54	8.0	351	-5.5
726	2009-12-24/03:28:00	2009-12-24/04:25:00	6.0	0.4	6.2	383	-12.4
727	2009-12-25/17:20:00	2009-12-25/21:00:00	8.8	0.3	5.5	330	-25.2
2010							
728	2010-01-03/11:00:00	2010-01-03/14:50:00	7.0	0.38	6.9	291	2.7
729	2010-01-04/03:02:00	2010-01-04/08:12:00	7.1	0.37	5.7	297	14.0
730	2010-01-04/14:00:00	2010-01-04/19:25:00	6.2	0.19	4.9	267	-4.7
731	2010-01-10/08:55:00	2010-01-10/11:25:00	6.1	0.28	6.7	299	-2.5
732	2010-01-11/06:48:00	2010-01-11/10:20:00	10.8	0.27	5.7	334	-19.7
733	2010-01-11/11:25:00	2010-01-11/13:10:00	10.8	0.25	5.3	389	-14.2
734	2010-01-11/13:50:00	2010-01-11/14:42:00	10.7	0.3	4.3	461	-25.6
735	2010-01-28/15:00:00	2010-01-28/19:28:00	6.1	0.44	6.8	375	8.1
736	2010-01-30/01:30:00	2010-01-30/07:02:00	8.2	0.24	6.3	347	19.8
737	2010-01-30/13:38:00	2010-01-30/16:48:00	7.4	0.18	5.0	354	3.4
738	2010-01-31/02:30:00	2010-01-31/04:25:00	7.6	0.31	6.1	438	4.0
739	2010-01-31/04:40:00	2010-01-31/07:45:00	7.6	0.27	4.7	425	3.5
740	2010-02-01/03:55:00	2010-02-01/08:20:00	7.0	0.13	5.7	345	-25.3
741	2010-02-06/12:38:00	2010-02-06/16:18:00	8.4	0.42	6.8	364	-2.3
742*	2010-02-11/07:30:00	2010-02-11/10:22:00	8.6	0.21	6.4	365	6.0
743*	2010-02-11/11:30:00	2010-02-11/22:22:00	7.0	0.07	5.4	358	-2.0
744	2010-02-16/03:40:00	2010-02-16/11:30:00	7.4	0.15	4.6	318	12.8
745	2010-02-16/16:25:00	2010-02-16/19:48:00	7.3	0.32	5.8	326	-1.9
746	2010-02-16/20:30:00	2010-02-17/02:13:00	6.9	0.19	5.9	332	0.6
747	2010-02-25/15:00:00	2010-02-25/19:12:00	7.1	0.12	5.9	359	-2.6
748	2010-02-28/06:00:00	2010-02-28/08:22:00	6.2	0.34	5.9	338	-5.6
749	2010-03-01/10:00:00	2010-03-01/13:28:00	8.6	0.17	5.7	331	1.2
750	2010-03-07/03:05:00	2010-03-07/04:05:00	9.7	0.43	4.8	419	-1.2
751	2010-03-07/05:55:00	2010-03-07/07:35:00	6.9	0.41	5.3	423	-0.7
752	2010-03-10/14:15:00	2010-03-10/16:42:00	8.7	0.25	4.4	400	-25.5
753	2010-03-17/03:45:00	2010-03-17/06:20:00	7.7	0.36	5.3	457	-0.7
754	2010-03-25/09:15:00	2010-03-25/10:45:00	7.6	0.15	6.5	327	-9.8
755	2010-03-25/12:25:00	2010-03-25/14:30:00	10.8	0.21	6.7	338	-0.8
756	2010-03-26/20:38:00	2010-03-26/22:00:00	7.0	0.3	4.1	418	-21.7
757	2010-03-26/22:20:00	2010-03-27/01:55:00	8.0	0.22	3.8	418	18.0
758	2010-03-31/23:15:00	2010-04-01/01:16:00	9.0	0.37	4.2	415	-3.7
759*	2010-04-05/11:00:00	2010-04-05/16:42:00	14.3	0.09	6.7	763	16.8
760	2010-04-12/19:35:00	2010-04-12/22:55:00	6.9	0.21	5.1	391	-0.2
761	2010-04-14/19:28:00	2010-04-14/22:30:00	12.3	0.5	6.2	419	3.3
762	2010-04-21/14:55:00	2010-04-21/20:30:00	7.6	0.3	6.0	407	-16.9

Table A.1: STs list from Wind Observation

No.	Start	End	B	β_p	M_A	V_p	V_{exp}
763	2010-04-29/00:28:00	2010-04-29/02:28:00	7.4	0.14	5.5	367	-1.3
764	2010-04-29/09:08:00	2010-04-29/10:50:00	6.8	0.32	6.2	362	4.1
765	2010-05-11/01:45:00	2010-05-11/03:35:00	7.2	0.18	6.8	370	-5.2
766	2010-06-16/00:45:00	2010-06-16/02:00:00	9.3	0.48	6.5	526	-12.4
767	2010-06-24/14:00:00	2010-06-24/15:35:00	6.8	0.42	6.7	335	-1.9
768	2010-06-25/11:42:00	2010-06-25/18:00:00	8.1	0.25	6.5	380	1.3
769	2010-06-26/02:28:00	2010-06-26/03:28:00	10.8	0.3	5.0	400	-27.4
770	2010-07-14/21:48:00	2010-07-14/23:22:00	16.1	0.1	3.6	428	-17.1
771	2010-07-23/08:00:00	2010-07-23/17:17:00	8.8	0.23	6.1	394	2.6
772	2010-07-23/21:15:00	2010-07-24/08:48:00	8.5	0.18	6.2	379	-4.1
773	2010-07-24/18:02:00	2010-07-24/20:12:00	8.1	0.3	5.3	358	0.3
774	2010-07-25/04:42:00	2010-07-25/05:55:00	7.7	0.21	5.4	357	5.6
775	2010-07-26/23:28:00	2010-07-27/02:22:00	8.3	0.39	6.6	465	-44.6
776*	2010-08-03/17:22:00	2010-08-03/19:20:00	14.6	0.32	5.1	571	-10.9
777	2010-09-02/07:35:00	2010-09-02/09:42:00	7.2	0.48	6.7	411	7.4
778	2010-09-05/21:38:00	2010-09-06/04:15:00	8.1	0.27	5.3	367	-28.4
779	2010-09-07/02:20:00	2010-09-07/06:18:00	6.9	0.24	5.7	350	-14.4
780	2010-09-07/07:15:00	2010-09-07/09:12:00	7.4	0.31	5.0	416	-10.9
781	2010-09-09/12:22:00	2010-09-09/13:17:00	6.8	0.12	6.4	389	5.8
782	2010-09-09/13:30:00	2010-09-09/16:25:00	7.8	0.13	5.3	399	-10.6
783	2010-09-14/05:17:00	2010-09-14/06:15:00	7.2	0.24	6.8	320	-3.6
784	2010-09-14/11:15:00	2010-09-14/13:45:00	9.1	0.21	6.1	334	2.6
785	2010-09-14/20:50:00	2010-09-14/22:20:00	9.3	0.34	5.1	377	1.9
786	2010-09-14/23:02:00	2010-09-15/00:20:00	7.6	0.42	6.8	382	-8.2
787	2010-09-21/02:16:00	2010-09-21/03:58:00	8.0	0.23	5.5	391	-11.3
788	2010-09-23/06:40:00	2010-09-23/14:27:00	10.7	0.33	5.9	378	-27.8
789	2010-09-23/16:45:00	2010-09-23/19:32:00	9.6	0.43	4.5	403	-17.7
790	2010-09-23/21:50:00	2010-09-24/04:55:00	9.3	0.33	5.0	460	-15.2
791	2010-10-04/21:00:00	2010-10-04/23:05:00	6.9	0.34	9.0	294	1.7
792	2010-10-05/07:48:00	2010-10-05/15:50:00	6.7	0.23	4.9	302	-6.4
793	2010-10-07/22:10:00	2010-10-08/02:45:00	6.2	0.22	6.2	319	-1.8
794	2010-10-19/07:20:00	2010-10-19/12:05:00	9.3	0.38	4.5	420	4.4
795	2010-10-22/08:30:00	2010-10-22/12:15:00	7.6	0.27	6.6	368	-25.7
796	2010-10-22/15:50:00	2010-10-22/19:22:00	8.9	0.15	5.1	467	-20.8
797	2010-10-22/21:40:00	2010-10-23/01:35:00	8.9	0.38	6.5	525	0.8
798	2010-11-10/18:22:00	2010-11-10/21:20:00	10.9	0.18	5.9	319	3.3
799	2010-11-11/01:00:00	2010-11-11/03:05:00	11.2	0.23	4.3	348	-18.7
800	2010-11-27/17:25:00	2010-11-27/19:38:00	13.2	0.33	4.4	393	-35.8
801	2010-11-27/20:15:00	2010-11-27/23:28:00	12.7	0.14	4.6	468	9.6
802	2010-11-28/00:40:00	2010-11-28/04:00:00	13.6	0.2	5.4	434	-9.4
803	2010-12-08/13:25:00	2010-12-08/15:02:00	6.1	0.28	5.5	379	-16.4
804	2010-12-12/16:12:00	2010-12-12/20:12:00	11.4	0.22	4.3	370	-25.1

Table A.1: STs list from Wind Observation

No.	Start	End	B	β_p	M_A	V_p	V_{exp}
805	2010-12-12/21:30:00	2010-12-12/23:45:00	7.9	0.38	6.5	415	-4.6
806	2010-12-20/08:48:00	2010-12-20/18:55:00	6.9	0.21	4.7	386	-26.1
807	2010-12-20/19:18:00	2010-12-20/21:25:00	6.8	0.19	6.6	376	-9.0
808	2010-12-25/15:45:00	2010-12-25/17:15:00	9.2	0.21	4.9	364	-9.8
809	2010-12-25/19:18:00	2010-12-25/23:20:00	8.2	0.33	5.1	389	-16.9
810*	2010-12-28/07:40:00	2010-12-28/12:30:00	10.9	0.08	5.0	342	-12.5
811	2010-12-28/15:25:00	2010-12-28/17:22:00	10.6	0.27	4.7	356	8.6
2011							
812	2011-01-03/20:42:00	2011-01-03/21:58:00	9.6	0.24	4.6	375	-3.0
813	2011-01-31/23:42:00	2011-02-01/00:30:00	10.9	0.25	4.6	284	9.9
814	2011-02-01/04:22:00	2011-02-01/05:22:00	11.9	0.24	5.6	355	1.6
815	2011-02-01/05:45:00	2011-02-01/15:12:00	8.8	0.31	5.7	394	-66.8
816*	2011-02-04/12:45:00	2011-02-04/18:05:00	13.1	0.24	5.8	411	-24.0
817*	2011-02-04/18:40:00	2011-02-04/20:05:00	21.1	0.1	4.2	430	-11.6
818	2011-02-14/18:58:00	2011-02-14/20:25:00	18.0	0.14	5.4	367	13.4
819	2011-02-14/20:50:00	2011-02-15/02:22:00	16.5	0.35	3.3	382	-13.4
820*	2011-02-18/04:10:00	2011-02-18/09:30:00	26.5	0.06	3.6	518	19.8
821	2011-03-01/06:18:00	2011-03-01/12:35:00	13.8	0.29	5.5	370	-11.4
822	2011-03-01/15:30:00	2011-03-01/20:42:00	13.1	0.46	5.1	499	-39.0
823	2011-03-11/00:30:00	2011-03-11/08:00:00	8.7	0.16	5.2	395	-9.9
824	2011-03-11/20:28:00	2011-03-11/21:12:00	15.7	0.16	3.5	441	-12.7
825	2011-03-22/14:50:00	2011-03-22/23:05:00	10.2	0.29	5.3	374	-20.2
826	2011-04-06/09:10:00	2011-04-06/11:22:00	14.3	0.36	6.2	534	-16.2
827	2011-04-11/18:02:00	2011-04-11/21:15:00	14.8	0.39	4.1	430	-21.2
828	2011-04-12/05:12:00	2011-04-12/08:55:00	10.5	0.25	5.0	515	6.5
829	2011-04-18/06:20:00	2011-04-18/10:18:00	11.5	0.27	7.6	370	-7.3
830	2011-04-19/06:38:00	2011-04-19/11:30:00	7.1	0.22	5.2	392	3.4
831	2011-04-20/01:45:00	2011-04-20/03:00:00	15.6	0.23	4.4	436	-5.5
832	2011-05-14/22:42:00	2011-05-15/01:42:00	10.6	0.24	5.5	359	-35.3
833	2011-05-15/04:20:00	2011-05-15/06:38:00	11.1	0.28	5.5	401	0.5
834	2011-05-26/14:25:00	2011-05-26/20:02:00	6.9	0.35	5.8	379	-1.2
835	2011-06-05/00:33:00	2011-06-05/07:25:00	18.6	0.12	5.0	532	2.8
836	2011-06-05/10:55:00	2011-06-05/17:18:00	7.8	0.12	5.8	497	7.3
837	2011-06-07/18:45:00	2011-06-07/22:40:00	9.2	0.09	5.3	450	-4.5
838	2011-06-09/19:22:00	2011-06-09/22:00:00	9.1	0.24	3.1	356	-35.8
839	2011-06-11/01:48:00	2011-06-11/05:10:00	9.3	0.22	6.1	386	3.5
840	2011-06-11/07:40:00	2011-06-11/12:02:00	9.8	0.18	5.3	393	-7.8
841	2011-06-11/14:00:00	2011-06-11/16:02:00	8.5	0.26	4.6	401	6.1
842	2011-06-22/17:35:00	2011-06-22/19:15:00	8.9	0.25	5.9	476	-12.6
843	2011-07-08/16:25:00	2011-07-08/22:35:00	7.5	0.11	6.0	346	12.5
844	2011-07-09/09:02:00	2011-07-09/13:58:00	8.8	0.46	5.5	376	-36.1
845	2011-07-09/15:02:00	2011-07-09/17:05:00	8.8	0.26	5.0	394	6.7

Table A.1: STs list from Wind Observation

No.	Start	End	B	β_p	M_A	V_p	V_{exp}
846	2011-07-10/03:20:00	2011-07-10/05:15:00	7.7	0.36	6.1	441	-18.7
847	2011-07-11/09:20:00	2011-07-11/11:10:00	12.2	0.41	6.3	503	14.5
848	2011-07-11/11:38:00	2011-07-11/15:12:00	10.0	0.28	6.2	481.7	5.0
849	2011-07-11/18:42:00	2011-07-11/22:12:00	7.6	0.35	5.1	635	-23.3
850	2011-07-18/03:32:00	2011-07-18/05:55:00	7.7	0.47	5.6	406	-50.7
851	2011-07-30/05:38:00	2011-07-30/12:35:00	9.8	0.25	5.5	396	-5.4
852*	2011-08-05/18:40:00	2011-08-05/19:45:00	30.0	0.24	4.7	611	-25.1
853*	2011-08-05/20:17:00	2011-08-06/00:15:00	26.5	0.16	3.3	592	6.1
854*	2011-08-06/06:12:00	2011-08-06/06:45:00	16.5	0.25	4.8	541	21.5
855*	2011-08-06/09:15:00	2011-08-06/11:20:00	14.7	0.16	4.8	552	20.6
856*	2011-08-06/11:38:00	2011-08-06/15:22:00	7.7	0.2	4.1	539	-31.4
857	2011-08-14/09:40:00	2011-08-14/11:40:00	8.9	0.25	6.1	382	0.1
858	2011-08-14/23:40:00	2011-08-15/00:32:00	10.3	0.38	5.3	527	14.0
859	2011-08-23/07:55:00	2011-08-23/13:55:00	9.4	0.37	5.5	430	-45.2
860*	2011-09-09/13:42:00	2011-09-09/18:00:00	18.5	0.44	3.4	475	-56.2
861*	2011-09-26/15:18:00	2011-09-26/18:32:00	32.7	0.14	2.2	586	-33.1
862*	2011-09-26/20:55:00	2011-09-27/00:10:00	11.7	0.14	4.9	667	-5.8
863*	2011-09-27/02:50:00	2011-09-27/06:00:00	7.9	0.11	5.1	647	-2.2
864*	2011-09-27/09:20:00	2011-09-27/13:20:00	7.4	0.16	5.9	594	5.7
865*	2011-09-27/15:58:00	2011-09-27/17:30:00	7.4	0.07	5.3	553	-9.2
866	2011-10-09/13:30:00	2011-10-09/16:16:00	7.2	0.18	5.3	327	-5.8
867	2011-10-11/08:40:00	2011-10-11/11:38:00	7.5	0.13	6.4	349	1.1
868	2011-10-24/06:50:00	2011-10-24/15:22:00	7.3	0.34	6.2	325	-8.5
869*	2011-10-30/14:32:00	2011-10-30/21:05:00	11.1	0.26	3.5	345	4.0
870	2011-10-31/20:35:00	2011-10-31/23:30:00	8.6	0.07	5.8	383	8.2
871	2011-11-06/07:32:00	2011-11-06/09:55:00	7.2	0.09	6.0	304	-2.6
872*	2011-11-07/16:15:00	2011-11-08/01:15:00	9.3	0.09	4.7	350	-15.8
873	2011-11-21/19:28:00	2011-11-21/21:18:00	8.2	0.3	6.0	297	-7.5
874	2011-11-22/01:32:00	2011-11-22/07:18:00	9.4	0.18	5.0	317	-7.2
875*	2011-11-29/00:20:00	2011-11-29/01:15:00	14.0	0.29	6.0	448	14.0
876*	2011-11-29/01:55:00	2011-11-29/04:23:00	16.6	0.11	4.6	452	12.9
877*	2011-11-29/04:48:00	2011-11-29/07:40:00	14.8	0.21	3.2	444	-17.8
878	2011-11-29/19:18:00	2011-11-29/21:45:00	9.0	0.22	5.7	444	8.7
879*	2011-12-29/22:23:00	2011-12-30/06:00:00	8.2	0.09	6.2	410	9.6
880	2011-12-19/03:10:00	2011-12-19/04:38:00	10.3	0.03	4.0	305	-0.6
881	2011-12-19/14:38:00	2011-12-19/19:15:00	7.6	0.23	5.1	360	-4.1
882	2011-12-20/04:05:00	2011-12-20/06:42:00	8.3	0.17	3.3	311	-2.1
883	2011-12-20/14:35:00	2011-12-20/18:32:00	7.2	0.24	5.6	345	-0.5
884	2011-12-28/12:10:00	2011-12-28/13:25:00	12.1	0.24	6.2	287	-0.1
885	2011-12-28/17:38:00	2011-12-28/20:45:00	9.5	0.32	6.0	304	-10.8
886	2011-12-30/17:55:00	2011-12-30/20:18:00	11.0	0.18	4.5	347	3.3
2012							

Table A.1: STs list from Wind Observation

No.	Start	End	B	β_p	M_A	V_p	V_{exp}
887	2012-01-16/07:58:00	2012-01-16/09:20:00	10.2	0.27	5.8	391	2.9
888	2012-01-16/10:15:00	2012-01-16/13:22:00	12.7	0.19	4.6	424	-21.5
889*	2012-01-22/08:15:00	2012-01-22/09:20:00	26.4	0.35	4.1	449	-8.3
890*	2012-01-22/09:38:00	2012-01-22/11:05:00	25.6	0.23	4.0	412	1.9
891*	2012-01-22/11:40:00	2012-01-22/17:28:00	21.2	0.15	4.4	410	3.0
892*	2012-01-22/18:48:00	2012-01-22/23:35:00	14.2	0.28	3.9	423	-11.4
893	2012-01-30/16:02:00	2012-01-30/17:35:00	10.7	0.24	5.7	411	-18.3
894	2012-02-13/09:40:00	2012-02-13/16:05:00	9.3	0.37	5.3	399	-16.0
895*	2012-03-08/19:20:00	2012-03-09/00:22:00	21.7	0.18	2.4	650	-28.8
896	2012-03-12/15:00:00	2012-03-12/15:50:00	15.2	0.18	2.4	502	-34.2
897	2012-03-23/00:50:00	2012-03-23/05:55:00	7.5	0.23	4.8	352	22.7
898	2012-03-31/14:22:00	2012-03-31/16:45:00	8.0	0.05	4.6	370	-2.0
899	2012-04-07/09:18:00	2012-04-07/12:30:00	8.0	0.26	5.1	334	-3.0
900	2012-04-17/15:02:00	2012-04-17/17:30:00	8.2	0.2	5.4	378	-17.0
901	2012-04-24/06:02:00	2012-04-24/07:30:00	10.3	0.2	3.4	406	9.8
902*	2012-04-25/18:12:00	2012-04-25/20:12:00	9.5	0.21	3.9	707	-4.3
903	2012-05-08/17:55:00	2012-05-08/22:27:00	14.6	0.36	5.3	365	-22.3
904	2012-05-29/13:48:00	2012-05-29/17:25:00	8.4	0.25	5.3	397	-12.5
905	2012-05-29/20:15:00	2012-05-29/21:35:00	9.3	0.24	4.1	440	4.1
906	2012-05-30/23:38:00	2012-05-31/07:15:00	9.3	0.23	5.0	421	9.1
907	2012-06-03/11:35:00	2012-06-03/13:02:00	10.8	0.11	5.5	342	-8.5
908	2012-06-03/14:38:00	2012-06-03/17:38:00	13.2	0.19	5.1	356	2.6
909	2012-06-17/19:55:00	2012-06-18/04:42:00	10.6	0.07	2.5	425	-5.3
910	2012-06-30/02:18:00	2012-06-30/04:05:00	11.5	0.25	5.3	405	-4.6
911	2012-06-30/06:38:00	2012-06-30/07:40:00	13.3	0.31	5.5	459	-7.5
912*	2012-07-06/03:18:00	2012-07-06/08:50:00	7.9	0.12	5.7	430	-2.1
913	2012-07-06/15:22:00	2012-07-06/22:00:00	10.0	0.13	4.2	467	-30.2
914*	2012-07-15/01:25:00	2012-07-15/02:32:00	16.9	0.27	4.9	641	13.7
915*	2012-07-21/16:30:00	2012-07-21/19:25:00	11.7	0.15	4.3	506	-11.4
916	2012-08-02/14:28:00	2012-08-02/19:00:00	10.3	0.3	6.8	447	4.8
917	2012-08-13/09:30:00	2012-08-13/12:50:00	9.3	0.29	4.1	450	-21.8
918*	2012-09-05/05:50:00	2012-09-05/17:35:00	11.1	0.07	4.9	507	29.4
919	2012-09-20/08:17:00	2012-09-20/11:00:00	9.1	0.18	4.9	502	-32.8
920	2012-09-26/12:30:00	2012-09-26/15:30:00	10.2	0.32	4.2	383	-15.3
921*	2012-10-01/12:30:00	2012-10-01/23:48:00	9.7	0.18	5.7	347	7.8
922	2012-10-02/00:35:00	2012-10-02/02:30:00	8.5	0.26	4.9	330	14.2
923*	2012-10-02/22:30:00	2012-10-03/01:25:00	7.6	0.02	2.5	312	17.5
924	2012-10-17/19:20:00	2012-10-17/23:22:00	8.2	0.24	4.5	467	-17.3
925	2012-11-07/00:16:00	2012-11-07/05:45:00	10.9	0.39	5.4	383	-26.8
926	2012-11-14/03:52:00	2012-11-14/08:05:00	16.8	0.15	3.0	393	5.1
927*	2012-11-23/21:38:00	2012-11-23/23:00:00	14.7	0.2	5.3	396	-3.7
928*	2012-12-14/07:38:00	2012-12-14/13:15:00	7.5	0.08	5.5	326	0.07

Table A.1: STs list from Wind Observation

No.	Start	End	B	β_p	M_A	V_p	V_{exp}
929	2012-12-17/06:58:00	2012-12-17/08:25:00	8.5	0.16	4.9	425	-19.9
930	2012-12-17/13:35:00	2012-12-17/18:30:00	8.8	0.21	5.1	477	2.6
2013							
931	2013-01-06/11:00:00	2013-01-06/14:32:00	7.5	0.16	7.2	317	-0.5
932	2013-01-06/15:58:00	2013-01-06/18:12:00	8.2	0.35	6.0	335	-4.5
933	2013-01-11/19:40:00	2013-01-11/22:38:00	8.1	0.34	5.5	328	-10.6
934	2013-01-12/23:20:00	2013-01-13/05:40:00	7.0	0.26	6.0	394	-2.8
935	2013-01-19/22:45:00	2013-01-20/03:42:00	7.4	0.13	5.4	426	17.1
936	2013-01-20/05:15:00	2013-01-20/07:00:00	8.3	0.07	4.4	439	5.4
937	2013-01-25/22:18:00	2013-01-25/23:18:00	12.2	0.32	6.4	398	-3.6
938	2013-01-26/13:40:00	2013-01-26/16:35:00	13.2	0.39	4.2	485	12.9
939	2013-02-07/08:00:00	2013-02-07/13:05:00	8.2	0.29	6.2	345	1.7
940	2013-02-07/23:22:00	2013-02-08/06:32:00	9.3	0.34	5.6	389	-19.1
941*	2013-02-13/15:32:00	2013-02-13/19:02:00	9.1	0.25	6.0	357	-5.8
942*	2013-02-17/11:10:00	2013-02-17/13:28:00	7.1	0.10	5.9	365	1.2
943	2013-02-18/23:25:00	2013-02-19/02:38:00	6.8	0.28	5.6	326	-0.2
944	2013-02-19/03:02:00	2013-02-19/03:48:00	7.1	0.39	5.7	318	-4.6
945	2013-02-25/13:20:00	2013-02-25/14:28:00	8.5	0.24	6.8	337	-0.7
946	2013-03-01/01:32:00	2013-03-01/09:16:00	13.1	0.23	4.9	424	-42.9
947	2013-03-14/02:48:00	2013-03-14/08:05:00	7.0	0.15	5.1	308	-3.3
948*	2013-03-17/14:30:00	2013-03-17/23:42:00	11.6	0.13	5.5	616	-9.3
949*	2013-03-20/16:48:00	2013-03-20/18:48:00	10.0	0.09	4.7	585	41.4
950*	2013-03-20/19:50:00	2013-03-20/23:35:00	8.7	0.15	5.1	516	7.0
951	2013-03-23/17:38:00	2013-03-23/19:18:00	9.5	0.19	6.9	384	-12.2
952	2013-03-25/17:35:00	2013-03-25/18:55:00	8.5	0.26	6.4	373	-4.1
953	2013-03-27/02:00:00	2013-03-27/06:55:00	9.7	0.2	6.1	376	-15.1
954	2013-03-27/07:32:00	2013-03-27/09:20:00	11.2	0.35	5.7	409	-7.4
955*	2013-04-13/22:16:00	2013-04-13/23:15:00	11.7	0.29	5.9	471	3.0
956	2013-04-24/06:02:00	2013-04-24/11:00:00	18.9	0.15	4.2	340	-14.2
957	2013-04-24/13:18:00	2013-04-24/18:00:00	15.2	0.25	3.6	380	-9.4
958	2013-04-25/08:55:00	2013-04-25/09:38:00	7.5	0.28	5.9	450	-5.3
959	2013-04-25/23:00:00	2013-04-26/00:32:00	8.2	0.38	5.4	500	21.0
960	2013-05-16/04:42:00	2013-05-16/10:15:00	6.8	0.07	6.1	396	7.4
961	2013-05-17/17:42:00	2013-05-18/01:38:00	8.3	0.11	5.4	395	-17.8
962	2013-05-20/03:00:00	2013-05-20/04:22:00	9.3	0.33	6.1	392	13.6
963	2013-05-22/19:30:00	2013-05-23/03:12:00	7.1	0.19	5.5	452	-5.0
964*	2013-05-25/14:10:00	2013-05-25/21:18:00	11.0	0.23	4.1	608	-101.3
965*	2013-05-26/00:40:00	2013-05-26/07:58:00	10.0	0.04	6.3	701	9.3
966	2013-05-31/23:38:00	2013-06-01/02:25:00	18.0	0.23	4.3	405	2.0
967	2013-06-01/03:30:00	2013-06-01/05:00:00	19.1	0.16	3.4	412	-6.0
968	2013-06-01/07:02:00	2013-06-01/08:50:00	19.2	0.35	3.9	499	-2.4
969	2013-06-10/18:50:00	2013-06-10/21:20:00	6.9	0.21	5.3	365	-1.9

Table A.1: STs list from Wind Observation

No.	Start	End	B	β_p	M_A	V_p	V_{exp}
970	2013-06-20/12:38:00	2013-06-20/16:28:00	13.6	0.22	3.7	371	-6.1
971	2013-06-20/22:30:00	2013-06-21/01:02:00	10.6	0.38	5.9	487	-6.2
972	2013-06-29/22:22:00	2013-06-30/00:45:00	10.0	0.39	5.9	459	2.5
973*	2013-07-05/03:48:00	2013-07-05/09:38:00	6.8	0.07	6.3	361	10.8
974*	2013-07-12/20:10:00	2013-07-13/01:22:00	10.7	0.15	4.0	497	14.6
975	2013-07-15/07:22:00	2013-07-15/08:02:00	7.4	0.3	5.7	391	0.3
976	2013-07-18/18:45:00	2013-07-19/03:42:00	11.3	0.33	4.9	511	-11.3
977	2013-07-25/17:02:00	2013-07-25/20:25:00	12.2	0.36	5.6	405	-41
978	2013-08-04/10:50:00	2013-08-04/13:00:00	12.1	0.29	5.0	325	11.8
979	2013-08-04/15:00:00	2013-08-04/17:30:00	14.8	0.24	3.8	388	-55.9
980	2013-08-04/18:42:00	2013-08-04/21:00:00	13.7	0.31	3.4	482	23.2
981	2013-08-09/10:30:00	2013-08-09/13:32:00	9.6	0.38	5.3	404	-21.3
982	2013-08-13/15:43:00	2013-08-13/18:00:00	10.2	0.13	4.6	410	-14.8
983*	2013-08-21/01:52:00	2013-08-21/04:15:00	10.4	0.18	4.2	426	-22.2
984	2013-08-27/05:50:00	2013-08-27/14:00:00	7.2	0.06	5.6	343	-12.4
985	2013-08-27/15:55:00	2013-08-27/18:25:00	13.1	0.13	5.9	394	-18.3
986	2013-08-30/09:38:00	2013-08-30/10:30:00	10.6	0.19	5.1	376	-8.9
987	2013-08-31/01:22:00	2013-08-31/02:12:00	8.3	0.45	5.7	410	-7.5
988	2013-08-31/05:55:00	2013-08-31/06:45:00	8.0	0.42	5.5	407	0.2
989	2013-09-17/19:20:00	2013-09-17/21:20:00	6.9	0.3	5.8	381	-5.7
990	2013-09-18/12:05:00	2013-09-18/13:28:00	8.9	0.24	6.4	421	-11.0
991	2013-10-01/06:25:00	2013-10-01/11:48:00	7.9	0.24	6.3	296	-9.8
992	2013-10-01/12:58:00	2013-10-01/15:42:00	8.5	0.35	4.9	330	0.4
993*	2013-10-02/03:55:00	2013-10-02/04:40:00	29.0	0.31	5.2	630	-0.6
994	2013-10-22/12:02:00	2013-10-22/16:02:00	8.3	0.15	5.7	316	2.5
995	2013-10-22/19:02:00	2013-10-22/21:48:00	7.9	0.26	4.6	346	6.0
996	2013-10-29/16:38:00	2013-10-29/17:30:00	8.2	0.14	5.4	329	-0.1
997	2013-10-29/22:05:00	2013-10-30/00:12:00	9.4	0.39	5.9	323	2.2
998	2013-10-30/06:25:00	2013-10-30/11:15:00	9.2	0.25	5.4	326	-13.2
999	2013-10-30/17:38:00	2013-10-31/05:00:00	8.9	0.2	4.6	341	16.6
1000	2013-10-31/10:33:00	2013-10-31/13:00:00	10.8	0.43	3.9	381	9.0
1001	2013-10-31/13:30:00	2013-10-31/16:28:00	9.4	0.22	5.6	398	-37.3
1002	2013-11-07/07:00:00	2013-11-07/13:12:00	10.0	0.25	5.4	363	13.3
1003*	2013-11-09/00:12:00	2013-11-09/06:27:00	12.8	0.18	6.3	412	-21.4
1004	2013-11-09/08:02:00	2013-11-09/10:12:00	11.9	0.19	3.8	462	-9.5
1005*	2013-11-11/17:45:00	2013-11-12/01:55:00	7.2	0.02	4.1	474	9.6
1006	2013-11-16/04:18:00	2013-11-16/06:42:00	10.5	0.33	5.4	356	-33.9
1007	2013-11-23/00:10:00	2013-11-23/09:28:00	8.4	0.25	5.1	337	-29.3
1008	2013-11-29/15:52:00	2013-11-29/17:10:00	10.6	0.1	4.6	310	-8.3
1009	2013-11-29/19:48:00	2013-11-29/23:18:00	8.5	0.41	5.3	331	-8.9
1010	2013-12-07/21:48:00	2013-12-07/22:32:00	15.8	0.21	5.7	413	-8.1
1011	2013-12-14/02:58:00	2013-12-14/05:05:00	12.2	0.45	5.7	342	3.1

Table A.1: STs list from Wind Observation

No.	Start	End	B	β_p	M_A	V_p	V_{exp}
1012*	2013-12-15/16:48:00	2013-12-16/01:15:00	8.3	0.01	2.4	460	16.1
1013	2013-12-28/14:18:00	2013-12-28/18:28:00	7.5	0.11	4.0	321	-7.1
1014	2013-12-28/20:45:00	2013-12-28/23:22:00	7.2	0.26	4.3	351	-12.8
2014							
1015	2014-01-01/12:00:00	2014-01-01/12:32:00	15.2	0.14	4.0	419	1.0
1016	2014-01-11/18:20:00	2014-01-11/21:50:00	7.9	0.14	3.8	401	4.5
1017	2014-01-21/19:35:00	2014-01-22/01:15:00	10.8	0.21	3.7	465	-29.7
1018	2014-01-28/13:15:00	2014-01-28/23:45:00	10.7	0.07	3.7	375	-52.2
1019*	2014-02-07/23:00:00	2014-02-07/23:45:00	11.6	0.15	4.3	446	-8.7
1020*	2014-02-07/23:50:00	2014-02-08/00:20:00	12.0	0.16	5.3	472	0.4
1021*	2014-02-08/08:15:00	2014-02-08/16:30:00	9.7	0.08	5.0	439	-6.2
1022*	2014-02-09/06:25:00	2014-02-09/10:40:00	9.0	0.06	4.2	380	0.2
1023*	2014-02-13/08:58:00	2014-02-13/10:12:00	8.7	0.1	5.2	380	16.8
1024*	2014-02-16/04:02:00	2014-02-16/14:15:00	14.9	0.07	3.8	382	17.7
1025	2014-02-16/19:10:00	2014-02-16/20:25:00	9.0	0.19	4.6	364	9.3
1026*	2014-02-19/14:00:00	2014-02-19/19:00:00	12.9	0.05	4.3	520	2.1
1027*	2014-02-20/03:45:00	2014-02-20/13:12:00	11.9	0.25	4.7	617	49.7
1028	2014-02-23/21:22:00	2014-02-23/23:10:00	8.8	0.15	3.8	467	16.2
1029	2014-02-27/20:42:00	2014-02-27/23:30:00	15.5	0.22	4.7	452	6.9
1030	2014-03-14/06:25:00	2014-03-14/12:00:00	8.3	0.11	3.7	467	9.9
1031	2014-03-18/19:48:00	2014-03-18/20:40:00	8.7	0.19	4.9	325	0.5
1032	2014-03-20/06:45:00	2014-03-20/09:00:00	10.0	0.11	4.6	338	-10.2
1033	2014-03-26/09:55:00	2014-03-26/11:58:00	8.4	0.12	5.3	405	12.5
1034	2014-03-27/01:30:00	2014-03-27/02:25:00	8.2	0.13	5.0	398	-2.2
1035	2014-04-07/09:28:00	2014-04-07/11:15:00	9.3	0.18	5.2	370	-16.4
1036	2014-04-07/17:00:00	2014-04-07/18:15:00	8.6	0.17	4.6	393	-5.2
1037	2014-04-12/23:05:00	2014-04-13/01:25:00	8.3	0.3	4.6	339	-5.2
1038*	2014-04-18/19:02:00	2014-04-18/23:02:00	9.6	0.1	4.8	499	-4.7
1039*	2014-04-19/01:00:00	2014-04-19/02:28:00	9.3	0.07	4.5	494	3.1
1040*	2014-04-30/18:00:00	2014-04-30/21:45:00	10.1	0.2	4.5	306	-8.1
1041	2014-05-05/03:00:00	2014-05-05/11:35:00	9.1	0.12	5.0	355	13.0
1042	2014-05-08/07:30:00	2014-05-08/08:15:00	11.8	0.07	3.2	345	11.0
1043	2014-05-23/02:35:00	2014-05-23/04:55:00	12.2	0.05	3.0	380	-38.4
1044	2014-06-03/00:45:00	2014-06-03/02:10:00	9.2	0.1	5.2	318	-1.8
1045	2014-06-03/12:00:00	2014-06-03/12:38:00	8.5	0.12	5.6	317	-4.7
1046	2014-06-03/17:30:00	2014-06-03/21:10:00	8.7	0.27	5.2	344	9.7
1047*	2014-06-08/04:25:00	2014-06-08/06:35:00	25.4	0.18	4.1	524	-42.6
1048*	2014-06-08/09:22:00	2014-06-08/10:30:00	17.0	0.15	4.2	503	-8.5
1049*	2014-06-08/12:10:00	2014-06-08/15:22:00	12.4	0.25	4.4	527	12.6
1050	2014-06-17/19:02:00	2014-06-17/21:45:00	9.6	0.22	3.8	409	-28.3
1051	2014-06-20/22:30:00	2014-06-20/23:12:00	8.6	0.24	4.4	429	-1.9
1052	2014-07-07/16:25:00	2014-07-08/02:00:00	8.3	0.15	3.9	313	2.9

Table A.1: STs list from Wind Observation

No.	Start	End	B	β_p	M_A	V_p	V_{exp}
1053	2014-07-14/18:45:00	2014-07-15/00:28:00	13.7	0.13	3.5	358	-9.5
1054	2014-07-21/20:30:00	2014-07-21/22:28:00	8.2	0.11	5.3	293	-5.3
1055	2014-07-28/10:25:00	2014-07-28/11:25:00	10.3	0.2	4.3	400	-5.0
1056	2014-08-10/13:00:00	2014-08-10/18:05:00	9.8	0.03	2.9	367	-25.8
1057	2014-08-10/18:32:00	2014-08-10/20:25:00	10.5	0.2	4.5	391	-31
1058	2014-08-17/07:40:00	2014-08-17/10:22:00	8.0	0.2	7.1	307	-3.5
1059	2014-08-28/02:05:00	2014-08-28/09:05:00	12.6	0.16	3.4	320	7.8
1060*	2014-09-17/20:45:00	2014-09-17/22:50:00	8.4	0.07	5.1	390	-3.4
1061*	2014-09-18/03:00:00	2014-09-18/11:40:00	8.1	0.07	4.2	365	6.9
1062	2014-10-08/08:40:00	2014-10-08/11:25:00	9.1	0.1	4.2	354	-0.3
1063	2014-10-13/06:00:00	2014-10-13/12:40:00	8.5	0.13	5.0	319	-12.5
1064	2014-10-14/12:20:00	2014-10-14/13:20:00	13.0	0.18	4.3	418	-2.7
1065	2014-10-14/18:00:00	2014-10-14/22:15:00	13.6	0.17	4.8	427	-22.5
1066	2014-12-06/09:00:00	2014-12-06/15:15:00	20.3	0.25	4.6	472	-10.4
1067	2014-12-12/01:25:00	2014-12-12/03:45:00	10.1	0.31	5.1	455	-16.3

Appendix B
The STs from STA

We observed 656 STs from STA from the year 2007 to 2014. The event number with "*" means this ST was in the time ranges which ICMEs have been observed. We call them "ICME-like STs" in this paper. The lists of the ICMEs observed by STA which have been used in this paper are got from: *Jian et al.*, 2006, www-ssc.igpp.ucla.edu/∼ jlan/STEREO/Level3/STEREO_Level3_ICME.pdf. The list is continually updated and cover our period completely.

The list of the STs observed by STA has been shown in the table below. We present the start time and end time of the STs, the average magnetic field strength ($< B >$), the average proton beta (β_p), the average Alfvén Mach number ($< M_A >$), the average proton velocity ($< V_p >$), the velocity expansion ($V_{exp} = \frac{V_{front} - V_{end}}{2}$).

Table B.1: STs list from STA Observation

No.	Start	End	B	β_p	M_A	V_p	V_{exp}
2007							
1	2007-02-24/12:50:00	2007-02-24/15:46:00	6.9	0.16	5.9	281	-8.2
2	2007-02-25/00:25:00	2007-02-25/01:20:00	6.4	0.09	6.7	284	-3.4
3	2007-02-25/01:50:00	2007-02-25/02:42:00	6.7	0.12	7.0	290	0.005
4	2007-02-25/21:30:00	2007-02-26/01:27:00	9.6	0.3	7.3	328	-4.3
5	2007-02-26/03:35:00	2007-02-26/06:02:00	11.5	0.13	3.2	361	-7.6
6	2007-02-27/09:06:00	2007-02-27/10:28:00	9.2	0.35	6.6	426	-1.9
7	2007-03-04/21:38:00	2007-03-04/23:30:00	7.9	0.36	6.2	384	-0.02
8	2007-03-07/01:45:00	2007-03-07/08:30:00	8.8	0.32	5.8	548	-16.0
9	2007-03-11/05:10:00	2007-03-11/08:15:00	7.8	0.28	6.6	336	-3.1
10	2007-03-12/19:15:00	2007-03-12/20:35:00	10.4	0.44	6.5	525	-17.9
11	2007-03-23/04:00:00	2007-03-23/04:40:00	7.7	0.15	7.2	284	-3.2
12	2007-03-24/00:30:00	2007-03-24/02:00:00	10.0	0.43	7.4	379	9.7
13	2007-03-24/02:38:00	2007-03-24/09:30:00	11.4	0.06	3.5	364	11.8
14	2007-03-27/06:58:00	2007-03-27/10:40:00	7.7	0.22	6.5	417	11.8
15	2007-03-31/20:15:00	2007-03-31/22:12:00	8.9	0.21	6.5	369	-14.2
16	2007-04-01/02:38:00	2007-04-01/05:05:00	10.0	0.36	5.7	406	-9.1
17	2007-04-01/20:38:00	2007-04-01/21:40:00	9.9	0.44	6.8	521	-2.6
18	2007-04-08/15:28:00	2007-04-08/16:28:00	7.1	0.12	5.1	327	-4.1
19	2007-04-08/21:00:00	2007-04-08/22:25:00	13.6	0.22	3.5	377	-2.1
20	2007-04-09/02:42:00	2007-04-09/03:30:00	9.3	0.33	5.7	413	3.0
21	2007-04-10/08:32:00	2007-04-10/10:05:00	9.9	0.19	5.4	387	9.5

Table B.1: STs list from STA Observation

No.	Start	End	B	β_p	M_A	V_p	V_{exp}
22	2007-04-10/11:40:00	2007-04-10/14:32:00	7.9	0.22	5.6	381	-13.9
23	2007-04-10/19:28:00	2007-04-10/21:12:00	10.0	0.32	6.2	444	17.9
24	2007-04-12/01:42:00	2007-04-12/03:38:00	6.5	0.34	7.6	482	5.0
25	2007-04-14/08:20:00	2007-04-14/11:50:00	6.8	0.12	4.7	360	4.9
26	2007-04-17/06:55:00	2007-04-17/08:10:00	8.7	0.22	3.8	334	14.2
27	2007-04-17/11:12:00	2007-04-17/16:00:00	8.1	0.14	3.5	342	17.3
28	2007-05-07/13:20:00	2007-05-07/14:32:00	19.0	0.14	3.3	342	0.2
29	2007-05-15/20:22:00	2007-05-15/21:58:00	6.5	0.2	6.2	303	-12.2
30	2007-05-18/10:10:00	2007-05-18/11:58:00	10.5	0.32	6.6	327	-13.2
31	2007-05-18/14:58:00	2007-05-18/15:40:00	18.7	0.14	4.1	425	-11.7
32	2007-05-18/18:05:00	2007-05-18/19:35:00	15.8	0.33	5.7	468	-5.7
33	2007-05-21/20:40:00	2007-05-21/21:42:00	8.8	0.06	5.9	473	-10.4
34	2007-05-24/03:55:00	2007-05-24/09:40:00	9.2	0.12	5.5	507	-2.8
35	2007-06-01/00:25:00	2007-06-01/01:30:00	7.1	0.32	6.7	332	0.4
36	2007-06-01/05:00:00	2007-06-01/07:02:00	8.9	0.27	5.8	359	-2.4
37	2007-06-01/07:20:00	2007-06-01/08:45:00	9.5	0.32	6.2	347	-3.3
38	2007-06-04/10:45:00	2007-06-04/12:25:00	7.1	0.29	7.1	346	-3.6
39	2007-06-04/12:30:00	2007-06-04/14:10:00	12.3	0.15	4.9	395	-36.3
40	2007-06-05/02:15:00	2007-06-05/06:00:00	6.2	0.19	6.2	471	28.4
41	2007-06-08/09:15:00	2007-06-08/11:00:00	9.9	0.08	4.6	358	-10.3
42	2007-06-09/13:18:00	2007-06-09/15:48:00	7.8	0.2	6.6	345	-5.4
43	2007-06-10/02:15:00	2007-06-10/03:32:00	8.3	0.46	6.8	410	-8.6
44	2007-06-10/07:22:00	2007-06-10/08:45:00	8.4	0.32	5.5	408	-21.0
45	2007-06-13/19:40:00	2007-06-13/23:32:00	8.7	0.21	6.2	317	-2.3
46	2007-06-14/03:40:00	2007-06-14/13:38:00	10.8	0.23	3.9	384	-25.2
47	2007-06-30/07:02:00	2007-06-30/10:00:00	10.4	0.48	5.5	385	-9.2
48	2007-07-01/05:00:00	2007-07-01/05:45:00	8.6	0.26	6.0	487	-6.8
49	2007-07-01/06:25:00	2007-07-01/07:55:00	8.4	0.21	5.7	490	25.9
50	2007-07-14/10:58:00	2007-07-14/16:20:00	7.1	0.09	5.4	384	-4.0
51	2007-07-14/18:05:00	2007-07-14/21:02:00	7.8	0.17	6.3	403	5.0
52	2007-07-15/03:28:00	2007-07-15/06:00:00	10.6	0.29	5.3	421	-31.3
53	2007-07-20/13:00:00	2007-07-20/14:05:00	8.6	0.15	6.0	336	0.9
54	2007-07-20/17:22:00	2007-07-20/19:45:00	10.8	0.11	5.2	340	8.7
55	2007-07-27/17:02:00	2007-07-27/18:20:00	8.8	0.15	5.0	400	-5.8
56	2007-07-29/08:30:00	2007-07-29/13:55:00	12.3	0.32	5.8	442	-63.6
57	2007-08-01/03:55:00	2007-08-01/14:25:00	8.1	0.27	5.2	501	-14.7
58	2007-08-07/05:45:00	2007-08-07/07:05:00	17.3	0.29	5.3	356	-11.4
59	2007-08-07/18:28:00	2007-08-07/19:35:00	11.2	0.35	6.2	461	-19.8
60	2007-08-10/18:45:00	2007-08-10/20:02:00	7.7	0.28	7.0	422	-3.1
61	2007-08-10/21:55:00	2007-08-11/03:50:00	10.0	0.26	6.4	409	-25.7
62	2007-08-17/01:50:00	2007-08-17/06:15:00	6.7	0.13	4.4	390	-12.3
63	2007-08-19/16:22:00	2007-08-19/19:20:00	7.3	0.17	5.4	373	-11.0

Table B.1: STs list from STA Observation

No.	Start	End	B	β_p	M_A	V_p	V_{exp}
64	2007-08-19/19:45:00	2007-08-19/22:50:00	9.8	0.1	5.0	430	-8.2
65	2007-09-01/23:32:00	2007-09-02/00:30:00	9.8	0.27	6.5	458	-7.6
66	2007-09-02/19:28:00	2007-09-02/20:10:00	7.0	0.21	5.0	479	1.2
67	2007-09-13/17:58:00	2007-09-13/21:18:00	7.5	0.04	4.2	282	-3.9
68	2007-09-19/16:02:00	2007-09-19/18:30:00	7.1	0.08	4.7	332	2.7
69	2007-09-20/01:00:00	2007-09-20/07:38:00	6.6	0.13	6.1	303	0.7
70	2007-09-21/17:45:00	2007-09-21/19:02:00	11.1	0.31	7.2	341	-1.3
71	2007-09-21/19:30:00	2007-09-21/20:15:00	12.1	0.4	6.1	325	-4.9
72	2007-09-28/18:50:00	2007-09-28/19:45:00	10.6	0.19	6.9	394	1.7
73	2007-10-04/04:50:00	2007-10-04/06:10:00	7.3	0.3	7.4	433	-9.4
74	2007-10-14/04:15:00	2007-10-14/08:02:00	7.0	0.32	6.0	358	-8.4
75	2007-10-15/22:02:00	2007-10-15/23:28:00	7.9	0.19	5.2	337	-0.6
76	2007-10-18/21:00:00	2007-10-18/21:30:00	11.5	0.13	5.3	348	-3.2
77	2007-10-18/23:00:00	2007-10-19/01:00:00	13.2	0.28	4.9	386	-38.7
78	2007-10-19/13:52:00	2007-10-19/16:55:00	10.1	0.35	6.2	348	-35.6
79	2007-10-25/19:30:00	2007-10-25/20:25:00	11.0	0.16	6.4	395	-0.1
80	2007-10-25/21:32:00	2007-10-25/22:45:00	10.7	0.26	7.1	410	-3.2
81	2007-10-26/00:20:00	2007-10-26/01:58:00	11.2	0.18	5.8	433	-6.0
82	2007-10-26/05:35:00	2007-10-26/06:25:00	9.6	0.39	6.8	490	-9.4
83	2007-10-30/19:02:00	2007-10-30/22:02:00	6.4	0.22	6.8	464	-2.5
84	2007-11-10/16:00:00	2007-11-10/17:02:00	11.7	0.44	5.6	428	-22.6
85	2007-11-14/02:30:00	2007-11-14/03:15:00	9.5	0.13	5.5	404	-15.2
86	2007-12-01/13:30:00	2007-12-01/14:40:00	6.4	0.24	6.0	439	-3.5
87	2007-12-11/15:50:00	2007-12-11/17:15:00	6.4	0.17	4.2	312	-0.9
88	2007-12-11/18:22:00	2007-12-11/19:55:00	7.1	0.22	4.6	349	-12.0
89	2007-12-11/21:45:00	2007-12-11/23:28:00	7.0	0.17	4.5	345	-6.6
90	2007-12-12/10:38:00	2007-12-12/12:30:00	9.6	0.15	6.1	417	4.5
91	2007-12-19/00:58:00	2007-12-19/02:10:00	9.9	0.24	4.8	457	15.9
92	2007-12-20/22:10:00	2007-12-20/22:55:00	14.1	0.11	4.3	505	-29.7
93	2007-12-31/22:22:00	2007-12-31/23:28:00	7.1	0.14	4.9	415	11.6
2008							
94	2008-01-01/10:20:00	2008-01-01/14:58:00	6.9	0.32	6.4	406	-35.1
95	2008-01-14/07:20:00	2008-01-14/12:32:00	6.0	0.17	5.5	433	0.3
96	2008-01-14/18:55:00	2008-01-14/23:02:00	7.1	0.13	5.4	417	7.7
97	2008-01-15/00:35:00	2008-01-15/04:45:00	9.9	0.18	4.9	398	17.7
98	2008-01-15/05:00:00	2008-01-15/07:00:00	7.7	0.09	3.1	378	-3.5
99	2008-02-02/09:45:00	2008-02-02/10:35:00	9.6	0.18	6.4	338	-0.2
100	2008-02-11/13:38:00	2008-02-11/14:25:00	11.5	0.31	5.8	402	9.3
101	2008-02-11/16:22:00	2008-02-11/20:18:00	12.4	0.4	5.3	418	-32.5
102	2008-02-11/21:02:00	2008-02-12/03:00:00	12.7	0.35	5.6	502	-12.3
103	2008-02-25/06:00:00	2008-02-25/11:05:00	7.7	0.06	4.8	368	-9.9
104	2008-02-26/07:30:00	2008-02-26/08:50:00	8.2	0.21	6.1	413	-3.3

Table B.1: STs list from STA Observation

No.	Start	End	B	β_p	M_A	V_p	V_{exp}
105	2008-02-26/09:40:00	2008-02-26/12:48:00	8.0	0.26	5.7	450	-9.5
106	2008-03-09/08:35:00	2008-03-09/11:00:00	15.8	0.24	5.8	431	4.4
107*	2008-03-21/08:35:00	2008-03-21/18:35:00	8.1	0.02	2.4	450	-4.9
108	2008-03-21/23:45:00	2008-03-22/04:05:00	6.9	0.14	5.1	411	5.6
109	2008-03-22/10:00:00	2008-03-22/13:10:00	7.2	0.23	6.0	434	-39.7
110	2008-03-25/08:55:00	2008-03-25/11:15:00	6.9	0.2	5.9	410	-5.0
111	2008-03-25/12:35:00	2008-03-25/15:00:00	6.3	0.29	6.1	469	-39.6
112	2008-03-27/21:02:00	2008-03-27/23:45:00	6.7	0.16	4.7	344	3.1
113	2008-03-28/06:16:00	2008-03-28/07:16:00	11.1	0.21	5.5	387	-3.8
114	2008-03-28/09:12:00	2008-03-28/11:22:00	12.9	0.13	3.8	423	-49.1
115	2008-04-06/17:00:00	2008-04-06/20:15:00	7.8	0.21	6.0	349	-4.6
116	2008-04-07/06:05:00	2008-04-07/10:25:00	10.5	0.08	2.8	387	-40.4
117	2008-04-22/18:38:00	2008-04-22/23:22:00	6.0	0.11	5.1	400	9.5
118	2008-05-01/19:25:00	2008-05-01/21:02:00	7.4	0.28	6.9	360	0.7
119	2008-05-06/08:32:00	2008-05-06/11:58:00	7.8	0.25	5.2	496	-37.1
120	2008-05-15/00:52:00	2008-05-15/05:25:00	6.8	0.13	4.8	332	7.5
121	2008-05-19/09:22:00	2008-05-19/10:15:00	7.1	0.17	5.8	304	-2.1
122	2008-05-19/10:42:00	2008-05-19/11:15:00	7.3	0.17	5.5	303	-1.3
123	2008-05-21/05:30:00	2008-05-21/07:10:00	8.9	0.21	6.0	303	4.1
124	2008-05-21/11:30:00	2008-05-21/21:48:00	11.2	0.34	4.9	415	-53.7
125	2008-05-30/00:05:00	2008-05-30/00:58:00	11.9	0.3	4.7	461	1.5
126	2008-05-30/14:00:00	2008-05-30/14:45:00	6.7	0.26	6.3	476	-17.7
127	2008-06-08/20:55:00	2008-06-08/24:00:00	11.4	0.22	4.7	356	-33.7
128	2008-06-09/21:00:00	2008-06-09/22:32:00	6.4	0.12	4.1	449	2.4
129	2008-06-10/00:30:00	2008-06-10/03:32:00	6.4	0.23	4.5	446	26.1
130	2008-06-16/11:20:00	2008-06-16/12:30:00	10.1	0.28	5.1	358	-13.4
131	2008-06-28/03:12:00	2008-06-28/10:42:00	7.9	0.24	5.1	438	-25.6
132	2008-07-02/09:45:00	2008-07-02/17:00:00	6.7	0.09	4.0	393	-22.4
133	2008-07-03/00:00:00	2008-07-03/01:50:00	6.4	0.11	4.6	404	1.8
134	2008-07-07/02:20:00	2008-07-07/08:40:00	9.5	0.34	5.4	325	-32.1
135	2008-07-10/20:45:00	2008-07-10/22:25:00	6.6	0.14	5.2	333	13.5
136	2008-07-13/06:10:00	2008-07-13/11:00:00	7.3	0.16	5.0	318	5.5
137	2008-07-13/15:20:00	2008-07-13/21:25:00	8.8	0.13	3.3	409	-70.5
138	2008-07-24/23:28:00	2008-07-25/06:10:00	6.2	0.14	5.1	349	10.4
139	2008-07-25/08:22:00	2008-07-25/09:20:00	9.5	0.23	6.2	374	-4.5
140	2008-07-26/16:30:00	2008-07-26/18:05:00	6.3	0.12	5.1	483	3.0
141	2008-07-30/01:28:00	2008-07-30/08:58:00	8.8	0.07	3.0	354	-26.3
142	2008-08-03/03:05:00	2008-08-03/04:20:00	7.8	0.22	4.7	354	-6.0
143	2008-08-10/11:22:00	2008-08-10/13:45:00	6.4	0.21	5.0	421	-12.6
144	2008-08-10/21:18:00	2008-08-10/22:10:00	7.0	0.28	5.4	456	-5.0
145	2008-08-29/13:30:00	2008-08-29/20:00:00	7.1	0.11	4.8	290	-2.3
146	2008-08-31/02:35:00	2008-08-31/12:18:00	5.9	0.08	4.3	288	-6.0

Table B.1: STs list from STA Observation

No.	Start	End	B	β_p	M_A	V_p	V_{exp}
147	2008-09-07/18:28:00	2008-09-07/22:30:00	7.3	0.23	5.4	405	-2.2
148	2008-09-16/20:20:00	2008-09-16/21:12:00	12.1	0.24	4.2	361	-12.8
149	2008-09-24/02:38:00	2008-09-24/12:12:00	6.8	0.15	4.4	313	10.4
150	2008-10-03/12:00:00	2008-10-03/18:58:00	7.8	0.2	5.5	336	-65.7
151	2008-10-04/04:00:00	2008-10-04/05:02:00	11.3	0.3	5.7	501	1.6
152	2008-10-13/00:55:00	2008-10-13/01:32:00	9.3	0.09	5.1	354	-1.4
153	2008-10-14/12:22:00	2008-10-14/13:05:00	6.2	0.14	4.7	480	-3.7
154	2008-10-15/01:40:00	2008-10-15/11:22:00	7.3	0.05	3.8	444	23.5
155	2008-10-22/14:50:00	2008-10-22/19:05:00	6.9	0.22	6.2	307	0.2
156	2008-10-23/01:05:00	2008-10-23/02:05:00	6.7	0.27	5.6	368	-8.6
157	2008-10-27/19:40:00	2008-10-28/00:15:00	8.4	0.18	6.4	293	5.4
158	2008-10-28/03:45:00	2008-10-28/08:30:00	6.5	0.16	5.1	301	-1.8
159*	2008-10-31/12:15:00	2008-10-31/17:32:00	14.0	0.07	3.6	378	-11.7
160	2008-11-07/05:12:00	2008-11-07/12:42:00	6.6	0.03	4.0	353	17.6
161	2008-11-09/04:25:00	2008-11-09/07:30:00	13.3	0.25	4.7	358	-25.6
162	2008-11-11/16:35:00	2008-11-11/22:45:00	5.9	0.06	3.1	419	12.3
163	2008-11-18/20:28:00	2008-11-18/23:50:00	6.6	0.06	4.5	296	2.5
164	2008-11-25/17:45:00	2008-11-25/18:58:00	6.2	0.22	5.9	299	-0.6
165	2008-11-28/08:02:00	2008-11-28/14:30:00	6.2	0.06	5.3	286	3.2
166*	2008-11-28/21:40:00	2008-11-28/23:45:00	18.0	0.14	4.2	361	-19.3
167	2008-12-06/12:40:00	2008-12-06/15:30:00	12.9	0.25	5.5	377	-18.8
168	2008-12-14/07:35:00	2008-12-14/09:02:00	6.0	0.08	4.0	385	11.1
169	2008-12-14/10:45:00	2008-12-14/14:05:00	6.8	0.12	4.2	374	-8.4
170	2008-12-15/00:45:00	2008-12-15/05:00:00	6.3	0.12	3.7	361	18.3
171	2008-12-16/00:22:00	2008-12-16/03:00:00	6.3	0.28	6.9	370	-13.4
172	2008-12-19/08:02:00	2008-12-19/08:42:00	6.5	0.15	5.2	325	-2.0
173	2008-12-21/06:25:00	2008-12-21/13:25:00	5.8	0.17	6.0	302	-0.02
174	2008-12-25/13:22:00	2008-12-25/15:42:00	8.4	0.32	5.8	337	-4.2
2009							
175	2009-01-05/21:45:00	2009-01-06/02:22:00	9.9	0.12	3.8	436	-14.0
176	2009-01-06/08:20:00	2009-01-06/10:20:00	7.7	0.26	5.2	490	-21.3
177	2009-01-08/10:58:00	2009-01-08/12:12:00	5.4	0.05	3.8	476	0.3
178	2009-01-12/13:00:00	2009-01-12/15:10:00	6.4	0.25	4.8	318	-9.3
179	2009-01-13/01:55:00	2009-01-13/04:02:00	5.7	0.23	5.4	342	-2.6
180	2009-01-19/18:18:00	2009-01-19/20:40:00	5.8	0.11	4.6	302	-1.5
181	2009-01-21/01:40:00	2009-01-21/08:05:00	7.7	0.17	4.9	360	-29.5
182	2009-01-22/20:15:00	2009-01-23/01:25:00	6.1	0.38	5.8	413	9.9
183	2009-01-25/09:30:00	2009-01-25/14:40:00	7.0	0.19	6.5	375	22.8
184	2009-02-02/00:15:00	2009-02-02/05:02:00	5.9	0.2	5.6	352	13.5
185	2009-02-02/10:45:00	2009-02-02/17:15:00	6.8	0.1	4.1	353	-36.9
186	2009-02-03/05:05:00	2009-02-03/05:50:00	7.5	0.32	5.2	440	-21.3
187	2009-02-04/03:50:00	2009-02-04/05:28:00	5.5	0.07	4.1	409	-4.1

Table B.1: STs list from STA Observation

No.	Start	End	B	β_p	M_A	V_p	V_{exp}
188	2009-02-13/19:02:00	2009-02-13/22:00:00	6.7	0.14	6.4	292	3.1
189	2009-02-14/06:02:00	2009-02-14/07:02:00	5.7	0.17	5.7	292	-2.1
190	2009-02-16/15:42:00	2009-02-16/17:30:00	6.6	0.12	5.5	288	2.9
191	2009-02-17/12:20:00	2009-02-17/13:38:00	12.8	0.23	5.9	350	-8.5
192	2009-02-21/09:55:00	2009-02-21/13:00:00	5.7	0.19	6.5	392	3.1
193	2009-02-25/07:18:00	2009-02-25/08:30:00	10.2	0.14	4.2	347	-7.3
194	2009-02-25/13:05:00	2009-02-25/15:40:00	8.1	0.2	4.3	353	11.2
195	2009-02-26/06:55:00	2009-02-26/16:00:00	6.9	0.15	4.0	333	-9.4
196	2009-02-26/21:30:00	2009-02-26/22:35:00	6.8	0.2	5.1	360	-2.5
197	2009-02-27/17:02:00	2009-02-27/18:30:00	6.7	0.18	6.0	430	10.5
198	2009-03-03/20:00:00	2009-03-03/22:20:00	6.2	0.39	6.6	326	-0.3
199	2009-03-04/01:42:00	2009-03-04/06:10:00	10.3	0.17	3.7	375	-7.1
200	2009-03-06/05:35:00	2009-03-06/06:50:00	6.1	0.2	5.4	424	5.2
201	2009-03-14/03:25:00	2009-03-14/07:22:00	5.6	0.21	5.5	333	5.5
202	2009-03-14/09:48:00	2009-03-14/13:20:00	5.6	0.16	4.8	343	1.6
203	2009-03-14/15:05:00	2009-03-14/19:30:00	6.5	0.24	4.8	330	7.3
204	2009-03-15/08:02:00	2009-03-15/14:12:00	7.5	0.21	5.4	385	-30.9
205	2009-03-15/16:48:00	2009-03-16/00:15:00	8.9	0.25	4.9	454	-48.6
206	2009-03-16/00:32:00	2009-03-16/01:32:00	9.3	0.27	6.0	498	6.8
207	2009-03-22/11:00:00	2009-03-22/18:30:00	5.9	0.23	6.7	333	-4.4
208	2009-03-23/19:38:00	2009-03-23/22:05:00	9.7	0.11	3.8	344	-0.7
209	2009-03-24/01:40:00	2009-03-24/05:42:00	7.3	0.36	5.9	366	-12.7
210	2009-03-25/09:30:00	2009-03-25/10:15:00	5.6	0.11	3.5	414	4.8
211	2009-03-29/09:20:00	2009-03-29/12:40:00	5.6	0.35	6.5	385	9.6
212	2009-03-31/03:02:00	2009-03-31/04:12:00	6.3	0.23	6.1	356	-3.7
213	2009-03-31/07:30:00	2009-03-31/10:10:00	5.4	0.11	5.4	349	-0.4
214	2009-04-05/06:25:00	2009-04-05/07:15:00	7.2	0.24	6.0	325	15.8
215	2009-04-05/12:18:00	2009-04-05/16:15:00	8.0	0.26	5.9	311	25.7
216	2009-04-20/16:20:00	2009-04-20/18:22:00	9.6	0.2	4.7	408	-23.4
217	2009-04-21/02:10:00	2009-04-21/02:50:00	5.8	0.3	5.7	434	-7.3
218	2009-04-30/17:02:00	2009-04-30/17:40:00	8.9	0.12	4.3	301	-10.7
219	2009-04-30/20:48:00	2009-05-01/03:50:00	7.8	0.07	4.0	311	5.7
220	2009-05-01/05:02:00	2009-05-01/09:02:00	6.1	0.2	5.1	307	4.5
221	2009-05-04/05:40:00	2009-05-04/06:45:00	6.5	0.24	5.2	333	6.7
222	2009-05-04/07:32:00	2009-05-04/10:38:00	5.8	0.2	5.6	336	4.9
223	2009-05-06/04:40:00	2009-05-06/06:30:00	6.8	0.26	5.8	305	1.1
224	2009-05-06/13:02:00	2009-05-06/17:55:00	5.3	0.2	6.2	300	0.7
225	2009-05-09/11:55:00	2009-05-09/12:35:00	16.9	0.11	3.1	421	2.0
226	2009-05-09/18:50:00	2009-05-09/22:15:00	8.9	0.3	4.8	465	-20.5
227	2009-05-14/07:30:00	2009-05-14/10:15:00	5.4	0.1	4.1	355	-8.8
228	2009-05-17/10:15:00	2009-05-17/12:15:00	6.2	0.18	5.2	402	3.6
229	2009-05-18/02:02:00	2009-05-18/05:30:00	6.0	0.1	4.5	414	-4

Table B.1: STs list from STA Observation

No.	Start	End	B	β_p	M_A	V_p	V_{exp}
230	2009-05-18/10:22:00	2009-05-18/12:20:00	5.5	0.24	5.5	411	-7.2
231	2009-05-24/17:20:00	2009-05-24/23:10:00	6.5	0.25	5.2	313	0.9
232	2009-05-27/00:20:00	2009-05-27/03:00:00	5.7	0.05	4.0	259	-3.5
233	2009-05-31/20:32:00	2009-05-31/22:35:00	9.7	0.23	4.5	430	-2.8
234	2009-06-05/14:05:00	2009-06-05/18:10:00	6.8	0.19	4.7	340	-0.9
235	2009-06-05/22:25:00	2009-06-06/04:30:00	6.5	0.13	3.9	338	7.4
236	2009-06-16/14:30:00	2009-06-16/18:40:00	6.0	0.13	5.1	307	6.7
237	2009-06-16/23:00:00	2009-06-17/04:15:00	5.9	0.17	4.7	348	-16.5
238	2009-06-20/11:30:00	2009-06-20/12:32:00	6.5	0.13	3.6	361	5.7
239	2009-06-21/02:50:00	2009-06-21/04:50:00	6.4	0.24	6.1	359	-3.9
240	2009-06-24/19:32:00	2009-06-24/21:15:00	8.4	0.27	5.9	384	-0.2
241	2009-06-28/08:12:00	2009-06-28/14:20:00	10.5	0.19	4.0	396	-31.1
242	2009-06-28/21:38:00	2009-06-28/23:25:00	6.8	0.28	6.7	493	-5.7
243	2009-07-06/16:45:00	2009-07-06/18:10:00	5.6	0.05	4.4	371	-2.1
244	2009-07-07/13:15:00	2009-07-07/22:38:00	6.6	0.28	5.8	326	-2.4
245	2009-07-11/20:48:00	2009-07-11/21:28:00	6.0	0.11	5.5	331	1.9
246	2009-07-13/09:20:00	2009-07-13/11:25:00	8.7	0.28	6.1	298	-1.1
247	2009-07-13/16:28:00	2009-07-13/18:40:00	13.6	0.21	4.4	407	-16.0
248	2009-07-13/21:30:00	2009-07-13/22:55:00	8.7	0.2	5.4	448	6.9
249	2009-07-23/14:00:00	2009-07-23/18:32:00	8.1	0.22	5.3	316	9.5
250	2009-07-26/13:50:00	2009-07-26/19:00:00	10.5	0.2	4.3	345	-69.995
251	2009-07-27/00:50:00	2009-07-27/02:15:00	6.8	0.24	5.1	468	-29.0
252	2009-07-27/03:00:00	2009-07-27/04:20:00	6.3	0.22	5.2	486	-6.9
253	2009-07-28/07:12:00	2009-07-28/09:02:00	5.4	0.2	4.8	512	-8.9
254	2009-08-07/04:42:00	2009-08-07/06:00:00	6.0	0.35	7.1	362	5.1
255	2009-08-08/14:00:00	2009-08-08/22:15:00	6.2	0.18	6.9	316	10.6
256	2009-08-09/08:20:00	2008-08-09/10:40:00	6.2	0.07	6.1	351	7.5
257	2009-08-17/03:30:00	2009-08-17/06:00:00	6.6	0.32	6.9	342	-8.7
258	2009-08-20/06:00:00	2009-08-20/08:00:00	5.9	0.21	6.2	298	2.8
259	2009-08-20/21:20:00	2009-08-21/06:30:00	6.0	0.03	4.4	282	3.4
260	2009-08-22/06:25:00	2009-08-22/09:58:00	8.7	0.27	6.1	303	0.8
261	2009-08-23/02:55:00	2009-08-23/12:45:00	6.1	0.3	5.7	362	-5.6
262	2009-08-23/13:45:00	2009-08-23/14:30:00	5.9	0.36	6.0	356	-8.4
263	2009-08-24/06:55:00	2009-08-24/07:42:00	6.0	0.09	4.2	353	-3.2
264	2009-08-27/20:20:00	2009-08-27/21:28:00	6.3	0.29	6.9	350	0.9
265	2009-08-28/00:10:00	2009-08-28/02:00:00	6.1	0.23	5.4	343	-3.1
266	2009-08-28/03:28:00	2009-08-28/07:32:00	5.9	0.17	5.7	355	2.9
267	2009-08-28/16:55:00	2009-08-28/19:35:00	5.9	0.12	4.2	355	-2.8
268	2009-09-08/10:00:00	2009-09-08/16:28:00	13.4	0.14	5.0	369	-20.2
269	2009-09-08/17:40:00	2009-09-08/19:25:00	11.1	0.25	4.7	438	-23.1
270	2009-09-09/00:10:00	2009-09-09/01:35:00	8.7	0.27	5.4	474	9.3
271	2009-09-15/16:30:00	2009-09-16/00:10:00	6.4	0.09	4.7	276	5.1

Table B.1: STs list from STA Observation

No.	Start	End	B	β_p	M_A	V_p	V_{exp}
272	2009-09-16/06:00:00	2009-09-16/07:25:00	6.4	0.03	3.0	257	1.9
273	2009-09-17/02:28:00	2009-09-17/05:30:00	5.9	0.14	4.3	265	-0.3
274	2009-09-17/20:48:00	2009-09-17/21:30:00	6.1	0.05	5.3	284	0.5
275	2009-09-18/02:20:00	2009-09-18/05:42:00	6.7	0.11	5.0	302	3.6
276	2009-09-18/20:55:00	2009-09-18/23:45:00	6.8	0.19	4.8	360	6
277	2009-09-21/10:20:00	2009-09-21/16:38:00	6.6	0.29	6.2	334	-7.6
278	2009-09-21/17:30:00	2009-09-21/18:38:00	7.9	0.09	4.0	350	5.9
279	2009-09-21/19:35:00	2009-09-21/21:30:00	6.8	0.28	5.1	372	-18.6
280	2009-09-25/22:20:00	2009-09-25/24:00:00	6.1	0.15	5.7	302	0.4
281	2009-09-28/17:00:00	2009-09-28/20:10:00	5.4	0.17	6.1	299	-5.0
282	2009-09-29/23:15:00	2009-09-30/04:25:00	7.0	0.14	5.4	305	2.3
283	2009-10-17/22:55:00	2009-10-18/00:40:00	9.8	0.04	2.4	329	-0.5
284	2009-10-18/02:42:00	2009-10-18/03:48:00	9.3	0.25	4.6	330	-2.2
285	2009-10-20/18:35:00	2009-10-20/21:18:00	6.3	0.12	5.2	322	-7.9
286	2009-10-29/02:30:00	2009-10-29/07:00:00	6.9	0.18	5.6	323	3.9
287	2009-10-29/07:28:00	2009-10-29/08:40:00	7.1	0.18	4.7	331	-6.5
288	2009-10-29/09:40:00	2009-10-29/13:35:00	7.1	0.2	5.0	334	-14.1
289*	2009-11-01/02:40:00	2009-11-01/08:28:00	6.5	0.03	3.1	528	6.0
290	2009-11-04/13:15:00	2009-11-04/15:30:00	7.0	0.22	6.1	359	-5.7
291	2009-11-06/09:28:00	2009-11-06/10:05:00	5.9	0.34	6.8	346	2.4
292	2009-11-12/10:42:00	2009-11-12/14:15:00	6.5	0.21	5.8	271	2.7
293*	2009-11-14/10:15:00	2009-11-14/18:00:00	9.0	0.17	6.5	304	-1.3
294	2009-11-23/05:42:00	2009-11-23/09:32:00	6.6	0.13	5.1	292	-9.6
295*	2009-11-25/23:00:00	2009-11-26/01:32:00	14.4	0.07	2.3	353	1.4
296	2009-11-26/06:25:00	2009-11-26/09:45:00	7.7	0.15	4.5	375	9.7
297	2009-11-26/11:02:00	2009-11-26/12:25:00	6.0	0.3	5.0	319	-8.4
298	2009-11-27/03:00:00	2009-11-27/05:28:00	6.8	0.2	4.6	344	2.2
299	2009-11-29/17:18:00	2009-11-29/21:02:00	7.7	0.17	5.0	392	-48.9
300	2009-11-30/02:30:00	2009-11-30/04:28:00	8.2	0.4	6.4	438	-5.8
301	2009-11-30/11:20:00	2009-11-30/13:30:00	6.3	0.28	6.0	430	-12.8
302*	2009-12-10/09:00:00	2009-12-10/12:10:00	12.0	0.09	5.5	312	-2.6
303	2009-12-11/01:18:00	2009-12-11/02:12:00	8.0	0.13	3.9	293	8.7
304	2009-12-11/11:25:00	2009-12-11/14:00:00	6.9	0.21	5.3	312	-6.1
305	2009-12-11/14:15:00	2009-12-11/18:00:00	5.6	0.25	6.0	300	4.8
306	2009-12-14/06:10:00	2009-12-14/12:40:00	6.0	0.12	5.6	289	4.2
307	2009-12-14/16:00:00	2009-12-14/19:30:00	5.5	0.15	6.3	290	-4.9
308	2009-12-21/17:35:00	2009-12-21/21:32:00	6.7	0.16	5.6	288	3.2
309	2009-12-22/12:22:00	2009-12-22/14:30:00	10.2	0.2	4.2	424	-39.9
310	2009-12-25/00:35:00	2009-12-25/01:20:00	5.7	0.12	5.2	374	-0.4
311	2009-12-25/01:45:00	2009-12-25/04:40:00	6.8	0.05	3.3	377	-13.1
312	2009-12-25/06:10:00	2009-12-25/07:42:00	7.2	0.11	3.5	398	6.5
313	2009-12-27/13:45:00	2009-12-27/15:30:00	6.8	0.18	5.3	355	-19.9

Table B.1: STs list from STA Observation

No.	Start	End	B	β_p	M_A	V_p	V_{exp}
314	2009-12-27/16:32:00	2009-12-27/18:30:00	6.3	0.33	4.6	391	-1.0
315	2009-12-31/15:30:00	2009-12-31/16:15:00	8.7	0.15	5.4	320	4.1
2010							
316	2010-01-07/01:00:00	2010-01-07/02:05:00	8.8	0.08	4.6	290	-2.7
317	2010-01-07/13:25:00	2010-01-07/15:25:00	10.4	0.14	4.7	352	0.7
318	2010-01-15/13:40:00	2010-01-15/17:50:00	11.1	0.15	4.7	319	-13.6
319	2010-01-16/03:00:00	2010-01-16/10:32:00	12.0	0.18	5.1	353	-12.4
320	2010-02-02/13:55:00	2010-02-02/19:32:00	7.1	0.26	5.4	329	5.1
321*	2010-02-05/09:30:00	2010-02-05/12:02:00	13.9	0.13	3.3	386	1.3
322	2010-02-10/09:45:00	2010-02-10/16:32:00	9.3	0.12	3.8	394	-14.6
323	2010-02-17/00:10:00	2010-02-17/06:15:00	9.1	0.14	4.7	485	6.8
324*	2010-03-05/19:00:00	2010-03-06/03:15:00	11.1	0.04	3.7	357	-33.0
325	2010-03-22/19:17:00	2010-03-22/23:45:00	10.8	0.2	3.6	428	8.0
326	2010-04-17/13:32:00	2010-04-17/15:59:00	8.5	0.06	3.1	405	-5.2
327	2010-04-19/10:10:00	2010-04-19/12:02:00	9.1	0.12	5.5	398	-0.1
328*	2010-04-23/06:30:00	2010-04-23/14:05:00	10.4	0.05	4.7	418	5.3
329	2010-05-19/16:28:00	2010-05-19/17:32:00	12.6	0.17	4.0	419	-1.1
330*	2010-05-30/21:45:00	2010-05-30/22:45:00	11.0	0.07	4.4	417	6.7
331*	2010-05-31/00:30:00	2010-05-31/05:50:00	8.9	0.15	4.9	414	-8.3
332*	2010-06-03/12:30:00	2010-06-03/13:35:00	12.7	0.03	3.2	376	0.6
333*	2010-06-03/18:30:00	2010-06-03/19:40:00	14.7	0.03	2.7	373	-2.9
334*	2010-06-03/20:38:00	2010-06-03/23:32:00	12.9	0.04	3.6	365	-3.9
335	2010-06-04/09:10:00	2010-06-04/16:02:00	15.6	0.08	4.4	366	1.6
336	2010-06-05/03:38:00	2010-06-05/04:40:00	11.9	0.17	3.5	562	-40.7
337*	2010-06-17/21:00:00	2010-06-18/03:30:00	7.2	0.04	4.3	408	26.3
338	2010-06-20/17:28:00	2010-06-20/18:45:00	16.0	0.11	3.9	372	2.5
339	2010-06-21/00:25:00	2010-06-21/03:02:00	14.9	0.14	5.0	412	-10.7
340	2010-06-21/05:38:00	2010-06-21/07:10:00	13.7	0.16	3.2	408	-4.6
341	2010-06-22/11:35:00	2010-06-22/14:30:00	7.4	0.14	4.9	473	16.7
342	2010-07-01/07:00:00	2010-07-01/07:10:00	12.0	0.23	4.4	437	-18.3
343	2010-07-02/04:00:00	2010-07-02/13:40:00	7.5	0.1	4.2	357	21.0
344	2010-07-16/07:45:00	2010-07-16/09:32:00	8.3	0.13	3.6	349	-5.1
345	2010-07-19/18:32:00	2010-07-19/22:20:00	6.7	0.09	3.9	323	6.7
346	2010-07-20/14:38:00	2010-07-20/16:30:00	8.0	0.2	5.5	309	-8.6
347	2010-07-20/21:35:00	2010-07-21/02:12:00	7.1	0.16	5.0	316	-7.0
348	2010-07-21/10:25:00	2010-07-21/12:00:00	6.8	0.08	3.6	336	4.6
349	2010-07-21/22:32:00	2010-07-21/23:45:00	7.0	0.12	4.2	356	-4.2
350	2010-08-11/16:00:00	2010-08-11/21:30:00	7.1	0.22	4.4	438	-28.6
351	2010-08-30/17:00:00	2010-08-30/17:38:00	12.1	0.14	3.9	429	-1.3
352*	2010-08-30/21:40:00	2010-08-31/08:42:00	14.0	0.06	3.3	446	-30.3
353	2010-08-31/16:12:00	2010-08-31/21:20:00	8.2	0.11	2.8	498	-5.7
354	2010-09-01/00:45:00	2010-09-01/02:12:00	7.9	0.13	4.7	512	-6.4

Table B.1: STs list from STA Observation

No.	Start	End	B	β_p	M_A	V_p	V_{exp}
355	2010-09-06/10:00:00	2010-09-06/13:10:00	7.8	0.05	4.0	396	-10.1
356*	2010-09-11/10:52:00	2010-09-11/11:30:00	20.7	0.1	2.8	588	-1.8
357	2010-09-17/01:38:00	2010-09-17/03:40:00	6.7	0.08	3.2	353	2.1
358	2010-09-17/19:30:00	2010-09-17/21:55:00	6.7	0.08	3.3	356	4.3
359	2010-09-22/23:05:00	2010-09-23/00:55:00	8.3	0.13	4.8	320	-16.3
360	2010-09-24/19:10:00	2010-09-24/21:38:00	8.0	0.09	4.8	350	-7.6
361	2010-09-24/23:30:00	2010-09-25/00:30:00	7.7	0.2	4.6	357	0.8
362	2010-09-25/00:38:00	2010-09-25/05:25:00	8.1	0.18	4.6	346	8.2
363	2010-09-25/09:38:00	2010-09-25/10:40:00	8.0	0.22	3.8	371	-15.0
364	2010-09-27/14:30:00	2010-09-27/15:28:00	9.0	0.12	3.8	401	-20.1
365	2010-10-10/23:20:00	2010-10-11/03:28:00	7.2	0.09	3.4	309	-1.2
366	2010-10-12/01:32:00	2010-10-12/03:16:00	6.6	0.27	5.6	329	5.5
367	2010-10-16/19:40:00	2010-10-17/03:45:00	7.5	0.12	5.1	313	5.8
368	2010-10-20/11:00:00	2010-10-20/14:58:00	9.0	0.08	4.5	360	-20.2
369	2010-10-25/11:35:00	2010-10-25/21:45:00	6.9	0.08	4.5	293	8.7
370	2010-10-30/12:50:00	2010-10-30/16:25:00	13.2	0.16	4.9	317	-12.3
371	2010-10-30/22:15:00	2010-10-30/23:32:00	17.6	0.12	4.7	361	-15.3
372	2010-10-31/01:02:00	2010-10-31/03:12:00	16.7	0.12	3.4	433	-71.9
373	2010-11-02/19:00:00	2010-11-02/22:45:00	6.7	0.25	4.9	531	15.9
374	2010-11-08/17:50:00	2010-11-08/19:35:00	7.0	0.13	4.0	505	3.6
375	2010-11-14/14:38:00	2010-11-14/16:48:00	9.5	0.15	3.5	351	-19.7
376	2010-11-25/09:45:00	2010-11-25/12:30:00	7.6	0.18	5.0	481	-5.3
377	2010-11-25/14:10:00	2010-11-25/15:22:00	8.3	0.11	4.3	494	22.6
378	2010-11-25/20:10:00	2010-11-25/22:55:00	13.6	0.08	4.0	490	-4.9
379	2010-11-26/05:28:00	2010-11-26/08:15:00	8.8	0.14	4.9	508	-32.4
380	2010-11-26/23:22:00	2010-11-27/00:20:00	7.3	0.21	4.8	459	1.6
381	2010-12-04/18:35:00	2010-12-04/21:00:00	9.4	0.09	4.1	314	-4.8
382	2010-12-04/22:30:00	2010-12-05/04:30:00	8.3	0.1	4.1	329	-2.7
383	2010-12-05/10:10:00	2010-12-05/12:20:00	9.5	0.19	4.4	344	-3.9
384	2010-12-06/17:30:00	2010-12-06/19:45:00	9.1	0.21	4.3	462	-5.8
385	2010-12-10/19:10:00	2010-12-10/20:00:00	6.8	0.16	4.4	338	-13.3
386	2010-12-12/20:20:00	2010-12-12/23:15:00	6.9	0.08	3.4	362	12.1
387	2010-12-14/09:30:00	2010-12-14/13:45:00	11.0	0.07	2.9	399	-3.8
388	2010-12-16/05:55:00	2010-12-16/11:55:00	13.5	0.09	4.6	471	-29.1
2011							
389	2011-01-04/17:10:00	2011-01-04/23:35:00	12.1	0.1	2.6	338	-16.9
390	2011-01-12/23:28:00	2011-01-13/01:00:00	9.1	0.12	2.6	398	1.9
391	2011-01-13/02:30:00	2011-01-13/04:00:00	8.2	0.16	4.6	370	18.9
392	2011-01-13/08:02:00	2011-01-13/09:00:00	10.7	0.17	4.8	469	-9.2
393*	2011-01-26/15:45:00	2011-01-27/02:30:00	7.8	0.02	2.8	443	6.3
394*	2011-02-03/19:22:00	2011-02-04/02:42:00	8.2	0.11	4.4	340	-10.4
395	2011-02-07/04:40:00	2011-02-07/07:00:00	9.1	0.17	5.1	314	-11.0

Table B.1: STs list from STA Observation

No.	Start	End	B	β_p	M_A	V_p	V_{exp}
396	2011-02-23/00:40:00	2011-02-23/03:02:00	8.1	0.06	4.2	348	-0.9
397	2011-03-04/01:10:00	2011-03-04/05:12:00	13.3	0.11	3.3	368	-31.8
398*	2011-03-19/12:45:00	2011-03-19/14:35:00	13.4	0.09	3.6	495	30.1
399*	2011-03-19/16:15:00	2011-03-19/22:05:00	12.8	0.16	4.0	476	-4.1
400*	2011-03-20/01:42:00	2011-03-20/11:00:00	11.0	0.02	2.1	467	18.2
401*	2011-03-22/17:55:00	2011-03-22/20:50:00	22.1	0.06	3.0	670	-118.3
402	2011-03-30/10:32:00	2011-03-30/11:30:00	16.2	0.11	3.7	332	-3.7
403	2011-04-04/13:30:00	2011-04-04/17:58:00	8.1	0.07	3.6	410	-11.2
404	2011-04-08/10:02:00	2011-04-08/18:12:00	8.3	0.11	3.7	445	-23.7
405	2011-04-16/10:25:00	2011-04-16/12:10:00	10.5	0.13	4.9	420	-5.6
406	2011-04-25/09:00:00	2011-04-25/10:55:00	8.2	0.14	5.1	307	5.1
407	2011-04-27/20:45:00	2011-04-27/21:50:00	7.6	0.18	5.1	385	-4.7
408	2011-04-30/15:40:00	2011-04-30/18:28:00	8.9	0.14	5.1	325	-6.2
409	2011-05-02/08:00:00	2011-05-02/10:00:00	7.8	0.07	2.7	323	5.8
410	2011-05-21/10:50:00	2011-05-21/16:20:00	17.6	0.16	4.6	430	18.3
411	2011-05-22/04:50:00	2011-05-22/06:18:00	11.5	0.05	4.3	496	6.9
412	2011-05-22/09:32:00	2011-05-22/10:58:00	15.2	0.05	3.5	507	0.3
413	2011-05-22/11:45:00	2011-05-22/17:10:00	15.7	0.09	3.4	492	27.0
414	2011-05-24/11:40:00	2011-05-24/16:35:00	7.6	0.09	3.3	458	-6.8
415	2011-05-31/03:45:00	2011-05-31/06:35:00	8.4	0.15	3.8	330	7.5
416	2011-06-10/13:32:00	2011-06-10/18:05:00	10.5	0.07	4.1	422	1.5
417	2011-06-28/11:50:00	2011-06-28/16:38:00	11.8	0.14	3.7	454	3.7
418	2011-06-29/08:22:00	2011-06-29/13:02:00	9.4	0.17	4.8	501	29.4
419	2011-07-03/21:38:00	2011-07-03/23:45:00	7.7	0.05	3.8	416	5.5
420	2011-07-08/20:12:00	2011-07-08/21:35:00	11.2	0.24	4.6	413	-5.2
421	2011-07-24/13:22:00	2011-07-24/14:35:00	12.5	0.13	3.4	357	6.2
422	2011-07-26/10:28:00	2011-07-26/11:20:00	13.4	0.29	4.6	428	-45.8
423	2011-07-26/14:20:00	2011-07-26/16:35:00	14.9	0.19	3.1	565	-14.8
424	2011-08-02/02:25:00	2011-08-02/08:50:00	9.3	0.13	3.4	411	-24.6
425*	2011-08-07/00:45:00	2011-08-07/01:50:00	8.0	0.12	4.9	415	0.5
426	2011-08-11/17:00:00	2011-08-11/19:30:00	11.6	0.15	4.7	566	5.6
427*	2011-08-13/22:42:00	2011-08-14/03:40:00	9.4	0.07	3.7	465	7.4
428	2011-08-22/10:00:00	2011-08-22/11:15:00	11.6	0.14	4.4	499	16.7
429	2011-08-22/12:00:00	2011-08-22/13:02:00	11.9	0.14	4.5	510	-4.2
430*	2011-09-05/00:15:00	2011-09-05/02:30:00	8.7	0.08	5.3	330	6.9
431	2011-09-12/12:15:00	2011-09-12/15:00:00	10.1	0.09	2.9	488	-12.2
432	2011-09-23/00:30:00	2011-09-23/02:15:00	7.4	0.04	4.4	351	1.8
433	2011-09-23/03:28:00	2011-09-23/07:28:00	7.9	0.1	4.9	348	-4.3
434	2011-09-23/08:20:00	2011-09-23/12:15:00	8.1	0.16	4.7	354	-3.6
435	2011-09-24/00:55:00	2011-09-24/02:22:00	8.2	0.04	4.3	354	2.4
436*	2011-09-25/06:22:00	2011-09-25/11:30:00	10.9	0.04	3.8	465	-5.9
437*	2011-09-25/14:35:00	2011-09-25/16:28:00	8.2	0.15	3.3	449	-3.5

Table B.1: STs list from STA Observation

No.	Start	End	B	β_p	M_A	V_p	V_{exp}
438	2011-10-01/22:32:00	2011-10-02/01:20:00	8.4	0.09	5.3	437	0.005
439	2011-10-08/05:20:00	2011-10-08/07:10:00	17.0	0.07	4.1	483	-31.9
440	2011-10-14/15:40:00	2011-10-14/19:00:00	7.8	0.03	3.5	364	1.6
441	2011-10-23/21:00:00	2011-10-24/05:28:00	9.8	0.08	4.7	350	-1.8
442	2011-10-24/18:05:00	2011-10-24/21:55:00	9.7	0.08	3.5	363	-14.1
443*	2011-10-25/15:55:00	2011-10-25/23:58:00	8.8	0.22	4.6	411	-5.6
444	2011-11-06/03:12:00	2011-11-06/04:35:00	14.6	0.19	5.2	320	-5.2
445	2011-11-16/15:22:00	2011-11-16/16:15:00	7.8	0.2	4.5	381	-8.5
446	2011-11-16/16:25:00	2011-11-16/17:05:00	7.7	0.23	4.3	389	-4.4
447	2011-11-19/23:20:00	2011-11-20/02:00:00	8.7	0.11	4.9	307	-5.4
448	2011-11-20/02:42:00	2011-11-20/04:05:00	9.5	0.1	4.3	341	-0.6
449	2011-11-20/04:55:00	2011-11-20/07:12:00	11.1	0.08	4.0	345	-12.5
450*	2011-11-27/00:22:00	2011-11-27/03:12:00	10.1	0.09	5.2	490	-9.0
451	2011-12-07/20:15:00	2011-12-07/21:20:00	8.3	0.11	4.6	344	-1.1
452	2011-12-08/08:48:00	2011-12-08/10:02:00	11.4	0.09	3.9	360	2.4
453	2011-12-08/14:55:00	2011-12-08/22:20:00	8.6	0.08	3.5	422	-19.9
454	2011-12-10/10:10:00	2011-12-10/11:50:00	7.8	0.14	5.1	428	-7.8
455	2011-12-15/02:30:00	2011-12-15/05:10:00	7.5	0.07	3.0	347	2.0
456	2011-12-17/04:10:00	2011-12-17/04:55:00	9.6	0.13	4.9	388	-6.9
457	2011-12-17/05:40:00	2011-12-17/10:28:00	11.0	0.1	3.4	415	0.9
458	2011-12-19/12:55:00	2011-12-19/14:38:00	8.8	0.08	3.8	369	-13.7
459	2011-12-19/17:40:00	2011-12-19/21:05:00	17.3	0.08	4.7	405	10.7
460	2011-12-28/06:00:00	2011-12-28/07:28:00	23.2	0.17	4.3	314	-4.8
2012							
461*	2012-01-01/22:02:00	2012-01-02/04:02:00	11.9	0.19	3.7	416	-1.7
462	2012-01-05/12:15:00	2012-01-05/14:00:00	10.1	0.16	4.8	472	-1.8
463	2012-01-13/21:02:00	2012-01-13/22:25:00	7.7	0.11	4.9	354	-11.7
464	2012-01-25/09:38:00	2012-01-25/11:40:00	8.8	0.21	4.7	637	-0.03
465*	2012-01-26/18:00:00	2012-01-26/20:40:00	8.3	0.1	4.7	459	3.5
466*	2012-01-29/13:02:00	2012-01-29/16:35:00	42.9	0.16	3.5	345	-57.0
467	2012-02-02/03:58:00	2012-02-02/05:38:00	8.1	0.02	3.3	380	10.5
468	2012-02-03/14:25:00	2012-02-03/18:30:00	9.1	0.12	4.1	313	6.5
469	2012-02-04/17:15:00	2012-02-04/22:15:00	9.2	0.09	3.4	384	2.6
470	2012-02-05/18:38:00	2012-02-05/22:20:00	8.3	0.16	4.8	457	-7.7
471	2012-02-06/03:20:00	2012-02-06/06:00:00	8.3	0.15	4.9	426	5.8
472	2012-02-21/02:38:00	2012-02-21/04:00:00	22.3	0.04	2.6	387	-3.7
473*	2012-02-21/05:05:00	2012-02-21/09:25:00	20.5	0.03	2.1	361	24.9
474	2012-02-21/10:18:00	2012-02-21/11:10:00	15.1	0.19	3.7	354	-3.9
475	2012-02-25/22:05:00	2012-02-26/00:32:00	11.6	0.06	2.5	399	-35.9
476	2012-02-26/03:30:00	2012-02-26/06:20:00	11.1	0.17	4.7	455	-25.1
477	2012-02-26/19:10:00	2012-02-26/22:00:00	9.6	0.12	4.3	439	-3.4
478*	2012-03-03/10:00:00	2012-03-03/18:10:00	13.6	0.04	2.9	397	17.3

Table B.1: STs list from STA Observation

No.	Start	End	B	β_p	M_A	V_p	V_{exp}
479	2012-03-04/05:48:00	2012-03-04/07:40:00	13.3	0.08	5.2	397	7.0
480*	2012-03-04/11:40:00	2012-03-04/18:35:00	10.2	0.04	4.3	411	3.1
481	2012-03-05/00:25:00	2012-03-05/02:12:00	8.5	0.08	4.3	382	3.8
482	2012-03-09/13:10:00	2012-03-09/14:05:00	17.9	0.21	4.1	406	-24.9
483	2012-03-09/20:40:00	2012-03-09/21:45:00	14.0	0.14	3.6	513	4.1
484	2012-03-15/05:25:00	2012-03-15/08:38:00	9.0	0.21	4.9	453	-27.8
485*	2012-03-17/04:18:00	2012-03-17/06:10:00	7.8	0.02	2.9	473	-4.4
486*	2012-03-19/11:35:00	2012-03-19/15:40:00	14.0	0.04	2.9	466	-5.1
487*	2012-03-19/19:18:00	2012-03-19/20:28:00	14.4	0.05	3.9	547	-28.1
488*	2012-03-20/01:38:00	2012-03-20/02:40:00	30.0	0.14	2.5	616	34.2
489*	2012-03-20/03:38:00	2012-03-20/04:45:00	21.0	0.1	3.2	671	6.6
490*	2012-03-20/06:15:00	2012-03-20/13:05:00	14.1	0.05	3.4	648	34.1
491	2012-03-23/22:38:00	2012-03-24/01:48:00	9.2	0.06	4.0	394	13.6
492	2012-03-24/20:00:00	2012-03-25/02:55:00	8.6	0.08	3.6	472	12.5
493	2012-04-05/03:00:00	2012-04-05/07:18:00	8.0	0.14	4.4	393	12.9
494	2012-04-09/11:00:00	2012-04-09/12:02:00	9.0	0.06	2.9	366	-0.2
495	2012-04-10/10:40:00	2012-04-10/14:50:00	9.8	0.13	4.7	409	-4.0
496	2012-04-10/18:18:00	2012-04-10/20:48:00	7.8	0.16	4.2	424	2.5
497	2012-04-12/23:35:00	2012-04-13/01:25:00	8.1	0.18	4.9	433	0.07
498	2012-04-29/22:15:00	2012-04-30/01:48:00	10.5	0.21	4.4	336	-3.0
499	2012-05-10/21:45:00	2012-05-11/00:22:00	13.4	0.11	2.8	304	-9.4
500	2012-05-11/02:00:00	2012-05-11/02:45:00	12.7	0.14	3.7	328	6.6
501	2012-05-11/12:28:00	2012-05-11/23:48:00	9.0	0.08	2.9	307	-3.0
502	2012-05-14/08:38:00	2012-05-14/10:38:00	14.3	0.1	3.4	382	-32.4
503	2012-05-14/17:05:00	2012-05-14/23:45:00	7.9	0.09	3.4	490	-13.9
504*	2012-05-24/01:02:00	2012-05-24/06:32:00	8.9	0.08	4.2	443	14.5
505	2012-06-12/04:20:00	2012-06-12/09:00:00	10.4	0.07	4.4	345	-0.5
506	2012-06-12/16:00:00	2012-06-12/18:10:00	18.1	0.11	2.7	380	16.6
507	2012-06-20/01:30:00	2012-06-20/03:42:00	8.1	0.13	4.4	347	-5.0
508*	2012-06-20/06:35:00	2012-06-20/08:20:00	8.6	0.05	3.4	351	-0.5
509*	2012-06-28/23:48:00	2012-06-29/11:10:00	8.6	0.03	1.7	382	-22.0
510	2012-07-01/04:00:00	2012-07-01/08:55:00	9.8	0.12	4.3	440	0
511	2012-07-05/06:45:00	2012-07-05/08:42:00	8.1	0.11	4.4	412	-6.5
512	2012-07-05/16:55:00	2012-07-05/19:00:00	11.9	0.17	5.4	403	-5.1
513*	2012-07-11/11:30:00	2012-07-11/13:50:00	13.8	0.02	3.7	683	-49.6
514*	2012-08-06/04:00:00	2012-08-06/12:32:00	10.4	0.02	2.4	453	32.3
515*	2012-08-14/02:30:00	2012-08-14/03:42:00	12.3	0.03	3.4	415	0.5
516*	2012-08-15/00:55:00	2012-08-15/03:32:00	9.8	0.04	3.2	422	-8.9
517	2012-08-22/16:45:00	2012-08-22/17:30:00	8.5	0.07	3.0	366	-13.3
518	2012-08-24/04:38:00	2012-08-24/07:45:00	8.8	0.11	4.2	391	-19.6
519	2012-09-05/15:05:00	2012-09-05/16:30:00	9.3	0.14	3.2	402	-13.3
520	2012-09-09/19:22:00	2012-09-09/20:50:00	8.6	0.05	2.5	375	-27.0

Table B.1: STs list from STA Observation

No.	Start	End	B	β_p	M_A	V_p	V_{exp}
521*	2012-09-12/06:45:00	2012-09-12/07:38:00	12.4	0.12	3.9	354	0.06
522	2012-09-14/11:35:00	2012-09-14/15:30:00	9.4	0.11	4.7	358	0.8
523*	2012-09-17/15:35:00	2012-09-17/16:40:00	8.6	0.1	4.2	370	1.7
524*	2012-09-17/17:28:00	2012-09-17/23:42:00	8.2	0.05	4.0	356	9.3
525	2012-09-18/11:12:00	2012-09-18/13:22:00	7.9	0.04	3.2	344	-0.03
526	2012-09-28/08:20:00	2012-09-28/15:30:00	8.0	0.07	4.7	358	17.2
527	2012-09-29/19:55:00	2012-09-29/20:32:00	12.1	0.06	2.9	340	3.2
528	2012-09-29/21:20:00	2012-09-30/00:35:00	9.1	0.11	3.5	334	5.2
529	2012-09-30/12:15:00	2012-09-30/13:05:00	10.6	0.17	4.4	356	-5.8
530	2012-09-30/21:35:00	2012-09-30/23:45:00	8.1	0.14	4.4	329	7.6
531	2012-10-01/07:30:00	2012-10-01/08:42:00	8.2	0.17	3.8	328	-4.1
532	2012-10-01/12:55:00	2012-10-01/13:55:00	7.9	0.22	5.0	349	2.3
533*	2012-10-05/08:05:00	2012-10-05/09:40:00	11.1	0.09	3.7	410	0.5
534*	2012-10-11/22:45:00	2012-10-12/02:00:00	10.9	0.05	3.5	371	7.5
535*	2012-10-23/21:10:00	2012-10-24/00:20:00	8.2	0.02	2.5	349	3.6
536*	2012-10-26/12:50:00	2012-10-26/20:22:00	8.6	0.03	3.4	365	-5.6
537*	2012-10-26/23:40:00	2012-10-27/08:12:00	8.6	0.05	3.4	358	14.8
538*	2012-11-11/03:30:00	2012-11-11/07:28:00	20.4	0.14	4.7	492	0.3
539*	2012-11-12/02:32:00	2012-11-12/03:30:00	16.0	0.04	2.2	452	2.8
540*	2012-11-12/04:40:00	2012-11-12/06:32:00	12.3	0.1	4.3	457	-5.0
541*	2012-11-12/11:45:00	2012-11-12/13:45:00	9.5	0.02	2.9	421	-3.2
542	2012-11-20/03:45:00	2012-11-20/05:38:00	14.1	0.11	3.1	411	-15.6
543*	2012-11-23/20:20:00	2012-11-23/21:38:00	15.0	0.06	2.1	411	-5.9
544*	2012-11-26/15:02:00	2012-11-26/19:12:00	10.8	0.06	4.9	490	27.9
545*	2012-11-27/02:58:00	2012-11-27/06:25:00	10.4	0.05	3.9	424	17.6
546*	2012-11-27/06:38:00	2012-11-27/07:15:00	10.5	0.07	3.1	417	8.6
547*	2012-11-27/10:20:00	2012-11-27/18:50:00	9.9	0.02	2.0	384	-0.8
548	2012-12-05/04:00:00	2012-12-05/05:25:00	8.2	0.07	3.7	293	-1.1
549	2012-12-27/07:35:00	2012-12-27/10:10:00	7.7	0.17	4.0	324	1.9
550	2012-12-28/05:02:00	2012-12-28/08:00:00	13.8	0.09	3.0	388	6.0
2013							
551	2013-01-06/18:40:00	2013-01-06/19:28:00	8.2	0.08	2.5	335	-28.5
552*	2013-01-25/14:40:00	2013-01-25/17:15:00	12.8	0.09	3.9	350	3.2
553	2013-01-27/09:00:00	2013-01-27/16:25:00	7.8	0.08	3.4	396	-5.6
554	2013-02-04/03:30:00	2013-02-04/06:25:00	8.4	0.08	4.4	307	5.3
555	2013-02-04/07:17:00	2013-02-04/09:00:00	7.9	0.12	4.8	304	5.3
556*	2013-02-08/19:12:00	2013-02-08/22:50:00	8.0	0.12	4.3	322	7.4
557*	2013-02-08/23:28:00	2013-02-09/09:15:00	8.7	0.06	3.8	306	4.8
558*	2013-02-19/07:48:00	2013-02-19/11:05:00	18.2	0.02	2.9	406	-1.5
559*	2013-02-19/22:38:00	2013-02-20/06:00:00	14.9	0.04	2.7	412	19.3
560*	2013-03-01/14:00:00	2013-03-01/17:35:00	14.0	0.08	3.1	415	-5.3
561*	2013-03-01/19:02:00	2013-03-01/21:02:00	12.8	0.08	3.2	414	-1.4

Table B.1: STs list from STA Observation

No.	Start	End	B	β_p	M_A	V_p	V_{exp}
562*	2013-03-08/04:00:00	2013-03-08/05:02:00	11.4	0.12	3.6	371	5.1
563	2013-03-10/17:25:00	2013-03-10/20:38:00	12.6	0.15	4.5	401	-8.2
564	2013-03-23/02:25:00	2013-03-23/03:25:00	8.3	0.13	4.7	316	-6.8
565	2013-03-30/07:42:00	2013-03-30/14:00:00	7.7	0.07	4.5	347	9.8
566*	2013-04-18/05:35:00	2013-04-18/11:15:00	9.2	0.02	2.0	358	17.7
567*	2013-04-22/19:48:00	2013-04-22/21:00:00	10.9	0.19	4.1	566	-7.1
568*	2013-04-28/08:00:00	2013-04-28/09:40:00	9.3	0.05	2.8	386	4.2
569*	2013-04-28/11:12:00	2013-04-28/14:00:00	8.0	0.04	2.8	375	12.5
570*	2013-05-03/05:48:00	2013-05-03/07:22:00	20.1	0.16	4.7	549	1.6
571	2013-05-06/13:16:00	2013-05-06/15:15:00	13.6	0.08	4.3	566	-3.7
572	2013-05-16/09:55:00	2013-05-16/11:30:00	26.6	0.14	3.9	445	-15.6
573	2013-06-02/14:40:00	2013-06-02/17:22:00	15.7	0.04	3.3	363	-2.9
574*	2013-06-27/16:22:00	2013-06-27/21:02:00	13.2	0.04	2.6	368	-9.9
575	2013-06-28/01:15:00	2013-06-28/02:30:00	9.1	0.08	3.3	362	-10.3
576	2013-06-28/15:00:00	2013-06-28/19:00:00	7.9	0.15	4.7	335	5.1
577	2013-07-03/01:00:00	2013-07-03/02:12:00	10.4	0.16	4.5	387	-6.7
578	2013-07-09/08:16:00	2013-07-09/11:10:00	8.8	0.14	4.1	436	-13.3
579	2013-07-18/17:28:00	2013-07-18/22:30:00	16.0	0.09	2.9	376	-29.7
580	2013-07-21/03:00:00	2013-07-21/08:32:00	8.3	0.1	3.1	477	-24.6
581*	2013-07-25/11:55:00	2013-07-25/14:35:00	38.1	0.05	1.7	482	-4.9
582	2013-07-26/13:22:00	2013-07-26/15:02:00	11.5	0.05	3.0	435	4.3
583*	2013-07-28/07:52:00	2013-07-28/10:00:00	7.8	0.07	4.3	539	8.2
584	2013-08-04/19:30:00	2013-08-04/22:17:00	12.0	0.07	2.6	389	9.0
585	2013-08-13/15:55:00	2013-08-13/16:45:00	10.1	0.02	3.0	376	-0.6
586	2013-08-13/21:00:00	2013-08-13/23:38:00	7.9	0.07	4.0	385	-7.9
587	2013-08-14/17:38:00	2013-08-14/19:40:00	8.7	0.11	4.0	402	-24.1
588	2013-08-19/00:00:00	2013-08-19/01:02:00	8.0	0.09	3.5	392	-2.7
589	2013-08-28/02:48:00	2013-08-28/05:45:00	12.0	0.09	3.3	369	-55.3
590*	2013-09-01/09:50:00	2013-09-01/14:50:00	8.3	0.1	3.1	354	9.6
591	2013-09-02/13:42:00	2013-09-02/15:45:00	9.9	0.15	2.9	363	-10.4
592	2013-09-02/18:40:00	2013-09-03/00:30:00	9.9	0.16	4.3	367	-10.9
593	2013-09-11/13:05:00	2013-09-11/15:02:00	8.5	0.15	4.4	432	-4.8
594	2013-09-11/22:38:00	2013-09-11/23:40:00	9.5	0.09	3.5	367	0.4
595	2013-09-12/00:35:00	2013-09-12/02:00:00	8.8	0.19	4.3	367	-0.96
596	2013-10-06/23:52:00	2013-10-07/01:10:00	9.3	0.08	3.7	309	-0.7
597	2013-10-07/12:00:00	2013-10-07/13:32:00	7.6	0.07	3.3	345	-0.5
598	2013-10-17/02:50:00	2013-10-17/07:28:00	9.3	0.07	3.1	307	-4.5
599	2013-10-21/21:40:00	2013-10-22/07:02:00	8.6	0.07	3.5	317	7.3
600*	2013-10-23/01:15:00	2013-10-23/03:25:00	9.3	0.1	3.6	323	-10.2
601*	2013-11-01/13:00:00	2013-11-01/14:00:00	17.4	0.1	3.2	449	-13.8
602*	2013-11-01/15:16:00	2013-11-01/18:22:00	15.2	0.11	3.6	417	10.8
603*	2013-11-05/16:50:00	2013-11-05/23:28:00	9.6	0.06	3.4	467	-4.9

Table B.1: STs list from STA Observation

No.	Start	End	B	β_p	M_A	V_p	V_{exp}
604*	2013-11-14/09:00:00	2013-11-14/13:00:00	9.0	0.02	2.9	411	-7.5
605*	2013-11-19/00:38:00	2013-11-19/03:15:00	8.6	0.17	4.8	324	-0.9
606	2013-11-21/10:15:00	2013-11-21/11:35:00	7.9	0.1	3.9	372	-5.0
607*	2013-11-26/19:30:00	2013-11-26/22:38:00	11.2	0.02	3.4	362	0.3
608*	2013-11-27/01:17:00	2013-11-27/04:00:00	11.8	0.03	3.2	363	-2.2
609*	2013-11-27/04:20:00	2013-11-27/05:40:00	10.6	0.04	4.0	390	-1.5
610	2013-12-16/00:35:00	2013-12-16/01:45:00	13.7	0.13	4.5	421	-0.9
611	2013-12-24/21:20:00	2013-12-25/06:00:00	16.4	0.09	4.1	381	-7.0
612*	2013-12-25/12:35:00	2013-12-25/22:12:00	11.2	0.06	2.9	381	-18.5
613	2013-12-26/01:25:00	2013-12-26/02:38:00	8.4	0.05	3.1	391	0.6
614	2013-12-30/03:42:00	2013-12-30/05:42:00	10.6	0.12	4.4	387	-4.9
615	2013-12-30/06:02:00	2013-12-30/06:50:00	11.1	0.11	2.7	395	-9.8
616	2013-12-30/11:12:00	2013-12-30/13:38:00	9.1	0.16	4.0	388	18.6
2014							
617	2014-01-06/00:20:00	2014-01-06/01:15:00	10.8	0.05	2.1	331	20.5
618*	2014-01-09/16:10:00	2014-01-09/17:42:00	19.5	0.04	3.3	537	2.6
619*	2014-01-09/19:00:00	2014-01-10/00:10:00	16.5	0.11	4.6	515	9.9
620*	2014-01-10/05:00:00	2014-01-10/05:40:00	13.0	0.03	2.8	518	4.0
621	2014-01-21/01:55:00	2014-01-21/03:45:00	11.0	0.18	4.6	361	11.5
622	2014-01-21/14:40:00	2014-01-21/18:25:00	13.0	0.17	4.0	422	-33.9
623*	2014-02-02/19:02:00	2014-02-02/21:35:00	13.1	0.03	3.7	382	6.0
624*	2014-02-03/03:45:00	2014-02-03/12:15:00	12.1	0.05	3.6	369	-16.6
625*	2014-02-07/23:25:00	2014-02-08/01:30:00	15.5	0.14	3.5	406	10.0
626	2014-02-16/02:35:00	2014-02-16/04:20:00	12.9	0.17	3.1	408	-37.8
627	2014-03-03/18:45:00	2014-03-03/21:05:00	8.3	0.08	3.5	304	-0.5
628	2014-03-04/01:30:00	2014-03-04/03:35:00	9.9	0.13	2.8	323	-9.96
629	2014-03-07/09:00:00	2014-03-07/10:12:00	8.4	0.24	4.3	403	-0.7
630*	2014-03-08/18:28:00	2014-03-08/21:22:00	8.6	0.12	5.1	499	2.9
631*	2014-03-11/12:00:00	2014-03-11/13:15:00	12.9	0.07	2.9	441	17.8
632*	2014-03-15/01:28:00	2014-03-15/12:00:00	9.1	0.17	4.0	578	94.4
633	2014-03-29/04:15:00	2014-03-29/06:15:00	8.2	0.11	3.8	327	9.0
634	2014-03-29/19:40:00	2014-03-30/04:48:00	9.9	0.15	4.3	345	-1.7
635	2014-03-30/07:10:00	2014-03-30/09:48:00	9.1	0.24	3.8	383	-0.8
636*	2014-04-01/14:50:00	2014-04-01/21:20:00	8.9	0.04	4.1	466	22.4
637*	2014-04-10/07:02:00	2014-04-10/13:48:00	12.1	0.04	3.3	390	5.7
638	2014-04-12/11:40:00	2014-04-12/17:40:00	8.4	0.03	3.1	435	21.8
639	2014-04-25/05:00:00	2014-04-25/10:15:00	10.0	0.16	4.4	398	-30.9
640	2014-04-29/05:25:00	2014-04-29/08:30:00	9.9	0.09	3.9	326	0.8
641	2014-04-29/09:28:00	2014-04-29/13:20:00	10.5	0.19	4.7	318	7.5
642	2014-04-30/11:22:00	2014-04-30/12:50:00	8.5	0.04	2.9	357	-5.1
643	2014-04-30/13:02:00	2014-04-30/16:45:00	8.1	0.14	3.1	350	9.2
644	2014-05-06/01:50:00	2014-05-06/04:18:00	8.1	0.13	4.1	336	-15.6

Table B.1: STs list from STA Observation

No.	Start	End	B	β_p	M_A	V_p	V_{exp}
645	2014-05-06/14:05:00	2014-05-06/15:50:00	12.3	0.15	4.1	427	-6.0
646	2014-05-06/17:30:00	2014-05-06/20:55:00	9.3	0.11	5.1	423	-14.1
647*	2014-05-12/08:35:00	2014-05-12/15:12:00	23.9	0.06	4.0	536	14.5
648*	2014-05-12/19:38:00	2014-05-13/04:32:00	9.8	0.08	3.4	576	13.3
649	2014-05-27/04:22:00	2014-05-27/13:12:00	8.3	0.05	2.9	263	-8.1
650	2014-07-05/04:32:00	2014-07-05/11:05:00	10.7	0.07	3.4	328	-8.1
651	2014-07-12/17:22:00	2014-07-12/23:05:00	18.2	0.1	4.1	419	7.8
652	2014-07-18/09:00:00	2014-07-18/10:15:00	9.7	0.04	2.6	343	-28.7
653	2014-07-28/00:22:00	2014-07-28/01:00:00	16.8	0.08	2.3	398	13.9
654	2014-07-28/03:38:00	2014-07-28/06:20:00	9.5	0.19	4.4	454	-4.8
655	2014-08-10/12:20:00	2014-08-10/16:30:00	8.4	0.07	4.0	355	2.2
656	2014-08-11/02:00:00	2014-08-11/05:30:00	8.1	0.04	3.2	328	-4.5

Appendix C

The STs from STB

We observed 625 STs from STB from the year 2007 to 2014. The event number with "*" means this ST was in the time ranges which ICMEs have been observed. We call them "ICME-like STs" in this paper. The lists of the ICMEs observed by STB which have been used in this paper are got from: *Jian et al.*, 2006, www-ssc.igpp.ucla.edu/∼ jlan/STEREO/Level3/STEREO_Level3_ICME.pdf. The list is continually updated and cover our period completely.

The list of the STs observed by STB has been shown in the table below. We present the start time and end time of the STs, the average magnetic field strength ($< B >$), the average proton beta (β_p), the average Alfvén Mach number ($< M_A >$), the average proton velocity ($< V_p >$), the velocity expansion ($V_{exp} = \frac{V_{front} - V_{end}}{2}$).

Table C.1: STs list from STB Observation

No.	Start	End	B	β_p	M_A	V_p	V_{exp}
2007							
1	2007-03-06/07:18:00	2007-03-06/08:25:00	9.6	0.33	5.3	432	-9.9
2	2007-03-11/10:02:00	2007-03-11/14:02:00	9.0	0.17	4.7	328	-16.2
3	2007-03-13/00:02:00	2007-03-13/01:32:00	10.1	0.2	5.5	603	-3.2
4	2007-03-23/06:32:00	2007-03-23/08:00:00	6.7	0.05	4.5	278	-3.2
5	2007-03-24/22:05:00	2007-03-25/03:22:00	11.7	0.14	5.4	359	-9.8
6	2007-03-25/04:32:00	2007-03-25/09:02:00	10.6	0.25	6.1	358	5.3
7	2007-03-26/00:35:00	2007-03-26/02:05:00	6.4	0.3	5.6	408	-6.8
8	2007-03-31/21:30:00	2007-04-01/01:00:00	7.7	0.23	5.6	338	-31.8
9	2007-04-01/22:00:00	2007-04-01/23:05:00	7.9	0.45	6.6	536	-1.8
10	2007-04-09/03:28:00	2007-04-09/04:20:00	17.6	0.29	5.5	347	1.7
11	2007-04-09/06:30:00	2007-04-09/08:35:00	15.2	0.06	2.1	305	18.4
12	2007-04-09/13:00:00	2007-04-09/14:05:00	9.7	0.34	6.2	447	-2.4
13	2007-04-11/05:17:00	2007-04-11/06:00:00	9.3	0.24	5.8	469	-8.6
14	2007-04-18/21:20:00	2007-04-18/22:32:00	6.9	0.3	6.3	350	10.7
15	2007-04-22/14:02:00	2007-04-22/15:00:00	9.7	0.37	6.6	327	-6.1
16	2007-04-22/17:15:00	2007-04-22/18:10:00	9.7	0.39	6.6	353	-2.9
17	2007-04-22/21:00:00	2007-04-22/22:45:00	9.0	0.52	5.5	411	-16.2
18	2007-04-23/02:10:00	2007-04-23/03:15:00	11.7	0.46	6.1	375	-13.0
19	2007-04-25/07:22:00	2007-04-25/08:30:00	5.7	0.48	6.5	422	-6.3
20	2007-04-26/20:35:00	2007-04-27/05:10:00	5.8	0.35	6.9	430	16.5
21	2007-05-07/22:25:00	2007-05-08/01:35:00	12.8	0.32	4.1	544	-82.0

Table C.1: STs list from STB Observation

No.	Start	End	B	β_p	M_A	V_p	V_{exp}
22	2007-05-17/21:25:00	2007-05-18/04:15:00	9.2	0.13	4.2	317	-1.9
23	2007-05-23/00:45:00	2007-05-23/03:35:00	10.5	0.26	5.7	407	-24.3
24	2007-05-23/22:20:00	2007-05-24/03:15:00	9.8	0.34	6.8	510	-20.4
25	2007-06-01/02:22:00	2007-06-01/05:20:00	6.1	0.35	6.9	324	-6.5
26	2007-06-01/14:30:00	2007-06-01/16:48:00	7.1	0.2	5.5	326	-5.5
27	2007-06-01/17:30:00	2007-06-01/18:45:00	7.5	0.14	4.7	325	6.1
28	2007-06-03/00:25:00	2007-06-03/02:35:00	8.1	0.48	7.0	434	3.5
29	2007-06-03/05:30:00	2007-06-03/10:22:00	6.1	0.48	6.6	383	11.2
30	2007-06-03/11:40:00	2007-06-03/13:48:00	6.1	0.31	6.0	412	-16.9
31	2007-06-08/05:45:00	2007-06-08/15:00:00	7.6	0.17	5.5	337	-9.0
32	2007-06-12/15:22:00	2007-06-12/18:30:00	5.9	0.09	4.3	318	-8.5
33	2007-06-12/19:00:00	2007-06-12/20:00:00	7.2	0.1	3.4	319	-13.6
34	2007-06-12/22:00:00	2007-06-12/23:22:00	6.6	0.22	4.6	319	8.5
35	2007-06-12/23:32:00	2007-06-13/00:32:00	6.1	0.05	4.3	309	4
36	2007-06-13/01:02:00	2007-06-13/03:30:00	5.9	0.03	3.7	304	-2
37	2007-06-28/16:30:00	2007-06-28/23:22:00	6.6	0.48	6.7	375	-14.3
38	2007-06-29/02:50:00	2007-06-29/04:20:00	5.9	0.45	7.2	397	4.8
39	2007-06-29/08:00:00	2007-06-29/08:38:00	6.6	0.41	6.2	369	0.8
40	2007-07-03/07:20:00	2007-07-03/13:38:00	8.0	0.26	5.2	411	-49.8
41	2007-07-10/17:45:00	2007-07-10/21:45:00	16.2	0.22	4.5	393	-40.3
42	2007-07-11/05:28:00	2007-07-11/06:30:00	9.5	0.37	5.5	527	-4.2
43	2007-07-14/02:40:00	2007-07-14/03:45:00	6.4	0.35	7.2	431	5.1
44	2007-07-14/09:35:00	2007-07-14/17:05:00	8.8	0.26	5.3	483	-61.3
45	2007-07-19/23:38:00	2007-07-20/03:28:00	12.1	0.11	4.3	339	-47.5
46	2007-07-26/05:20:00	2007-07-26/08:00:00	9.3	0.28	5.9	320	-8
47	2007-07-26/15:25:00	2007-07-26/16:12:00	10.4	0.57	6.4	433	-17.5
48	2007-07-28/18:16:00	2007-07-28/21:17:00	7.8	0.5	7.0	400	-42.5
49	2007-07-29/11:25:00	2007-07-29/16:30:00	6.6	0.25	6.1	470	24.0
50	2007-08-06/06:40:00	2007-08-06/07:40:00	11.4	0.24	5.2	411	-16.0
51	2007-08-06/09:32:00	2007-08-06/11:15:00	13.5	0.41	6.2	432	-5.7
52	2007-08-06/21:02:00	2007-08-06/22:10:00	9.4	0.39	6.2	598	-6.0
53	2007-08-15/03:15:00	2007-08-15/05:05:00	6.6	0.38	7.0	431	9.9
54	2007-08-24/15:00:00	2007-08-24/16:25:00	9.4	0.41	6.5	342	3.5
55	2007-08-25/07:22:00	2007-08-25/08:48:00	6.7	0.33	7.1	431	-1.5
56	2007-08-25/11:30:00	2007-08-25/15:17:00	8.1	0.35	6.0	422	-1.0
57	2007-08-26/07:40:00	2007-08-26/10:20:00	7.3	0.31	5.1	532	22.8
58	2007-08-26/15:48:00	2007-08-26/18:00:00	8.1	0.44	6.5	597	-69.5
59	2007-08-31/00:45:00	2007-08-31/02:32:00	6.6	0.2	6.1	350	6.9
60	2007-09-01/16:35:00	2007-09-01/18:05:00	8.3	0.33	6.1	578	-6.6
61	2007-09-06/05:25:00	2007-09-06/10:45:00	6.9	0.24	4.8	424	-14.0
62	2007-09-14/00:38:00	2007-09-14/09:25:00	9.3	0.08	4.0	299	-12.4
63	2007-09-19/20:15:00	2007-09-19/21:28:00	14.6	0.4	6.2	401	-3.8

Table C.1: STs list from STB Observation

No.	Start	End	B	β_p	M_A	V_p	V_{exp}
64	2007-09-20/14:35:00	2007-09-20/21:17:00	6.4	0.31	5.4	479	30.9
65	2007-09-27/07:48:00	2007-09-27/08:40:00	6.0	0.42	7.4	506	-1.1
66	2007-09-28/01:32:00	2007-09-28/05:00:00	8.5	0.21	5.0	497	-0.5
67	2007-09-29/04:40:00	2007-09-29/06:32:00	7.0	0.38	5.9	560	3.0
68	2007-10-12/12:10:00	2007-10-12/14:05:00	5.9	0.12	6.4	288	1.4
69	2007-10-12/16:30:00	2007-10-12/19:35:00	6.6	0.12	6.2	292	-1.6
70	2007-10-12/21:10:00	2007-10-12/22:55:00	7.3	0.1	5.5	296	-2.7
71	2007-10-13/04:02:00	2007-10-13/10:10:00	6.7	0.2	6.8	300	-6.6
72	2007-10-13/11:35:00	2007-10-13/17:20:00	6.4	0.19	6.3	301	-16.6
73	2007-10-13/18:38:00	2007-10-13/19:42:00	6.3	0.22	5.4	347	-5.3
74	2007-10-17/02:32:00	2007-10-17/07:15:00	8.0	0.25	6.0	441	-5.2
75	2007-10-24/16:35:00	2007-10-24/17:12:00	7.5	0.33	5.8	373	-1.4
76	2007-11-07/19:10:00	2007-11-07/20:50:00	5.9	0.13	6.7	290	-2.5
77	2007-11-07/21:35:00	2007-11-07/23:05:00	6.0	0.14	6.4	290	-1.0
78	2007-11-09/01:30:00	2007-11-09/05:45:00	7.9	0.11	5.3	306	-1.0
79	2007-11-09/06:00:00	2007-11-09/07:35:00	6.9	0.21	6.7	308	3.0
80	2007-11-09/19:02:00	2007-11-09/20:35:00	7.1	0.18	4.0	332	11.5
81	2007-11-09/23:20:00	2007-11-10/01:18:00	8.1	0.23	5.5	363	-23.3
82	2007-11-10/04:28:00	2007-11-10/05:32:00	6.5	0.45	6.6	351	4.4
83	2007-11-12/01:00:00	2007-11-12/03:16:00	7.9	0.28	6.2	331	-0.4
84	2007-11-12/07:22:00	2007-11-12/10:10:00	9.0	0.15	5.1	327	-6.5
85	2007-11-13/14:00:00	2007-11-13/16:10:00	8.0	0.34	5.1	508	5.9
86	2007-11-19/13:55:00	2007-11-19/15:35:00	8.4	0.36	7.2	343	-3.9
87*	2007-11-19/22:55:00	2007-11-20/02:20:00	16.6	0.1	4.7	446	-13.5
88*	2007-11-20/03:40:00	2007-11-20/11:02:00	10.1	0.31	5.9	463	-11.4
89	2007-11-20/12:00:00	2007-11-20/14:50:00	10.5	0.36	5.2	469	-20.7
90	2007-11-20/20:00:00	2007-11-20/22:05:00	6.9	0.22	6.4	583	-7.7
91	2007-11-23/14:18:00	2007-11-23/16:50:00	6.6	0.35	6.6	420	6.6
92	2007-12-04/04:30:00	2007-12-04/05:25:00	5.7	0.29	6.9	325	-2.0
93	2007-12-08/23:50:00	2007-12-09/04:28:00	7.9	0.17	5.4	304	10.0
94	2007-12-09/08:00:00	2007-12-09/13:55:00	13.7	0.33	4.9	365	-45.0
95	2007-12-25/11:25:00	2007-12-25/12:25:00	9.1	0.13	5.0	366	-0.4
96	2007-12-25/16:28:00	2007-12-25/19:25:00	7.8	0.36	6.3	348	4.2
97	2007-12-26/09:05:00	2007-12-26/11:20:00	6.5	0.37	6.9	346	9.5
2008							
98	2008-01-03/11:00:00	2008-01-03/17:00:00	12.1	0.39	5.2	364	-39.3
99	2008-01-03/18:10:00	2008-01-03/18:55:00	17.1	0.26	4.4	440	-8.3
100	2008-01-03/19:40:00	2008-01-03/21:00:00	14.6	0.57	6.4	530	-16.4
101	2008-01-10/16:00:00	2008-01-10/17:55:00	8.5	0.3	4.8	436	-12.2
102*	2008-02-07/04:40:00	2008-02-07/10:35:00	10.7	0.18	4.8	339	-1.0
103	2008-02-07/10:55:00	2008-02-07/14:32:00	11.2	0.25	3.8	353	2.6
104	2008-02-26/22:45:00	2008-02-27/01:25:00	10.0	0.26	4.4	359	-30.5

Table C.1: STs list from STB Observation

No.	Start	End	B	β_p	M_A	V_p	V_{exp}
105	2008-02-27/04:45:00	2008-02-27/05:42:00	16.9	0.35	5.6	436	-2.0
106*	2008-03-06/12:32:00	2008-03-06/16:25:00	15.4	0.28	4.7	391	5.3
107	2008-03-13/09:12:00	2008-03-13/11:10:00	5.5	0.23	6.0	569	12.6
108	2008-03-15/06:20:00	2008-03-15/07:30:00	5.7	0.35	7.1	565	3.9
109	2008-03-15/19:17:00	2008-03-15/20:05:00	5.6	0.36	7.4	496	3.2
110	2008-04-02/00:18:00	2008-04-02/01:22:00	8.3	0.28	6.1	336	-5.6
111	2008-04-02/21:38:00	2008-04-03/02:15:00	10.6	0.35	4.9	446	-24.1
112	2008-04-12/13:25:00	2008-04-12/15:30:00	5.4	0.27	7.0	525	15.6
113	2008-04-14/22:15:00	2008-04-15/05:20:00	5.9	0.16	5.7	451	-2.7
114	2008-04-15/08:55:00	2008-04-15/11:00:00	8.3	0.44	6.1	444	4.7
115	2008-04-15/12:30:00	2008-04-15/13:25:00	11.3	0.31	5.5	433	3.7
116	2008-04-15/13:55:00	2008-04-15/16:20:00	10.5	0.49	5.9	458	-24.4
117	2008-04-20/20:12:00	2008-04-20/21:38:00	5.9	0.24	6.3	348	-3.5
118	2008-04-21/22:25:00	2008-04-21/23:32:00	7.7	0.31	6.0	387	-0.9
119*	2008-04-29/23:15:00	2008-04-30/06:22:00	8.0	0.41	6.2	456	-12.0
120	2008-05-01/05:32:00	2008-05-01/10:02:00	9.3	0.28	5.7	449	-43.9
121	2008-05-05/04:30:00	2008-05-05/05:30:00	6.2	0.25	6.0	604	7.4
122	2008-05-12/23:35:00	2008-05-13/01:00:00	9.2	0.37	6.2	356	-3.2
123	2008-05-18/12:15:00	2008-05-18/13:17:00	6.3	0.41	7.1	370	-12.3
124	2008-05-27/02:22:00	2008-05-27/03:22:00	6.7	0.18	5.7	344	5.6
125	2008-05-27/05:05:00	2008-05-27/09:25:00	10.9	0.17	6.0	390	2.1
126	2008-05-27/21:17:00	2008-05-27/23:00:00	10.2	0.43	6.5	437	-0.4
127	2008-05-28/22:00:00	2008-05-29/09:00:00	7.2	0.29	5.4	428	-91.7
128	2008-05-29/12:17:00	2008-05-29/14:00:00	6.9	0.24	7.0	548	-16.5
129	2008-05-29/20:02:00	2008-05-29/22:42:00	7.1	0.13	5.4	482	18.7
130	2008-05-29/23:12:00	2008-05-29/23:55:00	6.9	0.15	5.3	462	9.1
131*	2008-06-06/18:15:00	2008-06-06/20:12:00	10.9	0.23	5.6	409	-2.7
132	2008-06-12/20:12:00	2008-06-12/22:20:00	7.9	0.07	4.4	332	-8.3
133	2008-06-13/00:40:00	2008-06-13/02:55:00	11.4	0.11	3.8	358	-22.2
134	2008-06-13/04:00:00	2008-06-13/06:55:00	8.5	0.1	3.6	377	-20.5
135	2008-06-25/05:38:00	2008-06-25/07:42:00	14.3	0.41	4.3	389	-19.9
136	2008-06-25/08:45:00	2008-06-25/12:40:00	9.3	0.42	6.0	399	8.1
137	2008-07-03/15:05:00	2008-07-03/19:17:00	7.2	0.1	3.8	350	-18.5
138	2008-07-09/12:30:00	2008-07-09/19:17:00	6.6	0.13	5.2	301	-9.5
139	2008-07-09/21:02:00	2008-07-09/23:32:00	8.6	0.18	4.0	329	-40.5
140	2008-07-10/23:22:00	2008-07-11/07:38:00	9.9	0.17	5.9	555	-16.0
141	2008-07-29/21:15:00	2008-07-29/22:52:00	5.7	0.13	6.6	328	-4.0
142	2008-07-30/00:30:00	2008-07-30/02:12:00	5.5	0.19	6.7	326	1.6
143	2008-08-04/22:17:00	2008-08-05/03:17:00	6.5	0.11	5.4	315	2.4
144	2008-08-05/05:25:00	2008-08-05/07:25:00	6.5	0.11	5.4	310	3.0
145	2008-08-06/14:12:00	2008-08-06/15:00:00	5.7	0.19	4.8	335	-6.3
146	2008-08-06/18:00:00	2008-08-06/18:58:00	7.0	0.24	6.3	346	6.2

Table C.1: STs list from STB Observation

No.	Start	End	B	β_p	M_A	V_p	V_{exp}
147	2008-08-13/14:38:00	2008-08-13/15:50:00	5.7	0.2	5.9	336	-7.5
148	2008-08-13/17:00:00	2008-08-14/00:40:00	5.6	0.25	6.5	331	0.97
149*	2008-08-15/12:30:00	2008-08-15/21:55:00	8.3	0.19	6.3	347	0.04
150	2008-08-16/00:45:00	2008-08-16/04:00:00	15.3	0.3	5.3	369	-9.3
151	2008-08-16/05:35:00	2008-08-16/06:22:00	14.4	0.27	4.2	399	-10.4
152	2008-08-26/01:20:00	2008-08-26/02:30:00	7.5	0.33	6.0	339	-1.3
153	2008-09-01/10:50:00	2008-09-01/12:12:00	11.3	0.34	4.3	354	-7.1
154	2008-09-01/13:38:00	2008-09-01/16:02:00	8.5	0.47	6.0	420	-11.7
155	2008-09-11/22:17:00	2008-09-11/23:45:00	6.2	0.22	5.7	322	0.5
156	2008-09-12/00:42:00	2008-09-12/02:25:00	6.2	0.41	6.9	328	1.5
157	2008-09-12/02:35:00	2008-09-12/04:20:00	5.7	0.49	7.5	322	8.5
158	2008-09-12/07:17:00	2008-09-12/08:20:00	6.0	0.14	6.3	309	-1.3
159	2008-09-12/15:22:00	2008-09-12/16:35:00	11.3	0.31	5.7	425	-2.3
160	2008-09-12/18:45:00	2008-09-12/20:02:00	11.9	0.25	5.8	457	-32.8
161	2008-09-25/17:25:00	2008-09-26/00:55:00	5.9	0.07	4.4	290	-3.2
162	2008-09-28/03:55:00	2008-09-28/11:35:00	8.2	0.11	4.7	352	1.4
163	2008-09-28/16:20:00	2008-09-28/17:48:00	9.7	0.57	6.5	442	-2.5
164	2008-09-30/14:25:00	2008-09-30/15:48:00	6.2	0.27	6.8	603	12.9
165	2008-10-08/09:45:00	2008-10-08/11:10:00	6.4	0.33	7.1	322	-1.5
166	2008-10-08/21:00:00	2008-10-08/23:30:00	6.7	0.49	6.8	360	-1.3
167	2008-10-09/00:05:00	2008-10-09/01:40:00	6.9	0.38	6.4	343	12.6
168*	2008-10-19/20:55:00	2008-10-20/00:30:00	6.5	0.4	5.7	317	1.9
169*	2008-10-20/07:28:00	2008-10-20/08:45:00	7.8	0.23	5.1	326	-4.6
170*	2008-10-20/09:15:00	2008-10-20/11:25:00	8.6	0.24	5.2	331	-6.9
171	2008-10-20/12:30:00	2008-10-20/15:25:00	8.3	0.35	5.3	347	-6.3
172	2008-10-24/21:32:00	2008-10-24/23:22:00	6.5	0.16	6.2	316	3.4
173	2008-10-25/04:12:00	2008-10-25/10:00:00	6.9	0.11	5.2	304	-1.3
174	2008-10-25/13:00:00	2008-10-25/14:02:00	6.3	0.59	6.4	335	1.5
175	2008-11-11/21:22:00	2008-11-11/22:38:00	7.1	0.34	5.9	341	-8.4
176	2008-11-12/00:22:00	2008-11-12/05:12:00	10.3	0.32	5.1	368	-28.8
177	2008-11-21/22:55:00	2008-11-21/23:45:00	10.1	0.3	6.2	315	0.5
178	2008-11-22/06:15:00	2008-11-22/13:48:00	7.3	0.37	5.6	432	1.9
179	2008-11-22/16:45:00	2008-11-22/17:32:00	8.1	0.26	6.5	414	-2.0
180	2008-11-22/20:28:00	2008-11-22/22:40:00	7.7	0.5	6.4	431	10.1
181	2008-11-30/21:35:00	2008-11-30/23:32:00	10.7	0.29	5.9	350	-6.4
182	2008-12-02/13:20:00	2008-12-02/15:02:00	6.0	0.44	6.7	398	7.3
183	2008-12-02/17:00:00	2008-12-02/18:01:00	6.2	0.38	6.6	421	-2.8
184	2008-12-07/11:58:00	2008-12-07/14:12:00	5.8	0.22	6.8	321	0.5
185	2008-12-08/17:10:00	2008-12-08/20:32:00	14.3	0.21	4.9	344	-16.1
186	2008-12-08/21:28:00	2008-12-08/22:35:00	19.4	0.2	4.0	364	-11.0
187	2008-12-15/04:00:00	2008-12-15/11:17:00	6.9	0.18	5.5	319	-5.0
188	2008-12-16/17:38:00	2008-12-17/03:00:00	6.2	0.11	6.0	324	11

Table C.1: STs list from STB Observation

No.	Start	End	B	β_p	M_A	V_p	V_{exp}
189	2008-12-17/03:50:00	2008-12-17/06:12:00	7.4	0.27	6.0	338	-9.5
190	2008-12-18/18:38:00	2008-12-18/21:20:00	6.8	0.25	5.7	349	12.5
191	2008-12-19/00:30:00	2008-12-19/01:45:00	8.5	0.25	4.5	390	-15.9
192	2008-12-20/06:02:00	2008-12-20/07:30:00	5.7	0.28	4.8	493	-1.5
193	2008-12-28/05:00:00	2008-12-28/05:30:00	9.3	0.3	5.3	415	-0.6
194	2008-12-29/09:22:00	2008-12-29/10:20:00	6.6	0.48	6.8	412	-9.3
2009							
195	2009-01-01/01:17:00	2009-01-01/03:30:00	5.2	0.13	4.9	367	6.6
196	2009-01-02/03:42:00	2009-01-02/07:17:00	5.0	0.27	6.6	394	-0.6
197	2009-01-05/03:25:00	2009-01-05/04:00:00	7.5	0.28	5.7	333	2.6
198	2009-01-05/17:28:00	2009-01-05/19:30:00	9.3	0.36	5.5	430	-2
199	2009-01-08/11:50:00	2009-01-08/13:26:00	5.5	0.21	5.6	333	7.4
200	2009-01-14/10:00:00	2009-01-14/11:28:00	9.6	0.34	6.3	385	-2.2
201	2009-01-19/02:25:00	2009-01-19/10:30:00	6.9	0.15	6.1	341	17.9
202	2009-01-19/19:30:00	2009-01-19/20:28:00	5.6	0.11	5.9	321	-0.4
203	2009-01-23/15:17:00	2009-01-23/16:25:00	12.2	0.17	4.3	312	-4.1
204	2009-01-23/17:00:00	2009-01-23/17:58:00	11.5	0.29	5.4	312	-3.8
205	2009-01-24/14:00:00	2009-01-24/14:58:00	5.7	0.31	5.8	361	8.5
206	2009-01-24/15:12:00	2009-01-24/22:45:00	5.6	0.26	6.1	344	-1
207	2009-01-25/01:25:00	2009-01-25/04:40:00	5.9	0.2	4.9	326	6.1
208	2009-01-25/20:15:00	2009-01-25/22:17:00	8.8	0.19	4.6	342	-1.2
209	2009-01-25/22:50:00	2009-01-25/23:30:00	8.4	0.23	5.1	346	1.3
210	2009-02-01/13:25:00	2009-02-01/20:55:00	5.0	0.1	6.5	288	-2.8
211	2009-02-01/21:48:00	2009-02-02/00:10:00	5.4	0.13	6.8	293	-0.1
212	2009-02-02/00:38:00	2009-02-02/10:42:00	6.8	0.12	5.6	306	-9.9
213	2009-02-02/13:42:00	2009-02-02/19:55:00	5.5	0.12	5.9	289	0.3
214	2009-02-02/22:58:00	2009-02-03/01:00:00	7.7	0.18	5.7	306	-8.0
215	2009-02-10/21:50:00	2009-02-11/02:40:00	14.8	0.21	3.7	425	-88.7
216	2009-02-18/08:48:00	2009-02-18/09:58:00	8.2	0.21	6.2	317	-12.9
217	2009-02-23/22:22:00	2009-02-24/05:22:00	7.4	0.16	4.6	328	-25.6
218	2009-02-24/06:22:00	2009-02-24/07:00:00	7.7	0.24	5.6	347	-9.9
219	2009-03-01/00:30:00	2009-03-01/07:17:00	5.5	0.07	4.5	294	3.6
220	2009-03-09/16:20:00	2009-03-09/17:28:00	6.1	0.14	5.2	307	2.6
221	2009-03-09/20:25:00	2009-03-10/00:48:00	6.1	0.06	4.1	296	-5.8
222	2009-03-14/14:38:00	2009-03-14/16:20:00	8.0	0.18	5.4	310	-3.2
223	2009-03-14/19:58:00	2009-03-14/23:22:00	9.2	0.13	4.5	357	2.4
224	2009-03-15/01:00:00	2009-03-15/09:00:00	6.7	0.25	4.9	372	-18.9
225	2009-03-23/15:00:00	2009-03-23/16:35:00	7.7	0.21	5.8	328	0.4
226	2009-03-23/19:22:00	2009-03-24/03:45:00	6.9	0.17	4.8	345	-36.4
227	2009-03-24/06:30:00	2009-03-24/09:55:00	7.6	0.22	4.4	422	9.0
228	2009-03-31/01:55:00	2009-03-31/02:40:00	9.3	0.24	4.2	352	-3.9
229	2009-03-31/04:00:00	2009-03-31/07:05:00	8.9	0.23	4.6	408	0.8

Table C.1: STs list from STB Observation

No.	Start	End	B	β_p	M_A	V_p	V_{exp}
230	2009-03-31/10:05:00	2009-03-31/13:32:00	8.2	0.37	5.3	402	6.1
231	2009-04-04/11:38:00	2009-04-04/13:25:00	7.1	0.08	3.3	334	-0.5
232	2009-04-04/15:45:00	2009-04-04/16:50:00	8.1	0.19	4.5	356	-4.4
233	2009-04-04/18:10:00	2009-04-04/20:05:00	7.4	0.28	5.4	362	-16.3
234	2009-04-13/06:28:00	2009-04-13/08:28:00	12.7	0.26	5.0	337	-8.9
235	2009-04-21/19:00:00	2009-04-21/23:00:00	5.7	0.25	6.5	438	6.6
236	2009-04-24/15:28:00	2009-04-24/18:58:00	5.7	0.27	5.4	329	0.7
237	2009-04-25/03:12:00	2009-04-25/05:00:00	5.0	0.3	6.3	344	4.4
238	2009-04-27/06:00:00	2009-04-27/13:45:00	6.7	0.12	5.5	306	-3.3
239	2009-04-27/14:40:00	2009-04-27/19:00:00	6.9	0.31	5.5	348	-23.7
240	2009-04-28/01:00:00	2009-04-28/02:28:00	5.3	0.36	6.7	354	-0.3
241	2009-04-28/11:45:00	2009-04-28/15:32:00	5.0	0.24	6.6	353	6.2
242	2009-05-02/07:28:00	2009-05-02/08:30:00	7.4	0.26	5.1	389	3.2
243	2009-05-12/03:42:00	2009-05-12/06:42:00	6.0	0.07	5.1	294	-5.8
244	2009-05-27/07:00:00	2009-05-27/08:00:00	7.8	0.38	5.9	320	-3.5
245	2009-05-27/23:30:00	2009-05-28/05:02:00	6.2	0.21	5.2	338	3.1
246	2009-05-30/23:25:00	2009-05-31/03:17:00	6.5	0.18	5.0	386	-11.5
247	2009-06-05/21:28:00	2009-06-05/23:15:00	11.2	0.13	4.0	321	-16.5
248	2009-06-06/01:50:00	2009-06-06/02:45:00	12.1	0.17	3.8	349	-3.0
249	2009-06-06/12:50:00	2009-06-06/18:12:00	5.7	0.22	4.7	348	23.0
250	2009-06-07/05:35:00	2009-06-07/06:45:00	5.1	0.16	5.8	350	1.5
251*	2009-06-19/01:00:00	2009-06-19/04:30:00	6.8	0.11	5.0	302	-6.5
252*	2009-06-19/07:40:00	2009-06-19/11:10:00	9.9	0.05	4.5	347	-16.5
253	2009-06-21/13:55:00	2009-06-21/16:15:00	7.3	0.02	2.4	310	-0.97
254	2009-06-22/02:12:00	2009-06-22/04:35:00	7.1	0.28	5.4	352	-15.5
255	2009-06-26/11:00:00	2009-06-26/12:25:00	9.3	0.16	3.8	359	-7.8
256	2009-06-26/13:00:00	2009-06-26/15:58:00	9.1	0.13	3.2	358	11.5
257	2009-06-28/03:17:00	2009-06-28/05:00:00	8.4	0.04	2.9	354	22.5
258	2009-07-03/18:28:00	2009-07-03/22:32:00	6.0	0.3	6.0	321	3.0
259	2009-07-05/08:30:00	2009-07-05/10:00:00	5.3	0.24	5.8	327	2.0
260	2009-07-05/10:30:00	2009-07-05/20:28:00	5.9	0.07	3.6	319	13.3
261	2009-07-07/11:00:00	2009-07-07/12:00:00	5.4	0.14	6.0	301	-1.3
262	2009-07-07/14:42:00	2009-07-07/16:30:00	5.4	0.12	6.1	295	-1.8
263	2009-07-07/17:02:00	2009-07-07/18:45:00	5.8	0.1	5.3	294	0.7
264	2009-07-07/21:12:00	2009-07-08/01:02:00	7.8	0.09	3.3	346	-22.1
265	2009-07-10/04:02:00	2009-07-10/05:02:00	9.7	0.08	3.0	354	-23.6
266	2009-07-10/07:00:00	2009-07-10/10:58:00	6.5	0.3	5.3	409	-20.3
267	2009-07-17/21:58:00	2009-07-18/01:20:00	6.2	0.27	5.2	349	3.1
268	2009-07-18/13:17:00	2009-07-18/16:32:00	15.1	0.19	4.0	402	-14.0
269	2009-07-18/17:28:00	2009-07-18/18:45:00	17.5	0.13	4.3	438	-12.8
270	2009-07-30/18:10:00	2009-07-30/22:00:00	9.1	0.17	3.6	371	-1.4
271*	2009-07-31/02:20:00	2009-07-31/10:32:00	9.2	0.05	3.7	383	44.4

Table C.1: STs list from STB Observation

No.	Start	End	B	β_p	M_A	V_p	V_{exp}
272	2009-08-02/16:45:00	2009-08-02/21:35:00	5.1	0.03	2.8	327	-1.5
273	2009-08-03/12:22:00	2009-08-03/15:00:00	5.6	0.23	6.6	410	0.1
274	2009-08-13/20:00:00	2009-08-13/21:48:00	6.7	0.1	5.2	297	0.2
275	2009-08-13/23:25:00	2009-08-14/00:30:00	7.4	0.13	5.2	300	-15.8
276	2009-08-14/01:00:00	2009-08-14/03:58:00	10.0	0.12	4.9	314	-6.4
277	2009-08-14/04:38:00	2009-08-14/08:35:00	11.1	0.05	4.2	339	-2.4
278	2009-08-14/14:30:00	2009-08-14/23:48:00	6.8	0.27	4.8	363	-4.7
279	2009-08-15/02:58:00	2009-08-15/10:58:00	6.3	0.18	4.3	389	-66.0
280	2009-08-20/15:58:00	2009-08-20/17:45:00	5.4	0.19	4.4	399	-12.8
281	2009-09-06/21:18:00	2009-09-07/02:40:00	6.4	0.07	5.3	297	4.3
282	2009-09-07/05:30:00	2009-09-07/07:48:00	5.2	0.11	5.2	291	1.8
283*	2009-09-09/17:35:00	2009-09-09/21:45:00	6.5	0.07	4.3	312	1.1
284*	2009-09-09/22:30:00	2009-09-10/02:00:00	6.7	0.1	4.3	312	-3.3
285	2009-09-12/10:22:00	2009-09-12/11:32:00	11.6	0.21	3.9	405	-11.2
286	2009-09-23/01:00:00	2009-09-23/03:12:00	5.2	0.1	6.4	289	0.07
287	2009-09-24/06:40:00	2009-09-24/08:10:00	8.1	0.14	4.4	343	-2.4
288*	2009-09-28/03:12:00	2009-09-28/11:38:00	6.1	0.05	3.3	315	-5.2
289*	2009-10-02/17:12:00	2009-10-02/18:32:00	8.9	0.08	4.7	290	-3.4
290	2009-10-06/18:28:00	2009-10-07/00:28:00	12.9	0.1	3.0	345	-22.6
291	2009-10-19/09:48:00	2009-10-19/10:58:00	6.2	0.14	5.0	312	-7.4
292	2009-10-21/12:33:00	2009-10-21/13:58:00	5.8	0.15	5.5	303	2.0
293	2009-10-21/17:22:00	2009-10-21/19:55:00	6.0	0.19	4.6	348	-11.6
294	2009-10-26/18:45:00	2009-10-26/22:22:00	7.7	0.22	4.4	324	11.0
295	2009-10-29/20:30:00	2009-10-30/02:55:00	5.4	0.27	5.8	325	2.2
296	2009-10-30/05:12:00	2009-10-30/11:00:00	5.3	0.18	5.3	313	3.5
297	2009-11-03/08:00:00	2009-11-03/09:22:00	7.9	0.16	5.4	320	4.1
298	2009-11-03/09:38:00	2009-11-03/11:00:00	7.7	0.15	4.0	345	-15.4
299	2009-11-04/20:15:00	2009-11-05/00:50:00	4.9	0.18	5.2	404	4.3
300	2009-11-08/20:00:00	2009-11-08/21:40:00	5.6	0.09	5.0	297	5.0
301	2009-11-10/14:45:00	2009-11-10/17:28:00	6.1	0.21	5.4	341	17.0
302	2009-11-11/20:30:00	2009-11-11/21:25:00	7.7	0.25	4.3	374	-17.0
303	2009-11-12/15:28:00	2009-11-12/16:30:00	5.7	0.23	5.4	365	-0.9
304	2009-11-15/05:28:00	2009-11-15/09:50:00	8.0	0.13	4.0	379	6.4
305	2009-11-23/12:45:00	2009-11-23/14:05:00	5.2	0.05	3.3	309	-0.5
306*	2009-11-27/12:38:00	2009-11-27/20:32:00	9.9	0.1	4.3	319	-7.5
307	2009-11-27/20:50:00	2009-11-27/21:48:00	8.8	0.24	6.0	326	-4.0
308	2009-12-08/19:55:00	2009-12-09/05:12:00	7.1	0.04	3.6	306	-0.5
309	2009-12-09/12:48:00	2009-12-09/19:20:00	7.3	0.18	3.8	381	-68.5
310	2009-12-12/12:28:00	2009-12-12/16:42:00	5.3	0.13	4.1	343	3.5
311	2009-12-12/20:12:00	2009-12-13/00:50:00	6.6	0.22	5.3	355	-9.1
312	2009-12-20/19:05:00	2009-12-20/21:45:00	7.2	0.09	4.2	288	-1.0
313	2009-12-20/22:00:00	2009-12-20/23:30:00	6.8	0.16	4.8	296	-6.6

Table C.1: STs list from STB Observation

No.	Start	End	B	β_p	M_A	V_p	V_{exp}
314	2009-12-21/00:35:00	2009-12-21/03:45:00	8.1	0.2	4.3	335	-11.0
315	2009-12-21/04:00:00	2009-12-21/07:25:00	6.5	0.26	5.3	355	-5.9
316	2009-12-25/00:45:00	2009-12-25/04:30:00	5.1	0.2	5.6	320	-3.0
317*	2009-12-29/17:50:00	2009-12-30/01:45:00	8.5	0.1	4.2	314	-11.9
318*	2009-12-30/02:02:00	2009-12-30/09:15:00	10.3	0.04	2.8	303	9.5
2010							
319	2010-01-01/05:22:00	2010-01-01/06:02:00	7.3	0.15	4.4	342	-14.5
320	2010-01-01/12:35:00	2010-01-01/15:50:00	6.3	0.28	4.9	355	-0.7
321	2010-01-06/07:00:00	2010-01-06/09:35:00	15.2	0.21	3.7	371	-23.5
322	2010-01-14/13:58:00	2010-01-14/17:30:00	6.4	0.14	3.7	350	-1.3
323	2010-01-24/22:00:00	2010-01-25/00:25:00	8.7	0.1	3.9	310	-0.4
324	2010-01-25/02:30:00	2010-01-25/03:22:00	8.0	0.26	5.2	380	-28.4
325	2010-01-28/00:16:00	2010-01-28/01:50:00	6.6	0.18	4.6	332	-2.7
326	2010-01-31/01:58:00	2010-01-31/04:35:00	8.1	0.13	3.6	368	-12.4
327	2010-01-31/23:20:00	2010-02-01/01:40:00	8.2	0.06	2.9	428	-19.3
328	2010-02-01/04:00:00	2010-02-01/07:45:00	9.4	0.22	4.0	468	-48.2
329	2010-02-16/00:25:00	2010-02-16/02:05:00	5.9	0.26	4.8	437	-8.3
330	2010-02-24/06:10:00	2010-02-24/06:50:00	8.1	0.06	4.8	291	-0.7
331	2010-02-24/12:23:00	2010-02-24/13:15:00	9.5	0.1	4.9	300	-8.2
332	2010-02-24/14:30:00	2010-02-24/18:28:00	8.5	0.1	4.2	308	0.3
333	2010-02-24/18:38:00	2010-02-25/06:00:00	7.7	0.12	3.7	326	-32.3
334	2010-03-02/17:00:00	2010-03-02/21:00:00	8.3	0.19	4.0	493	-5.3
335	2010-03-04/10:20:00	2010-03-04/12:00:00	6.1	0.2	4.0	522	15.0
336	2010-03-05/02:12:00	2010-03-05/06:30:00	7.8	0.09	4.2	506	7.5
337	2010-03-07/08:02:00	2010-03-07/10:35:00	5.9	0.17	4.2	414	4.1
338	2010-03-07/12:00:00	2010-03-07/14:00:00	5.9	0.24	5.1	435	6.3
339	2010-03-19/14:15:00	2010-03-19/15:02:00	12.4	0.07	4.0	298	0.2
340	2010-03-19/20:15:00	2010-03-19/22:28:00	14.1	0.17	3.3	359	-11.6
341	2010-03-24/11:30:00	2010-03-24/13:42:00	6.2	0.1	4.7	314	14.2
342	2010-04-01/20:28:00	2010-04-01/22:05:00	9.9	0.3	4.7	520	-2.7
343	2010-04-08/08:35:00	2010-04-08/09:20:00	7.1	0.1	3.8	300	-1.9
344	2010-04-08/19:28:00	2010-04-08/23:22:00	8.1	0.13	3.8	365	-38.7
345	2010-04-10/09:50:00	2010-04-10/11:10:00	6.1	0.03	3.1	309	-0.9
346	2010-04-13/02:32:00	2010-04-13/04:28:00	8.6	0.18	4.5	357	1.3
347	2010-04-16/12:28:00	2010-04-16/14:27:00	7.7	0.14	5.1	414	4.8
348	2010-04-18/02:00:00	2010-04-18/03:00:00	6.1	0.2	5.1	366	8
349	2010-04-18/09:32:00	2010-04-18/10:18:00	6.5	0.22	4.3	383	14.4
350	2010-04-18/11:02:00	2010-04-18/22:00:00	6.8	0.13	3.8	356	3.7
351	2010-04-21/10:50:00	2010-04-21/14:28:00	7.4	0.15	3.9	431	-61.3
352	2010-04-27/12:00:00	2010-04-27/14:48:00	9.4	0.09	4.4	298	-19.5
353	2010-05-05/23:12:00	2010-05-06/00:40:00	11.5	0.15	4.9	352	-4.3
354	2010-05-06/01:30:00	2010-05-06/03:35:00	13.4	0.27	5.2	375	-18.7

Table C.1: STs list from STB Observation

No.	Start	End	B	β_p	M_A	V_p	V_{exp}
355	2010-05-06/09:22:00	2010-05-06/13:45:00	9.7	0.23	5.0	438	-17.2
356	2010-05-20/18:40:00	2010-05-20/19:22:00	6.4	0.29	5.9	331	-3.6
357*	2010-06-07/22:28:00	2010-06-08/05:00:00	10.2	0.13	5.6	379	17.5
358	2010-06-11/15:00:00	2010-06-11/16:40:00	12.5	0.1	3.9	437	9.97
359	2010-06-21/08:00:00	2010-06-21/09:00:00	7.7	0.11	5.5	295	0.9
360	2010-06-21/11:00:00	2010-06-21/13:30:00	14.1	0.21	4.5	318	0.7
361	2010-06-21/17:38:00	2010-06-21/18:45:00	12.8	0.2	4.2	347	4.8
362	2010-06-21/20:00:00	2010-06-21/22:48:00	13.6	0.16	2.5	416	-20.2
363	2010-07-08/17:45:00	2010-07-08/19:23:00	10.7	0.19	5.0	310	-8.0
364	2010-07-22/07:10:00	2010-07-22/15:15:00	7.9	0.08	4.1	388	15.5
365	2010-08-02/19:55:00	2010-08-02/23:20:00	14.3	0.28	4.9	453	-4.1
366	2010-08-03/01:20:00	2010-08-03/02:35:00	12.3	0.13	3.9	426	4.1
367*	2010-08-03/04:12:00	2010-08-03/08:45:00	26.4	0.05	2.2	590	-99.6
368	2010-09-01/08:12:00	2010-09-01/12:22:00	8.9	0.16	3.7	339	-19.2
369	2010-09-08/02:22:00	2010-09-08/08:30:00	7.1	0.24	5.5	359	9
370	2010-09-08/13:12:00	2010-09-08/16:00:00	7.5	0.1	4.6	350	8.8
371	2010-09-15/09:50:00	2010-09-15/11:22:00	6.6	0.13	5.8	297	-2.5
372	2010-09-30/05:02:00	2010-09-30/06:38:00	7.7	0.11	4.9	299	1.6
373	2010-09-30/09:45:00	2010-09-30/10:48:00	7.8	0.12	4.0	314	-0.3
374	2010-09-30/11:40:00	2010-09-30/12:28:00	7.7	0.23	4.4	332	-5.5
375	2010-10-07/06:30:00	2010-10-07/11:00:00	7.4	0.09	5.1	325	2.6
376	2010-10-07/11:38:00	2010-10-07/13:23:00	7.5	0.12	3.9	321	-8.4
377	2010-10-13/03:05:00	2010-10-13/08:30:00	7.7	0.3	4.9	388	-18.2
378	2010-10-15/13:28:00	2010-10-15/16:30:00	6.9	0.24	5.2	403	4.1
379	2010-10-17/04:12:00	2010-10-17/10:12:00	11.0	0.24	4.2	499	-11.5
380	2010-11-14/19:00:00	2010-11-14/21:35:00	6.3	0.26	5.0	457	6.5
381*	2010-11-20/01:40:00	2010-11-20/03:00:00	8.2	0.21	4.6	438	12.6
382	2010-11-22/06:02:00	2010-11-22/08:45:00	6.2	0.18	5.8	361	-4.3
383	2010-11-22/23:45:00	2010-11-23/01:20:00	10.2	0.24	4.2	403	-3.0
384	2010-11-30/03:38:00	2010-11-30/04:55:00	6.4	0.09	5.6	292	-0.4
385	2010-11-30/08:15:00	2010-11-30/10:20:00	9.2	0.08	4.5	302	7.9
386*	2010-12-03/09:50:00	2010-12-03/11:05:00	6.5	0.17	4.6	347	0.5
387	2010-12-04/02:38:00	2010-12-04/04:05:00	9.3	0.27	5.2	403	1.6
388	2010-12-04/19:40:00	2010-12-04/21:48:00	8.2	0.19	5.2	512	-16.6
389	2010-12-12/22:00:00	2010-12-12/23:38:00	8.3	0.27	5.5	474	-0.95
390	2010-12-20/09:22:00	2010-12-20/20:30:00	6.1	0.21	4.5	334	4.9
391	2010-12-27/10:38:00	2010-12-27/12:50:00	9.5	0.09	3.5	307	0.005
392	2010-12-29/13:15:00	2010-12-29/14:00:00	11.3	0.31	5.0	344	-0.005
393	2010-12-29/23:00:00	2010-12-29/23:40:00	10.1	0.09	4.1	395	-5.0
2011							
394	2011-01-07/00:32:00	2011-01-07/01:15:00	7.2	0.11	3.2	359	2.6
395*	2011-01-18/00:35:00	2011-01-18/02:42:00	8.6	0.14	4.8	354	-0.4

Table C.1: STs list from STB Observation

No.	Start	End	B	β_p	M_A	V_p	V_{exp}
396*	2011-01-18/12:45:00	2011-01-18/23:12:00	7.3	0.06	2.7	323	-5.7
397	2011-01-19/03:05:00	2011-01-19/05:15:00	7.2	0.12	3.8	325	-5.9
398	2011-01-22/21:45:00	2011-01-22/23:00:00	7.8	0.06	3.6	298	-0.5
399	2011-01-25/02:30:00	2011-01-25/05:45:00	8.6	0.18	5.1	354	2.6
400	2011-02-02/19:00:00	2011-02-02/20:40:00	7.8	0.19	3.7	419	2.8
401	2011-02-17/11:38:00	2011-02-17/13:30:00	11.2	0.04	3.1	346	-8.1
402	2011-02-17/13:58:00	2011-02-17/15:16:00	10.7	0.12	3.9	362	-16.3
403	2011-02-17/20:00:00	2011-02-17/21:00:00	12.5	0.06	3.4	357	-2.9
404*	2011-03-07/20:08:00	2011-03-07/22:45:00	16.8	0.07	3.3	417	2.1
405*	2011-03-08/02:12:00	2011-03-08/05:02:00	13.8	0.05	3.1	430	4.3
406*	2011-03-12/06:30:00	2011-03-12/11:40:00	8.4	0.05	3.2	390	16.0
407	2011-03-12/15:05:00	2011-03-12/18:00:00	6.9	0.16	4.4	384	12.5
408	2011-03-16/17:25:00	2011-03-16/20:10:00	7.2	0.18	4.5	393	-27.4
409	2011-03-17/02:25:00	2011-03-17/04:38:00	8.5	0.15	4.8	416	-10.6
410	2011-03-23/15:40:00	2011-03-23/17:50:00	8.1	0.09	3.6	448	-16.1
411	2011-03-23/20:00:00	2011-03-23/22:22:00	14.5	0.13	3.9	511	-4.8
412	2011-03-23/23:00:00	2011-03-24/01:00:00	13.5	0.09	2.9	600	-25.1
413*	2011-03-28/18:30:00	2011-03-28/22:12:00	12.7	0.01	2.9	649	16.0
414*	2011-04-01/03:00:00	2011-04-01/11:30:00	18.4	0.27	4.5	531	25.8
415	2011-04-10/15:23:00	2011-04-10/20:00:00	11.4	0.17	4.0	339	-9.6
416	2011-04-11/15:17:00	2011-04-11/20:00:00	8.6	0.16	5.4	409	-6.9
417	2011-04-13/00:28:00	2011-04-13/03:45:00	6.8	0.12	4.3	347	-5.6
418	2011-04-13/04:50:00	2011-04-13/06:00:00	7.0	0.2	4.5	367	7.9
419	2011-04-13/07:00:00	2011-04-13/09:48:00	7.9	0.22	4.4	377	-27.3
420	2011-04-13/17:15:00	2011-04-13/20:30:00	9.1	0.18	5.0	447	-3.2
421	2011-04-20/19:02:00	2011-04-20/20:45:00	7.1	0.05	2.3	375	15.6
422	2011-04-23/09:00:00	2011-04-23/11:40:00	8.3	0.17	4.8	356	8.8
423	2011-04-23/12:15:00	2011-04-23/16:05:00	11.4	0.23	4.4	392	-24.6
424*	2011-05-04/21:35:00	2011-05-05/08:25:00	13.9	0.13	4.0	392	-6.1
425	2011-05-07/20:02:00	2011-05-08/01:38:00	7.1	0.12	3.6	414	20.1
426	2011-05-08/22:52:00	2011-05-09/00:12:00	7.6	0.23	5.5	549	-0.3
427	2011-05-18/12:52:00	2011-05-18/23:15:00	7.9	0.1	4.6	335	-0.1
428	2011-05-19/08:00:00	2011-05-19/11:58:00	8.0	0.24	4.1	344	-5.9
429	2011-05-19/23:25:00	2011-05-20/02:40:00	8.3	0.17	4.5	331	9.9
430	2011-05-20/05:38:00	2011-05-20/13:05:00	9.8	0.12	3.2	328	-0.2
431	2011-05-31/05:16:00	2011-05-31/08:00:00	6.7	0.21	5.4	303	-7.3
432	2011-06-05/07:15:00	2011-06-05/12:12:00	10.0	0.15	3.6	421	-29.3
433	2011-06-06/03:38:00	2011-06-06/14:42:00	7.0	0.25	4.1	490	15.6
434	2011-06-06/15:40:00	2011-06-06/17:02:00	7.7	0.23	3.7	483	19.3
435	2011-06-10/12:20:00	2011-06-10/17:02:00	7.3	0.07	1.9	376	17.8
436	2011-06-15/16:02:00	2011-06-15/17:35:00	6.8	0.18	4.9	366	-0.8
437	2011-06-15/21:00:00	2011-06-15/23:00:00	9.6	0.21	5.1	427	-5.1

Table C.1: STs list from STB Observation

No.	Start	End	B	β_p	M_A	V_p	V_{exp}
438	2011-06-25/12:28:00	2011-06-25/23:20:00	7.6	0.06	4.3	305	-5.3
439*	2011-06-26/18:15:00	2011-06-26/23:15:00	13.3	0.12	3.9	394	-18.7
440*	2011-06-30/13:22:00	2011-07-01/00:12:00	8.2	0.09	4.6	356	-0.9
441	2011-07-01/00:25:00	2011-07-01/01:12:00	9.2	0.1	3.5	344	0.2
442	2011-07-01/06:00:00	2011-07-01/10:12:00	7.7	0.21	4.7	346	0.6
443	2011-07-02/04:38:00	2011-07-02/08:02:00	6.6	0.13	3.6	380	-20.9
444	2011-07-07/18:25:00	2011-07-07/22:38:00	6.9	0.2	5.4	414	7.5
445	2011-07-07/23:48:00	2011-07-08/01:38:00	7.3	0.16	5.2	421	-2.9
446	2011-07-12/21:58:00	2011-07-13/00:32:00	8.3	0.26	4.1	420	-6.0
447	2011-07-20/01:05:00	2011-07-20/02:50:00	10.9	0.19	4.0	331	-5.8
448*	2011-07-23/07:30:00	2011-07-23/11:28:00	7.5	0.03	3.6	286	3.6
449	2011-07-23/13:50:00	2011-07-23/16:30:00	8.2	0.04	4.2	290	1.6
450	2011-07-23/18:30:00	2011-07-23/23:30:00	10.9	0.1	4.5	306	-14.2
451	2011-07-25/15:00:00	2011-07-25/21:00:00	7.9	0.08	4.0	454	9.4
452	2011-07-26/20:35:00	2011-07-26/21:35:00	7.8	0.24	4.7	367	11.1
453	2011-08-09/05:42:00	2011-08-09/10:15:00	22.3	0.25	3.3	408	-44.2
454	2011-08-27/08:40:00	2011-08-27/09:55:00	17.3	0.14	4.2	354	-4.6
455	2011-09-04/23:22:00	2011-09-05/02:12:00	9.7	0.14	3.9	342	-24.7
456	2011-09-10/10:40:00	2011-09-10/16:25:00	6.7	0.09	5.1	374	-6.9
457	2011-09-17/19:02:00	2011-09-18/02:15:00	7.0	0.09	3.7	339	14.6
458	2011-10-03/17:00:00	2011-10-03/19:15:00	9.7	0.17	4.1	344	-6.8
459*	2011-10-04/02:55:00	2011-10-04/11:25:00	21.8	0.01	2.0	682	9.9
460*	2011-10-18/20:22:00	2011-10-19/03:00:00	15.6	0.11	4.1	398	15.3
461*	2011-10-19/04:25:00	2011-10-19/07:45:00	13.1	0.14	4.2	366	5.1
462	2011-10-19/13:50:00	2011-10-19/18:30:00	12.1	0.13	3.1	394	-2.2
463	2011-10-28/21:30:00	2011-10-29/04:12:00	7.8	0.09	3.3	327	-18.6
464	2011-11-02/22:10:00	2011-11-03/00:55:00	7.9	0.15	4.6	360	9.2
465	2011-11-04/20:00:00	2011-11-04/23:20:00	7.5	0.07	3.4	340	-4.6
466	2011-11-04/23:45:00	2011-11-05/02:15:00	7.7	0.13	3.8	349	-3.7
467	2011-11-18/07:10:00	2011-11-18/09:20:00	7.5	0.25	5.7	324	3.3
468	2011-11-20/00:45:00	2011-11-20/09:35:00	7.5	0.11	4.2	312	-5.1
469	2011-12-12/03:15:00	2011-12-12/13:35:00	9.7	0.13	3.9	315	13.8
470	2011-12-12/18:12:00	2011-12-12/21:55:00	13.5	0.14	2.7	342	-31.9
471	2011-12-19/12:02:00	2011-12-19/14:30:00	7.4	0.02	2.9	276	3.0
472	2011-12-26/06:10:00	2011-12-26/07:42:00	6.6	0.07	5.3	291	-1.1
473	2011-12-26/14:10:00	2011-12-26/15:28:00	6.8	0.05	3.7	295	-2.6
474*	2011-12-27/23:38:00	2011-12-28/06:00:00	14.5	0.09	3.6	369	-12.8
475	2011-12-28/23:40:00	2011-12-29/03:15:00	7.2	0.12	3.8	403	0.6
476	2011-12-29/06:12:00	2011-12-29/09:25:00	7.2	0.26	4.9	386	7.7
2012							
477	2012-01-06/12:17:00	2012-01-06/17:40:00	10.2	0.07	4.4	298	-1.5
478	2012-01-07/05:00:00	2012-01-07/07:28:00	9.0	0.14	4.8	302	-5.8

Table C.1: STs list from STB Observation

No.	Start	End	B	β_p	M_A	V_p	V_{exp}
479	2012-01-07/19:32:00	2012-01-08/01:45:00	10.1	0.11	3.7	350	-5.8
480*	2012-01-10/14:38:00	2012-01-10/15:42:00	11.0	0.24	5.1	436	-13.2
481*	2012-01-11/08:45:00	2012-01-11/11:22:00	8.8	0.08	4.4	463	-17.7
482*	2012-01-19/02:22:00	2012-01-19/05:02:00	15.3	0.06	3.7	451	-12.6
483	2012-01-24/13:30:00	2012-01-24/16:00:00	7.9	0.09	4.3	319	-6.7
484	2012-01-25/04:15:00	2012-01-25/05:00:00	8.8	0.13	4.2	314	0.05
485	2012-01-25/07:38:00	2012-01-25/10:02:00	8.6	0.25	4.6	333	-9.9
486	2012-01-25/11:20:00	2012-01-25/14:00:00	8.7	0.27	4.8	348	6.5
487	2012-01-25/15:00:00	2012-01-25/17:35:00	8.8	0.2	4.1	359	-11.6
488	2012-02-03/14:23:00	2012-02-03/15:23:00	9.6	0.31	4.2	444	-49.7
489	2012-02-10/09:28:00	2012-02-10/17:25:00	12.2	0.11	2.6	424	-0.1
490	2012-02-20/21:17:00	2012-02-20/23:30:00	11.9	0.14	4.4	306	-6.2
491	2012-02-21/20:22:00	2012-02-21/22:48:00	10.9	0.13	3.3	356	-1.6
492	2012-02-22/01:22:00	2012-02-22/05:15:00	10.8	0.15	3.7	409	4.8
493	2012-02-29/20:12:00	2012-03-01/02:05:00	9.6	0.12	4.1	312	1.1
494	2012-03-05/01:02:00	2012-03-05/04:05:00	8.9	0.19	4.2	344	6.3
495*	2012-03-12/10:25:00	2012-03-12/18:50:00	8.3	0.08	4.8	480	22.2
496	2012-03-23/05:25:00	2012-03-23/13:35:00	8.1	0.11	4.1	354	-10.1
497*	2012-03-28/23:17:00	2012-03-29/01:42:00	31.3	0.08	2.9	637	-14.4
498	2012-04-13/17:12:00	2012-04-13/18:22:00	7.6	0.1	4.3	313	1.4
499	2012-04-13/18:55:00	2012-04-13/20:00:00	7.5	0.05	3.6	304	-1.8
500	2012-04-19/05:22:00	2012-04-19/09:55:00	8.9	0.09	2.8	501	3.9
501	2012-04-20/06:00:00	2012-04-20/08:35:00	7.8	0.18	4.4	487	12.1
502	2012-04-21/16:30:00	2012-04-21/18:00:00	8.2	0.14	4.5	406	-0.4
503	2012-04-21/18:32:00	2012-04-21/23:40:00	10.0	0.12	4.2	404	-16.5
504	2012-04-28/10:00:00	2012-04-28/11:50:00	6.9	0.1	4.5	309	-2.8
505	2012-04-30/09:42:00	2012-04-30/20:40:00	10.3	0.16	4.5	354	-55.1
506	2012-05-07/04:20:00	2012-05-07/07:17:00	10.4	0.19	4.6	365	0.8
507	2012-05-07/08:22:00	2012-05-07/10:20:00	10.3	0.13	4.3	355	2.6
508	2012-05-07/12:22:00	2012-05-07/17:12:00	11.1	0.1	3.6	350	7.7
509	2012-05-19/11:00:00	2012-05-19/12:15:00	10.6	0.18	4.4	371	-20.9
510	2012-05-19/13:40:00	2012-05-19/19:30:00	9.0	0.24	4.3	396	10.1
511	2012-05-20/19:25:00	2012-05-21/05:22:00	8.7	0.12	3.2	433	7.4
512	2012-06-05/15:00:00	2012-06-05/20:45:00	6.8	0.03	3.6	298	-0.09
513	2012-06-08/20:58:00	2012-06-09/02:02:00	7.9	0.13	3.5	410	-30.8
514	2012-06-12/19:20:00	2012-06-12/21:55:00	8.5	0.09	5.3	423	-5.1
515	2012-06-14/05:48:00	2012-06-14/08:27:00	9.9	0.08	4.2	420	14.2
516	2012-06-20/18:28:00	2012-06-21/00:18:00	11.5	0.13	4.2	455	5.5
517	2012-06-27/02:10:00	2012-06-27/03:35:00	10.5	0.14	4.8	479	2.7
518*	2012-07-24/15:48:00	2012-07-24/19:35:00	8.6	0.07	3.4	346	11.2
519	2012-07-25/15:55:00	2012-07-25/19:25:00	11.9	0.06	3.2	353	1.0
520*	2012-07-28/17:12:00	2012-07-29/00:45:00	10.1	0.14	4.7	420	-6.3

Table C.1: STs list from STB Observation

No.	Start	End	B	β_p	M_A	V_p	V_{exp}
521	2012-08-05/00:28:00	2012-08-05/03:48:00	6.9	0.11	3.8	359	-2.1
522	2012-08-24/19:22:00	2012-08-24/20:38:00	17.5	0.06	3.3	401	-34.0
523*	2012-08-24/22:25:00	2012-08-25/02:23:00	16.2	0.07	3.1	349	37.4
524	2012-08-28/07:02:00	2012-08-28/10:28:00	8.3	0.15	4.0	344	2.2
525	2012-09-08/00:45:00	2012-09-08/02:05:00	7.6	0.18	5.3	455	11.2
526	2012-09-11/13:40:00	2012-09-11/15:02:00	11.1	0.11	3.8	404	-10.8
527	2012-09-19/13:25:00	2012-09-19/15:22:00	7.7	0.14	4.3	314	-9.9
528*	2012-09-23/11:42:00	2012-09-23/13:28:00	27.2	0.21	4.5	432	23.8
529*	2012-09-24/00:10:00	2012-09-24/09:45:00	12.0	0.12	3.8	383	-5.3
530	2012-09-24/10:15:00	2012-09-24/12:30:00	9.2	0.3	4.7	380	2.8
531	2012-10-09/02:05:00	2012-10-09/03:17:00	9.2	0.1	4.0	342	5.3
532	2012-10-09/06:20:00	2012-10-09/08:25:00	11.3	0.2	5.2	398	-1.5
533*	2012-10-18/01:00:00	2012-10-18/03:35:00	8.5	0.08	3.8	305	3.0
534*	2012-10-25/21:02:00	2012-10-25/23:22:00	17.4	0.12	3.1	345	-25.2
535	2012-11-09/01:38:00	2012-11-09/04:00:00	6.9	0.02	3.3	282	0.6
536	2012-11-09/09:25:00	2012-11-09/12:20:00	9.3	0.05	3.9	290	-9.5
537*	2012-11-19/17:28:00	2012-11-19/23:25:00	19.0	0.11	3.5	409	8.8
538*	2012-11-20/02:00:00	2012-11-20/12:32:00	16.1	0.04	2.9	377	26.6
539	2012-11-30/16:50:00	2012-11-30/20:15:00	7.4	0.29	5.0	349	-6.7
540	2012-11-30/22:58:00	2012-12-01/04:15:00	7.3	0.15	4.2	391	-42.6
541	2012-12-04/06:40:00	2012-12-04/11:10:00	7.2	0.11	3.8	354	-1.9
542	2012-12-16/21:15:00	2012-12-16/23:12:00	7.7	0.08	3.7	344	-3.2
543*	2012-12-25/07:17:00	2012-12-25/08:22:00	13.3	0.21	4.6	390	-0.99
544*	2012-12-25/12:02:00	2012-12-25/13:50:00	11.2	0.15	3.6	353	-1.1
2013							
545	2013-01-15/21:35:00	2013-01-16/07:12:00	8.4	0.05	3.1	352	6.3
546	2013-01-23/08:02:00	2013-01-23/11:40:00	9.7	0.1	4.4	301	5.3
547	2013-01-23/13:12:00	2013-01-23/14:30:00	11.3	0.09	2.8	335	-9.9
548	2013-01-24/21:25:00	2013-01-25/01:38:00	10.4	0.15	4.4	397	14.4
549	2013-02-14/17:45:00	2013-02-14/20:02:00	7.0	0.04	3.1	309	9.4
550	2013-02-19/19:35:00	2013-02-20/00:35:00	7.4	0.09	4.8	413	-22.3
551	2013-02-23/12:02:00	2013-02-23/13:02:00	10.2	0.21	3.2	387	3.8
552	2013-02-25/15:35:00	2013-02-25/19:45:00	6.6	0.07	2.3	419	4.8
553	2013-03-05/20:32:00	2013-03-05/23:42:00	7.4	0.04	3.3	287	2.4
554	2013-04-24/14:00:00	2013-04-24/15:17:00	6.4	0.13	3.7	401	-1.3
555	2013-04-24/16:00:00	2013-04-24/21:58:00	7.3	0.08	2.8	340	11.3
556*	2013-05-04/07:50:00	2013-05-04/09:15:00	17.1	0.11	3.6	352	-5.2
557	2013-05-12/05:50:00	2013-05-12/06:38:00	10.8	0.15	4.0	353	4.1
558	2013-05-12/07:00:00	2013-05-12/09:38:00	11.0	0.15	3.5	368	-21.6
559	2013-05-12/20:15:00	2013-05-12/23:45:00	8.5	0.24	4.6	346	2.6
560	2013-05-13/07:58:00	2013-05-13/10:05:00	8.5	0.14	3.8	360	-0.5
561	2013-05-13/17:02:00	2013-05-13/23:05:00	9.8	0.12	3.8	397	-10.7

Table C.1: STs list from STB Observation

No.	Start	End	B	β_p	M_A	V_p	V_{exp}
562	2013-05-22/22:42:00	2013-05-23/06:05:00	17.2	0.08	3.9	436	-36.0
563	2013-05-30/14:10:00	2013-05-30/17:00:00	7.4	0.1	4.2	312	10.9
564*	2013-06-03/13:28:00	2013-06-03/23:45:00	9.7	0.12	3.6	431	-7.1
565	2013-06-08/04:20:00	2013-06-08/06:00:00	11.8	0.21	4.5	347	8.5
566	2013-06-16/22:22:00	2013-06-16/23:45:00	6.5	0.09	4.9	357	10.0
567*	2013-06-19/17:28:00	2013-06-19/20:12:00	8.2	0.05	4.9	581	0.9
568	2013-06-26/14:00:00	2013-06-26/17:45:00	7.8	0.05	3.9	303	-0.1
569	2013-06-26/20:40:00	2013-06-26/21:42:00	7.9	0.08	4.8	307	-0.5
570	2013-06-27/03:15:00	2013-06-27/06:45:00	9.9	0.04	3.5	309	-5.0
571	2013-06-27/12:25:00	2013-06-27/15:30:00	12.2	0.15	3.6	346	-19.0
572*	2013-07-05/08:00:00	2013-07-05/12:00:00	11.3	0.11	4.1	347	12.5
573	2013-07-08/04:28:00	2013-07-08/08:25:00	8.8	0.16	4.7	324	-7.0
574	2013-07-08/10:00:00	2013-07-08/15:02:00	11.2	0.09	3.7	323	-23.0
575	2013-07-15/22:25:00	2013-07-16/08:45:00	7.1	0.07	3.9	296	7.5
576	2013-07-16/13:20:00	2013-07-16/18:15:00	9.6	0.08	3.9	302	-6.0
577	2013-08-05/17:50:00	2013-08-05/20:15:00	8.9	0.1	3.4	342	-6.1
578	2013-08-05/21:02:00	2013-08-06/02:45:00	8.6	0.11	3.1	374	-8.2
579	2013-08-20/08:25:00	2013-08-20/10:58:00	10.2	0.23	4.3	342	-14.3
580*	2013-08-22/13:15:00	2013-08-22/15:30:00	8.9	0.23	4.7	588	0.2
581	2013-09-03/02:20:00	2013-09-03/03:25:00	8.0	0.17	4.8	322	-0.08
582*	2013-09-03/16:22:00	2013-09-03/17:32:00	16.5	0.18	4.1	432	-19.0
583*	2013-09-10/07:12:00	2013-09-10/13:25:00	10.5	0.04	3.0	432	4.3
584*	2013-09-15/17:22:00	2013-09-15/18:23:00	8.8	0.09	4.1	313	-0.5
585	2013-09-20/19:48:00	2013-09-21/01:25:00	8.8	0.05	3.1	301	-13.6
586	2013-09-23/09:02:00	2013-09-23/14:48:00	8.0	0.13	3.3	422	-2.2
587	2013-10-01/12:55:00	2013-10-01/13:30:00	8.8	0.04	3.4	296	-3.2
588	2013-10-05/18:17:00	2013-10-05/20:30:00	7.6	0.08	3.9	308	-7.6
589	2013-10-06/04:25:00	2013-10-06/06:32:00	7.9	0.12	3.8	345	-6.7
590	2013-10-17/18:15:00	2013-10-17/19:32:00	8.2	0.04	3.9	298	0.4
591	2013-10-17/22:12:00	2013-10-17/22:45:00	9.1	0.08	3.7	307	-0.5
592	2013-10-26/11:30:00	2013-10-26/12:25:00	7.0	0.03	2.9	306	-4.2
593*	2013-11-05/11:05:00	2013-11-05/12:02:00	11.3	0.17	3.9	353	4.9
594	2013-11-18/17:22:00	2013-11-18/18:37:00	6.9	0.11	4.4	314	5.5
595	2013-11-21/02:38:00	2013-11-21/04:48:00	7.3	0.19	3.8	343	-5.8
596	2013-11-25/00:40:00	2013-11-25/03:02:00	6.7	0.11	3.8	375	-2.9
597*	2013-12-17/22:30:00	2013-12-18/02:02:00	8.8	0.12	3.8	421	-4.4
598	2013-12-22/00:15:00	2013-12-22/02:50:00	17.7	0.13	4.3	385	-0.9
599*	2013-12-29/00:30:00	2013-12-29/04:10:00	21.0	0.17	3.5	466	-28.8
600*	2013-12-29/04:30:00	2013-12-29/08:32:00	18.7	0.19	4.2	506	9.2
601*	2013-12-29/09:15:00	2013-12-29/18:38:00	17.2	0.03	1.9	474	37.7
2014							
602	2014-01-11/08:55:00	2014-01-11/18:00:00	8.9	0.05	2.9	322	-12.0

Table C.1: STs list from STB Observation

No.	Start	End	B	β_p	M_A	V_p	V_{exp}
603	2014-01-18/06:12:00	2014-01-18/09:50:00	9.7	0.13	4.7	343	-1.4
604	2014-01-18/11:25:00	2014-01-18/17:45:00	10.8	0.1	4.0	340	-1.9
605	2014-01-18/18:10:00	2014-01-18/21:10:00	12.3	0.08	3.4	366	5.7
606	2014-01-25/02:20:00	2014-01-25/09:55:00	8.6	0.08	1.8	361	-6.6
607	2014-02-05/18:00:00	2014-02-06/02:15:00	9.3	0.15	3.6	338	-30.4
608	2014-02-08/17:25:00	2014-02-08/18:25:00	8.6	0.13	3.4	321	-2.6
609	2014-03-12/09:30:00	2014-03-12/13:10:00	7.8	0.08	2.8	450	-14.1
610	2014-03-15/05:18:00	2014-03-15/15:05:00	21.5	0.11	3.1	521	-26.2
611	2014-04-12/10:35:00	2014-04-12/15:20:00	16.2	0.15	4.3	420	14.5
612	2014-04-12/16:45:00	2014-04-12/18:50:00	15.4	0.15	3.6	404	25.4
613	2014-05-01/19:30:00	2014-05-01/22:28:00	8.3	0.09	4.5	307	-1.4
614	2014-05-23/13:00:00	2014-05-23/14:35:00	8.4	0.1	4.5	308	3.0
615	2014-05-23/18:00:00	2014-05-23/21:45:00	9.1	0.15	3.5	322	-22.2
616	2014-07-01/20:22:00	2014-07-01/23:35:00	26.6	0.09	2.3	569	-51.5
617	2014-07-07/17:28:00	2014-07-07/23:30:00	7.6	0.11	3.8	322	16.5
618	2014-07-22/02:00:00	2014-07-22/06:45:00	9.2	0.06	3.0	294	-7.3
619	2014-07-29/19:40:00	2014-07-30/01:00:00	8.5	0.04	3.5	283	-0.4
620	2014-07-30/09:50:00	2014-07-30/12:35:00	9.4	0.06	3.8	293	-10.4
621	2014-07-30/16:25:00	2014-07-30/18:42:00	15.9	0.27	4.2	331	-18.7
622	2014-08-06/19:15:00	2014-08-06/20:22:00	16.1	0.17	3.5	336	-9.6
623	2014-08-10/11:30:00	2014-08-10/14:30:00	12.6	0.17	4.6	399	1.2
624	2014-08-25/01:02:00	2014-08-25/02:00:00	7.3	0.04	3.8	301	5.5
625	2014-08-26/02:22:00	2014-08-26/04:17:00	11.4	0.21	4.1	402	-3.2

Appendix D

Analytical model with circular cross-section

We assume the flux rope that locally be considered as a cylinder with circular cross-section. We assume the current density is $(0, j_\varphi, j_z)$, and j_φ and j_z are constants. We assume there is no radial component, $B_r = 0$, so in the cylinder coordinate,

$$\bigtriangledown \times B = \mu_0 j \Rightarrow \begin{cases} \frac{1}{r}\frac{\partial B_z}{\partial \varphi} - \frac{\partial B_\varphi}{\partial z} = 0 \\ -\frac{\partial B_z}{\partial r} = \mu_0 j_\varphi \\ \frac{1}{r}\frac{\partial (rB_\varphi)}{\partial r} = \mu_0 j_z \end{cases} \tag{D.1}$$

Considered j_φ and j_z are constants, solve the above equations, we get:

$$\begin{cases} B_r = 0 \\ B_\varphi = \frac{\mu_0 j_z r}{2} \\ B_z = \mu_0 j_\varphi (R - r) \end{cases} \tag{D.2}$$

D.1 The solution in GSE coordinate system

To get the relationship between the 3 magnetic field components in the flux-rope coordinate and the GSE coordinate system, we define flux-rope coordinate with the axis along z_{FR} (see Figure D-1). So

$$z_{FR} = (cos\theta cos\phi, cos\theta sin\phi, sin\theta) \tag{D.3}$$

, then we define,

$$\begin{aligned} x_{FR} &= (1, 0, 0) \times z_{FR} \\ &= (0, -sin\theta, cos\theta sin\phi) \end{aligned} \tag{D.4}$$

, and

$$\begin{aligned} y_{FR} &= z_{FR} \times x_{FR} \\ &= ((sin\theta)^2 + (cos\theta sin\phi)^2, -(cos\theta)^2 sin\phi cos\phi, -sin\theta cos\theta cos\phi) \end{aligned} \tag{D.5}$$

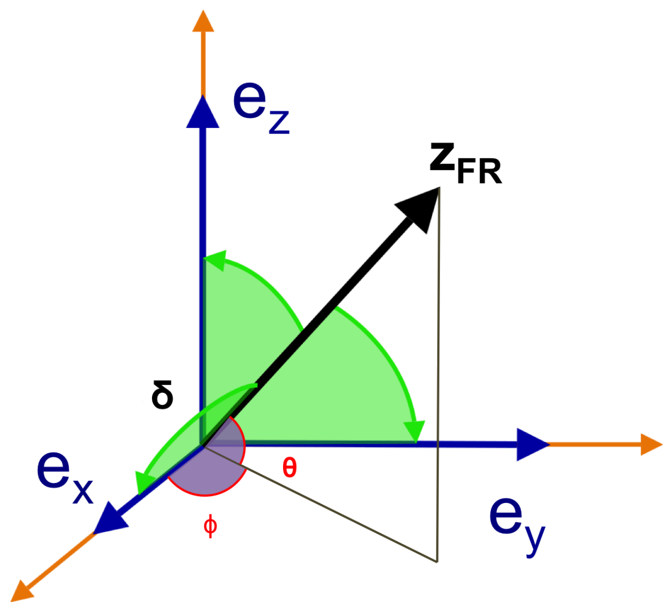

Figure D-1: The flux-rope axis in the GSE coordinate.

To normalize the above 3 coordinate components, we define

$$N^2 = (sin\theta)^2 + (cos\theta sin\phi)^2 \tag{D.6}$$

. Then the 3 normalized Cartesian coordinate components in the flux rope system is:

$$\begin{cases} x_{FR} = \frac{1}{N}(0, -sin\theta, cos\theta sin\phi) \\ y_{FR} = \frac{1}{N}(N^2, -(cos\theta)^2 sin\phi cos\phi, -sin\theta cos\theta cos\phi) \\ z_{FR} = (cos\theta cos\phi, cos\theta sin\phi, sin\theta) \end{cases} \tag{D.7}$$

So,

$$\begin{pmatrix} x_{FR} \\ y_{FR} \\ z_{FR} \end{pmatrix} = \begin{pmatrix} 0 & -\frac{sin\theta}{N} & \frac{cos\theta sin\phi}{N} \\ N & -\frac{(cos\theta)^2 sin\phi cos\phi}{N} & -\frac{sin\theta cos\theta cos\phi}{N} \\ cos\theta cos\phi & cos\theta sin\phi & sin\theta \end{pmatrix} \cdot \begin{pmatrix} x_{GSE} \\ y_{GSE} \\ z_{GSE} \end{pmatrix} \tag{D.8}$$

, where

$$M = \begin{pmatrix} 0 & -\frac{sin\theta}{N} & \frac{cos\theta sin\phi}{N} \\ N & -\frac{(cos\theta)^2 sin\phi cos\phi}{N} & -\frac{sin\theta cos\theta cos\phi}{N} \\ cos\theta cos\phi & cos\theta sin\phi & sin\theta \end{pmatrix} \tag{D.9}$$

, and

$$M^{-1} = \begin{pmatrix} 0 & N & cos\theta cos\phi \\ -\frac{sin\theta}{N} & -\frac{(cos\theta)^2 sin\phi cos\phi}{N} & cos\theta sin\phi \\ \frac{cos\theta sin\phi}{N} & -\frac{sin\theta cos\theta cos\phi}{N} & sin\theta \end{pmatrix} \tag{D.10}$$

So for any vector X, $X_{FR} = M \cdot X_{GSE}$, and $X_{GSE} = M^{-1} \cdot X_{FR}$.

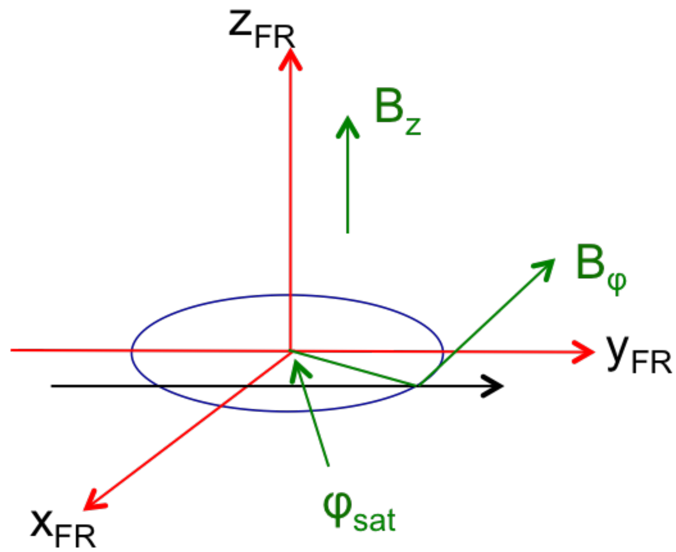

Figure D-2: The magnetic field components in the flux rope coordinate.

In the flux rope frame (see Figure D-2),

$$B_{FR} = \begin{pmatrix} -B_{\varphi} sin\varphi_{sat} \\ B_{\varphi} cos\varphi_{sat} \\ B_z \end{pmatrix} \tag{D.11}$$

So we could get the relationship between $(B_{xGSE}, B_{yGSE}, B_{zGSE})$ and (B_r, B_{φ}, B_z),

$$\begin{aligned} B_{GSE} &= M^{-1} \cdot B_{FR} \\ &= \begin{pmatrix} 0 & N & cos\theta cos\phi \\ -\frac{sin\theta}{N} & -\frac{(cos\theta)^2 sin\phi cos\phi}{N} & cos\theta sin\phi \\ \frac{cos\theta sin\phi}{N} & -\frac{sin\theta cos\theta cos\phi}{N} & sin\theta \end{pmatrix} \cdot \begin{pmatrix} -B_{\varphi} sin\varphi_{sat} \\ B_{\varphi} cos\varphi_{sat} \\ B_z \end{pmatrix} \\ &= \begin{pmatrix} NB_{\varphi} cos\varphi_{sat} + B_z cos\theta cos\phi \\ \frac{1}{N} B_{\varphi} sin\varphi_{sat} sin\theta - \frac{1}{N} B_{\varphi} cos\varphi_{sat} (cos\theta)^2 sin\phi cos\phi + B_z cos\theta sin\phi \\ -\frac{1}{N} B_{\varphi} sin\varphi_{sat} cos\theta sin\phi - \frac{1}{N} B_{\varphi} cos\varphi_{sat} sin\theta cos\theta cos\phi + B_z sin\theta \end{pmatrix} \end{aligned} \tag{D.12}$$

The relationship between the magnetic field components observed in the MC coordinate and the magnetic field components observed in the GSE system is:

$$\begin{cases} B_x^{GSE} = NB_{\varphi} cos\varphi_{sat} + B_z cos\theta cos\phi \\ B_y^{GSE} = \frac{1}{N} B_{\varphi} sin\varphi_{sat} sin\theta - \frac{1}{N} B_{\varphi} cos\varphi_{sat} (cos\theta)^2 sin\phi cos\phi + B_z cos\theta sin\phi \\ B_z^{GSE} = -\frac{1}{N} B_{\varphi} sin\varphi_{sat} cos\theta sin\phi - \frac{1}{N} B_{\varphi} cos\varphi_{sat} sin\theta cos\theta cos\phi + B_z sin\theta \end{cases} \tag{D.13}$$

When the flux-rope is observed at 1 AU, assume the spacecraft passes along the x-GSE

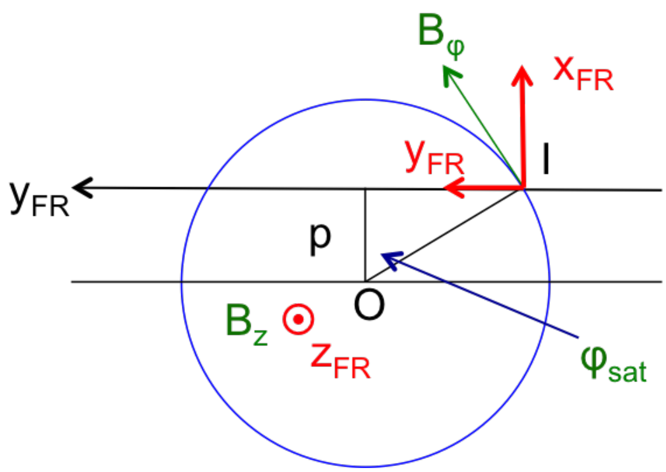

Figure D-3: The trajectory of the spacecraft in the flux-rope coordinate.

direction. And at time t, the position of the spacecraft is

$$r_{GSE}(t) = \begin{pmatrix} V_{SW}(t-t_0) \\ 0 \\ 0 \end{pmatrix} \tag{D.14}$$

In the flux-rope frame, with origin at point I (on the boundary of the flux-rope, see figure D-3), the position of SC is:

$$r'_{FR}(t) = M \cdot r_{GSE}(t) = \begin{pmatrix} 0 \\ NV_{SW}(t-t_0) \\ cos\theta cos\phi V_{SW}(t-t_0) \end{pmatrix} \tag{D.15}$$

Consider the origin of the flux rope is on the axis, which is at the point O (see figure D-3). And at time $t_{center} = \frac{(t_1-t_0)}{2}$ (t_0 - start time, t_1 - ending time), the distance between the spacecraft and the flux rope axis is minimum p. Define δ is the angle between the x_{GSE} direction and the z_{RF}. So the position of the spacecraft in the flux rope coordinate with the origin at the axis is (see figure D-1, and figure D-4):

$$r_{FR}(t) = \begin{pmatrix} p \\ NV_{SW}(t-t_0) - \frac{V_{SW}(t_1-t_0)sin\delta}{2} \\ cos\theta cos\phi V_{SW}(t-t_0) - \frac{V_{SW}(t_1-t_0)cos\delta}{2} \end{pmatrix} \tag{D.16}$$

From Figure D-1, we have,

$$cos\delta = cos\theta cos\phi \tag{D.17}$$

$$\rightarrow sin\delta = N \tag{D.18}$$

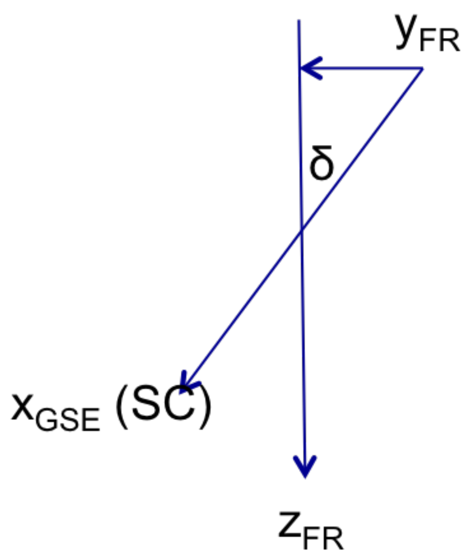

Figure D-4: The trajectory of the spacecraft in the GSE coordinate.

So,

$$r_{FR}(t) = \begin{pmatrix} p \\ NV_{SW}(t - t_0) - \frac{NV_{SW}(t_1 - t_0)}{2} \\ cos\theta cos\phi V_{SW}(t - t_0) - \frac{V_{SW}(t_1 - t_0) cos\theta cos\phi}{2} \end{pmatrix} \quad (D.19)$$

Since r_{sat} is the distance from the spacecraft to the z_{FR}, so,

$$r_{sat} = \sqrt{p^2 + [NV_{SW}(t - t_0) - \frac{NV_{SW}(t_1 - t_0)}{2}]^2} \quad (D.20)$$

where (see Figure D-3),

$$sin\varphi_{sat} = \frac{NV_{SW}(t - t_0) - NV_{SW}(t_1 - t_0)/2}{r_{sat}} \quad (D.21)$$

$$cos\varphi_{sat} = \frac{p}{r_{sat}} \quad (D.22)$$

This model has five free parameters: (i) the latitude, θ; (ii) the longitude, ϕ; (iii) the closest approach distance, p; (iv) j_φ; (v) j_z are corresponding components of the plasma current density. So, with the above equations, we could fit the theoretical magnetic field vector $(B_x^{GSE}, B_y^{GSE}, B_z^{GSE})$ to the observed magnetic field data in GSE coordinate system $(B_x^{obs}, B_y^{obs}, B_z^{obs})$.

D.2 The solution in RTN coordinate system

In RTN coordinate system, we could also follow the steps we derived in the GSE coordinate system, and we have the relationship between magnetic field components (B_r, B_φ, B_z)

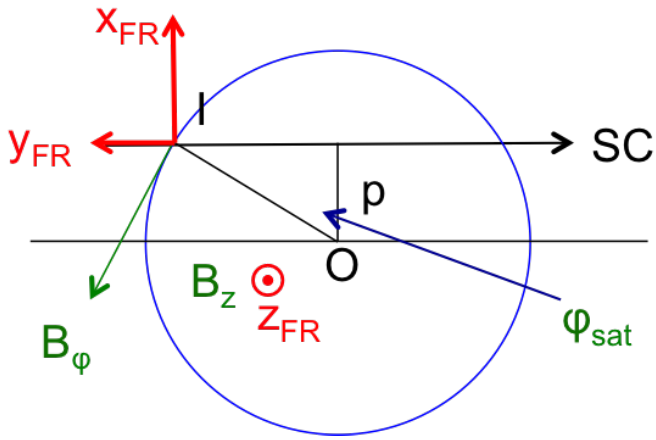

Figure D-5: The trajectory of the spacecraft in the flux-rope coordinate when we observed in RTN coordinate.

observed in the MC coordinate and the (B_R, B_T, B_N) observed in the RTN system is:

$$\begin{cases} B_R = NB_\varphi cos\varphi_{sat} + B_z cos\theta cos\phi \\ B_T = \frac{1}{N} B_\varphi sin\varphi_{sat} sin\theta - \frac{1}{N} B_\varphi cos\varphi_{sat} (cos\theta)^2 sin\phi cos\phi + B_z cos\theta sin\phi \\ B_N = -\frac{1}{N} B_\varphi sin\varphi_{sat} cos\theta sin\phi - \frac{1}{N} B_\varphi cos\varphi_{sat} sin\theta cos\theta cos\phi + B_z sin\theta \end{cases} \tag{D.23}$$

In this case, the spacecraft passes along the -R direction. At time t, the position of the spacecraft is

$$r_{RTN}(t) = \begin{pmatrix} -V_{SW}(t - t_0) \\ 0 \\ 0 \end{pmatrix} \tag{D.24}$$

In the flux-rope frame, with origin at point I (on the boundary of the flux-rope, see figure D-5), the position of SC is:

$$r'_{FR}(t) = M \cdot r_{RTN}(t) = \begin{pmatrix} 0 \\ -NV_{SW}(t - t_0) \\ -cos\theta cos\phi V_{SW}(t - t_0) \end{pmatrix} \tag{D.25}$$

Consider the origin of the flux rope is on the axis, which is at the point O (see figure D-5). And at time $t_{center} = \frac{(t_1 - t_0)}{2}$ (t_0 - start time, t_1 - ending time), the distance between the spacecraft and the flux rope axis is minimum p. Define δ is the angle between the R direction and the z_{RF}. So the position of the spacecraft in the flux rope coordinate with the origin at the axis is (see figure D-1):

$$r_{FR}(t) = \begin{pmatrix} p \\ -NV_{SW}(t - t_0) + \frac{V_{SW}(t_1 - t_0) sin\delta}{2} \\ -cos\theta cos\phi V_{SW}(t - t_0) + \frac{V_{SW}(t_1 - t_0) cos\delta}{2} \end{pmatrix} \tag{D.26}$$

And,

$$\begin{aligned} cos\delta &= cos\theta cos\phi && \text{(D.27)} \\ \rightarrow sin\delta &= N && \text{(D.28)} \end{aligned}$$

So,

$$r_{FR}(t) = \begin{pmatrix} p \\ -NV_{SW}(t-t_0) + \frac{NV_{SW}(t_1-t_0)}{2} \\ -cos\theta cos\phi V_{SW}(t-t_0) + \frac{V_{SW}(t_1-t_0)cos\theta cos\phi}{2} \end{pmatrix} \quad \text{(D.29)}$$

Since r_{sat} is the distance from the spacecraft to the z_{FR}, so,

$$r_{sat} = \sqrt{p^2 + [-NV_{SW}(t-t_0) + \frac{NV_{SW}(t_1-t_0)}{2}]^2} \quad \text{(D.30)}$$

where (see Figure D-5),

$$\begin{aligned} sin\varphi_{sat} &= \frac{-NV_{SW}(t-t_0) + NV_{SW}(t_1-t_0)/2}{r_{sat}} && \text{(D.31)} \\ cos\varphi_{sat} &= \frac{p}{r_{sat}} && \text{(D.32)} \end{aligned}$$

So with the above solutions, we could get the fitting in the RTN coordinate system.

Appendix E

Analytical model with elliptical cross-section

Some flux ropes have unsymmetrical structure in the total magnetic field strength. The main reason of this unsymmetrical is probably the interaction of the flux ropes with the solar wind, which distort the local shape of the cloud.

In this section, we assume the flux ropes are locally have a cylindrical structure with elliptical cross-section. We start with solving the Maxwell equations and the continuity equation in the elliptical cylindrical coordinate. The elliptical cylindrical coordinate is defined:

$$\begin{cases} x = ccosh\eta cos\varphi \\ y = csinh\eta sin\varphi \\ z = z \end{cases} \tag{E.1}$$

, where two foci F1 and F2 are fixed at -c and +c, η is a nonnegative real number and $\varphi \in (0, 2\pi)$.

[1] Solve the j and B in the elliptical cylindrical coordinate.

We assume the magnetic field has only two components: the poloidal component B_φ and axial component B_z. Then in this case, the radial component is $B_\eta = 0$. For the current density, we assume j_η is constant, and $\frac{\partial}{\partial z} = 0$. In elliptic cylindrical coordinates, the scale factor is:

$$h = h_\eta = h_\varphi = c\sqrt{(cosh\eta)^2 - (cos\varphi)^2} = c\sqrt{(sinh\eta)^2 + (sin\varphi)^2} \tag{E.2}$$

$$h_z = 1 \tag{E.3}$$

So,

$$\frac{\partial h}{\partial \eta} = \frac{c^2 sinh\eta cosh\eta}{h} \tag{E.4}$$

$$\frac{\partial h}{\partial \varphi} = \frac{c^2 sin\varphi cos\varphi}{h} \tag{E.5}$$

From the Maxwell relations and continuity equation:

$$\nabla \times B = \mu_0 J \tag{E.6}$$

$$\nabla \cdot B = 0 \tag{E.7}$$

$$\nabla \cdot j = 0 \tag{E.8}$$

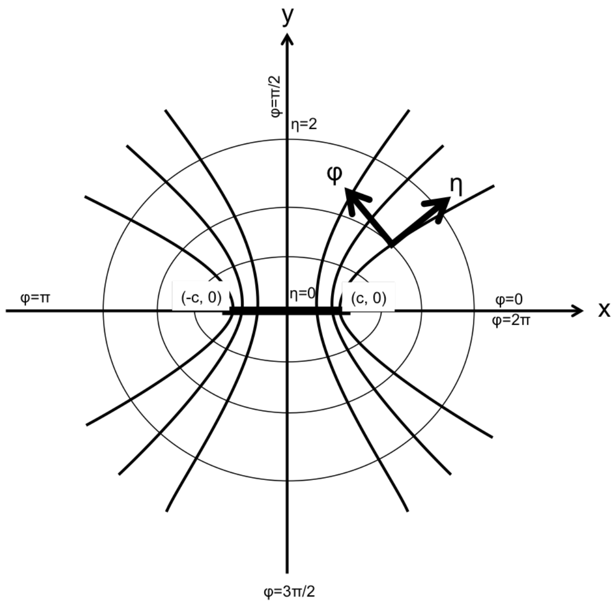

Figure E-1: The elliptical coordinate system.

, we have

$$\frac{1}{h}[\frac{\partial}{\partial\varphi}B_z - \frac{\partial}{\partial z}(hB_\varphi)] = \mu_0 j_\eta \tag{E.9}$$

$$\frac{1}{h}[\frac{\partial}{\partial z}(hB_\eta) - \frac{\partial}{\partial\eta}B_z] = \mu_0 j_\varphi \tag{E.10}$$

$$\frac{1}{h^2}[\frac{\partial}{\partial\eta}(hB_\varphi) - \frac{\partial}{\partial\varphi}(hB_\eta)] = \mu_0 j_z \tag{E.11}$$

$$\frac{\partial}{\partial\eta}(B_\eta h) + \frac{\partial}{\partial\varphi}(B_\varphi h) + h^2\frac{\partial B_z}{\partial z} = 0 \tag{E.12}$$

$$\frac{\partial}{\partial\eta}(j_\eta h) + \frac{\partial}{\partial\varphi}(j_\varphi h) + h^2\frac{\partial}{\partial z}j_z = 0 \tag{E.13}$$

Under the assumptions $B_\eta = 0$, $j_\eta = constant$ and $\frac{\partial}{\partial z} = 0$, we have

$$\frac{\partial}{\partial\varphi} B_z = \mu_0 j_\eta h \tag{E.14}$$

$$\frac{\partial}{\partial\eta} B_z = -\mu_0 j_\varphi h \tag{E.15}$$

$$\frac{\partial}{\partial\eta}(h B_\varphi) = \mu_0 j_z h^2 \tag{E.16}$$

$$\frac{\partial}{\partial\varphi}(B_\varphi h) = 0 \tag{E.17}$$

$$j_\eta \frac{\partial}{\partial\eta} h + \frac{\partial}{\partial\varphi}(j_\varphi h) = 0 \tag{E.18}$$

1. From the equation (E.18) to solve the j_φ.
Plug (E.4) into (E.18),

$$j_\eta \frac{c^2 sinh\eta cosh\eta}{h} + \frac{\partial}{\partial\varphi}(j_{varphi} h) = 0$$
$$\rightarrow \frac{\partial}{\partial\varphi}(j_\varphi h) = (-j_\eta c^2 sinh\eta cosh\eta)\frac{1}{h}$$
$$\rightarrow j_\varphi h = (-j_{eta} c^2 sinh\eta cosh\eta)\int \frac{1}{h} d\varphi + f_1(\eta)$$

, where $f_1(\eta)$ is a function only depend on η. And $\int \frac{1}{h} d\varphi = \int \frac{1}{c\sqrt{(cosh\eta)^2 - (cos\varphi)^2}} d\varphi = \int \frac{d\varphi}{ccosh\eta\sqrt{1 - \frac{(cos\varphi)^2}{(cosh\eta)^2}}}$. So

$$j_\varphi h = -j_\eta csinh\eta \int \frac{d\varphi}{\sqrt{1 - \frac{(cos\varphi)^2}{(cosh\eta)^2}}} + f_1(\eta)$$
$$\rightarrow j_\varphi = -j_\eta \frac{csinh\eta}{h} \int \frac{d\varphi}{\sqrt{1 - \frac{(cos\varphi)^2}{(cosh\eta)^2}}} + \frac{f_1(\eta)}{h}$$
$$\rightarrow j_\varphi = -j_\eta \frac{sinh\eta}{\sqrt{(cosh\eta)^2 - (cos\varphi)^2}} \int \frac{d\varphi}{\sqrt{1 - \frac{(cos\varphi)^2}{(cosh\eta)^2}}} + \frac{f_1(\eta)}{h}$$

Let

$$w = cos\varphi \rightarrow dw = -sin\varphi d\varphi$$
$$k = \frac{1}{cosh\eta}, S = \frac{\sqrt{(sin\varphi)^2}}{sin\varphi}$$

Then,

$$\begin{aligned}
j_\varphi &= -j_\eta \frac{sinh\eta}{\sqrt{(cosh\eta)^2-(cos\varphi)^2}} \int \frac{dw}{-\sqrt{1-w^2}} S \frac{1}{\sqrt{1-\frac{w^2}{(cosh\eta)^2}}} + \frac{f_1(\eta)}{h} \\
&= -j_\eta \frac{sinh\eta}{\sqrt{(cosh\eta)^2-(cos\varphi)^2}} \int \frac{dw}{-\sqrt{1-w^2}} S \frac{1}{\sqrt{1-k^2w^2}} + \frac{f_1(\eta)}{h} \\
&= j_\eta \frac{sinh\eta S}{\sqrt{(cosh\eta)^2-(cos\varphi)^2}} \int \frac{dw}{\sqrt{(1-w^2)(1-k^2w^2)}} + \frac{f_1(\eta)}{h} \\
&= j_\eta \frac{sinh\eta S}{\sqrt{(cosh\eta)^2-(cos\varphi)^2}} F(w,k) + \frac{f_1(\eta)}{h} \\
&= j_\eta \frac{sinh\eta S}{\sqrt{(cosh\eta)^2-(cos\varphi)^2}} F(cos\varphi, \frac{1}{cosh\eta}) + \frac{f_1(\eta)}{h}
\end{aligned}$$

, where $F(w,k) = F(cos\varphi, \frac{1}{cosh\eta})$ is the incomplete elliptic integral of first kind. Expand $F(cos\varphi, \frac{1}{cosh\eta}) \approx cos\varphi$. Then we got,

$$j_\varphi = j_{eta} \frac{sinh\eta S}{\sqrt{(cosh\eta)^2-(cos\varphi)^2}} cos\varphi + \frac{f_1(\eta)}{h} \tag{E.19}$$

2. From (E.14) and (E.15) to solve the B_z.
Since j_η is constant by assumption,

$$\begin{aligned}
B_z &= \int \mu_0 j_\eta h d\varphi + f_1(\eta) \\
&= \mu_0 j_\eta \int h d\varphi + f_2(\eta)
\end{aligned}$$

, where $f_2(\eta)$ is a function only depend on η.
And,

$$\begin{aligned}
\int h d\varphi &= \int c\sqrt{(cosh\eta)^2-(cos\varphi)^2} d\varphi \\
&= \int c\sqrt{(cosh\eta)^2-w^2} \frac{dw}{-sin\varphi} \\
&= ccosh\eta \int \sqrt{1-\frac{w^2}{(cosh\eta)^2}} \frac{dwS}{-\sqrt{1-w^2}} \\
&= -ccosh\eta S \int \frac{\sqrt{1-k^2w^2}}{\sqrt{1-w^2}} dw \\
&= -ccosh\eta S E(cos\varphi, k)
\end{aligned}$$

, where $E(cos\varphi, k)$ is the incomplete elliptic integral of second kind. Expand $E(cos\varphi, k) \approx$

$cos\varphi$, so

$$\int h d\varphi = -ccosh\eta S cos\varphi$$
$$\rightarrow B_z = -\mu_0 j_\eta ccosh\eta S cos\varphi + f_2(\eta) \quad \text{(E.20)}$$

Input (E.20) into (E.15), left: $\frac{\partial}{\partial\eta}B_z = -\mu_0 j_\eta csinh\eta S cos\varphi + \frac{\partial f_2(\eta)}{\partial\eta}$; right: $-\mu_0 j_\varphi h = -\mu_0 j_\eta \frac{sinh\eta S}{\sqrt{(cosh\eta)^2-(cos\varphi)^2}} cos\varphi h - \mu_0 f_1(\eta) = -\mu_0 j_\eta csinh\eta S cos\varphi - \mu_0 f_1(\eta)$.

The left = right, we have,

$$\frac{\partial f_2(\eta)}{\partial\eta} = -\mu_0 f_1(\eta)$$
$$\rightarrow f_2(\eta) = -\mu_0 \int f_1(\eta) d\eta + C1, \quad \text{, where C1 is a constant}$$
$$\rightarrow B_z = -\mu_0 j_\eta ccosh\eta S cos\varphi - \mu_0 \int f_1(\eta) d\eta + C1$$

To make the consistent with the Circular model we studied before (see Appendix-D). That is, when $\eta \rightarrow \infty$, we have the same solution of j_φ and B_z with the circular model. So we choose $f_1(\eta) = j_\varphi^0 csinh\eta$, and $C1 = \mu_0 j_\varphi^0 R_0$, where j_φ^0 is a constant, and R_0 is the distance of spacecraft to the axis at the time t_0 (see the section of the equation x_0 and y_0).

$$\rightarrow f_2(\eta) = -\mu_0 \int f_1(\eta) d\eta + C1 = -\mu_0 j_\varphi^0 ccosh\eta + \mu_0 j_\varphi^0 R_0$$

So plug $f_1(\eta)$ and $f_2(\eta)$ into eqs. (E.19) and (E.20), we have

$$j_\varphi = j_\eta \frac{csinh\eta S}{h} cos\varphi + \frac{j_\varphi^0 csinh\eta}{h} \quad \text{(E.21)}$$
$$B_z = -\mu_0 j_\eta ccosh\eta S cos\varphi - \mu_0 j_\varphi^0 ccosh\eta + \mu_0 j_\varphi^0 R_0 \quad \text{(E.22)}$$

, the R_0 is the distance of the spacecraft to the axis at the time t_0, which we will get later.

3. From (E.16) and (E.17) to get the j_z and B_φ.

$$\frac{\partial}{\partial\varphi}(B_\varphi h) = 0$$
$$\rightarrow B_\varphi h = g(\eta), \quad \text{, where g}(\eta)\text{ is a function only depends on }\eta.$$

Input the above result into (E.16),

$$\frac{\partial}{\partial \eta}(hB_\varphi) = \mu_0 j_z h^2$$
$$\rightarrow \frac{\partial}{\partial \eta} g(\eta) = \mu_0 j_z h^2$$
$$\rightarrow g(\eta) = \int \mu_0 j_z h^2 d\eta$$

Since $g(\eta)$ only depends on η, so $\int \mu_0 j_z h^2 d\eta$ also only depends on η. $\rightarrow j_z h^2$ only depends on η. Let,

$$j_z h^2 = q(\eta) \rightarrow j_z = \frac{q(\eta)}{h^2} \tag{E.23}$$

, where $q(\eta)$ is a function only depends on η. So,

$$g(\eta) = \int \mu_0 j_z h^2 d\eta = \mu_0 \int q(\eta) d\eta$$
$$\rightarrow B_\varphi = \frac{\mu_0}{h} \int q(\eta) d\eta$$

Here, we choose $q(\eta) = j_z^0 c^2 (sinh\eta)^2, j_z^0$ is a constant. So

$$j_z = \frac{j_z^0 c^2 (sinh\eta)^2}{h^2} \tag{E.24}$$
$$B_\varphi = \frac{\mu_0 j_z^0 c^2 sinh\eta cosh\eta}{2h} - \frac{\mu_0 j_z^0 c^2 \eta}{2h} \tag{E.25}$$

So, we get the solutions of j and B by solving the MHD equations and the continuity equation in the elliptical cylindrical coordinate, the solutions of j and B are:

$$j_\eta = constant \tag{E.26}$$
$$j_\varphi = \frac{j_\eta c sinh\eta S cos\varphi}{h} + \frac{j_\varphi^0 c sinh\eta}{h} \tag{E.27}$$
$$j_z = \frac{j_z^0 c^2 (sinh\eta)^2}{h^2} \tag{E.28}$$
$$B_\eta = 0 \tag{E.29}$$
$$B_\varphi = \frac{\mu_0 j_z^0 c^2 sinh\eta cosh\eta}{2h} - \frac{\mu_0 j_z^0 c^2 \eta}{2h} \tag{E.30}$$
$$B_z = -\mu_0 j_\eta c cosh\eta S cos\varphi - \mu_0 j_\varphi^0 c cosh\eta + \mu_0 j_\varphi^0 R_0 \tag{E.31}$$

, where j_φ^0 and j_z^0 are constant, $S = \frac{\sqrt{(sin\varphi)^2}}{sin\varphi}$, and R_0 is the distance of the spacecraft to the axis of flux rope at time t_0.

[2] Get the relationship of the magnetic field components between the space-center (GSE coordinate) and the body-center (Cartesian coordinate on the flux rope with the axis be the z'', major axis lie on the x'', and minor axis lie on the y'').

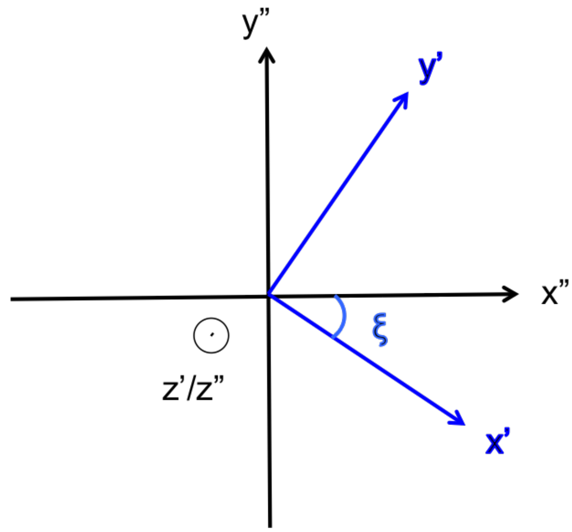

Figure E-2: The flux rope coordinate system.

When the flux rope is observed at 1 AU, we assume the axis has angle θ with respect to the ecliptic plane, and ϕ in the ecliptic plane. The mapping of the trajectory has an angle ξ with respect to the minor-axis of the elliptical cross-section (see Figure E-1). Following the same step with the circular model, define the flux rope's axis along $z^{'}$. So $z^{'} = (cos\theta cos\phi, cos\theta sin\phi, sin\theta)$. Then we define

$$x^{'} = (1,0,0) \times z^{'} = (0, -sin\theta, cos\theta sin\phi)$$
$$y^{'} = z^{'} \times x^{'} = ((sin\theta)^2 + (cos\theta sin\phi)^2, -(cos\theta)^2 sin\phi cos\phi, -sin\theta cos\theta cos\phi)$$

Define $N^2 = (sin\theta)^2 + (cos\theta sin\phi)^2$, then the $x^{'}y^{'}z^{'}$ could be normalized.

$$x^{'} = \frac{1}{N}(0, -sin\theta, cos\theta sin\phi)$$
$$y^{'} = \frac{1}{N}(N^2, -(cos\theta)^2 sin\phi cos\phi, -sin\theta cos\theta cos\phi)$$
$$z^{'} = (cos\theta cos\phi, cos\theta sin\phi, sin\theta)$$

So,

$$\begin{pmatrix} x^{'} \\ y^{'} \\ z^{'} \end{pmatrix} = \begin{pmatrix} 0 & -\frac{sin\theta}{N} & \frac{cos\theta sin\phi}{N} \\ N & -\frac{(cos\theta)^2 sin\phi cos\phi}{N} & -\frac{sin\theta cos\theta cos\phi}{N} \\ cos\theta cos\phi & cos\theta sin\phi & sin\theta \end{pmatrix} \cdot \begin{pmatrix} x_{GSE} \\ y_{GSE} \\ z_{GSE} \end{pmatrix}$$

, where

$$M1 = \begin{pmatrix} 0 & -\frac{sin\theta}{N} & \frac{cos\theta sin\phi}{N} \\ N & -\frac{(cos\theta)^2 sin\phi cos\phi}{N} & -\frac{sin\theta cos\theta cos\phi}{N} \\ cos\theta cos\phi & cos\theta sin\phi & sin\theta \end{pmatrix} \quad \text{(E.32)}$$

Now the $y^{'}$ is the spacecraft's trajectory mapping on the flux rope's cross-section plane.

The angle between the trajectory and the minor axis ($y^{''}$) of the elliptical cross-section is ξ (see the picture E-2). Now we transform from $(x^{'}, y^{'}, z^{'})$ to $(x^{''}, y^{''}, z^{''})$ by matrix M2.

$$\begin{pmatrix} x^{''} \\ y^{''} \\ z^{''} \end{pmatrix} = \begin{pmatrix} cos\xi & sin\xi & 0 \\ -sin\xi & cos\xi & 0 \\ 0 & 0 & 1 \end{pmatrix} \cdot \begin{pmatrix} x^{'} \\ y^{'} \\ z^{'} \end{pmatrix}$$

, where

$$M2 = \begin{pmatrix} cos\xi & sin\xi & 0 \\ -sin\xi & cos\xi & 0 \\ 0 & 0 & 1 \end{pmatrix} \tag{E.33}$$

So the transformation matrix is $M = M2 \cdot M1$ (which transforms the vectors in the GSE coordinate system to the Cartesian coordinate system on the MC, which with $z^{''}$ along the axis, $x^{''}$ along the major axis of the elliptical cross-section, and $y^{''}$ along the minor axis).

$$V^{''} = MV_{GSE}$$

So $B_{GSE} = M^{-1}B^{''}$, and $r^{''} = Mr_{GSE}$, where $B^{''}$ and $r^{''}$ are on the cartesian coordinate on the flux rope. And

$$\begin{aligned} M &= M2 \cdot M1 \\ &= \begin{pmatrix} cos\xi & sin\xi & 0 \\ -sin\xi & cos\xi & 0 \\ 0 & 0 & 1 \end{pmatrix} \cdot \begin{pmatrix} 0 & -\frac{sin\theta}{N} & \frac{cos\theta sin\phi}{N} \\ N & -\frac{(cos\theta)^2 sin\phi cos\phi}{N} & -\frac{sin\theta cos\theta cos\phi}{N} \\ cos\theta cos\phi & cos\theta sin\phi & sin\theta \end{pmatrix} \\ &= \begin{pmatrix} Nsin\xi & -\frac{sin\theta cos\xi + (cos\theta)^2 sin\phi cos\phi sin\xi}{N} & \frac{cos\theta sin\phi cos\xi - sin\theta cos\theta cos\phi sin\xi}{N} \\ Ncos\xi & \frac{sin\theta sin\xi - (cos\theta)^2 sin\phi cos\phi cos\xi}{N} & -\frac{cos\theta sin\phi sin\xi + sin\theta cos\theta cos\phi cos\xi}{N} \\ cos\theta cos\phi & cos\theta sin\phi & sin\theta \end{pmatrix} \end{aligned} \tag{E.34}$$

, and

$$M^{-1} = \begin{pmatrix} Nsin\xi & Ncos\xi & cos\theta cos\phi \\ -\frac{sin\theta cos\xi + (cos\theta)^2 sin\phi cos\phi sin\xi}{N} & \frac{sin\theta sin\xi - (cos\theta)^2 sin\phi cos\phi cos\xi}{N} & cos\theta sin\phi \\ \frac{cos\theta sin\phi cos\xi - sin\theta cos\theta cos\phi sin\xi}{N} & -\frac{cos\theta sin\phi sin\xi + sin\theta cos\theta cos\phi cos\xi}{N} & sin\theta \end{pmatrix} \tag{E.35}$$

The relationship between the magnetic field components observed in the flux rope coordinate and the components observed in the GSE system is $B_{GSE} = M^{-1} \cdot B^{''}$:

$$\begin{cases} B_{xGSE} = Nsin\xi B_x^{''} + Ncos\xi B_y^{''} + cos\theta cos\phi B_z^{''} \\ B_{yGSE} = -\frac{1}{N}(sin\theta cos\xi + (cos\theta)^2 sin\phi cos\phi sin\xi)B_x^{''} + \frac{1}{N}(sin\theta sin\xi - (cos\theta)^2 sin\phi cos\phi cos\xi)B_y^{''} \\ +cos\theta sin\phi B_z^{''} \\ B_{zGSE} = \frac{1}{N}(cos\theta sin\phi cos\xi - sin\theta cos\theta cos\phi sin\xi)B_x^{''} - \frac{1}{N}(sin\theta cos\theta cos\phi cos\xi + cos\theta sin\phi sin\xi)B_y^{''} \\ +sin\theta B_z^{''} \end{cases} \tag{E.36}$$

, where $N = \sqrt{(sin\theta)^2 + (cos\theta sin\phi)^2}$.

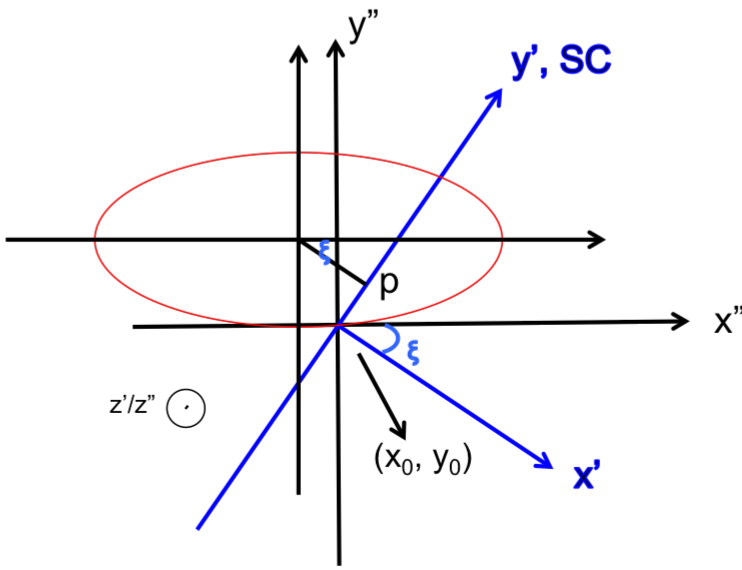

Figure E-3: The mapping of the spacecraft's trajectory on the elliptical cross plane.

And $(B_x^{''}, B_y^{''}, B_z^{''})$ are determined by the expressions

$$\begin{cases} B_x^{''} = -\frac{c}{h} cosh\eta sin\varphi B_\varphi \\ B_y^{''} = \frac{c}{h} sinh\eta cos\varphi B_\varphi \\ B_z^{''} = B_z \end{cases} \tag{E.37}$$

[3] Get the c and φ_{sat} when observed in GSE coordinate system.

So now we are prepared to compare the theory with observed data. Where is the data gathered? We need to take the spacecraft's path in both GSE coordinate and flux rope coordinate. In GSE system, the spacecraft is along x-GSE, so

$$r_{GSE}(t) = \begin{pmatrix} V_{SW}(t - t_0) \\ 0 \\ 0 \end{pmatrix} \tag{E.38}$$

Then, with the transformation matrix, we could get the spacecraft's path in the flux rope coordinate,

$$r^{''}(t) = M \cdot r_{GSE}(t) = V_{SW}(t - t_0) \begin{pmatrix} N sin\xi \\ N cos\xi \\ cos\theta cos\phi \end{pmatrix} \tag{E.39}$$

When the spacecraft cross the boundary of the flux rope, the position of it is (x_0, y_0) away from the center of the flux rope (see Figure E-3). So the distance from the spacecraft to the center of the flux rope is:

$$r_{sat}(t) = \begin{pmatrix} V_{SW}(t-t_0)Nsin\xi + x_0 \\ V_{SW}(t-t_0)Ncos\xi + y_0 \end{pmatrix}$$

To get the x_0, y_0.

In the flux rope's Cartesian coordinate, $\frac{x^2}{a^2} + \frac{y^2}{b^2} = 1$, and the line of the trajectory is $y = \frac{cos\xi}{sin\xi}x - \frac{p}{sin\xi}$. The two points $(x_0, y_0), (V_{SW}(t_1-t_0)Nsin\xi + x_0, V_{SW}(t_1-t_0)Ncos\xi + y_0)$ are on the both equations.

$$\begin{cases} \frac{x_0^2}{a^2} + \frac{y_0^2}{b^2} = 1 \\ y_0 = \frac{cos\xi}{sin\xi}x_0 - \frac{p}{sin\xi} \end{cases}$$

Let, $L = V_{SW}(t_1-t_0)N$. And plug the two points into the above equations to get the solution of x_0 and y_0.

$$\begin{cases} x_0 = -\frac{Lsin\xi}{2} + \frac{pcos\xi(cosh\eta)^2}{(cos\xi)^2+(sinh\eta)^2} \\ y_0 = -\frac{Lcos\xi}{2} - \frac{psin\xi(sinh\eta)^2}{(cos\xi)^2+(sinh\eta)^2} \end{cases} \quad (E.40)$$

Then we get at time $t = t_0$, the distance from the spacecraft to the axis is:

$$R_0 = \sqrt{x_0^2 + y_0^2} = \sqrt{(\frac{L}{2} - \frac{pcos\xi sin\xi}{(cos\xi)^2 + (sinh\eta)^2})^2 + p^2} \quad (E.41)$$

And the position of spacecraft at any time t is:

$$\begin{cases} x = V_{SW}(t-t_0)Nsin\xi + x_0 \\ y = V_{SW}(t-t_0)Ncos\xi + y_0 \end{cases} \quad (E.42)$$

Since,

$$\begin{cases} x = ccosh\eta cos\varphi \\ y = csinh\eta sin\varphi \end{cases}$$

Therefore, at any time t, the distance of spacecraft to the axis is determined by

$$r_{sat} = \sqrt{[V_{SW}(t-t_0)Nsin\xi + x_0]^2 + [V_{SW}(t-t_0)Ncos\xi + y_0]^2} \quad (E.43)$$

and,

$$\varphi_{sat} = tan^{-1}(\frac{y}{x} \cdot \frac{cosh\eta}{sinh\eta}) \quad (E.44)$$

$$c = \sqrt{\frac{x^2+y^2}{(cos\varphi_{sat})^2 + (sinh\eta)^2}} \quad (E.45)$$

At time t_0, the distance of the spacecraft to the axis is:

$R_0 = \sqrt{x_0^2 + y_0^2} = \sqrt{(\frac{L}{2} - \frac{pcos\xi sin\xi}{(cos\xi)^2+(sinh\eta)^2})^2 + p^2}$.

This model has eight free parameters: (i) the latitude, θ; (ii) the longitude, ϕ; (iii) the orientation of the elliptical cross section, ξ; (iv) the closest approach distance, p; (v)

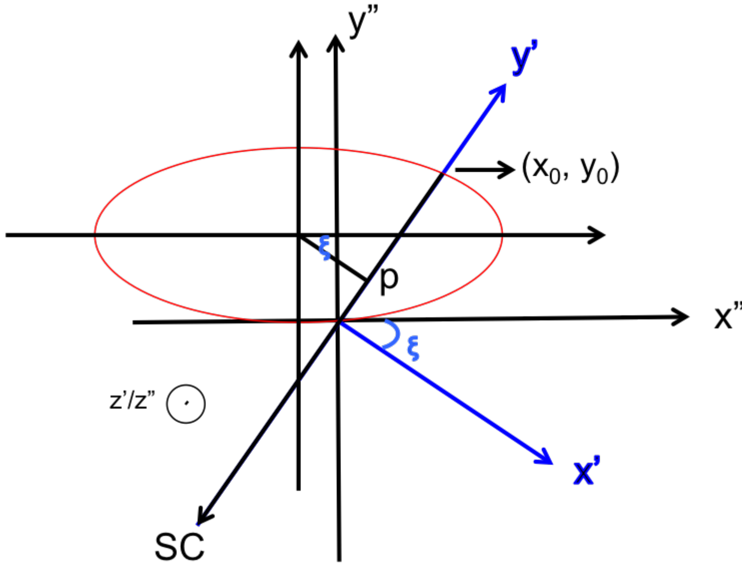

Figure E-4: The mapping of the spacecraft's trajectory on the elliptical cross plane when observed in RTN coordinate.

the parameter associated with the eccentricity, η; (vi) j_η; $(vii) j^0_\varphi$; $(viii) j^0_z$ are corresponding components of the plasma current density. So with the above equations, we could fit the observed magnetic field components by using this elliptical model.

[4] Get the c and φ_{sat} when observed in RTN coordinate system.

When we observe in RTN coordinate system, the spacecraft is along -R direction, so

$$r_{RTN}(t) = \begin{pmatrix} -V_{SW}(t-t_0) \\ 0 \\ 0 \end{pmatrix} \tag{E.46}$$

Then, with the transformation matrix, we could get the spacecraft's path in the flux rope coordinate,

$$r''(t) = M \cdot r_{RTN}(t) = -V_{SW}(t-t_0) \begin{pmatrix} N sin\xi \\ N cos\xi \\ cos\theta cos\phi \end{pmatrix} \tag{E.47}$$

When the spacecraft cross the boundary of the flux rope, the position of it is (x_0, y_0) away from the center of the flux rope (see Figure E-4). So the distance from the spacecraft to the center of the flux rope is:

$$r_{sat}(t) = \begin{pmatrix} x_0 - V_{SW}(t-t_0) N sin\xi \\ y_0 - V_{SW}(t-t_0) N cos\xi \end{pmatrix}$$

To get the x_0, y_0.

In the flux rope's Cartesian coordinate, $\frac{x^2}{a^2} + \frac{y^2}{b^2} = 1$, and the line of the trajectory is

$y = \frac{cos\xi}{sin\xi}x - \frac{p}{sin\xi}$. The two points $(x_0, y_0), (x_0 - V_{SW}(t_1 - t_0)Nsin\xi, y_0 - V_{SW}(t_1 - t_0)Ncos\xi)$ are on the both equations.

Then we have,

$$\begin{cases} x_0 = \frac{Lsin\xi}{2} + \frac{pcos\xi(cosh\eta)^2}{(cos\xi)^2+(sinh\eta)^2} \\ y_0 = \frac{Lcos\xi}{2} - \frac{psin\xi(sinh\eta)^2}{(cos\xi)^2+(sinh\eta)^2} \end{cases} \tag{E.48}$$

, where $L = V_{SW}(t_1 - t_0)N$.

Then we get at time $t = t_0$, the distance from the spacecraft to the axis is:

$$R_0 = \sqrt{x_0^2 + y_0^2} = \sqrt{(\frac{L}{2} + \frac{pcos\xi sin\xi}{(cos\xi)^2 + (sinh\eta)^2})^2 + p^2} \tag{E.49}$$

And the position of spacecraft at any time t is:

$$\begin{cases} x = x_0 - V_{SW}(t - t_0)Nsin\xi \\ y = y_0 - V_{SW}(t - t_0)Ncos\xi \end{cases} \tag{E.50}$$

Since,

$$\begin{cases} x = ccosh\eta cos\varphi \\ y = csinh\eta sin\varphi \end{cases}$$

Therefore, at any time t, the distance of spacecraft to the axis is determined by

$$r_{sat} = \sqrt{[x_0 - V_{SW}(t - t_0)Nsin\xi]^2 + [y_0 - V_{SW}(t - t_0)Ncos\xi]^2} \tag{E.51}$$

and,

$$\varphi_{sat} = tan^{-1}(\frac{y}{x} \cdot \frac{cosh\eta}{sinh\eta}) \tag{E.52}$$

$$c = \sqrt{\frac{x^2 + y^2}{(cos\varphi_{sat})^2 + (sinh\eta)^2}} \tag{E.53}$$

At time t_0, the distance of spacecraft to the axis is $R_0 = \sqrt{x_0^2 + y_0^2} = \sqrt{(\frac{L}{2} + \frac{pcos\xi sin\xi}{(cos\xi)^2+(sinh\eta)^2})^2 + p^2}$.

Appendix F

Codes for selecting data and non-force free analytical model

F.1 Searching code

Part of our automatic searching code is described below to indicate our criteria for selecting STs. (i) Duration between [0.5, 12] hours. (ii) Magnetic field strength (B) which is higher than the yearly average (1.3 times the yearly average B). (iii) Low proton beta (β_p less than 0.7 times yearly average) or low proton temperature, where by "low" we mean T_p/T_{exp} less than 0.7. (iv) Low Alfvén Mach Number (M_A less than 0.7 yearly average), or large rotations of magnetic field components.

Below is the program we used in our study to select the time ranges which satisfy our criteria for selecting the STs. With the output data, we plot them out and use eye to check the boundaries of the selected events. Later, we removed the alfvénic structures by checking if they satisfy the relation $\Delta \mathbf{V}_\perp = \frac{\Delta \mathbf{B}_\perp}{\sqrt{\mu_0 \rho}}$.

Below we select the data in Jan, 2009 from Wind spacecraft.

```
;Read in the data from three instruments of Wind
input_MFI = 'WI_H0_MFI_200901.txt'; magnetic fields data from MFI instrument
input_H5 = 'WI_H5_SWE_200901.txt' ; electron data from SWE instrument
input_SWE = 'WI_K0_SWE_200901.txt'; proton data from SWE instrument
;get the number of lines of the input data
num_MFI = file_lines(input_MFI)
num_H5 = file_lines(input_H5)
num_SWE = file_lines(input_SWE)
;input the yearly average values
b_ave = 3.89
betaproton_ave = 0.94
day0 = 01
;readin magnetic field data
vect1 = fltarr(13L, num_MFI)
openr,51,input_MFI
readf,51,vect1
close,51
daymfi = vect1(0,*)
monthmfi = vect1(1,*)
hourmfi = vect1(3,*)
```

```
minmfi = vect1(4,*)
secmfi = vect1(5,*)
b = vect1(6,*)
bxgse = vect1(7,*)
bygse = vect1(8,*)
bzgse = vect1(9,*)
;calculate the observed date and time in hours.
hourmfi1 = 24*(daymfi-day0)+double(hourmfi)+double(minmfi/60)+double(secmfi/3600)
;readin electron data
vect2=dblarr(8L, num_H5)
openr,52,input_H5
readf,52,vect2
close,52
dayswete = vect2(0,*)
monthswete = vect2(1,*)
hourswete =vect2(3,*)
minswete = vect2(4,*)
secswete = vect2(5,*)
swete = vect2(7,*)
swene = vect2(6,*)
hourswete1 = 24*(dayswete-day0)+double(hourswete)+double(minswete/60)+double (secswete/3600)
;readin proton data
vect3=dblarr(11L, num_SWE)
openr,53,input_SWE
readf,53,vect3
close,53
dayswetp = vect3(0,*)
monthswetp = vect3(1,*)
yearswetp = vect3(2,*)
hourswetp =vect3(3,*)
minswetp = vect3(4,*)
secswetp = vect3(5,*)
vth = vect3(6,*)
np = vect3(7,*)
vxgse = vect3(8,*)
vygse = vect3(9,*)
vzgse = vect3(10,*)
vp = sqrt (vxgse^2+vygse^2+vzgse^2)
tp = 60.1*vth*vth
hourswetp1 = 24*(dayswetp-day0)+double(hourswetp)+double(minswetp/60)+double (secswetp/3600)
;interpol the data into the same data period.
swete_int = interpol(swete, hourswete1, hourswetp1)
swene_int = interpol(swene, hourswete1, hourswetp1)
```

```
te_tp = swete_int/tp
b_int = interpol(b, hourmfi1, hourswetp1)
pp = np*tp*1.3807e-8 ; nkT thermal pressure
pe_int = (swene_int)*(swete_int)*1.3807e-8 ; electrons pressure
pplasma = pp + pe_int ; Total PLASMA pressure
pm = b_int*b_int*3.979e-4
pt = pplasma + pm
beta_proton = pp/pm
ma = (vp*sqrt(np))/(21.812*b_int)
beta_plasma = pplasma/pm
;Expected temperature,
number = n_elements(vp)
tempexp = dblarr(number)
FOR k = 0L, number - 1 DO BEGIN
IF vp(k) LT 500.0 then begin
tempexp(k) = (0.028*vp(k)-3.81)^2*1000
ENDIF
IF vp(k) GE 500.0 then begin
tempexp(k)=(0.574*vp(k)-188)*1000
ENDIF
ENDFOR
tp_tempexp = tp/tempexp
;select the data which have the magnetic field higher than 1.3 yearly average value, low proton beta or low proton temprature.
a=where((b_int GT 1.3*b_ave) and ((tp_tempexp LT 0.7) or (beta_proton LT 0.7 * betaproton_ave)))
vect4=fltarr(6, n_elements(a))
vect4[0,*]=dayswetp(a)
vect4[1,*]=monthswetp(a)
vect4[2,*]=yearswetp(a)
vect4[3,*]=hourswetp(a)
vect4[4,*]=minswetp(a)
vect4[5,*]=secswetp(a)
openw, 34, 'wind_choose_days_200901.txt'
printf, 34, vect4, format='(6F10.3)'
close, 34
end
```

Then the output data will be used to plotted out which we used to check the boundaries. Further, we deal with the selected data to check the final criteria. That is we check if they have low Alfvén Mach Number signature or large rotations of magnetic field components (which we use the minimum variance analysis to get the ratio of the eigenvalues; and we require the ratio be greater than 5).

F.2 Code of non-force free analytical model with circular cross-section

The code of the non-force free analytical model with circular cross-section (the details of this model is presented in the Appendix D). In this code, we use the MPFIT fitting routine (Markwardt [2009]) to do the fitting in this non-force free model.

```
;non-force free model with circular cross-section
FUNCTION MC_COSINE, time, P
AU = 1.4959d11 ;m
mu0 = 1.26d-6 ; H m-1
theta = P[0]*!dtor ; transfer theta to rad
phi = P[1]*!dtor ; transfer theta to rad
z0 = P[2]*AU ; transfer z0 from unit AU to meters
j_phi = P[3]*10^-12 ; C m^-2 s^-1
j_psi = P[4]*10^-12
Vsw_par = P[5]*1000 ; transfer Vsw from km/s to m/s
t = time*3600 ; transfer t from hours to senconds
nr = n_elements(t)
t0 = t[0]
t1 = t[nr -1]
;define a0
a01 = (sin(theta))^2
a02 = (cos(theta)*sin(phi))^2
a0 = sqrt(a01+a02)
;define xc
xc1 = a0*V*(t-t0)
xc2 = .5*a0*V*(t1-t0)
xc = xc1-xc2
;define zc
zc = z0
;define rsat
rsat = sqrt(zc^2 + xc^2)
sin_phi_sat = xc/rsat
cos_phi_sat = zc/rsat
;define Rc
rc1 = .5*a0*V*(t1-t0)
Rc = sqrt(zc^2 +rc1^2)
;define B_phi, B_psi in MC frame; and transfer them to nT.
B_phi_MC = .5*mu0*j_psi*rsat ; in T
B_psi_MC = mu0*j_phi*(Rc-rsat) ; T
B_phi_MC = B_phi_MC*10^9 ; in nT
B_psi_MC = B_psi_MC*10^9 ; nT
;get Bx, By, Bz in GSE coordinates by using M transfermation matrix got from direction-cosine.
```

```
bx1 = a0*B_phi_MC*cos_phi_sat
bx2 = B_psi_MC*cos(theta)*cos(phi)
Bx_GSE = bx1+bx2
by1 = -B_phi_MC*cos_phi_sat*cos(theta)*cos(theta)*sin(phi)*cos(phi)/a0
by2 = B_psi_MC*cos(theta)*sin(phi)
by3 = B_phi_MC*sin_phi_sat*sin(theta)/a0
By_GSE = by1+by2+by3
bz1 = -B_phi_MC*cos_phi_sat*sin(theta)*cos(theta)*cos(phi)/a0
bz2 = B_psi_MC*sin(theta)
bz3 = -B_phi_MC*sin_phi_sat*cos(theta)*sin(phi)/a0
Bz_GSE = bz1+bz2+bz3
B_DATA = [[Bx_GSE], [By_GSE], [Bz_GSE]]
return, B_DATA
END
;..............................
input_MFI = 'WI_H0_MFI_20090115.txt'
input_SWE = 'WI_K0_SWE_20090115.txt'
input_H0 = 'WI_H5_SWE_20090115.txt'
file_name='Wind_circular_20090115'
title_name = 'Wind_circular_20090115'
num_MFI = file_lines(input_MFI)
num_SWE = file_lines(input_SWE)
num_H0 = file_lines(input_H0)
;readin the magnetic field
vect21=fltarr(13, num_MFI)
openr,51,input_MFI
readf,51,vect21
close,51
dayb = vect21(0,*)
hourb = vect21(3,*)
minb = vect21(4,*)
secb = vect21(5,*)
day0 = dayb[0]
hourmfi= 24.0*(dayb-day0) + float(hourb)+float(minb)/60.0+float(secb/3600.)
b_mfi = vect21(6,*)
bx_mfi = vect21(7,*)
by_mfi = vect21(8,*)
bz_mfi = vect21(9,*)
nt = n_elements(hourmfi)
nr = nt - 1
t = hourmfi(0 : nr) ; get time from data WI_H0_MFI.
btotal_obs = b_mfi(0 : nr)
bx_obs = bx_mfi(0 : nr)
by_obs = by_mfi(0 : nr)
bz_obs = bz_mfi(0 : nr)
```

B_obs = [[Bx_obs], [By_obs], [Bz_obs]]

; readin the velocity

vect22=fltarr(11, num_SWE)

openr,52,input_SWE

readf,52,vect22

close,52

dayswetp = vect22(0,*)

hourswetp = vect22(3,*)

minswetp = vect22(4,*)

secswetp = vect22(5,*)

hourswetp_1 = 24.0*(dayswetp-day0)+float(hourswetp)+float(minswetp/60.)+float (secswetp/3600.)

swevth = vect22(6,*)

swenp = vect22(7,*)

swevxgse = vect22(8,*)

swevygse = vect22(9,*)

swevzgse = vect22(10,*)

vp = sqrt(swevxgse^2+swevygse^2+swevzgse^2)

Vsw_aver = moment(vp(0 : nv), /nan) ; get the average Vsw between MC from data WI_K0_SWE.

Vsw = Vsw_aver[0]

;fit cosine's function. The start theta0 and phi0 are selected in fitting the functions. We usually used the results got from minimum variance analysis.

theta0 = 10

phi0 = 90

start_A_C = [theta0, phi0, 0.0001, 1., 1., Vsw]

err_C = fltarr(n_elements(t), 3)

err_C[*] = 1

;setting the parameter limits

pi_C = replicate(fixed:0, limited:[0,0], limits:[0.D,0.D],6)

pi_C[0].limited[0] = 1 ;theta = P[0]

pi_C[0].limited[1] = 1

pi_C[0].limits[0] = -90

pi_C[0].limits[1] = 90

pi_C[1].limited[0] = 1 ;phi = P[1]

pi_C[1].limited[1] = 1

pi_C[1].limits[0] = 0

pi_C[1].limits[1] = 360

pi_C[2].limited[0] = 0 ;z0 = P[2]

pi_C[2].limited[1] = 0

pi_C[3].limited[0] = 0 ;j_phi = P[3]

pi_C[3].limited[1] = 0

pi_C[4].limited[0] = 0 ;j_psi = P[4]

pi_C[4].limited[1] = 0

pi_C[5].fixed = 1 ; Vsw always fixed

;fit the data by using OUR COSINE's model

P_C = MPFITFUN('MC_COSINE', t, b_obs, err_C, start_A_C, /NAN,

PARINFO=pi_C,

BESTNORM = bestnorm, ; the value of the summed squared residuals for the returned parameter values.

BEST_RESID = best_resid, ;upon return, an array of best-fit deviates normalized by the weights or errors.

COVAR = covar, ;The square root of the diagonal elements gives the formal 1-sigma statistical errors on the parameters IF errors were treated "properly" in MYFUNC;

STATUS = status_C,

yfit = yfit_c)

;print the output of the fitting results.

print, "theta_H = ", P_C[0]

print, "phi_H = ", P_C[1]

print, "z0_H = ", P_C[2]

print, "j_phi_H = ", P_C[3]

print, "j_psi_H = ", P_C[4]

print, "status_H = ", status_C

Btotal_fit_c = sqrt((yfit_c[*, 0])^2 + yfit_c[*, 1]^2 +yfit_c[*, 2]^2)

bx_c = yfit_c[*,0]

by_c = yfit_c[*,1]

bz_c = yfit_c[*,2]

nd2_c = ((bx_obs - bx_c)^2+(by_obs - by_c)^2+(bz_obs - bz_c)^2)/(btotal_obs)^2

nchi2_c = total(nd2_c, /nan)/(3*nt)

print, "nchi2_H = ", nchi2_c

end

Bibliography

S-I Akasofu. The development of the auroral substorm. *Planetary and Space Science*, 12(4): 273–282, 1964.

S-I Akasofu. The relationship between the magnetosphere and magnetospheric/auroral substorms. In *Annales Geophysicae*, volume 31, pages 387–394. Copernicus GmbH, 2013.

Joachim Birn and Eric Ronald Priest. *Reconnection of magnetic fields: magnetohydrodynamics and collisionless theory and observations*. Cambridge University Press, 2007.

Space Studies Board et al. *Severe Space Weather Events–Understanding Societal and Economic Impacts: A Workshop Report*. National Academies Press, 2008.

JL Burch. Preconditions for the triggering of polar magnetic substorms by storm sudden commencements. *Journal of Geophysical Research*, 77(28):5629–5632, 1972.

L. Burlaga, E. Sittler, F. Mariani, and R. Schwenn. Magnetic Loop Behind an Interplanetary Shock: Voyager, Helios, and IMP 8 Observations. *J. Geophys. Res.*, 86(A8):6673–6684, 1981. doi: 10.1029/JA086iA08p06673.

L.F. Burlaga. Magnetic clouds and force-free fields with constant alpha. *Journal of Geophysical Research: Space Physics*, 93(A7):7217–7224, 1988. doi: 10.1029/JA093iA07p07217.

Michael N Caan, Robert L McPherron, and Christopher T Russell. Substorm and interplanetary magnetic field effects on the geomagnetic tail lobes. *Journal of Geophysical Research*, 80(1):191–194, 1975.

M.L. Cartwright and M.B. Moldwin. Comparison of small-scale flux rope magnetic properties to large-scale magnetic clouds: Evidence for reconnection across the hcs? *Journal of Geophysical Research: Space Physics*, 113(A9), 2008. doi: 10.1029/2008JA013389.

M.L. Cartwright and M.B. Moldwin. Heliospheric evolution of solar wind small-scale magnetic flux ropes. *Journal of Geophysical Research: Space Physics*, 115(A8), 2010. doi: 10.1029/2009JA014271.

Sydney Chapman and Julius Bartels. *Geomagnetism*, volume 2. Clarendon Press, 1940.

P. Démoulin. Interaction of icmes with the solar wind.

P. Démoulin. Why do temperature and velocity have different relationships in the solar wind and in interplanetary coronal mass ejections? *Solar Physics*, 257(1):169–184, 2009. doi: 10.1007/s11207-009-9338-5.

H.A. Elliott, D.J. McComas, N.A. Schwadron, J.T. Gosling, R.M. Skoug, G. Gloeckler, and T.H. Zurbuchen. An improved expected temperature formula for identifying interplanetary coronal mass ejections. *Journal of Geophysical Research: Space Physics*, 110(A4), 2005. doi: 10.1029/2004JA010794.

C.J. Eyles, R.A. Harrison, C.J. Davis, N.R. Waltham, B.M. Shaughnessy, H.C.A. Mapson-Menard, Danielle Bewsher, S.R. Crothers, J.A. Davies, G.M. Simnett, et al. The heliospheric imagers onboard the stereo mission. *Solar Physics*, 254(2):387–445, 2009. doi: 10.1007/s11207-008-9299-0.

J Fainberg, VA Osherovich, RG Stone, RJ MacDowall, and A Balogh. Ulysses observations of electron and proton components in a magnetic cloud and related wave activity. In *American Institute of Physics Conference Series*, volume 382, pages 554–557, 1996. doi: 10.1063/1.51513.

C.J. Farrugia, L.F. Burlaga, V.A. Osherovich, and R.P. Lepping. A comparative study of dynamically expanding force-free, constant-alpha magnetic configurations with applications to magnetic clouds. In *Solar Wind Seven Colloquium*, volume 1, pages 611–614, 1992.

C.J. Farrugia, N.V. Erkaev, H.K. Biernat, and L.F. Burlaga. Anomalous magnetosheath properties during earth passage of an interplanetary magnetic cloud. *Journal of Geophysical Research: Space Physics*, 100(A10):19245–19257, 1995.

C.J. Farrugia, L.F. Burlaga, and R.P. Lepping. Magnetic clouds and the quiet-storm effect at earth. *Magnetic storms*, pages 91–106, 1997. doi: 10.1029/GM098p0091.

C.J. Farrugia, B. Harris, M. Leitner, C. Möstl, A.B. Galvin, K.D.C. Simunac, R.B. Torbert, M.B. Temmer, A.M. Veronig, N.V. Erkaev, et al. Deep solar activity minimum 2007–2009: Solar wind properties and major effects on the terrestrial magnetosphere. *Solar Physics*, 281(1):461–489, 2012. doi: 10.1007/s11207-012-0119-1.

U Feldman, E Landi, and NA Schwadron. On the sources of fast and slow solar wind. *Journal of Geophysical Research: Space Physics*, 110(A7), 2005.

YI Feldstein, VG Vorobjev, and VL Zverev. Comment on the importance of auroral features in the search for substorm onset process by syun-ichi akasofu, aty lui, and c.-i. meng. *Journal of Geophysical Research: Space Physics*, 116(A2), 2011.

H.Q. Feng, D.J. Wu, and J.K. Chao. Size and energy distributions of interplanetary magnetic flux ropes. *Journal of Geophysical Research: Space Physics*, 112(A2), 2007. doi: 10.1029/2006JA011962.

H.Q. Feng, D.J. Wu, C.C. Lin, J.K. Chao, L.C. Lee, and L.H. Lyu. Interplanetary small- and intermediate-sized magnetic flux ropes during 1995–2005. *Journal of Geophysical Research: Space Physics*, 113(A12), 2008. doi: 10.1029/2008JA013103.

HQ Feng, JK Chao, LH Lyu, and LC Lee. The relationship between small interplanetary magnetic flux rope and the substorm expansion phase. *Journal of Geophysical Research: Space Physics*, 115(A9), 2010.

A.B. Galvin, L.M. Kistler, M.A. Popecki, C.J. Farrugia, K.D.C. Simunac, L. Ellis, E. Möbius, M.A. Lee, M. Boehm, J. Carroll, et al. The plasma and suprathermal ion composition (plastic) investigation on the stereo observatories. *Space Science Reviews*, 136(1-4):437–486, 2008. doi: 10.1007/s11214-007-9296-x.

M.N. Gnevyshev. Essential features of the 11-year solar cycle. *Solar Physics*, 51(1):175–183, 1977.

H. Goldstein. On the field configuration in magnetic clouds. In *NASA conference publication*, volume 228, 1983.

Walter D Gonzalez and Bruce T Tsurutani. Criteria of interplanetary parameters causing intense magnetic storms (dst¡- 100 nt). *Planetary and Space Science*, 35(9):1101–1109, 1987.

J.T. Gosling, V. Pizzo, and S.J. Bame. Anomalously Low Proton Temperatures in the Solar Wind following Interplanetary Shock Waves - Evidence for Magnetic Bottles? *J. Geophys. Res.*, 78(13), 1973.

L-N Hau and Bengt UÖ Sonnerup. Two-dimensional coherent structures in the magnetopause: Recovery of static equilibria from single-spacecraft data. *Journal of Geophysical Research: Space Physics*, 104(A4):6899–6917, 1999.

MA Hidalgo. A study of the expansion and distortion of the cross section of magnetic clouds in the interplanetary medium. *Journal of Geophysical Research: Space Physics*, 108(A8), 2003.

MA Hidalgo. Correction to a study of the expansion and distortion of the cross section of magnetic clouds in the interplanetary medium. *Journal of Geophysical Research: Space Physics*, 110(A3), 2005.

MA Hidalgo, C Cid, AF Vinas, and J Sequeiros. A non-force-free approach to the topology of magnetic clouds in the solar wind. *Journal of Geophysical Research: Space Physics*, 107 (A1), 2002a.

M.A. Hidalgo, T. Nieves-Chinchilla, and C. Cid. Elliptical cross-section model for the magnetic topology of magnetic clouds. *Geophysical research letters*, 29(13), 2002b. doi: 10.1029/2001GL013875.

R.A. Howard, J.D. Moses, A. Vourlidas, J.S. Newmark, D.G. Socker, S.P. Plunkett, C.M. Korendyke, J.W. Cook, A. Hurley, J.M. Davila, et al. Sun earth connection coronal and heliospheric investigation (secchi). *Space Science Reviews*, 136(1-4):67–115, 2008. doi: 10.1007/s11214-008-9341-4.

Qiang Hu and Bengt UÖ Sonnerup. Magnetopause transects from two spacecraft: A comparison. *Geophysical research letters*, 27(10):1443–1446, 2000.

Qiang Hu and Bengt UÖ Sonnerup. Reconstruction of magnetic flux ropes in the solar wind. *Geophysical research letters*, 28(3):467–470, 2001.

Qiang Hu and Bengt UÖ Sonnerup. Reconstruction of magnetic clouds in the solar wind: Orientations and configurations. *Journal of Geophysical Research: Space Physics*, 107 (A7), 2002.

Alexey Isavnin, Emilia KJ Kilpua, and Hannu EJ Koskinen. Grad–shafranov reconstruction of magnetic clouds: overview and improvements. *Solar Physics*, 273(1):205–219, 2011.

P.A. Isenberg. The solar wind. In *Geomagnetism*, volume 1, pages 1–85, 1991.

M. Janvier, P. Démoulin, and S. Dasso. In situ properties of small and large flux ropes in the solar wind. *Journal of Geophysical Research: Space Physics*, 119(9):7088–7107, 2014a. doi: 10.1002/2014JA020218.

Miho Janvier, Pascal Démoulin, and Sergio Dasso. Are there different populations of flux ropes in the solar wind? *Solar Physics*, 289(7):2633–2652, 2014b. doi: 10.1007/s11207-014-0486-x.

L. Jian, C.T. Russell, J.G. Luhmann, and R.M. Skoug. Properties of interplanetary coronal mass ejections at one au during 1995–2004. *Solar Physics*, 239(1-2):393–436, 2006. doi: 10.1007/s11207-006-0133-2.

S.W. Kahler and D.F. Webb. V arc interplanetary coronal mass ejections observed with the solar mass ejection imager. *Journal of Geophysical Research: Space Physics*, 112(A9), 2007. doi: 10.1029/2007JA012358.

Y Kamide, PD Perreault, S-I Akasofu, and JD Winningham. Dependence of substorm occurrence probability on the interplanetary magnetic field and on the size of the auroral oval. *Journal of Geophysical Research*, 82(35):5521–5528, 1977.

Y Kamide, W Baumjohann, IA Daglis, WD Gonzalez, M Grande, JA Joselyn, RL McPherron, JL Phillips, EGD Reeves, G Rostoker, et al. Current understanding of magnetic storms: Storm-substorm relationships. *Journal of Geophysical Research: Space Physics*, 103(A8):17705–17728, 1998.

K Kawasaki, S-I Akasofu, F Yasuhara, and C-I Meng. Storm sudden commencements and polar magnetic substorms. *Journal of Geophysical Research*, 76(28):6781–6789, 1971.

E.K. Kilpua, J.G. Luhmann, J. Gosling, Y. Li, H. Elliott, C.T. Russell, L. Jian, A.B. Galvin, D. Larson, P. Schroeder, et al. Small solar wind transients and their connection to the large-scale coronal structure. *Solar Physics*, 256(1-2):327–344, 2009. doi: 10.1007/s11207-009-9366-1.

E.K.J. Kilpua, L.K. Jian, Y. Li, J.G. Luhmann, and C.T. Russell. Observations of icmes and icme-like solar wind structures from 2007–2010 using near-earth and stereo observations. *Solar Physics*, 281(1):391–409, 2012. doi: 10.1007/s11207-012-9957-0.

L.W. Klein and L.F. Burlaga. Interplanetary magnetic clouds at 1 au. *Journal of Geophysical Research*, 87(A2):613–624, 1982.

S Kokubun, RL McPherron, and CT Russell. Triggering of substorms by solar wind discontinuities. *Journal of Geophysical Research*, 82(1):74–86, 1977.

B. Lavraud, J.E. Borovsky, A.J. Ridley, E.W. Pogue, M.F. Thomsen, H. Rème, A.N. Fazakerley, and E.A. Lucek. Strong bulk plasma acceleration in earth's magnetosheath: A magnetic slingshot effect? *Geophysical Research Letters*, 34(14), 2007. doi: 10.1029/2007GL030024.

Benoit Lavraud and Joseph E. Borovsky. Altered solar wind-magnetosphere interaction at low mach numbers: Coronal mass ejections. *Journal of Geophysical Research: Space Physics*, 113(A9), 2008. doi: 10.1029/2008JA013192.

M. Leitner and C.J. Farrugia. Solar wind quasi invariant within icmes. In *Twelfth International Solar Wind Conference*, volume 1216, pages 652–654. AIP Publishing, 2010. doi: 10.1063/1.3395951.

M. Leitner, C.J. Farrugia, A. Galvin, K.D.C. Simunac, H.K. Biernat, and V.A. Osherovich. The solar wind quasi-invariant observed by stereo a and b at solar minimum 2007 and comparison with two other minima. *Solar Physics*, 259(1-2):381–388, 2009. doi: 10.1007/s11207-009-9412-z.

R.P. Lepping, J.A. Jones, and L.F. Burlaga. Magnetic field structure of interplanetary magnetic clouds at 1 au. *Journal of Geophysical Research*, 95(A8):11957–11965, 1990.

R.P. Lepping, M.H. Acũna, L.F. Burlaga, W.M. Farrell, J.A. Slavin, K.H. Schatten, F. Mariani, N.F. Ness, F.M. Neubauer, Y.C. Whang, et al. The wind magnetic field investigation. *Space Science Reviews*, 71(1-4):207–229, 1995.

R.P. Lepping, D.B. Berdichevsky, C.-C. Wu, A. Szabo, T. Narock, F. Mariani, A.J. Lazarus, and A.J. Quivers. A summary of wind magnetic clouds for years 1995-2003: model-fitted parameters, associated errors and classifications. 24(1):215–245, 2006.

S.T. Lepri and T.H. Zurbuchen. Correction to iron charge state distributions as an indicator of hot icmes: Possible sources and temporal and spatial variations during solar maximum. *Journal of Geophysical Research: Space Physics*, 109(A6), 2004a. doi: 10.1029/2004JA010455.

S.T. Lepri and T.H. Zurbuchen. Iron charge state distributions as an indicator of hot icmes: Possible sources and temporal and spatial variations during solar maximum. *Journal of Geophysical Research: Space Physics*, 109(A1), 2004b. doi: 10.1029/2003JA009954.

S.T. Lepri, T.H. Zurbuchen, L.A. Fisk, I.G. Richardson, H.V. Cane, and G. Gloeckler. Iron charge distribution as an identifier of interplanetary coronal mass ejections. *Journal of Geophysical Research. A. Space Physics*, 106:29, 2001.

Kan Liou. Large, abrupt pressure decreases as a substorm onset trigger. *Geophysical Research Letters*, 34(14), 2007.

Ramon E. Lopez and John W. Freeman. Solar wind proton temperature-velocity relationship. *Journal of Geophysical Research: Space Physics*, 91(A2):1701–1705, 1986. doi: 10.1029/JA091iA02p01701.

R.E. Lopez. Solar cycle invariance in solar wind proton temperature relationships. *Journal of Geophysical Research*, 92:11189–11194, 1987.

N. Lugaz, A. Vourlidas, and I.I. Roussev. Deriving the radial distances of wide coronal mass ejections from elongation measurements in the heliosphere-application to cme-cme interaction. *arXiv preprint arXiv:0909.0534*, 2009.

J.G. Luhmann, D.W. Curtis, P. Schroeder, J. McCauley, R.P. Lin, D.E. Larson, S.D. Bale, J.-A. Sauvaud, C. Aoustin, R.A. Mewaldt, et al. Stereo impact investigation goals, measurements, and data products overview. *Space Science Reviews*, 136(1-4):117–184, 2008. doi: 10.1007/s11214-007-9170-x.

Stig Lundquist. Magneto-hydrostatic fields. *Arkiv for Fysik*, 2(4):361–365, 1950.

Craig B Markwardt. Non-linear least squares fitting in idl with mpfit. *arXiv preprint arXiv:0902.2850*, 2009.

K Marubashi and RP Lepping. Long-duration magnetic clouds: a comparison of analyses using torus-and cylinder-shaped flux rope models. In *Annales Geophysicae*, volume 25, pages 2453–2477, 2007.

K. Marubashi, K.S. Cho, Y.D. Park, M. Maksimovic, K. Issautier, N. Meyer-Vernet, M. Moncuquet, and F. Pantellini. Torsional alfvén waves as pseudo-magnetic flux ropes. In *Aip Conference Proceedings*, volume 1216, page 240, 2010. doi: 10.1063/1.3395845.

D.J. McComas, R.W. Ebert, H.A. Elliott, B.E. Goldstein, J.T. Gosling, N.A. Schwadron, and R.M. Skoug. Weaker solar wind from the polar coronal holes and the whole sun. *Geophysical Research Letters*, 35(18), 2008. doi: 10.1029/2008GL034896.

Robert L McPherron, CT Russell, and MP Aubry. Satellite studies of magnetospheric substorms on august 15, 1968: 9. phenomenological model for substorms. *Journal of Geophysical Research*, 78(16):3131–3149, 1973.

Mark B Moldwin and W Jeffrey Hughes. Plasmoids as magnetic flux ropes. *Journal of Geophysical Research: Space Physics*, 96(A8):14051–14064, 1991.

M.B. Moldwin, J.L. Phillips, J.T. Gosling, E.E. Scime, D.J. McComas, S.J. Bame, A. Balogh, and R.J. Forsyth. Ulysses observation of a noncoronal mass ejection flux rope: Evidence of interplanetary magnetic reconnection. *Journal of Geophysical Research: Space Physics*, 100(A10):19903–19910, 1995. doi: 10.1029/95JA01123.

M.B. Moldwin, S. Ford, R. Lepping, J. Slavin, and A. Szabo. Small-scale magnetic flux ropes in the solar wind. *Geophysical research letters*, 27(1):57–60, 2000. doi: 10.1029/1999GL010724.

C Möstl, T Rollett, N Lugaz, CJ Farrugia, JA Davies, M Temmer, AM Veronig, RA Harrison, S Crothers, JG Luhmann, et al. Arrival time calculation for interplanetary coronal mass ejections with circular fronts and application to stereo observations of the 2009 february 13 eruption. *The Astrophysical Journal*, 741(1):34, 2011. doi: 10.1088/0004-637X/741/1/34.

Christian Möstl, Christiane Miklenic, CJ Farrugia, Manuela Temmer, Astrid Veronig, AB Galvin, Bojan Vršnak, and HK Biernat. Two-spacecraft reconstruction of a magnetic cloud and comparison to its solar source. In *Annales Geophysicae*, volume 26, pages 3139–3152. Copernicus GmbH, 2008.

T Mulligan and CT Russell. Multispacecraft modeling of the flux rope structure of interplanetary coronal mass ejections: Cylindrically symmetric versus nonsymmetric topologies. *Journal of Geophysical Research: Space Physics*, 106(A6):10581–10596, 2001.

M. Neugebauer, J.T. Steinberg, R.L. Tokar, B.L. Barraclough, E.E. Dors, R.C. Wiens, D.E. Gingerich, D. Luckey, and D.B. Whiteaker. Genesis on-board determination of the solar wind flow regime. In *The Genesis Mission*, pages 153–171. Springer, 2003.

Marcia Neugebauer and Raymond Goldstein. *Particle and field signatures of coronal mass ejections in the solar wind*. Wiley Online Library, 1997.

J.A. Newbury, C.T. Russell, J.L. Phillips, and S.P. Gary. Electron temperature in the ambient solar wind: Typical properties and a lower bound at 1 au. *Journal of Geophysical Research*, 103(A5), 1998. doi: 10.1029/98JA00067.

K.W. Ogilvie, D.J. Chornay, R.J. Fritzenreiter, F. Hunsaker, J. Keller, J. Lobell, G. Miller, J.D. Scudder, E.C. Sittler Jr., R.B. Torbert, et al. Swe, a comprehensive plasma instrument for the wind spacecraft. *Space Science Reviews*, 71(1-4):55–77, 1995. doi: 10.1007/BF00751326.

Vladimir A. Osherovich, J. Fainberg, and R.G. Stone. Multi-tube model for interplanetary magnetic clouds. *Geophysical research letters*, 26(3):401–404, 1999.

Mathew James Owens, VG Merkin, and P Riley. A kinematically distorted flux rope model for magnetic clouds. *Journal of Geophysical Research: Space Physics*, 111(A3), 2006.

Eugene N Parker. Dynamics of the interplanetary gas and magnetic fields. *The Astrophysical Journal*, 128:664, 1958.

JL Phillips, SJ Bame, WC Feldman, BE Goldstein, et al. Ulysses solar wind plasma observations at high southerly latitudes. *Science*, 268(5213):1030, 1995.

I.G. Richardson and H.V. Cane. Regions of abnormally low proton temperature in the solar wind (1965–1991) and their association with ejecta. *Journal of Geophysical Research: Space Physics*, 100(A12):23397–23412, 1995.

I.G. Richardson and H.V. Cane. Near-earth interplanetary coronal mass ejections during solar cycle 23 (1996–2009): Catalog and summary of properties. *Solar Physics*, 264(1): 189–237, 2010. doi: 10.1007/s11207-010-9568-6.

I.G. Richardson, C.J. Farrugia, and H.V. Cane. A statistical study of the behavior of the electron temperature in ejecta. *Journal of Geophysical Research: Space Physics*, 102(A3): 4691–4699, 1997.

Pete Riley and NU Crooker. Kinematic treatment of coronal mass ejection evolution in the solar wind. *The Astrophysical Journal*, 600(2):1035, 2004.

Pete Riley, JA Linker, R Lionello, Z Mikić, D Odstrcil, MA Hidalgo, C Cid, Q Hu, RP Lepping, BJ Lynch, et al. Fitting flux ropes to a global mhd solution: A comparison of techniques. *Journal of atmospheric and solar-terrestrial physics*, 66(15):1321–1331, 2004.

E. Robbrecht, D. Berghmans, and R.A.M. Van der Linden. Automated lasco cme catalog for solar cycle 23: are cmes scale invariant? *The Astrophysical Journal*, 691(2):1222, 2009. doi: 10.1088/0004-637X/691/2/1222.

T. Rollett, C. Möstl, M. Temmer, A.M. Veronig, C.J. Farrugia, and H.K. Biernat. Constraining the kinematics of coronal mass ejections in the inner heliosphere with in-situ signatures. *Solar Physics*, 276(1-2):293–314, 2012. doi: 10.1007/s11207-011-9897-0.

Gordon Rostoker. Triggering of expansive phase intensifications of magnetospheric substorms by northward turnings of the interplanetary magnetic field. *Journal of Geophysical Research: Space Physics*, 88(A9):6981–6993, 1983.

A.P. Rouillard, N.R. Sheeley Jr., T.J. Cooper, J.A. Davies, B. Lavraud, E.K.J. Kilpua, R.M. Skoug, J.T. Steinberg, A. Szabo, A. Opitz, et al. The solar origin of small interplanetary transients. *The Astrophysical Journal*, 734(1):7, 2011. doi: 10.1088/0004-637X/734/1/7.

P. Ruan, A. Korth, E. Marsch, B. Inhester, S. Solanki, T. Wiegelmann, Q.-G. Zong, R. Bucik, and K.-H. Fornacon. Multiple-spacecraft study of an extended magnetic structure in the solar wind. *Journal of Geophysical Research: Space Physics*, 114(A2), 2009. doi: 10.1029/2008JA013769.

JC Samson and KL Yeung. Some generalizations on the method of superposed epoch analysis. *Planetary and space science*, 34(11):1133–1142, 1986.

JP Schieldge and GL Siscoe. A correlation of the occurrence of simultaneous sudden magnetospheric compressions and geomagnetic bay onsets with selected geophysical indices. *Journal of Atmospheric and Terrestrial Physics*, 32(11):1819–1830, 1970.

Rainer Schwenn. Average solar wind in the inner heliosphere: structures and slow variations. Technical report, Max-Planck-Institut fuer Aeronomie, Katlenburg-Lindau (Germany, FR), 1983.

N.R. Sheeley Jr., Y.-M. Wang, S.H. Hawley, G.E. Brueckner, K.P. Dere, R.A. Howard, M.J. Koomen, C.M. Korendyke, D.J. Michels, S.E. Paswaters, et al. Measurements of flow speeds in the corona between 2 and 30 $r_\odot$? *The Astrophysical Journal*, 484(1):472, 1997.

N.R. Sheeley Jr., J.H. Walters, Y.-M. Wang, and R.A. Howard. Continuous tracking of coronal outflows: Two kinds of coronal mass ejections. *Journal of Geophysical Research: Space Physics*, 104(A11):24739–24767, 1999.

E.C. Sittler and L.F. Burlaga. Electron temperatures within magnetic clouds between 2 and 4 au: Voyager 2 observations. *Journal of Geophysical Research: Space Physics*, 103(A8): 17447–17454, 1998.

JA Slavin, RP Lepping, J Gjerloev, DH Fairfield, M Hesse, CJ Owen, MB Moldwin, T Nagai, A Ieda, and T Mukai. Geotail observations of magnetic flux ropes in the plasma sheet. *Journal of Geophysical Research: Space Physics*, 108(A1), 2003.

Edward J. Smith and Andre Balogh. Decrease in heliospheric magnetic flux in this solar minimum: Recent ulysses magnetic field observations. *Geophysical Research Letters*, 35 (22), 2008. doi: 10.1029/2008GL035345.

BENGT U.*Ö* Sonnerup and Maureen Scheible. Minimum and maximum variance analysis. *Analysis methods for multi-spacecraft data*, pages 185–220, 1998.

BU Sonnerup and M Guo. Magnetopause transects. 1996.

B.U.*Ö*. Sonnerup and L.J. Cahill Jr. Magnetopause structure and attitude from explorer 12 observations. *Journal of Geophysical Research*, 72(1):171–183, 1967. doi: 10.1029/JZ072i001p00171.

Hui Tian, Shuo Yao, Qiugang Zong, Jiansen He, and Yu Qi. Signatures of magnetic reconnection at boundaries of interplanetary small-scale magnetic flux ropes. *The Astrophysical Journal*, 720(1):454, 2010. doi: 10.1088/0004-637X/720/1/454.

Y.-M. Wang and R. Colaninno. Is solar cycle 24 producing more coronal mass ejections than cycle 23? *The Astrophysical Journal Letters*, 784(2):L27, 2014. doi: 10.1088/2041-8205/784/2/L27.

Y.-M. Wang, N.R. Sheeley Jr., D.G. Socker, R.A. Howard, and N.B. Rich. The dynamical nature of coronal streamers. *Journal of Geophysical Research: Space Physics*, 105(A11): 25133–25142, 2000. doi: 10.1029/2000JA000149.

W. Yu, C.J. Farrugia, A.B. Galvin, K.D.C. Simunac, E.K.J. Kilpua, M.A. Popecki, C. Moestl, N. Lugaz, J.G. Luhmann, A. Opitz, et al. Small solar wind transients: Stereo-a observations in 2009. In *SOLAR WIND 13: Proceedings of the Thirteenth International Solar Wind Conference*, volume 1539, pages 311–314. AIP Publishing, 2013. doi: 10.1063/1.4811050.

W. Yu, C.J. Farrugia, N. Lugaz, A.B. Galvin, E.K.J. Kilpua, H. Kucharek, C. Möstl, M. Leitner, R.B. Torbert, K.D.C. Simunac, et al. A statistical analysis of properties of small transients in the solar wind 2007–2009: Stereo and wind observations. *Journal of Geophysical Research: Space Physics*, 119(2):689–708, 2014. doi: 10.1002/2013JA019115.

W Yu, CJ Farrugia, AB Galvin, Noé Lugaz, JG Luhmann, KDC Simunac, and E Kilpua. Small solar wind transients at 1 au: Stereo observations (2007–2014) and comparison with near-earth wind results (1995–2014). *Journal of Geophysical Research: Space Physics*, 2016.

X-Y Zhang, MB Moldwin, and M Cartwright. The geo-effectiveness of interplanetary small-scale magnetic fluxropes. *Journal of Atmospheric and Solar-Terrestrial Physics*, 95:1–14, 2013.

Thomas H. Zurbuchen and Ian G. Richardson. In-situ solar wind and magnetic field signatures of interplanetary coronal mass ejections. *Space Science Reviews*, 123(1-3):31–43, 2006. doi: 10.1007/s11214-006-9010-4.